

METEOR-Berichte

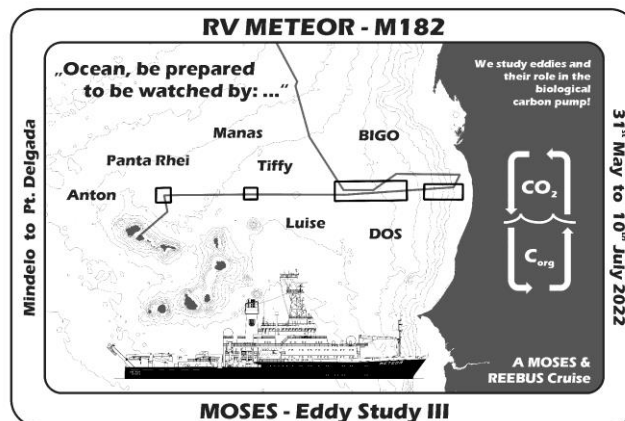
Role of Eddies in the Carbon Pump of Eastern Boundary Upwelling Systems, REEBUS

Cruise No. M182

31.05. – 10.07.2022

Mindelo (Cap Verde) – Pt. Delgada (Azores)

MOSES Eddy Study III



Mareike Kampmeier, Andrew W. Dale, Jens Greinert, Hendrik-Jan Hoving, Benjamin Pontiller, Danilo Scheppukat, Stefan Sommer, Emanuel Wenzlaff

Prof. Dr. Jens Greinert

GEOMAR Helmholtz Centre for Ocean Research Kiel

Table of Contents

1	Cruise Summary.....	4
1.1	Summary in English	4
1.2	Zusammenfassung	4
2	Participants.....	5
2.1	Principal Investigators	5
2.2	Scientific Party	5
2.3	Participating Institutions.....	6
3	Research Program	7
3.1	Description of the Work Area	7
3.2	Aims of the Cruise.....	8
3.3	Agenda of the Cruise	8
4	Narrative of the Cruise.....	10
5	Preliminary Results	14
5.1	Water Column Biogeochemistry	14
5.2	Water Column Biology.....	22
5.3	Benthic Biogeochemistry	26
5.4	Benthic Insitu-Fluxes.....	28
5.5	Benthic Observations.....	33
5.7	AUV Tests	47
5.8	Dedicated Acoustic Mapping	53
5.9	Underway Studies.....	56
5.10	Expected Results.....	58
6	Ship's METEORological Station.....	59
6.1	Weather and Route during the Trip M182.....	59
7	Station List	61
8	Data and Sample Storage and Availability	75
9	Acknowledgements.....	75
10	References	76
11	Abbreviations	79
12	Appendices	80
12.1	Water Column Biogeochemistry	80
12.2	Water Colum Biology.....	87

12.3	Benthic Biogeochemistry	90
12.4	Benthic Insitu-Fluxes.....	93
12.5	Benthic Observations.....	96
12.6	AUV Test.....	126
12.7	Dedicated Acoustic Mapping	128
12.8	Maps of the Research Areas	129

1 Cruise Summary

1.1 Summary in English

The research cruise M182 (MOSES Eddy-III) concludes a trilogy of research cruises conducted in the frame of the Helmholtz Association's Modular Observation Solutions for Earth Systems (MOSES) infrastructure, aiming at a comprehensive multi- and interdisciplinary study of ocean eddies in the northern tropical Atlantic. As an integral part of the BMBF-funded project "Role of eddies in the carbon pump of eastern upwelling systems - Demonstration Case Canary Current System" (REEBUS), launched in 2019, this study focuses on investigating the multi-layered influence of eddies on the lateral transport of biogeochemical properties and the carbon pump within deep-sea ecosystems. Ocean eddies have a significant impact on the physical, biogeochemical and biological aspects of coastal upwelling regions. Given the profound socio-economic impact of coastal upwelling areas, REEBUS takes a multidisciplinary approach to investigate the influence of ocean eddies on these systems. This expedition is motivated by the objective of acquiring novel insights into the functional dynamics of eddies, specifically elucidating their role in the CO₂ source and sink functions inherent to eastern boundary upwelling systems. Furthermore, our investigative efforts encompassed a thorough examination of the biological carbon pump within both the designated upwelling areas and their associated oligotrophic regions. The synthesis of data from all REEBUS cruises, coupled with the inclusion of data from prior expeditions (MOSES Eddy-I and II) within this geographical region, promises to yield a high scientific potential.

1.2 Zusammenfassung

Die Forschungsfahrt M182 (MOSES Eddy-III) bildet den Abschluss einer Trilogie von Forschungsfahrten, die im Rahmen der MOSES-Infrastruktur (Modular Observation Solutions for Earth Systems) der Helmholtz-Gemeinschaft durchgeführt wurden und die eine umfassende multi- und interdisziplinäre Untersuchung von Ozeanwirbeln im nördlichen tropischen Atlantik zum Ziel haben. Als integraler Bestandteil des vom BMBF geförderten Projekts "Role of eddies in the carbon pump of eastern upwelling systems - Demonstration Case Canary Current System" (REEBUS), das 2019 startete, konzentriert sich diese Studie auf die Untersuchung des vielschichtigen Einflusses von Wirbeln auf den lateralen Transport biogeochemischer Eigenschaften und die Kohlenstoffpumpe in Tiefsee-Ökosystemen. Ozeanwirbel haben einen erheblichen Einfluss auf die physikalischen, biogeochemischen und biologischen Aspekte von Auftriebsgebieten an der Küste. Angesichts der tiefgreifenden sozioökonomischen Auswirkungen von Auftriebsgebieten an der Küste verfolgt REEBUS einen multidisziplinären Ansatz, um den Einfluss von Ozeanwirbeln auf diese Systeme zu untersuchen. Ziel dieser Expedition war es, neue Erkenntnisse über die funktionelle Dynamik von Wirbeln zu gewinnen und insbesondere ihre Rolle bei der CO₂-Quellen- und -Senkenfunktion von Auftriebssystemen an der Ostgrenze zu klären. Darüber hinaus haben wir die biologische Kohlenstoffpumpe sowohl in den ausgewiesenen Auftriebsgebieten als auch in den dazugehörigen oligotrophen Regionen eingehend untersucht. Die Synthese der Daten aller REEBUS-Fahrten in Verbindung mit der Einbeziehung der Daten früherer Expeditionen

(MOSES Eddy-I und II) in dieser geografischen Region verspricht ein hohes wissenschaftliches Potenzial.

2 Participants

2.1 Principal Investigators

Name	Institution
Greinert, Jens, Prof. Dr.	GEOMAR
Hoving, Hendrik Jan Ties, Dr.	GEOMAR
Sommer, Stefan, Dr.	GEOMAR
Dale, Andrew, Dr.	GEOMAR
Pontiller, Benjamin, Dr.	GEOMAR



Fig. 2.1 Participants of the scientific crew of M182.

2.2 Scientific Party

Name	Discipline	Institution
Prof. Dr. Greinert, Jens	Marine Geology / Chief Scientist	GEOMAR
M.Sc. Kampmeier, Mareike	Marine Geology / Hydroacoustics, Benthic Observations	GEOMAR

Dr. Hoving, Hendrik Jan Ties	Marine Biology	GEOMAR
M.Sc. von See, Tim Benedict	Robotics /AUVs Girona500	GEOMAR
M. Eng.. Heger, Karl	AUV Abyss	GEOMAR
Dr. Sommer, Stefan	Marine Geochemistry	GEOMAR
Dipl.-Ing.Türk, Matthias	Lander, Deepsea Rover	GEOMAR
M.Sc. Hansen, Nis	Marine Biology	GEOMAR
B.Eng. Nolte, Gabriel	Lander, Deepsea Rover, XOFOS	GEOMAR
Dr. Linke, Peter	Lander, Deepsea Rover, XOFOS	GEOMAR
Dr. Dale, Andrew	Marine Geochemistry	GEOMAR
CTA Surberg, Regina	Marine Geochemistry	GEOMAR
CTA Domeyer, Bettina	Marine Geochemistry	GEOMAR
Dr. Chuang, Pei-Chuan	Marine Geochemistry	GEOMAR
Spiegel, Timo	Marine Geochemistry	GEOMAR
M.Eng.Striewski, Peter	AUV Abyss	GEOMAR
M.Eng.Wenzlaff, Emanuel	AUV Abyss	GEOMAR
M.Eng. Kurbjuhn, Torge	AUV Abyss	GEOMAR
M.Sc. Mohrmann, Jochen	Hydroacoustics	GEOMAR
M.Sc. Hinz, Anina-Kaja	Hydroacoustics, Benthic Observations	GEOMAR
M.Eng. Scheppukat, Danilo	AUVs Girona500	GEOMAR
M.Eng.Fabrizius, Eduard	Lander, XOFOS	GEOMAR
Dr. Pontiller, Benjamin	Marine Biogeochemistry	GEOMAR
M.Sc. Golde, Sandra	Marine Biogeochemistry	GEOMAR
M.Sc. Devresse, Quentin Romain Michel	Marine Biogeochemistry	GEOMAR
von Jackowski, Anabel Charlotte	Marine Biogeochemistry	GEOMAR
M.Sc.Weyand, Phillip	Marine Geochemistry	GEOMAR

2.3 Participating Institutions

GEOMAR Helmholtz-Centre for Ocean Research Kiel

with research division Ocean Circulation and Climate Dynamics (onshore support), Marine Biogeochemistry and Marine Ecology

3 Research Program

3.1 Description of the Work Area

The main research areas, labelled E1 to E5, are located along the 18th parallel north and were already partially bathymetrically mapped during the M156 research expedition in 2019. These areas are complemented by additional mapping strategically positioned sampling stations, including the CVOO long-term station and Cape Blanc (CB) to the north, which is on the way to the Azores.

The entire study area around 18° North is referred to as an "eddy alley", as eddies repeatedly form on the Mauritanian shelf and eventually detach from the coastal periphery and migrate westwards.

Significantly, regions E1 to E3 are characterized by homogeneous flat deep-sea facies, while E1 Hill, Senghor SMT, E4 and E5 show distinct morphological features. In particular, E1 Hill comprises a seamount of 500 m height above seafloor, E4 is characterized by a smaller (300 m height above seafloor) and more gentle sloping seamount accompanied by a proximal channel system and E5 represents the nearshore area of the Mauritanian shelf with a discrete reef structure. From all research areas, the Senghor SMT is the most prominent site, featuring a seamount that rises from abyssal depths to 110 meters below the sea surface.

Maps showing the individual research areas with its corresponding sampling stations can be found inside the appendix.

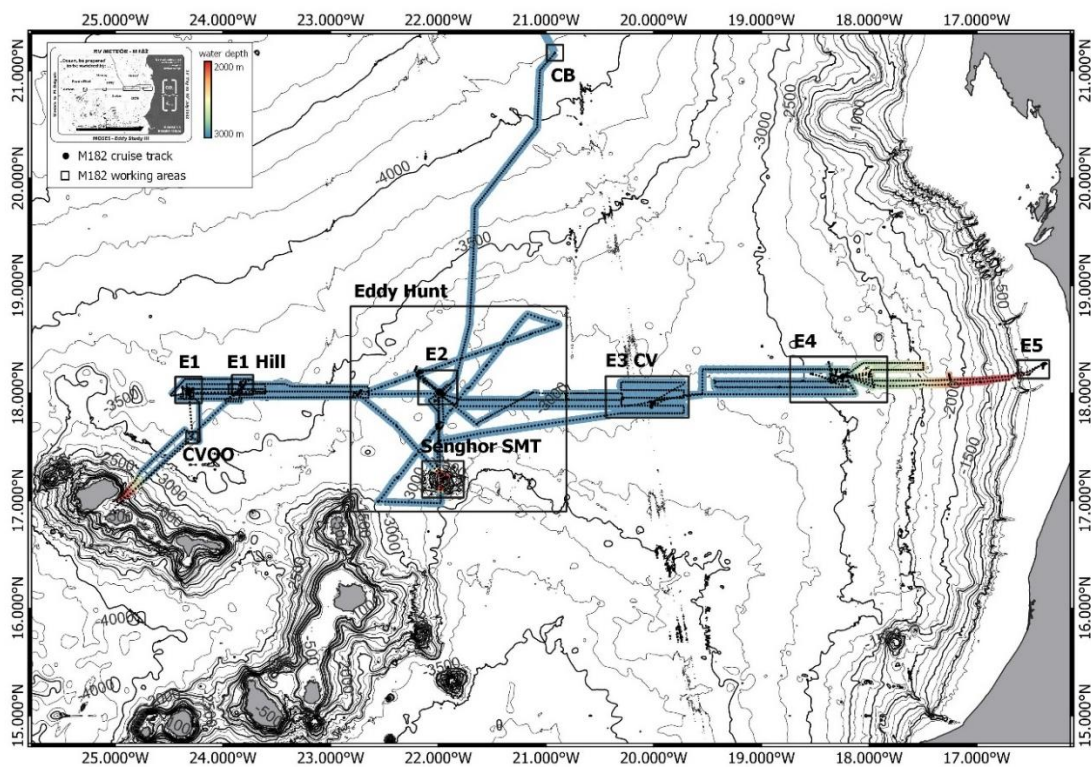


Fig. 3.1 Map inclusive cruise track and bathymetric Multibeam data of the cruise M182.

3.2 Aims of the Cruise

Cruise M182 is the third and last research cruise within the frame of the BMBF funded REEBUS project with the overarching objective of studying regional eddies in eastern boundary upwelling systems and their impact on pelagic biogeochemical processes and the modulation of the carbon export towards the seafloor. In parallel, it is part of the Helmholtz funded technology project MOSES that aimed of developing modular systems for Earth System studies. Both projects jointly conducted the previous two RV METEOR cruises M156 and M160. The study area of the REEBUS project is the northern tropical Atlantic between Cabo Verde and Mauretania along an E-W transect at about 18° north. The two previous cruises focussed on water column investigations including eddy hunting by using physical oceanography tools and approaches (ship based ADCPs, CTD, glider) with parallel water column sampling for biogeochemical investigations. In addition, seafloor studies with sediment sampling, optical and acoustic mapping as well as in-situ biogeochemical flux measurements with landers were performed. M160 even did a coordinated mission with the Stemme S10 VTX motorglider from Aachen University for detecting eddies.

During M182 we focused on biogeochemical investigation of the seafloor but also did a substantial water column sampling program including an ADCP and CTD-based eddy hunt survey. As the time between applying for the cruise and the actual cruise happening was rather long, an additional group looking at gelatinous organisms in the water column joined and broadened our studies. For achieving our overarching objective, a number of tasks guided the work during M182 which can be summarized as follows:

- Map, characterise and ‘pin-point’ an eddy using physical oceanography (ship-based ADCP, CTD) and satellite-based sea-surface height information
- Sample the eddy along a cross-transect for biogeochemical investigations
- Perform vertical water column sampling and optical investigations along horizontal transects for gelatinous organisms
- Investigate the potentially small scaled heterogeneity of the biogeochemical carbon turnover on the seafloor using
 - AUV based mapping technologies (acoustically and optically)
 - XOFOs-based high resolution optical seafloor mapping
 - detailed sediment sampling with TV-MUC and GC
 - and in-situ biogeochemical flux measurements with BIGO landers and the Panta Rhei rover

Deploy the BBL lander (CTD, ADCP, sediment trap, time laps camera) and the deep-sea rover Panta Rhei (benthic oxygen flux chambers, ADCP, CTD, cameras) to investigate the potential impact of a passing eddy until their recovery on 15 January 2023 with RV MS MERIAN.

3.3 Agenda of the Cruise

As delineated above, the research cruise was driven by two principal objectives: the first, the discovery and acquisition of samples from an oceanic eddy, and the second, the comprehensive

exploration of the variability characterizing diverse benthic seafloor attributes encompassing biogeochemistry, morphology, and physical properties.

Since Eddies do form frequently within proximity of the west African coast, but their lifespan and propagation path are difficult to predict, an extensive benthic and pelagic program was launched within the zonal eddy passage situated at 18° latitude before a suitable eddy was identified. It extends from the vicinity of Cabo Verde to the Mauritanian continental shelf (designated as E1-E4). A sequence of benthic stations was designated at varying water depths and in proximity to the continental shelf, serving as locations for systematic sampling. Furthermore, deviating from the initial cruise proposal, the itinerary was expanded to incorporate investigations at the Senghor Seamount and the E1 hill station. When selecting these additional sites, it was considered that seamounts represent unique ecological niches in the surrounding deep-sea environment. In parallel, the water column was sampled through the deployment of a multi-net apparatus. The scientific undertakings commenced with a multinet haul and the deployment of a Conductivity, Temperature, and Depth (CTD) profiler at the Cabo Verde Ocean Observatory site (CVOO), an established long-term monitoring station that undergoes periodic sampling. In each working area, sediment was sampled via TV-MUC and gravity corer for geochemical analysis. The deep-sea rover (DSR) Panta Rhei and the BIGO (Benthic In situ Gravimetric Observatory) lander were deployed with the primary aim of quantifying benthic fluxes over an extended observational period spanning several days. Additionally, the cruise incorporated the use of a towed extended ocean floor observation system (XOFOS), which allows high-resolution visual documentation of the seafloor surface through video profiles. This program enabled the investigation of variabilities in bioturbation patterns, macrofaunal communities, small-scale seafloor heterogeneity, and the intricacies of biogeochemical carbon turnover processes. It was repeated in each research area.

Eventually, one eddy was identified via satellite images and could be sampled in the second week of the cruise. Acquired underway ADCP and CTD data was sent on a regular basis to GEOMAR for parallel analysis, which supported the eddy detection and identification. Additional ADCP surveys crossing the eddy from different directions are needed to identify the eddy core location for sampling to investigate the characteristics and dynamics of oceanic eddies, including their physical properties and potential impact on carbon fluxes. Once the eddy is found, it was sampled along a cross-transect for biogeochemical and microbiological investigations.

Towards the end of the cruise an area needed to be defined, which is well-suited in order to deploy the BBL lander and the Panta Rhei rover for the long-term measurements.

According to the ship time proposal, we successfully conducted measurements at all planned stations. We followed the DFG regulations summarized in the „Erklärung zu einer verantwortungsvollen Meeresforschung“ and the (OSPAR) Code „Code of Conduct for Responsible Marine Research in the Deep Seas and High Seas of the OSPAR Maritime Area“ to avoid unnecessary environmental and ecosystem disturbances. The impact of the conducted work to the environment can be considered as very minor. There were no activities, which could lead to substantial physical, chemical, biological or geological changes or damage of marine habitats. Care was taken to avoid activities, which could disturb the experiments and

observations of other scientists. We made use of the most environmentally-friendly and appropriate study methods, which are presently available, and avoided collections that are not essential to conduct the scientific research. The number of samples was reduced to the necessary minimum.

4 Narrative of the Cruise

M182 had five full weeks of station work, followed by a transit of 4.5 days from our last sampling location, the Cape Blanc site, to Pt Delgada on the Azores. Fig. 3.1 shows the cruise track from Mindelo up to Cape Blanc. During all the time the EM122 multibeam, the ship-based 38kHz ADCP and the thermosalinograph kept running to acquire needed data for the eddy hunt and also to add underway data e.g. for mapping uncharted parts of the seafloor and add them to the GEBCO compiled data of our oceans. Members of the scientific party started to arrive on Sao Vicente, an island of the archipelago of Cape Verde in the Atlantic Ocean at 16°53' N and 25° 00' W, already on 27th of May. The last member of the scientific party arrived on 30th after an unplanned stop-over in Lisbon. The 29th and 30th May were busy with loading and installing equipment and making it ready to leave harbor the next morning.

Week 1 – 31st May to 6th June

The M182 expedition started at 9:00 a.m. local time on 31st May in Mindelo on Sao Vicente. We arrived at our first station the Cabo Verde Ocean Observatory site (CVOO) at 13:35 local time, where we conducted a multi-net haul (station 001) and our first of 52 CTD casts. On June 1st, two LBL transponders were deployed in our western-most working area (E1) to prepare for AUV Abyss dives. The second CTD was taken (station 005) as the eastern most CTD station of a long E-W transect stretching from the E1 to E5 area. This CTD section is a repetition of an equivalent transect performed during M156. After our first TV-MUC sampling we deployed the BIGO lander in E1 to measure benthic fluxes for several days (stations 008 and 010). Subsequently, the XOFOS was deployed for the first time and all its functions were checked and tested and the seafloor was surveyed optically. More multibeam data were acquired while RV METEOR approached the next multi-net and CTD position between work area E1 and E2 marking the second CTD station on the E-W transect (stations 013 and 014). The multibeam echo sounder on the transit revealed a seamount structure (E1-Hill), which we selected for the second BIGO deployment in the early night of June 2nd (station 015). To save time, the heel frame normally used to deploy the lander was sent on a reconnaissance trip in NE direction to explore the sediment surface and bioturbation type and intensity in the lander vicinity. On the morning of June 3rd, a TV-MUC (station 016) was taken near the lander position before we returned to the E1 area.

Back at E1 the Panta Rhei rover (station 018) was deployed for the first time in such great water depth and particularly the group around Stefan Sommer was very much looking forward to its recovery and hopefully successful completion of the mission. A second XOFOS surveyed the E1 area again (station 019) before another sediment core was taken for a colleague at GEOMAR (station 020). After that, we continued mapping to the east to take a multi-net, a CTD, a TV-MUC and an XOFOS to visually inspect the top 1000 m of the water column

(stations 025 to 028) at the E1-Hill site. This site turned out to be the NW periphery of the eddy that we sampled in more detail later.

We went back to the E1-Hill site to conclude sampling at this area by deploying the BIGO lander once more, take a second TV-MUC at the top of the hill and run a XOFOS seafloor survey down the hill in northward direction. At the end of the XOFOS transect we sampled for organisms in the upper 1500m using the multi-net (stations 030 to 033). With 33 stations, we concluded the first week of work by heading back to the E1 area.

Week 2 – 7th to 13th June

Back at E1 we took our first gravity corer of the cruise and recovered the two LBL transponders. Unfortunately, AUV Abyss could not be deployed as an O-Ring of the inertial navigation sensor was broken and despite a large number of spare O-rings on board this particular one was not present. So, after a USBL test-station for AUV Anton (station 038) and two further XOFOS stations (station 039 and 040) for biological water column investigations. Before we headed back towards Mindelo for the delivery of AUV spare parts, the missing O-ring and an additional fluorescence sensor that was kindly supplied by the Ocean Science Centre Mindelo.

After the successful hand over, we turned back north to take a night multi-net at CVOO (station 042) followed by a long multibeam survey towards the east and the start of the Eddy-Hunt CTD transect. Satellite images showed sea surface height anomaly indicative of an eddy with a core position roughly at the E2 area. The supposed eddy had dimensions of about 115 km by 180 km and as such was rather big. Starting early morning at 00:44 the first (station 045) of 15 CTDs physically explored the eddy every 8 nmi. In addition, the ship-based 38kHz ADCP was used to measure the water current direction and speed in the upper 800m to 900m in 32m thick layers. A short additional USBL testing for AUV Anton was performed at the location of CTD station 053 for solving issues with lever-arm offsets which are needed for accurate underwater navigation. After finishing the physical exploration of the eddy towards 70° we turned southward on a 220° course to sample the eddy every 16nmi. The last CTD station along this transect was station 068 in the morning of 12th June.

To take the needed gravity core at E2 we headed back to this area but after sampling went back south to take a CTD, a water column XOFOS and a multi-net at the supposed eddy centre at 17°41.229' N and 21°59.659' W (stations 71 to 73). We used the chance to investigate the central part of the eddy in more detail by deploying AUV Abyss in a zig-zag water column mapping mode. This new possibility came with the upgrade of the system after 2.5 years of repairs. This first dive of Abyss (station 074) was a success after the delay due to the missing of the O-ring. After the Abyss dive we went back to E2, deployed the LBL transponders and the BIGO and took another CTD before in late night of 13th June the ninth XOFOS went into the water to observe the seafloor across the sampling and lander site of E2.

Week 3 and one day – 14th to 20th June

After finishing the XOFOS in the E2 area we acquired additional multibeam data of the E2 area and before we took a multi corer and deployed the deepsea rover and the AUV to perform

their monitoring and mapping missions (stations 080 to 082). While these two devices were running we sampled a station 16nmi towards the NW at the periphery of the eddy with two CTD cast a water column XOFOS and a multi-net (stations 083 to 086). After recovering the AUV we headed south again to the eddy core location for further CTD, sediment and biological water column sampling (stations 088 to 092). Continuing the CTD stations across the eddy towards the south we took CTD station 093 at the northern flank of the Senghor seamount and performed an EM122 multibeam survey of the top of the seamount to prepare for an AUV Anton dive in about 105 m depth. Prior to the AUV deployment we surveyed the top to ensure that no lost fishing gear as nets or lines could cause damage to the AUV. The fauna on the seamount was spectacular and colorful and was very much contrasting to the much more homogenous and ‘brown’ seafloor in the abyss.

After Anton’s successful recovery, we continued sampling the western periphery of the eddy (CTD stations 098) and continued in the same direction towards the E1-E2 mountain range for a final TV-MUC sampling. We went back to E2 and deployed AUV Abyss for another camera and sidescan sonar mapping survey (station 100) and used the time of the mapping to move back to the NW eddy periphery to take an XOFOS and a multi-net during the day (stations 101 and 102). Three consecutive CTDs were performed on our way towards the east adding more stations along the long E-W CTD transect (stations 103 – 105). During the transit towards the E3 area we recognized a mountain range like area that we decided to map in greater detail for subsequent sediment sampling. After acquiring the TV-MUC sample at the top of the range, we deployed AUV Abyss again in the E2 area (station 108) and after retrieval of the AUV and the LBL transponders we completed a second CTD cast. The station was located at an updated eddy core location a bit south of the previous core location (station 111). Afterwards, we went on a long multibeam survey to cover the supposed to be ‘new’ long-term monitoring area for the BBL and rover deployment in Cabo Verde waters (area E3-CV). The time of the multibeam mapping (station 112) was used to celebrate the mid of the cruise and a combined birthday of 11 crew members and scientists.

Week 4 – 21st to 27th June

The next six stations after our midterm break aimed at characterizing this new working area; this included a TV-MUC (station 113) an AUV deployment, GC sediment recovery, BIGO and rover deployments with CTD station 118 as last station on 21st June. During the very early morning of 22nd June, two XOFOS dives took place one for inspecting the water column, the second for exploring the seafloor of the supposed long-term monitoring area. We left the site and one BIGO lander and headed further towards the east to start working in area E4. On the way, we took another CTD of the long E-W transect (station 124) and started with GC sampling upon arrival in E4. Until noon of 28th we stayed in the E4 area mapping and sampling different habitats and geological structure of this much more versatile area. Changing between multibeam mapping and XOFOS transects during the night to lander and TV-MUC deployments during the day and in between AUV deployments and recoveries, we undertook stations 121 to 152 during this time.

Week 5 – 28th June to 5th July

In the afternoon of 28th June we started steaming further towards the east and lowered CTD number 47 (station 154) early evening of the 28th followed by a water column XOFOS station between working area E4 and E5 in about 2150m water depth. Work in E5 started in the morning of 29th June with one CTD at 176m water depth, the most eastern CTD of the long E-W transect and an even shallower CTD at 75m water depth (stations 156 and 157), at an area that was studied already during M107 as part of SFB754 studies. Next to sampling this area we aimed at more intensely deploying the small Girona 500 AUVs. In preparation for this we lowered a USBL transponder of the small AUVs and performed a number of loop and crossing transects over it to further develop and compare position offsets of GEOMARs Beluga software and the commercial equivalent. This work happened during the night after the BIGO was deployed for a 3 days measurement and two TV-MUCs were taken (station 160 and 161). An XOFOS in the evening showed as the shallow water habitats of this heavily fished area. METEOR was surrounded by eight and sometimes more large fishing vessels which apparently focus on pelagic fishing, as the seafloor that we inspected showed little impact of bottom trawling. In the morning of 30th July both small AUVs, Anton and Luise were launched to perform a camera survey (Anton) and a number of automated water column surveys (Luise). During recovery of Luise she was pulled below the ship's hull and due to her internal safety features, stayed below the surface and could not be retrieved immediately; we could pick her up about 2h later after she had drifted off about 2.5nmi towards the south. Following this short search and recover operation, we successfully deployed AUV Abyss for two camera missions (station 167). After two additional seafloor XOFOS transects during the night, we left the E5 area to retrieve the rover in the E4 and the BIGO in the E3-CV area. On the way two additional TV-MUCs were taken in a canyon system of E5 and at 1700m water depth further to the west (stations 171 and 172 and an additional CTD for the E-W transect was taken between E4 and E5. The recovery of the rover and the BIGO went well, although the recovery of the rover during the night with 2m waves was challenging. Due to the visual and sidescan inspection of the seafloor within E3-CV we decided earlier to shift the longterm monitoring location towards E2, where we arrived early morning on 3rd July readily prepared to deploy the BBL lander and the rover until 15th January 2023 (stations 176 and 177) and undertake a camera and sidescan inspection of their deployment area. A final CTD at E2 aimed at characterizing the geochemistry of the long-term deployment at this site.

Moving north towards the Cape Blanc area we added multibeam data where GEBCO maps did not show existing coverage. We arrived after 24 h, performed our three last physical sample stations, a CTD, TV-MUC and GC, before we concluded sampling, and started our transit towards the Azores. Until the 200nmi zone of the EEZ we continued acquiring multibeam and ADCP data and continued without data recording until we arrived the pilot station at 19:30 on 9th July.

5 Preliminary Results

5.1 Water Column Biogeochemistry

(B. Pontiller, A. von Jackowski, Q. Devresse, S. Golde, P. Weyand, B. Domeyer, R. Surberg, and A. Engel)

Overview

A characteristic feature of Eastern Boundary Upwelling Systems (EBUS) is the upwelling of nutrient-rich deep water and, therefore, typically high primary production. The physical properties associated with the large-scale movement of water masses also support the formation of circular water movements at a much smaller scale (eddies). These eddies conserve the characteristics of the coastal upwelling zone and transport nutrients (e.g. carbon and nitrogen) from the productive coastal to the open oligotrophic ocean. While mesoscale eddies can extend over 100 km in the horizontal dimension, they typically affect the upper ocean chemistry and biology, reaching a few hundred meters deep into the water column. These effects are visible by distinct chemical, biological, and physical signatures of the water inside the eddy compared to the surrounding water. In cyclonic eddies (CE), nutrient upwelling supports higher primary production and heterotrophic bacterial activities than measured in ambient waters. However, knowledge on how mesoscale eddies affect the balance between the production and degradation of dissolved organic matter (DOM) along the coast to offshore migration path has yet to advance. Therefore, we conducted an intensive sampling program to investigate the horizontal and vertical variability of biogeochemical parameters and microbial activity between Cape Verde Islands and Mauritanian, a hotspot of eddies migrating towards the open ocean.

We identified a cyclonic eddy based on CTD profiles and ADCP data from the upper ocean water column and retrieved seawater samples using 24 x 10 L Niskin bottles attached to a CTD rosette frame. The overarching objectives of M182 were to study the influence of (sub)mesoscale eddies formed in EBUS regions on (i) upper ocean organic carbon distribution; (ii) microbial productivity and organic matter turnover, and (iii) supply of organic matter to the central Atlantic Ocean.

Our main objective of the CTD-rosette sampling program was the detailed acquisition of upper ocean water column profiles. At 25 CTD stations, we collected water samples, mostly from 7 depths, for the analysis of a variety of biogeochemical and microbiological parameters. These included dissolved, non-sinking, and other particulate organic matter components, nutrients, oxygen, microbial extracellular enzymatic (EEA) activity, microbial cell abundance, microbial community composition, and functioning (Table 12.1). Overall, we collected 162 DOM samples (in replicates) and 138 samples (in replicates) for POM, microgels, biogenic silica, and extracellular enzymatic activity. Moreover, at four stations and four depths, we conducted polysaccharide hydrolysis assays (48 samples, three polysaccharides in triplicates). Additionally, we collected 110 DNA and RNA samples for characterizing microbial community composition and functioning. All samples were shipped frozen or cooled to the home laboratory at GEOMAR where analyses will be carried out within the coming year.

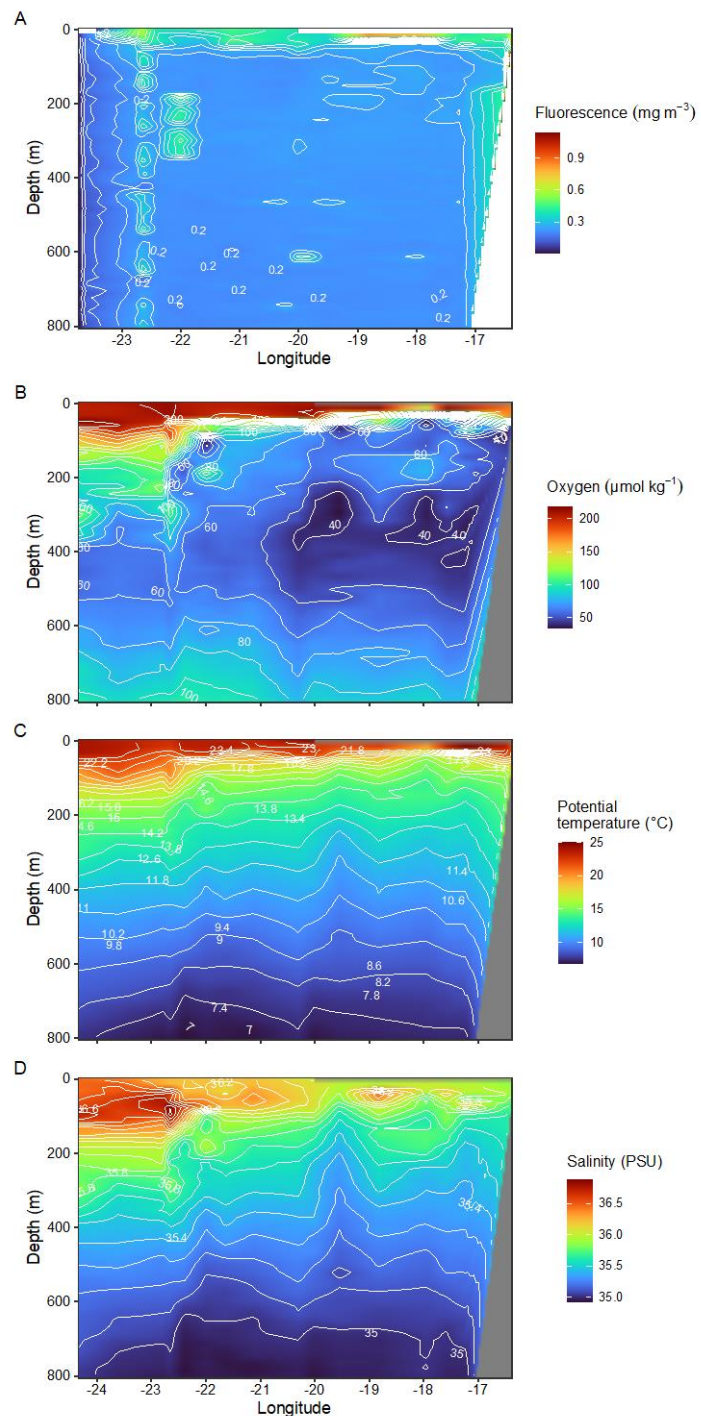
Sampling method and tables can be found in the appendix (12.1 Water Column Biogeochemistry).

CTD Preliminary Results

During M182, a total of 52 CTD profiles were conducted, reaching a maximum depth of ~3680 m. We deployed 24 CTD-casts together with ADCP data to locate an eddy and 25 CTD-casts to collect water samples for biogeochemical and microbiological analysis (Table 12.1 and Table 12.2). The remaining CTD profiles were used by the deep-sea biology group (Dr. Henk-Jan Hoving) for eDNA analysis (Water Column Biology). The CTD casts at regular stations reached 20 m above the seafloor. Two depth layers, one roughly 100-200 m above the seafloor and one at 1500 m depths were sampled in addition to six roughly evenly spaced depths (depending on the water column characteristics), including water samples for oxygen and nutrient concentrations. Eddy stations, in turn, were sampled down to 1500 m depth. In total, we sampled seven depth layers for biogeochemical and genomic parameters, except for TEP and CSP which comprised six depths and reaching 800 m deep. This sampling strategy ensured comparability of the result with the previously conducted expeditions M156 and M160. The GPS positions and details of water column sampling are listed in Table 12.1. For calibration of the CTD conductivity and oxygen sensors, water samples were collected with Niskin bottles from almost every CTD profile. Sampling depths were chosen to cover a wide range of parameters (i.e., depth, temperature, conductivity, oxygen, and time). Oxygen concentrations were determined from 169 water samples using Winkler titration.

A full CTD section from S1 (17° 59.996' N, 24° 20.006' W) to E5 (18° 15.906' N, 16° 23.781' W), including the eddy centre (17° 32.960' N, 22° 00.017' W) consisting of 17 CTD profiles was visualized. Chlorophyll a (determined by fluorescence) was generally low, increased slightly towards the Mauritanian coast, but did not increase inside the eddy (Fig. 5.1 A). However, the eddy showed notably lower oxygen concentrations inside the core, where minimum oxygen concentrations were well below 60 $\mu\text{mol kg}^{-1}$ between 80 and 100 m depth (Fig. 5.1 B). Also, salinity and temperature anomalies were found around the eddy centre (Fig. 5.1 C and D).

Fig. 5.1 CTD section along the W-S transect including the eddy (center at 17° 32.960' N, 22° 00.017' W). From top to bottom panel: Fluorescence (Chl a) (A), oxygen concentrations (B), potential water temperature (C), and salinity (D). Data is shown for the upper 800 m (but for most CTD casts available to a depth of 20 m above seafloor). Note the x-axis is shifted in panel A because the CTD cast M182_005 was excluded from analysis due to missing sensor data.



Biogeochemistry and Microbiology

Dissolved organic matter sampling (DOM)

Photosynthesis by phytoplankton in the euphotic surface layer is the main source of oceanic dissolved organic matter (DOM). Marine DOM, here the fraction passing through a 0.45 μm pore-size filter, is at 662 Gt C, the largest pool of reduced organic carbon in the ocean (Hansell et al., 2009). The marine DOM pool is composed of a myriad of organic compounds, which

fuel heterotrophic microbial activity and supplement nutrient-limited autotrophs with e.g., nitrogen and phosphorous (Hansell and Carlson, 2015).

During M182, we collected water samples for the analysis of dissolved organic carbon (DOC), total dissolved nitrogen (TDN), and dissolved organic phosphorus (DOP) concentrations. Moreover, we collected samples to determine the concentration and composition of dissolved amino acids (DAA) and dissolved carbohydrates (DCHO). Collectively, these biogeochemical parameters will allow us to describe the *in-situ* substrate availability of bacteria and archaea inside and around the mesoscale eddy and along the transect from the open ocean to the Mauritanian coast. All samples were filtered on-board and stored at +4°C or -20°C. Once the samples arrive at our home laboratory, they will be analyzed using established methods and according to established protocols. In brief, DOC analysis will be carried out according to (Sugimura and Suzuki, 1988) and (Engel and Galgani, 2016) using a high temperature combustion method. DOP will be analyzed after (Grasshof et al., 1999) and DAA according to (Lindroth and Mopper, 2002) using high-performance liquid chromatography. DCHO will be analyzed following the protocol by (Engel and Händel, 2011). Chromophoric dissolved organic matter (CDOM) and fluorescent dissolved organic matter (FDOM) will be estimated from spectral adsorption and spectral fluorescence measurements, respectively, as described in (Loginova et al., 2016).

Particulate organic matter sampling (POM)

The ocean harbors ~670 Gt C of total organic carbon (TOC) (Ogawa and Tanoue, 2003; Hansell and Carlson, 2015). This TOC pool can be separated into the operationally defined fractions of dissolved organic carbon (DOC) and particulate organic carbon (POC). Particulate organic carbon (POC) includes living and nonliving components of suspended and sinking submicron particles, gels, and colloids in the size range of 1 nm–1 µm (Benner and Amon, 2015, and references therein). Phytoplankton in the ocean account for roughly half of global net primary production and are the main producers of particulate organic matter (POM), which plays a key role in oceanic carbon cycling (Field et al., 1998). For instance, roughly half of the POM is converted into DOM within the upper mixed layer by genetically diverse bacteria (Azam, 1998; Arnosti, 2011), which modulate the recycling and export of organic matter in and out of the euphotic zone (Sanders et al., 2014). More recently, it has been shown that mesoscale eddies have the potential to alter surface ocean POC fluxes (Omand et al., 2015). However, research aiming to shed light on the impact of mesoscale eddies and their role in shaping the biogeochemical cycling and the export of POM and DOM in EBUS is needed. Therefore, we collected samples to determine the total POC content. All POM samples were filtered onto GFF filters and stored at -80 °C until further analysis in the home laboratory.

Microgels (TEP and CSP)

Phytoplankton (including Cyanobacteria) play a vital role in the global carbon cycle by transforming, via photosynthesis, inorganic carbon into organic matter. During this process, a small amount of carbon escapes rapid remineralization in the upper ocean and is stored in the deep ocean (biological pump) (Falkowski et al., 1998). However, under nutrient scarcity, phytoplankton tends to increase the exudation of exopolymers, including surface active carbohydrates and protein (Engel et al., 2002; Thornton and Chen, 2017). These dissolved

precursors (e.g., acidic polysaccharides or amino acids with aliphatic and aromatic side chains) can abiotically aggregate into larger gels (microgels) called transparent exopolymer particles (TEP) and protein-containing particles known as Coomassie-stainable particles (CSP) because of their sticky surface characteristics (Verdugo et al., 2004). These gels can reach sizes of hundreds of micrometers up to centimeter-scale owing to stable calcium ion bridges, thereby, linking the dissolved and the particulate organic matter phase in the marine water column (Engel, 2002; Verdugo et al., 2004). Both types of these microgel particles are important nutrient hotspots and are colonized by bacterioplankton (Mari and Kiørboe, 1996; Busch et al., 2017). Moreover, TEP and CSP play a crucial role in nutrient export fluxes from the euphotic zone to the deep sea (Engel et al., 2004).

To study TEP and CSP particle characteristics inside and around the eddy and along the transect, we collected seawater samples from 6 different depth layers and most CTD stations (Table 12.1) following the procedures described in (Alldredge et al., 1993) and (Long and Azam, 1996). The analysis includes vacuum filtration of water samples to collect the gel-like particles on filters (0.45 μm pore-size) and subsequent staining with either Alcian Blue or Coomassie Brilliant Blue for TEP and CSP, respectively. All of these steps were performed onboard and the quality of filters and the filter volume were checked immediately after staining and embedding the filters on the microscopy slides. The filters will be shipped frozen to the home laboratory, where we conduct a thorough analysis using microscopic and colorimetric analyses to obtain particle counts, size distribution, and concentrations as described in (Engel, 2009).

Total extracellular enzymatic activity assays

Organic matter in the ocean consists of a plethora of organic compounds spanning over orders of magnitude in size (Kujawinski, 2011; Moran et al., 2016; Dittmar et al., 2021). Two fractions of the organic matter pool are operationally defined based on a filter-pore size (e.g., 0.45 μm) into particulate organic matter (POM) and dissolved organic matter (DOM) (Hansell and Carlson, 2015). Heterotrophic bacterioplankton (here bacteria and archaea) rely on organic compounds but the uptake of these molecules through the cell membrane is generally limited to <600 Da (Weiss et al., 1991). Microorganisms synthesize a diverse suite of extracellular enzymes to hydrolyze peptide and glycosidic bonds of protein and polysaccharides into amino acids and oligo or monosaccharides, respectively (Arnosti, 2011). To measure *in-situ* extracellular enzymatic activity of bacteria and archaea inside and around a mesoscale eddy, we collected water from the upper 1500 m, used fluorogenic model substrates (Hoppe, 1993; Baltar et al., 2009) and fluorescently labeled polysaccharides (Arnosti, 2003). Potential peptidase, glucosidase, acetylglucosaminidase, and phosphatase activities were measured onboard using peptide, glucose, acetylglucosamine and phosphate substrate analogs, respectively. Exo-acting (terminal cleaving) leucine aminopeptidase activities were measured using the methylcoumarin-labeled substrate analog leucine, likewise glucosidase, acetylglucosamine, and phosphatase activities were measured using methylumbelliferyl-labeled α -glucopyranoside and β -glucopyranoside in addition to N-acetyl- β -D-glucosaminid, and phosphate. In order to measure polysaccharide hydrolase activities, we used laminarin [β (1,3-glucose)], xylan (xylose), and chondroitin sulphate (sulphated N-acetylgalactosamine, and glucuronic acid). All samples for polysaccharide hydrolase activity measurements were incubated and filtered

onboard, and stored at -20°C . These samples will be shipped to our collaborator Prof. Dr. Carol Arnosti, measured via gel permeation chromatography, and hydrolysis rates calculated as previously described (Arnosti, 2003).

Microbial community composition and cell counts

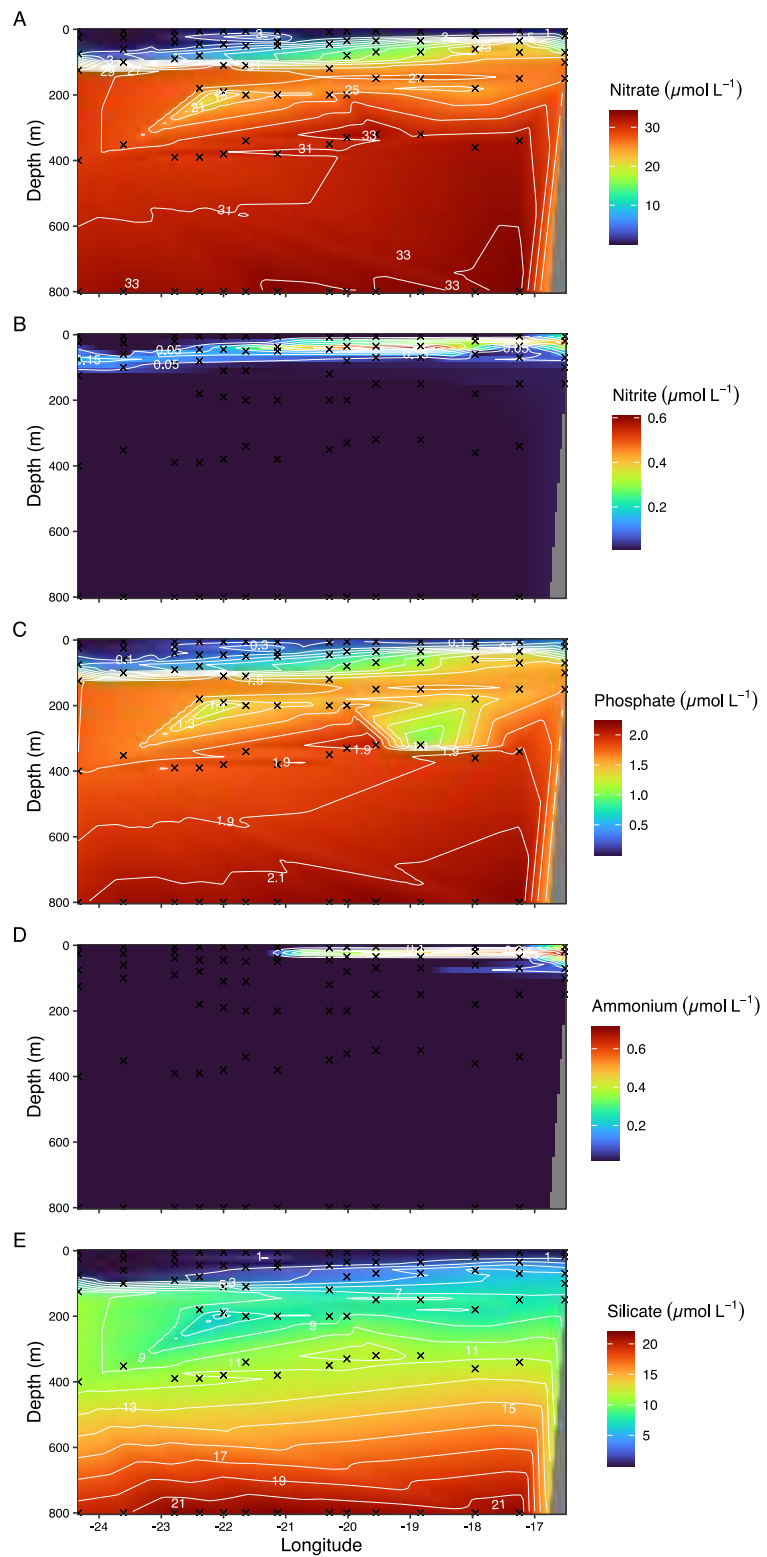
Microorganisms are the engines that drive biogeochemical cycles (Falkowski et al., 2008). Still, a plethora of natural bacteria and archaea escape any cultivation attempt and therefore their contribution to biogeochemical cycles remains an enigma. Fortunately, rapid advances in culture-independent analyses of microorganisms by using high-throughput sequencing of DNA and RNA allow studying natural microbial assemblages without the need to culture them. These analyses showed that natural microorganisms are phylogenetically and metabolically diverse (Sunagawa et al., 2015; Salazar and Sunagawa, 2017; Parks et al., 2018; Salazar et al., 2019) and actively involved in the cycling of elements (Satinsky et al., 2017; Pontiller et al., 2020; Pontiller et al., 2021). To determine the community composition and functioning of bacteria and archaea inside and around a mesoscale eddy, we collected and filtered water from the upper 1500 m onboard and stored the samples at -80°C . All of the samples will be shipped to the home laboratory where DNA and RNA will be extracted. To assess the bacterioplankton community composition, we will extract total DNA using the DNeasy PowerWater Kit (Qiagen, USA) and subsequently amplify the V4 and V5 hypervariable region of the ribosomal 16S rDNA gene using the primers pairs 515F-Y and 926R (Parada et al., 2016). The resulting 16S amplicons will be sequenced on a MiSeq platform (Illumina, USA) to generate 2 x 300 bp paired-end reads. To study the functional gene expression of bacteria and archaea inside and outside the eddy, we will extract total RNA using the RNeasy Mini Kit (Qiagen, USA) according to (Poretsky et al., 2009) as described in (Pontiller et al., 2020). Messenger RNA will be sequenced on a NovaSeq 6000 platform (Illumina, USA). Moreover, we collected samples for flow cytometry to determine the abundance, distribution, and community structure of pico- and nanophytoplankton as well as bacteria and viruses. These samples were fixed onboard, flash-frozen, and stored at -80°C . We'll transport these samples together with samples for genomic analyses on dry ice to the home laboratory at GEOMAR.

Water column nutrient and oxygen concentrations

Water samples for nutrient analysis and oxygen were obtained from 10 L Niskin bottles mounted to a CTD water sampling rosette. Water samples for oxygen and nutrients were taken immediately after retrieval of the CTD to minimize sampling artifacts and the risk of contamination. In total, 169 nutrient samples (in replicates) were sampled indicated with "O₂ & nutrients" in the station list (Table 12.1). The samples were stored in a fridge until further analysis within 24 hours after sampling. The concentrations of nitrate (NO_3^-), nitrite (NO_2^-), phosphate (PO_4^{3-}), and dissolved silica ($\text{Si}(\text{OH})_4$) were measured onboard according to (Grasshof et al., 1999) using a QuAatro autoanalyzer (Seal Analytical) with a detection limit of $1 \mu\text{mol L}^{-1}$ and analytical precision of 1%, $0.1 \mu\text{mol L}^{-1}$ (2%), $0.05 \mu\text{mol L}^{-1}$ (2%), and $0.24 \mu\text{mol L}^{-1}$, respectively.

In addition, ammonium (NH_4^+) was measured fluorometrically with the autoanalyzer using the ortho-phthalaldehyde (OPA) reagent with a detection limit of $1 \mu\text{mol L}^{-1}$ and analytical precision of 5% following. Oxygen concentrations were determined from water samples using Winkler titration of dissolved oxygen. Subsamples were filled in 66 mL glass bottles (Wheaton), which were rinsed with at least three times the bottle volume to ensure air-bubble-free samples. Subsequently, 1 mL of each of the two fixation solutions (NaI/NaOH and MnCl_2) was added using high precision bottle-top dispenser (0.4-2.0 mL, Ceramus classic, Hirschmann) to fix the oxygen. Finally, the samples were stored in the dark until titration with thiosulfate solution within the Wheaton bottles using a 5 mL Burette Metrohm 876 Dosimat Plus Titration unit. As already outlined in section 5.1 for CTD profiles, discrete water samples for nutrient analyses were visualized from S1 ($17^\circ 59.996' \text{ N}$, $24^\circ 20.006' \text{ W}$) to S11 ($18^\circ 10.249' \text{ N}$, $16^\circ 30.852' \text{ W}$), including the eddy (center at $17^\circ 32.960' \text{ N}$, $22^\circ 00.017' \text{ W}$), consisting of 15 CTD profiles. In general, nitrate, phosphate, and silicate concentrations increased with depth. Interestingly, in the eddy core, we found that nitrate, phosphate, and silicate concentrations between 200 and 400 m depth were slightly lower than the surrounding (Fig. 5.2 A, C, and E). Nitrite concentrations were highest in the upper 100 m, increasing towards the coast of Mauritanian (Fig. 5.2 B). Ammonium concentrations were generally low, often below the detection limit of the instrument, and increased towards the coast of Mauretania (Fig. 5.2 D).

Fig. 5.2 CTD section along the W-S transect including the eddy center (17° 32.960' N, 22° 00.017' W). From top to bottom panel: (A) nitrate (NO_3^-), (B) nitrite (NO_2^-), (C) phosphate (PO_4^{3-}), (D) ammonium (NH_4^+), and (E) dissolved silica (SiO_2). Crosses indicate sampling points. Data is shown for the upper 800 m (but available to depths of ~3000 m).



5.2 Water Column Biology

(H. J. Hoving, N. Hansen)

Background

The mesopelagic zone extends from 200 to 100 m depth. Many mesopelagic organisms migrate to the sea surface during the night to profit from the high productivity and hide in the darker, deeper mesopelagic zone during the day to avoid visual predators. By doing so, they contribute to the active flux of the biological carbon pump and transport organic carbon from the sea surface to deeper layers (*i.e.* the mesopelagic migration pump). Quantifying the role and biomass of mesopelagic organisms is very important for integrative understanding of the biological carbon pump. The diversity, abundance and biomass of the mesopelagic community is not the same in all ocean regions but may vary in respect to the sea surface primary productivity. For example, upwelling areas and mesoscale eddies, regions with increasing sea surface productivity, show a dominance of filter and flux feeders that exploit the increasing downwards flux of particulate matter. During M182, we were interested in the variability in diversity, abundance, and biomass of pelagic zooplankton along a west (oligotrophic, low sea surface productivity) to east (eutrophic, high sea surface productivity) transect, in and outside mesoscale eddies, and between day and night. Historically, zooplankton communities were studied with nets but the recent applications of *in situ* observations have revealed a poorly known gelatinous food web. This illustrates that every instrument that is deployed in the ocean has its advantages and disadvantages. Another example is that the use of acoustics can show biomass aggregations but is unable to show high taxonomic resolution or species associations. During M182, we applied a combination of nets, acoustics, observational tools, and water and sediment sampling to quantify diversity, distribution, abundance of pelagic organisms and their potential role in transporting carbon through the water column down to the sea floor (*i.e.* benthic-pelagic coupling).

HYDROBIUS Maxi MultiNet

With the HYDROBIUS opening and closing net, Maxi MultiNet (335 μm), we sampled 9 discrete depths from 0 m to 1000 m at 9 stations during day (4 stations) and night (5 stations). During the cruise the flowmeters did not work and one of the four support cables from the net frame to the frame that holds the cod-ends broke. The broken cable was replaced by a new cable. We fixed the zooplankton samples in Formaldehyde (4%) in 500 ml Kautex bottles for later analysis in the GEOMAR Helmholtz Centre for Ocean Research Kiel laboratories. There, we identify the organisms to the lowest possible taxonomic level, and measure and count the individuals. The measurements will give us a verification for the size and biomass measurements that we will obtain with the video data (see below). We will compare vertical distribution, abundance, and diversity data between stations along a west to east productivity gradient (Fig. 5.2) and also between day and night. We caught krill and other pelagic crustaceans, jellyfish, and mesopelagic fish with the multinet. A first inspection of our multinet samples shows a clear difference between day and night tows. The collected multinet data are part of the Ph.D. thesis of Nis Hansen and of peer-reviewed scientific publications.

Stereo Camera

We also deployed a novel stereo camera system during horizontal video transects. The two cameras were Ximea MX245CG-SY-X2G2-FL built with 24.5 MP Sony IMX540 sensors and DUW Distagon deep ocean metric 4.2mm f4 lenses developed by Carl Zeiss Jena GmbH in collaboration with the GEOMAR Helmholtz Centre for Ocean Research Kiel. The calibrated cameras were mounted on the XOFOS frame and had a fixed tilted inwards angle of 18°. We performed horizontal tows at 1 knot (0.51 m s⁻¹) of 13 minutes at up to 14 individual depths between 0 m and 1500 m. Depth was monitored via CTD and ADCP allowed measurements of current speed. We obtained two synchronized videos both with a 4k by 4k resolution at 25 fps for each transect. We performed stereo camera deployments at 10 stations during day (4 stations) and night (6 stations) and collected over 30 hours of footage. This is the first field-collected footage from this camera. We will calculate the sampled water volume to determine abundance using ADCP data. Unfortunately, the ADCP was not working for the last two dives.

From the live preview on board, we already saw more gelatinous fauna than in our multinet samples. Preliminary comparison between day and night transects showed a clear difference in observed fauna, similar to the multinet. At GEOMAR Helmholtz Centre for Ocean Science Kiel we will process the data from the stereo camera using computer vision and photogrammetry methods in order to support detection, to characterize size, and potentially some deformation properties. We will annotate (identify the organisms in our footage) the video footage and link distribution, abundance and diversity to environmental parameters that we obtained from a CTD attached to the XOFOS frame. At the third dive (M182_85) the CTD did not work for the depths 500m, 700m, and 900m and for the depth 25m at the fourth dive (M182_89). Via triangulation of the stereo footage (Fig. 5.3) and allometric equations, the size and volume of each organisms (> 1 cm) can be quantified. For many gelatinous organisms, their properties will be quantified for the first time. Examples of observed gelatinous fauna include *Vampyroctena* sp. (Fig. 5.4A), which was only recently described and for which we provide one of the first *in situ* observations; *Kiyohimea usagi* (Fig. 5.4B), a large ctenophore that was only recently observed for the first time in the Atlantic Ocean; *Solmissus* sp. (Fig. 5.4C), which occurred throughout the water column and we observed repeatedly; *Atolla wyvillei* (Fig. 5.4D), a common crown jelly that is abundant in the mesopelagic and which we also caught in the multinet; the abundant epipelagic ctenophore *Cestum veneris* (Fig. 5.4E); and *Praya* sp. (Fig. 5.4F), which is a colonial cnidarian that can grow up to more than 30 m. We will compare vertical distribution, abundance, and diversity data between stations and between day and night along a west to east productivity gradient. The collected footage from the stereo camera is part of the Ph.D. thesis of Nis Hansen and of peer-reviewed scientific publications. Sampling and station tables can be found in the appendix (12.2 Water Column Biology).

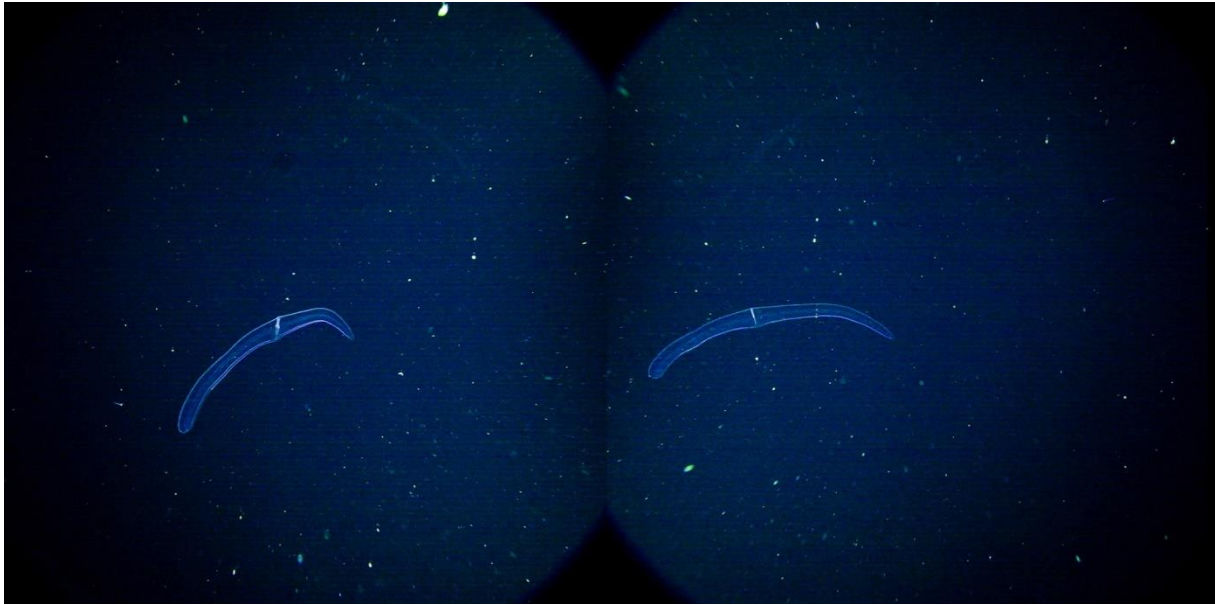


Fig. 5.3 Stereo footage of *Cestum veneris* from the left and right camera. Via the disparity between the left and right camera, the position of *C. veneris* in the three dimensions can be determined and its size and volume quantified.

eDNA

We sampled eDNA at 3 stations by filtering 2 liters of water in triplicates (3 filters) each at the depths 900m, 700m, 500m, 400, 250m, 160, 100m, 65m, and 25m. At the fourth station we sampled triplicates each at the depths 1500m, 800m, 380m, 180m, 82m, and 52m, and at the last station we sampled one filter at 1500m and one at 800m. We took controls (MilliQ water) at each station except for the last. We sampled a total of 105 eDNA Sterivex™ filters from CTD water of 5 stations. We will apply DNA metabarcoding protocols to identify species that avoid towed instruments and that we do not see in pelagic video transect nor catch with the multinet (*e.g.* larger nekton such as cephalopods and fish). We will extract the DNA from the filters via standardized extraction kits, then perform polymerase chain reactions (PCRs) to amplify the DNA region of interest. The amplified DNA will be sequenced via Next Generation Illumina Sequencing. Furthermore, we also sampled sediment from the upper 1 cm of cores taken with the TV Multicorer at 7 stations. With these samples we will also apply DNA metabarcoding to identify pelagic species that may play a role in benthic-pelagic coupling.

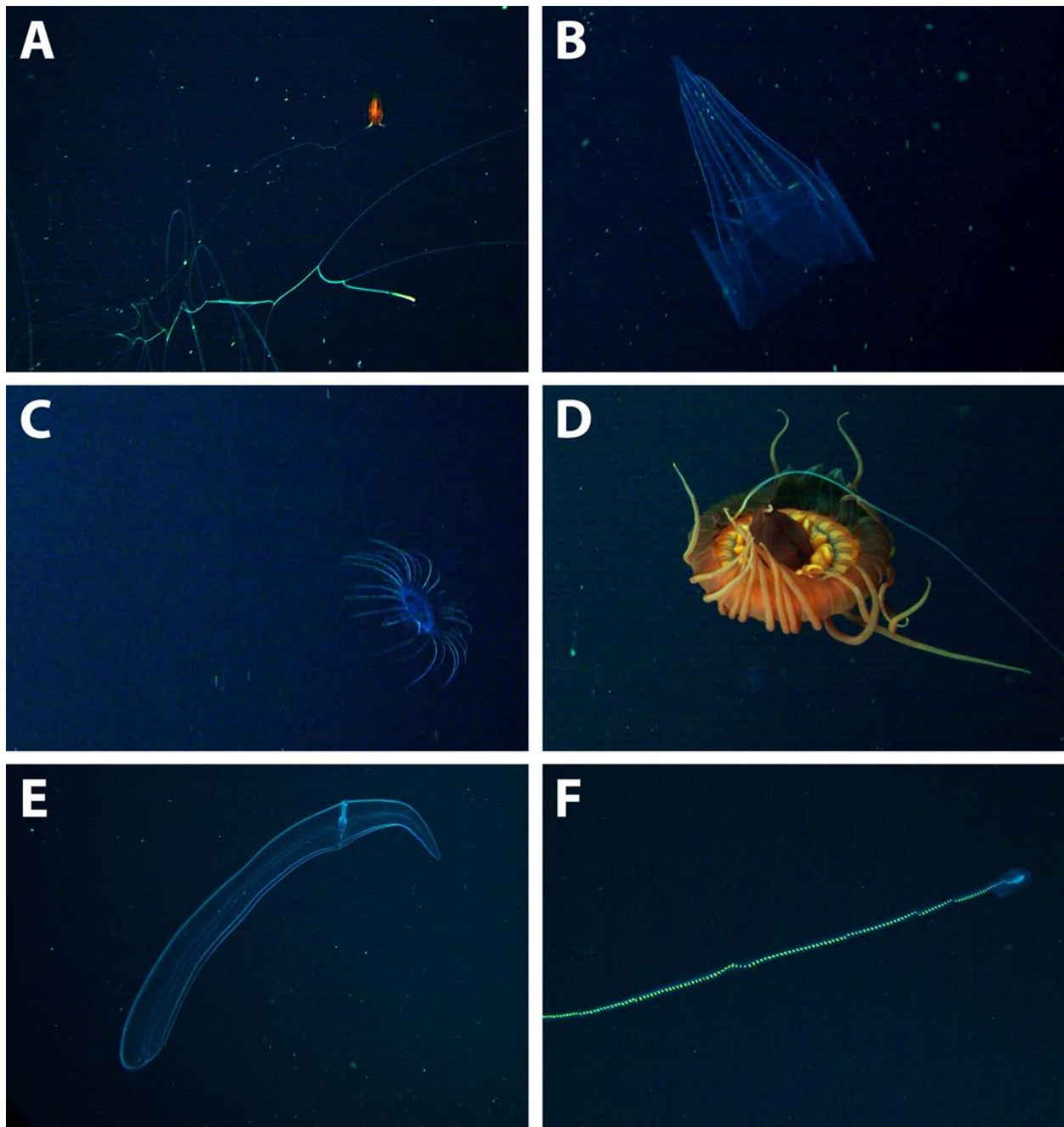


Fig. 5.4 Observations from horizontal pelagic tows with the stereo camera on the XOFOS frame. A) *Vampyroctena* sp., B) *Kiyohimea usagi*, C) *Solmissus* sp., D) *Atolla wyvillei*, E) *Cestum veneris*, F) *Praya* sp.

Echo Sounder

During almost all of our stations, we also had the Simrad EK80 single beam echo sounder running at 70 kHz and an opening angle of 18°. With the acoustic data we will infer the scatter layer and its biomass in the upper 300 m and to compared this with our samples, observations, and biomass estimates. During the cruise we repeatedly documented the diel vertical migration to the sea surface and back to the mesopelagic zone via acoustics (Fig. 5.5). The acoustic backscatter data are part of the Ph.D. thesis of Nis Hansen and of peer-reviewed scientific publications.

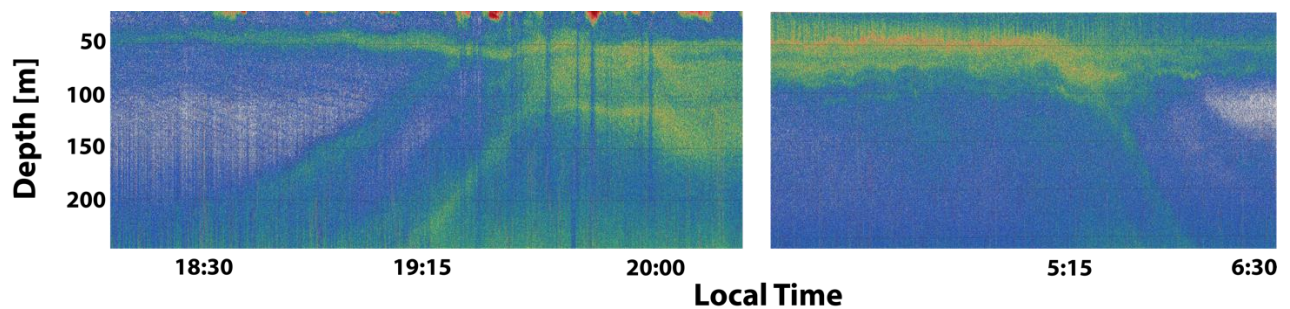


Fig. 5.5 Acoustic backscatter profile from the 06.06.2022. Vertical migration to the sea surface occurred in two distinct pulses, starting at 18:30 and 19:15 (-1:00 UTC) from below 200 m. Vertical migration to the mesopelagic zone occurred in one pulse starting at 5:15 (- 1:00 UTC).

5.3 Benthic Biogeochemistry

(A. Dale, P.-C. Chuang, B.Domeyer, T.Spiegel, R. Surberg)

Objectives

The porewater composition of surface sediments was investigated on the Cape Verde Terrace and eastwards to the oxygen-deficient waters offshore Mauritania. The main aim was to characterize and quantify sediment diagenetic processes, organic carbon burial rates and carbon burial efficiencies at the sites where the deep-sea rover and BIGO lander were deployed, and to further the general understanding of how carbon turnover is affected by seafloor topography. Specific emphasis was placed on the biogeochemical cycling and distribution of redox sensitive elements such as N, P and Fe and their relation to benthic oxygen respiration rates. Sampling method and tables can be found in the appendix (12.3 Benthic Biogeochemistry).

Onboard Results

Examples of sediment porewater geochemistry from the two westernmost sites E1 and E2 are compared in Fig. 5.6. The MUC device recovered the uppermost 20 – 30 cm of sediments, whereas the GC recovered 280 cm at E1 and 460 cm at E2, presumably due to differences in sediment porosity and particle grain size. The differences in the distributions of dissolved NO_3^- , Fe^{2+} and NH_4^+ are striking. At E1, NO_3^- was measurable down to the bottom of the GC whereas NO_3^- disappeared by 70 cm in the GC. Being closer to the mainland, E2 most probably receives a greater amount of organic carbon from the water column than E1. This is further evidenced by the higher concentrations of H_4SiO_4 at E2. The degradation of organic material as it becomes progressively buried in the sediment contributes to greater respiration rates of NO_3^- by denitrifying organisms at E2. The MUC data show that NO_3^- starts to decrease below 5 cm in MUC 6,7, and 8, whereas at E1 NO_3^- remains high throughout the top 20 cm due to lower microbial respiration rates. MUC 9 at E1 is an exception. Taken from the top of a small hill (ca. 300 m above the abyssal plain), the NO_3^- in this core decreases much more rapidly. Further work on the particulate material will help to understand the reasons for this extensive decrease. Overall, the MUC data at each site show a high degree of similarity, with only relatively minor differences between each core, especially for E1. The MUC data are also

nearly identical to data recovered during an earlier cruise M156 to the same locations (Fig. 5.6).

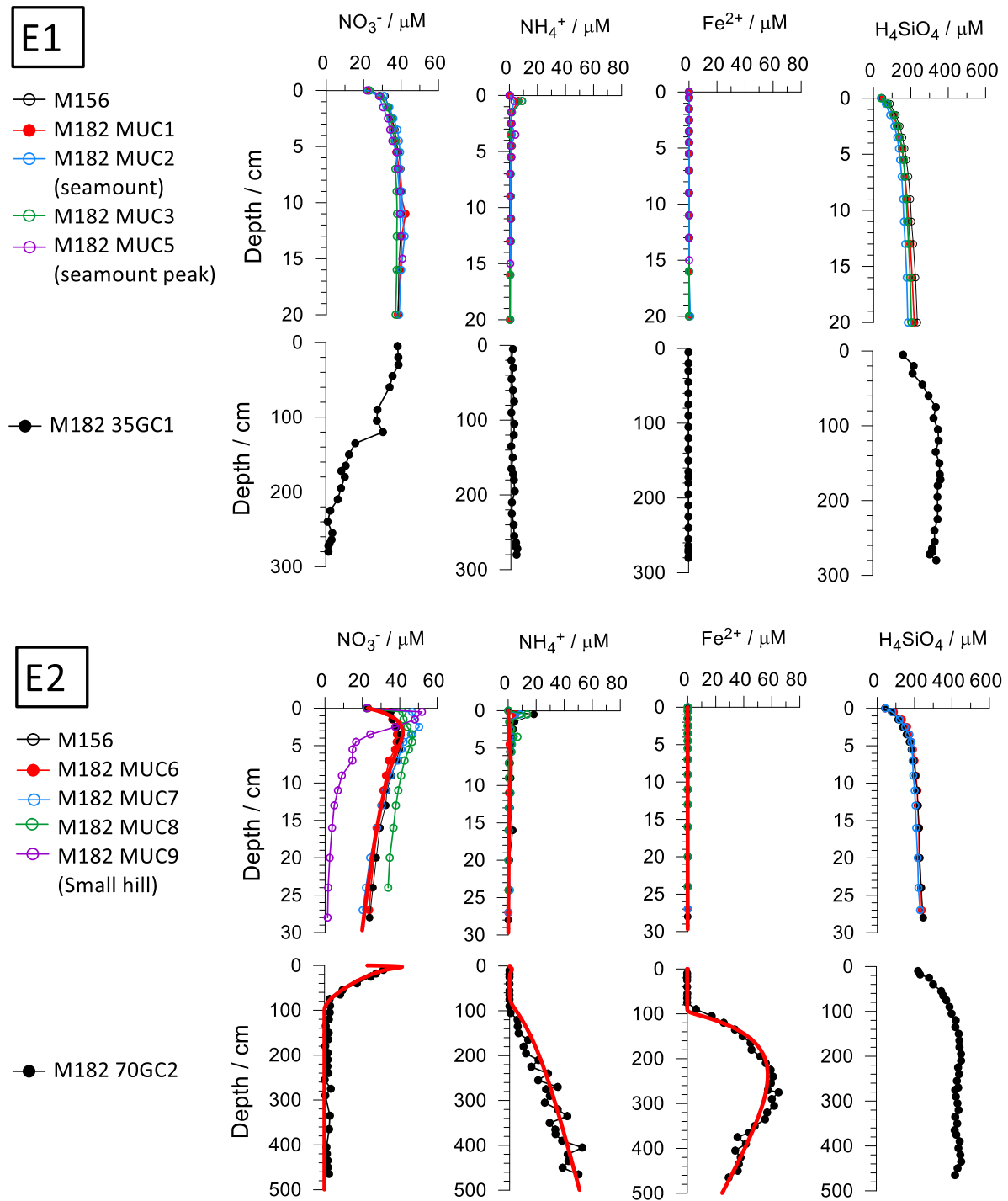


Fig. 5.6 Measured (symbols) concentration profiles of selected porewater constituents in sediments at sites E1 and E2. The upper panels at each site correspond to data recovered with the MUC, whilst the lower panels are GC data. The red curves for E2 show preliminary model results.

At site E2, concentrations of dissolved Fe^{2+} and NH_4^+ begin to increase once NO_3^- is exhausted. The vertical spatial separation of dissolved NO_3^- and Fe^{2+} in the porewater strongly indicates

that Fe^{2+} is rapidly oxidized by NO_3^- , potentially coupled to denitrification and the formation of iron (oxy)hydroxide mineral phases (Dhakar and Burdige, 1996; Scholz et al., 2016):



Modelling of the porewater data (e.g. Dale et al., 2019) supports this idea (Fig. 5.6, red curves), although these model results were generated on board and are very preliminary. Similarly, the appearance of NH_4^+ after the depletion of NO_3^- suggest that the former is oxidized anaerobically:



These data suggest that NO_3^- is an important electron acceptor for ferrous iron and ammonium oxidation in the deep-sea. As more data become available following further geochemical analysis at GEOMAR, we can expect to observe how this pattern is altered moving closer to land, and within sites with heterogeneous bottom topography such as site E4.

5.4 Benthic In situ-Fluxes

(S. Sommer, P. Chuan, A. Dale, B. Domeyer, P. Linke, G. Nolte, Timo Spiegel, R. Surberg, M. Türk)

Major goal was to quantify the magnitude and variability of material turnover in the sediments underneath the eddy passage and to possibly link the benthic carbon turnover to eddy induced enhanced export production at the sea surface. Furthermore, organic matter degradation along a zonal depth section at 18° N was investigated encompassing a depth range of 3700 m (E1) to the shelf (E5-SFB754) representing an area, which is known as major westward passage for mesoscale eddies that form off the coast of Mauritania.

In the typically oligotrophic deep-sea sediments organic carbon degradation is predominantly driven by using oxygen as the major electron acceptor. Hence major emphasis was placed on the measurement of total oxygen uptake (TOU) from which the organic carbon degradation can be calculated. At selected stations in addition to the TOU in situ fluxes of silicate, total alkalinity, DIC, NO_3^- , NO_2^- , NH_4^+ , and PO_4^{3-} across the sediment water interface were determined to study carbon cycling and that of associated major elements in deep-sea sediments off Cape Verde and Mauritania including the shelf station E5-SFB754, Table 12.6. At the stations E1 and E2 only oxygen consumption was measured due to the low reactivity of the sediments. Sampling and station tables can be found in the appendix (12.4 Benthic In situ-Fluxes).

Onboard Results

Deployment of the BIGO Lander

Apart from a few minor failures the BIGO Lander worked reliably providing predominantly oxygen fluxes and at the shallower stations nutrient fluxes (see Table 12.6). The analysis of the fluxes will be conducted at GEOMAR.

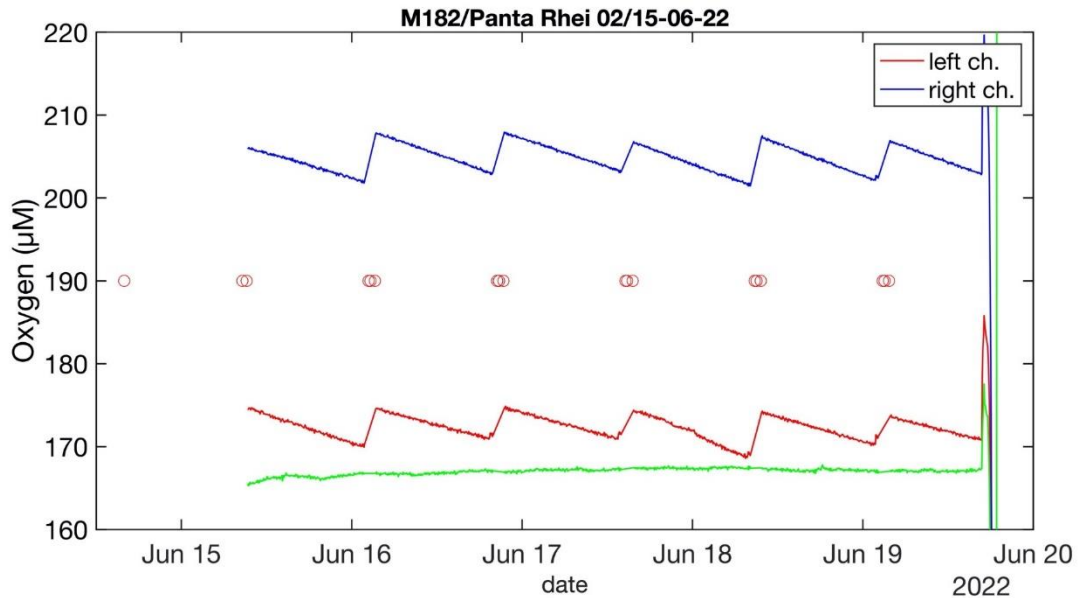


Fig. 5.7 Raw oxygen concentrations measured during deployment DSR-02 at the E2 working area in a water depth of 3294 m. Measurements in the left chamber (red line, sensor no. 1), the right chamber (blue line, sensor no. 7) and in the ambient bottom water time when (green line, sensor no. 4) are indicated. The measurements of the remaining 7 sensors are not shown for the sake of clarity. The red dots indicate the time when photos of the sediment were taken.

Deployment of the DSR Panta Rhei

For the first time the DSR Panta Rhei was successfully deployed in the deep-sea. As an example, results obtained of the deployment DSR-02 at the working area E2 is shown below, Fig. 5.7. The DSR performs repeated oxygen flux measurements at different locations. In between the flux measurements it very slowly moves forward a distance of 0.7 m. During the deployment DSR-02, 6 flux measurements in the left and the right chamber were conducted as can be recognized by the decreasing oxygen concentrations, Fig. 5.7. As already indicated by the similar slopes of the oxygen decline during the various flux measurements a high variability of oxygen consumption is not to expect. Preliminary total oxygen uptake (TOU) varied between -0.25 and -0.38 $\text{mmol m}^{-2} \text{d}^{-1}$. Average TOU was -0.28 $\text{mmol m}^{-2} \text{d}^{-1}$ ($n = 10$). During METEOR cruise M156 a TOU of -0.82 $\text{mmol m}^{-2} \text{d}^{-1}$ ($n = 1$) was measured using a BIGO.

It's a major advantage of the Rover that in comparison to Lander based flux measurements it enables flux measurements in absolutely undisturbed pristine sediments, potential deposits of e.g. fluffy detritus layers at the sediment surface will not become re-suspended. Fig. 5.8 shows the sediment surface at three different stages, i. before the chamber is inserted into the sediment, ii. the actual flux measurement when the chamber is inserted into the sea floor and iii. after the flux measurement when the chamber has been retrieved out of the sediment.



Fig. 5.8 Oblique view (camera 2) of (a) the sediment sampled by the left chamber of the DSR before the chamber is driven into the sediment, (b) during der flux measurement and (c) after the measurement when the chamber is retrieved out of the seafloor leaving a circular imprint in the sediment (white arrow). The black arrows indicate radial feeding tracks emanating from a small burrow entry hole.

By this the DSR allows to address the question of how variability of the TOU relate to the small-scale sea floor topography affecting deposition of particulate organic carbon and to the biological activity of in- and epifaunal benthic organisms as can be discerned from seafloor images. Many deep-sea animals are quite small and most of them live within the sediment. During feeding and burrowing, these animals form a variety of features called *lebensspuren*, defined as any sedimentary structure produced by a living organism (Dundas & Przeslawski, 2009). During deployment DSR-02 a predominantly flat barren seafloor with no conspicuous features was encountered. In two pictures a cluster of small sediment cones can be identified (Fig. 5.8), where the highest O₂ uptake was measured. At this site a small burrow entry hole with thick, radial feeding explorations from the central burrow was visible, which according to Dundas & Przeslawski, (2009) might be caused by echinurans or polychaetes. At other pictures ophiuroids and a vermiform organism is visible.

Environmental conditions during DSR-02 deployment

CTD based pressure measurements indicate a semi-diurnal tidal regime with periodicities of 12.1 and 6.0 hours, Fig. 5.9.

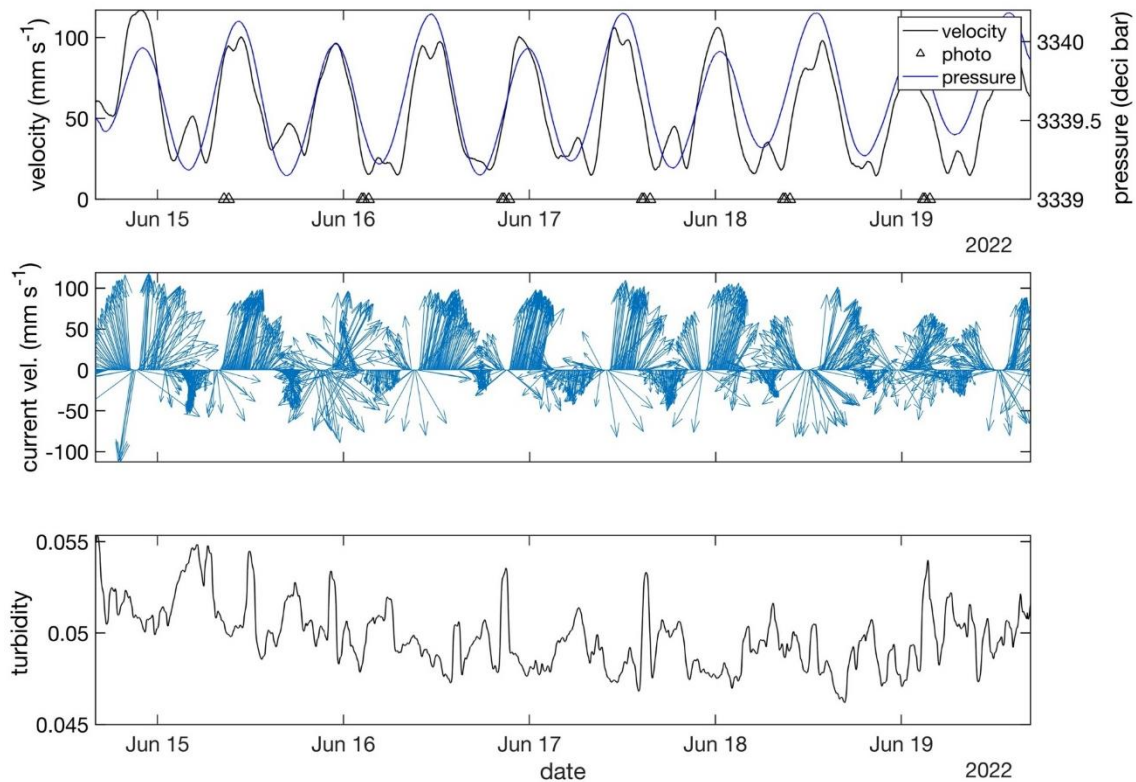


Fig. 5.9 Upper panel, current velocity and pressure measured during the DSR-02 deployment at E2; middle panel, current velocity and direction; lower panel, turbidity. Current velocity was sampled at a rate of 0.0033 Hz, pressure and turbidity were sampled at rate of 0.0667 Hz. All parameters were smoothed using a moving average over 1 hour. Triangles indicate when photos were taken.

Current velocity and current direction was related to tidal currents showing periodic distinct changes between strong northwards directed currents with a velocity of up to 10 cm s^{-1} and less pronounced southward directed currents. Current velocities and directions were averaged over the first 15 bins representing the first 30 m of the bottom boundary layer. The first bin was 4.19 m above the upward looking ADCP mounted at the upper side of the DSR. The heading of the Rover was about 30° . Turbidity was low, yet appeared to be generally increased during phases of slow southward directed currents. Major peaks of turbidity coincide with periods of Rover movements as is indicated by the temporal match between the triangles (times of photos taken and the Rover movement to the next site) and peaks of turbidity.

Long-term deployment of the DSR Panta Rhei-04

At the 03.07.2022 we finally deployed the Rover at E2 for its long-term stay at the sea floor until its recovery in January with RV MS Merian (MSM114). This site was selected based on three major criteria i. the consistency of the sediment must be suitable for the Rover movement, ii. it should not have a hummocky small scale topography or any major obstacles, and iii. to best-possibly decipher the effects of allochthonous input of particulate organic carbon on the deep-sea benthic carbon turnover, other effects on carbon deposition originating from larger scale sea floor topography (such as gulleys, major depression, hills) in interaction with the current regime should be minimal. Site selection was performed based on seafloor multi-beam bathymetrical mapping and visual seafloor inspection by the OFOS and AUV. Every 40 hours the Rover will perform oxygen flux measurements. Between each flux measurement the Rover

will move a distance of 0.7 m, hence during its entire deployment duration of 6 months the Rover hopefully will perform about 107 flux measurements in two benthic chambers and travels a distance of 85 m including the 10m distance the Rover moves after it has been placed at the seafloor. Fig. 5.10 shows the Rover several hours after it has been deployed during a survey with the GEOMAR AUV ABYSS. The tracks of its first movement away from the landing site can be easily recognized. Next to the Rover a DOS Lander was deployed for the same long-term period as the DSR to record physical properties, to perform time lapse imaging of the seafloor and to measure the particle flux using a sediment trap. We very much hope that the Rover and the Lander complete their mission successfully and look forward to their recovery in January 2023.

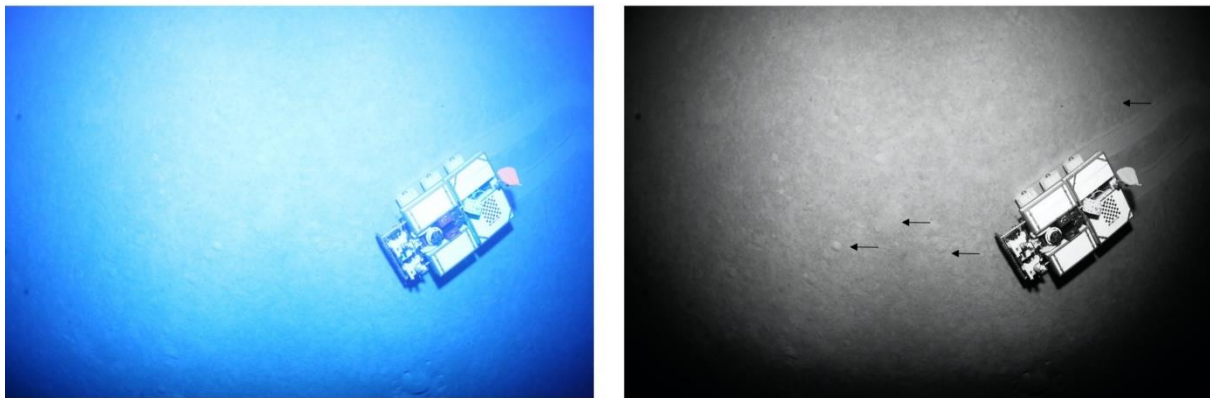


Fig. 5.10 Left panel, DSR Pantarhei as viewed from the AUV ABYSS flying over it in a distance of about 4 m; right panel, same image converted into black & white to enhance contrasts nicely showing details of the seafloor such as cones, irregular or circular arrangements of worm holes (arrows) as well as the tracks of the DSR. Photo AUV team.

Expected Results

We expect to strongly contribute to expand the data base of in situ benthic fluxes of the still largely under-sampled deep-sea. The data sets obtained during M182 and the previous cruise M156 will be combined to get insight into the carbon turnover of the deep-sea benthos along a zonal depth section at 18° N in an area where mesoscale eddies export higher surface water productivity into the open ocean. We set out the working hypothesis that the investigated area largely benefits from an intense pelagic-benthic coupling resulting in higher benthic carbon turnover and total oxygen uptake. We will address this hypothesis by the comparison of combined flux data base in comparison with the already existing data base for the North Atlantic.

Regarding the long-term Rover deployment at the working area E2, we hope to be able to clearly show the response of the deep-sea benthos to the enhanced carbon deposition during the passage of a productive eddy at the sea surface and to assess its implications for the deep-sea benthic ecosystem. As described above during the long-term deployment the Rover will make about 100 measurements of TOU in both benthic chambers, hence in case of a successful deployment about 200 flux measurements were conducted in variety of different sea floor features. Giving such a large data set, we hope that we can correlate variability of the benthic TOU to specific small scale sediment features

The Rover enlarges the highly limited availability of benthic vehicles for in situ biogeochemical measurements at the seafloor. It offers a wide range of application in a variety of benthic ecosystems and bears a high potential for the future investigation of benthic ecosystems.

5.5 Benthic Observations

(M. Kampmeier, J. Mohrmann, J. Greinert, A. K. Hinz, E. Fabrizius, G. Nolte)

XOFOS

Technical description can be found in the appendix (12.5 Benthic Observations).

Preliminary Results

Working area E1

The seafloor of E1 is rather flat with only few bioturbation mounts. The most abundant features are different types of feeding rosettes (small, messy, large) and thin holothurian trails. Just a few burrows form mounts larger than 15 cm.

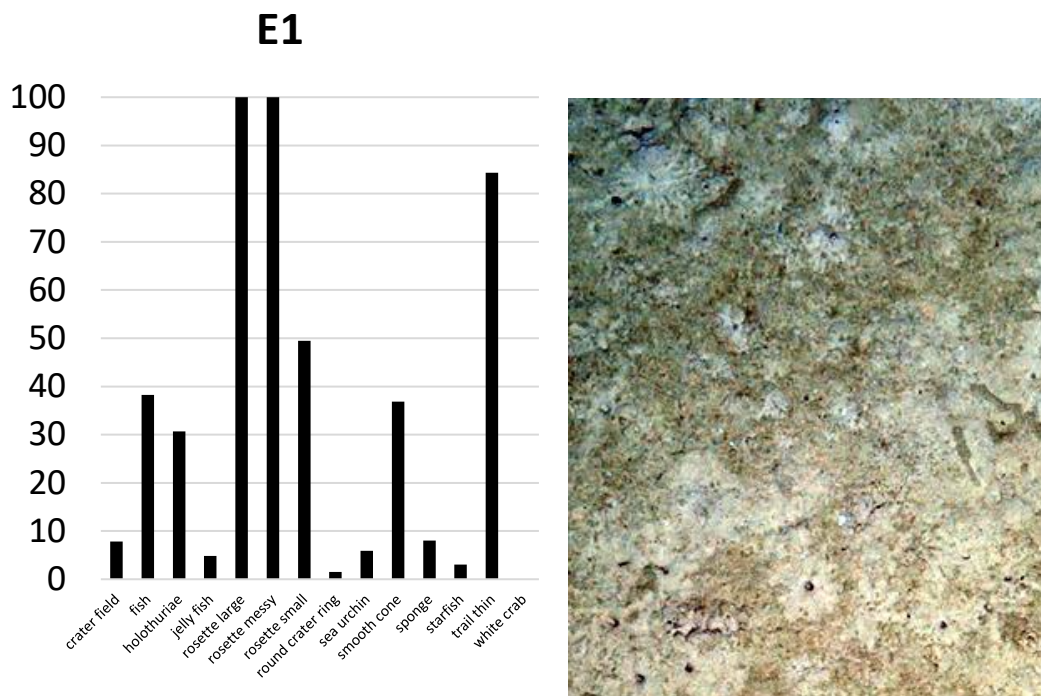


Fig. 5.11 Overview of annotated features in XOFOS videos. The annotations of all deep-sea areas (E1, E1 Hill E2, E3 CV and E4) have been normalized to percentages (100% = maximum of all annotations of the feature within all areas). Right side: Characteristic image of the seafloor from OIS showing small feedings rosettes and holothurian faecal casts.

Working area E1 Hill

The XOFOS profile in this area started on top of the hill plateau and went downslope. On a small-scale, the bathymetry was not visible, but the differences in benthic features to E1 are significant. Whereby the macro fauna like fish and holothurians are similar to E1, there are far

less feeding rosettes and a high number of starfishes. Besides, features of unknown origin can be observed: a number of sharp edged holes spread over the whole XOFOS track and a trail on the seafloor that looks like from a vehicle (Fig. 5.12).

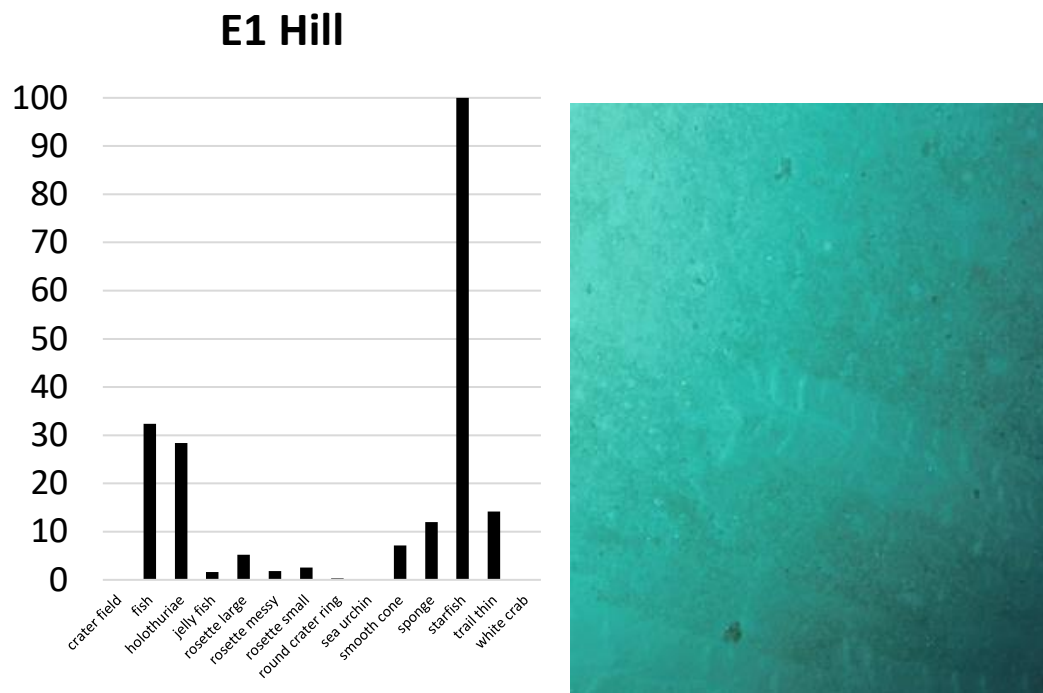


Fig. 5.12 Left side: Overview of annotated features in XOFOS videos. The annotations of all deep-sea areas (E1, E1 Hill E2, E3 CV and E4) have been normalized to percentages (100% = maximum of all annotations of the feature within all areas). Right side: Characteristic image of the seafloor from OIS showing a track of unknown origin.

Working area Eddy periphery NW

This area has one very characteristic feature: The round crater ring structures are dominant. Those ring-build structures typically have a diameter of ca 50 cm and are perfectly geometric. Besides that, feeding rosettes and macro fauna are quite abundant as well.

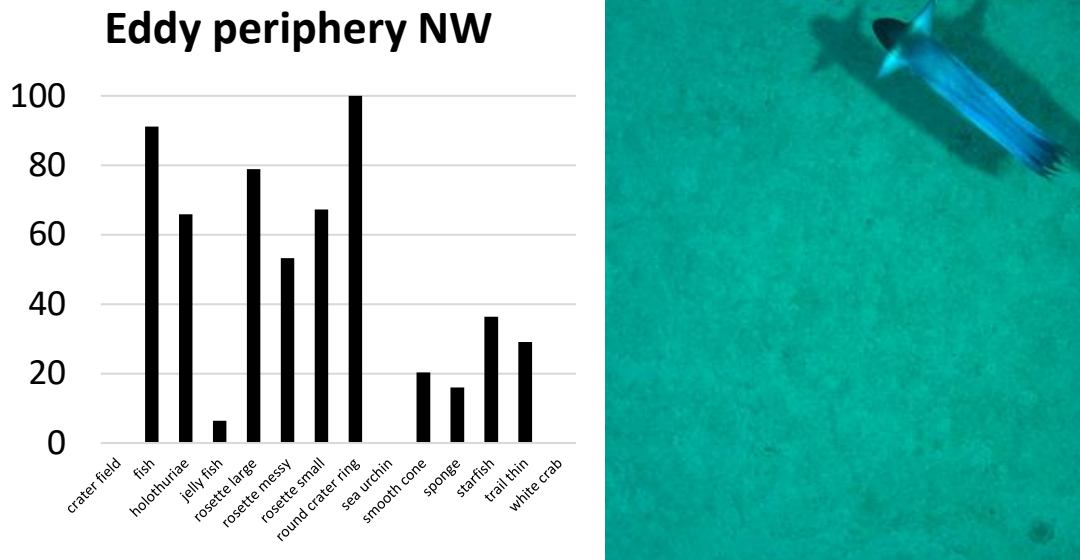


Fig. 5.13 Left side: Overview of annotated features in XOFOS videos. The annotations of all deep-sea areas (E1, E1 Hill E2, E3 CV and E4) have been normalized to percentages (100% = maximum of all annotations of the feature within all areas). Right side: Characteristic image of the seafloor from OIS showing an Octopus.

Working area E2

The seafloor in E2 is similar to the previous ones, except of the almost complete absence of round crater rings and sponges. On the other hand, small white crabs occur here.

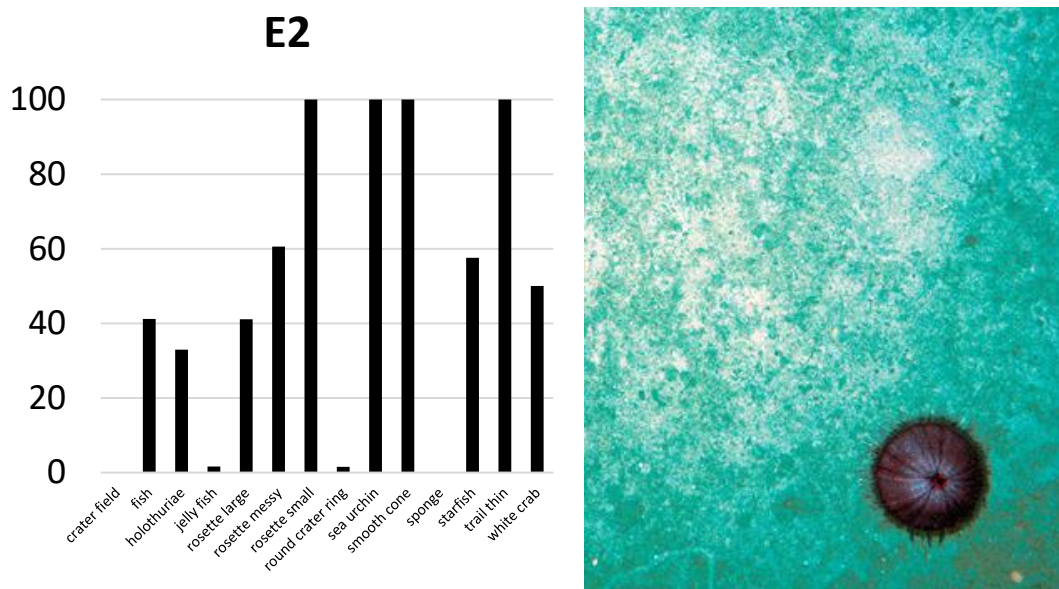


Fig. 5.14 Left side: Overview of annotated features in XOFOS videos. The annotations of all deep-sea areas (E1, E1 Hill E2, E3 CV and E4) have been normalized to percentages (100% = maximum of all annotations of the feature within all areas). Right side: Characteristic image of the seafloor from OIS showing a sea urchin on sediment with small feeding rosettes.

Working area Senghor Seamount

The Senghor Seamount differs extremely from all other locations. The XOFOS profile starts on the plateau in 80 m water depth and extends downhill until ca 250 m. Numerous brittle stars and spiral corals cover the seafloor. Schools of fish followed the XOFOS and make it impossible to generate a photomosaic from the data. On hard substrate grow sponges and corals and live different kinds of fish. Below the photic zone in around 110 m, the macro fauna abundance decreases and the seafloor looks like the deep seafloor: plain sediment with few bioturbation marks.

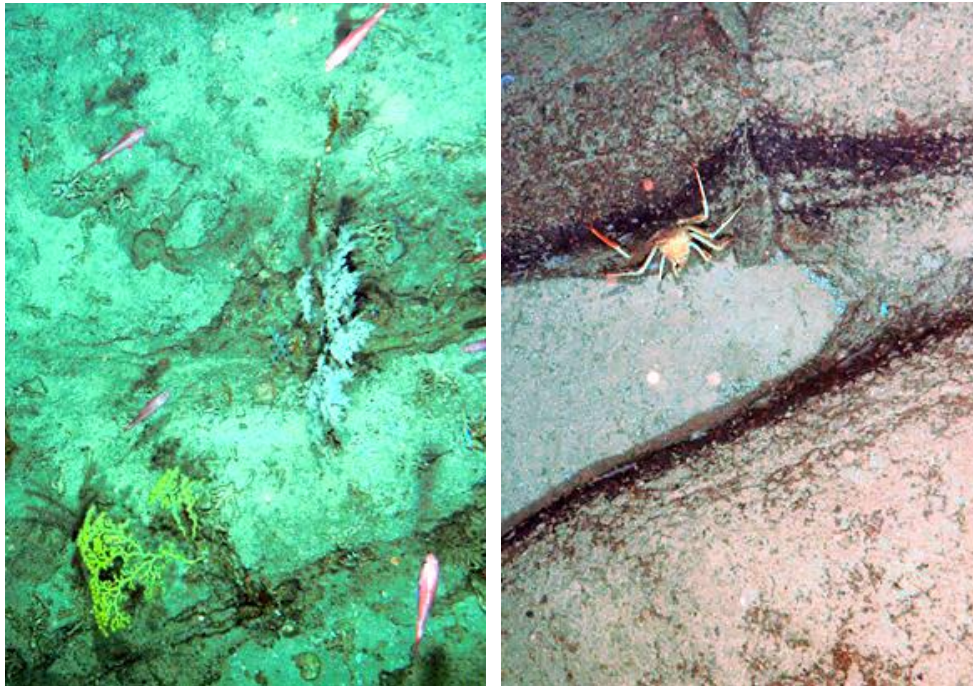


Fig. 5.15 Images from the OIS. Left: Yellow and white corals growing on hard substrate. Right: A crab is hiding in between rocks.

Working area E3 CV

This area resembles the previous deep-sea sites. The main difference is the size of bioturbation cones, which can reach roughly 20 cm height. Bright sediments give the impression that feeding structures might be still young. Several features do overlay each other and the benthic activity seems to be high.

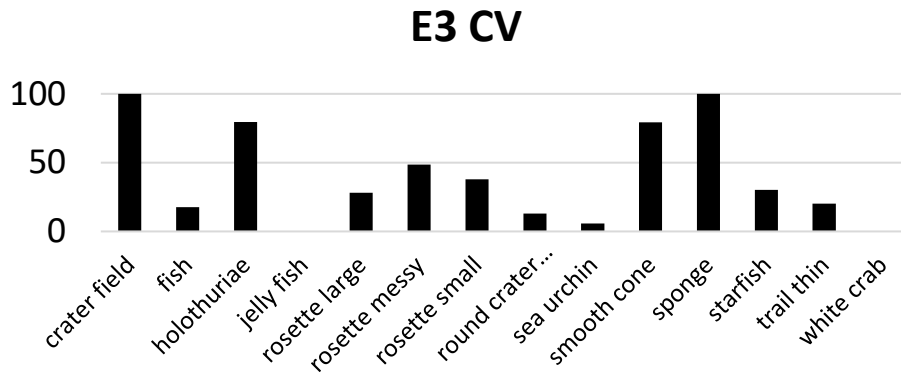


Fig. 5.16 Left side: Overview of annotated features in XOFOS videos. The annotations of all deep-sea areas (E1, E1 Hill E2, E3 CV and E4) have been normalized to percentages (100% = maximum of all annotations of the feature within all areas).

Working area E4

The seafloor morphology of this area is quite different to the other sites. It is not just plain but crisscrossed by channels, which lead around a 300 m high, diapiric mount. The first XOFOS profile went through one of the channels. White glass sponges grow on the steep channel edges and indicate higher current regimes. The channel bottom gives no hint of increased current velocities or recent sediment transport. Feeding structures in here seem to be stable and undisturbed. The second XOFOS dive started on top of the hill and went downslope, where the glass sponge density is high as well.

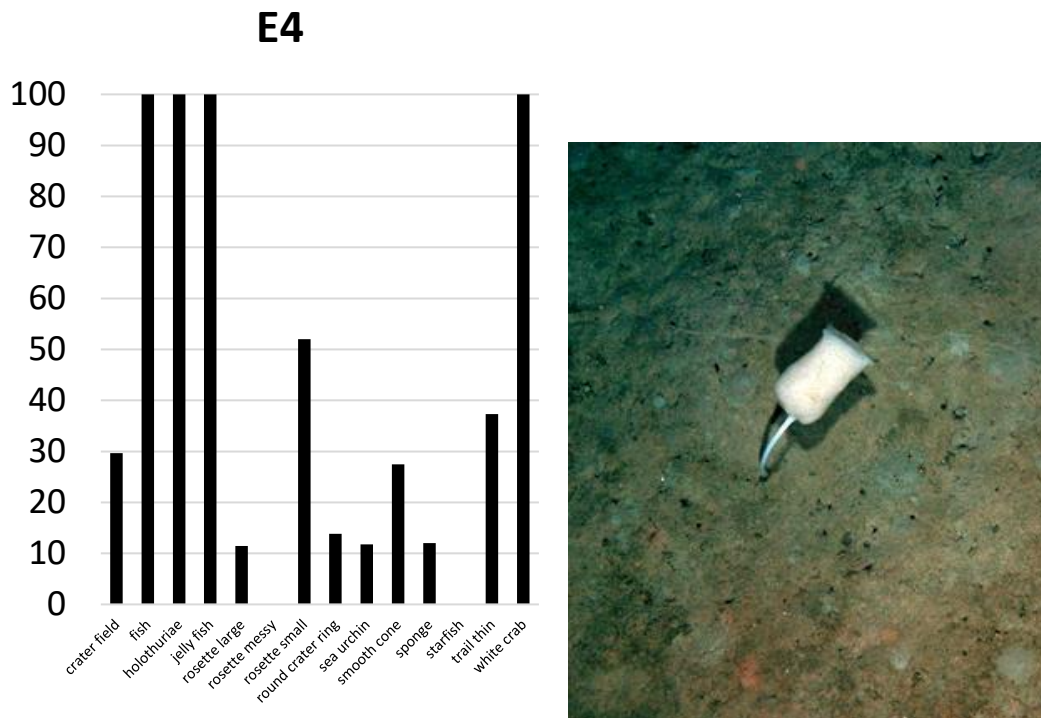


Fig. 5.17 Left side: Overview of annotated features in XOFOS videos. The annotations of all deep-sea areas (E1, E1 Hill E2, E3 CV and E4) have been normalized to percentages (100% = maximum of all annotations of the feature within all areas). Right side: Characteristic image of the seafloor from OIS showing a glass sponge.

Working area E5

The shallowest area is the coastal area E5. Only 13 NM off the Mauritanian coast, the water is influenced by increased particle concentrations and the visibility is rather low. Therefore, this area cannot be directly compared to the deep-sea areas. There are less pronounced bioturbation structures and more macro fauna, such as fish, starfish and crabs.



Fig. 5.18 Images from the OIS. Left: Different types of fish and an anemone. Right: Unknown flora or fauna on the seafloor. The sediment in both images is mixed with shells and gravel sized grains.

BBL-Lander

The Benthic Boundary Layer (BBL) lander was deployed for two times. The first deployment was done in the area E3 CV for 5 days (23-28th June 2022). Unfortunately did the flash of the OIS not work and no pictures were acquired. The second deployment was the long-term deployment in area E2. Therefore, it is equipped with a 300 kHz ADCP, a Seabird CTD, sediment trap from KUM and the OIS.

The cups of the sediment tarp were prepared with a formol solution, which is denser than the bottom water, which prevents it from spilling out of the cups.

Table 5.1 BBL settings for the long-term deployment.

Device	Start	Sampling interval
OIS Camera	03/07/2022 15:45	1 photo / hour
ADCP	03/07/2022 12:00	15 minutes
CTD	03/07/2022 12:00	15 minutes; 10/s
Sediment trap	Cup 1	1 cup / 9 days 18 hours

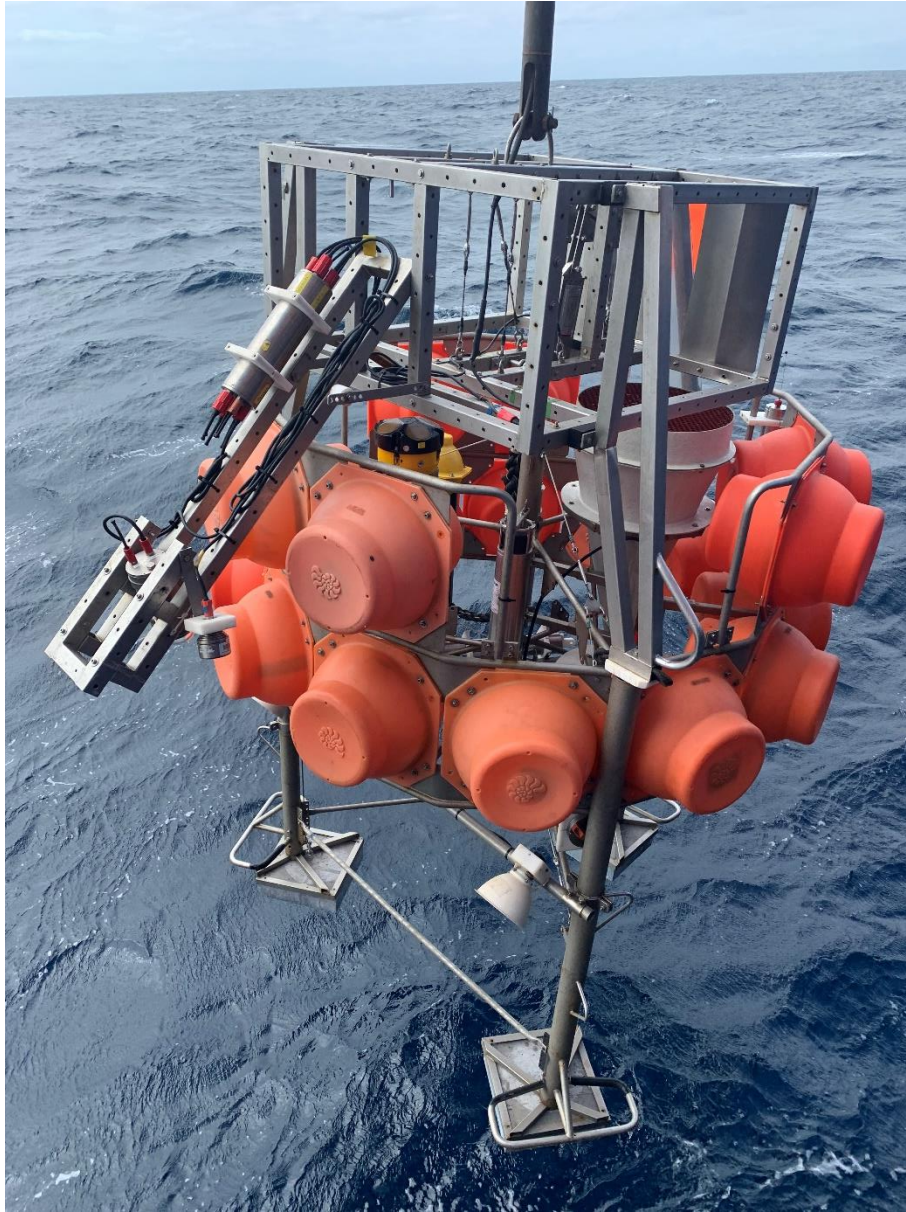


Fig. 5.19 BBL Lander is launched with a video guided launching system and is released just above the seafloor. For recovery the foot weights will be released via an acoustic signal and the positive buoyant lander will ascend (photo: P. Linke).

AUV Mapping

(T. Kurbjuhn, E. Wenzlaff, P.Striewski, D.Scheppukat, T. B. von See, K. Heger)

The Autonomous Underwater Vehicle (AUV) „ABYSS“ is a modular AUV designed to survey the ocean, combining geophysical studies of the seafloor with oceanographic investigations of the overlying water column (Fig. 5.20). The basic mission of ABYSS is deep-sea exploration, specifically in volcanically and tectonically active parts, such as mid-ocean ridges. With a maximum mission depth of 6000 meters, the AUV uses several technologies to map the seafloor accurately and determine its geological structure with applications from geology to biology to mineral exploration. Purchased in 2007, the AUV fulfilled many dives until 2020 and after a major water damage on its 355th dive the AUV was subject of a major restoration

at Woods Hole Oceanographic Institution. Since 2022 AUV Abyss is used again on research expeditions around the world.



Fig. 5.20 AUV Abyss on the searface.

The detailed AUV- and station description can be found in the appendix (12.5 Benthic Observations).

AUV GIRONA 500

Anton and Luise are reconfigurable autonomous underwater vehicle (AUV) of the type Girona 500. They are designed for a maximum operating depth of up to 500 m. The vehicle is composed of an aluminium frame which supports three torpedo-shaped hulls of 0.3 m in diameter and 1.5 m in length as well as other elements like the thrusters. This design offers a good hydrodynamic performance and a large space for housing the equipment while maintaining a compact size, which allows operating the vehicle from small boats.

AUV GIRONA500 dives

Due to a restriction in staff who is operating the AUVs, the number of dives which could be done on the cruise was limited. Operating the Gironas in the open sea without bottom lock of DVL requires a calm sea state and a good working USBL Positioning. The Evelogics USBL system which is mandatory for a safe operation, did not provide a good performance on the vessel. Therefore, the Gironas were only used in shallow water conditions. The detailed technical AUV- description can be found in the appendix (12.5 Benthic Observations).

Table 5.2 Overview of AUV GIRONA500 dives.

Station Number	Dive Number	Area	Sensors	Date	Mission Time	Distance In meter
97	Anton230	Senghor Seamount	Coramo Downlooking	16.06.2022	3:05	3725
165	233	E5	Coramo Downlooking	30.06.2022	6:07	7378

Anton 230 - 231

The area where the dive took place is located on the Senghor Seamount plateau. Before the AUV was deployed in the area, an XOFOS dive was conducted to determine a suitable location for the mission.

The goal was a photo survey of the top of the seamount. Anton 230 consists of 2 dives, due to starting problems dive 230 didn't make it to the bottom. Dive 231 was successful and brought a set of 3500 images back.

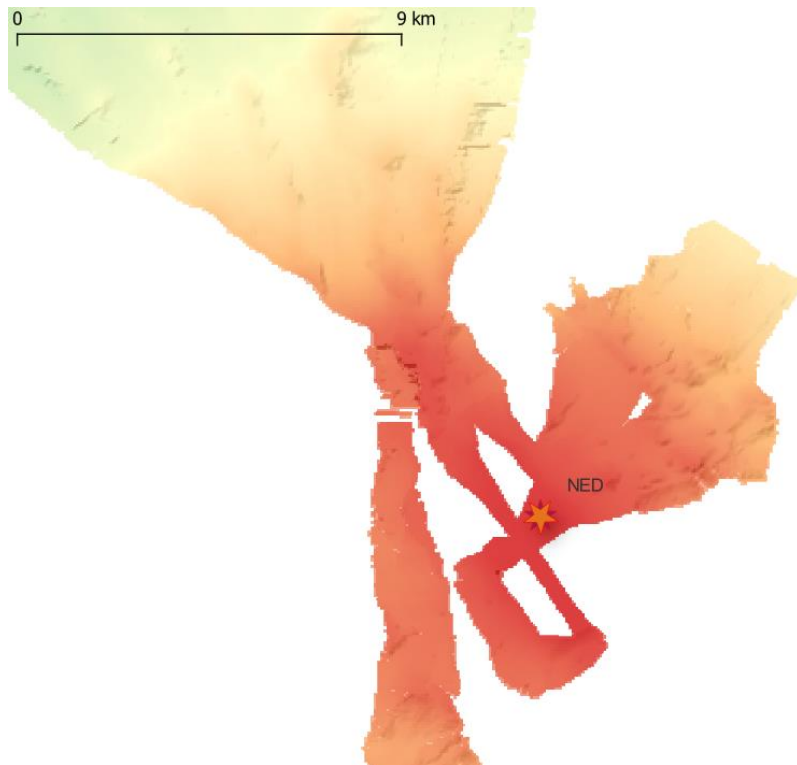


Fig. 5.21 Dive Area on Seamount.

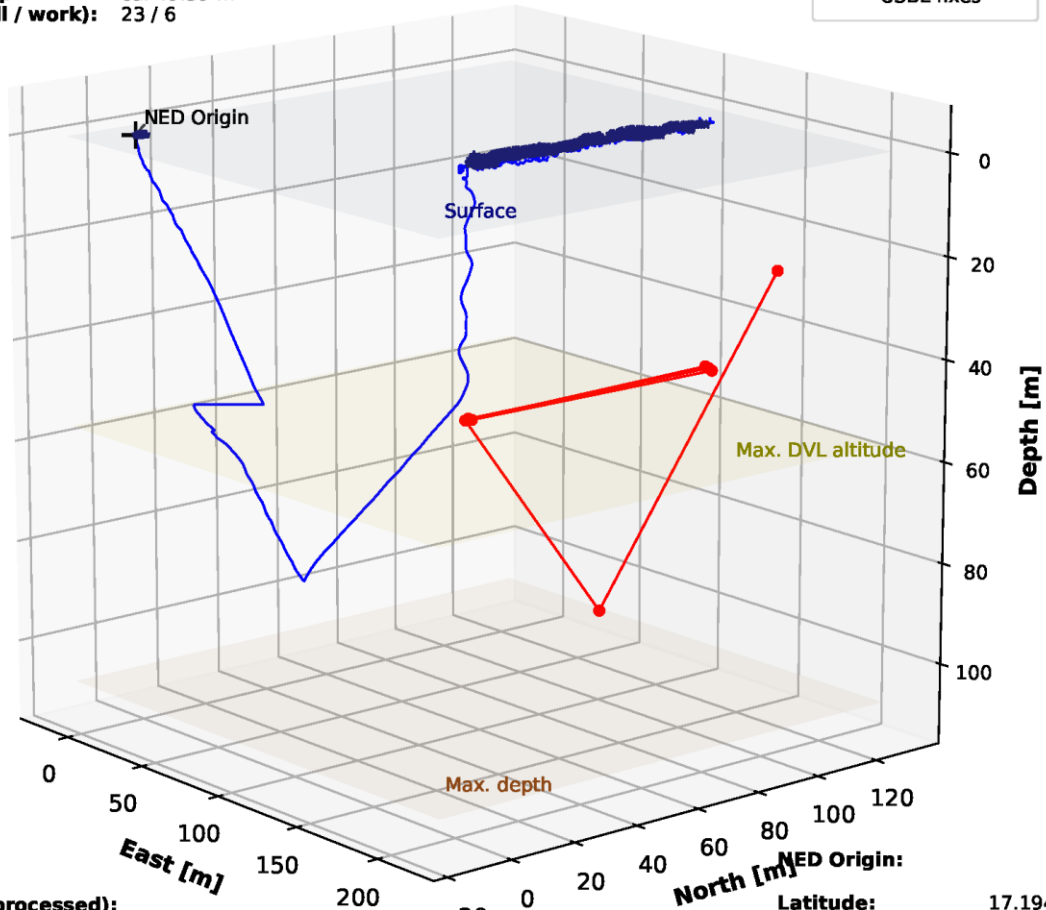
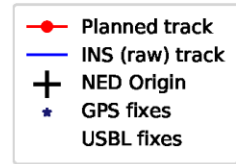
First Girona deployment on M182. Mission failed due to invalid mission parameters.

Mission started: 2022-06-16 12:56
Mission finished: 2022-06-16 13:12

Statistics (planned):

Overall length: 393.98 m
Overall duration: 00:17 hrs
Working area: 122.5 x 194.6 m = 23837.8 m²
Working depth: ca. 49.39 m
Sections (all / work): 23 / 6

Anton_230



Statistics (processed):
 Please provide Phins C3 INS log:
 1. Enable postprocessing log in iXBlue Phins C3 INS
 2. Open log in iXBlue DELPH software
 3. Run forward/backwards/smoothing processing
 4. Export 'primary navigation' to provided template

Note: All times are UTC

NED Origin:
Latitude: 17.19417°
Longitude: -21.95570°
GPS altitude: 30.70 m
Maximum depth: 107.94 m
Max DVL altitude: 51.13 m

Fig. 5.22 Anton 230 aborted dive.

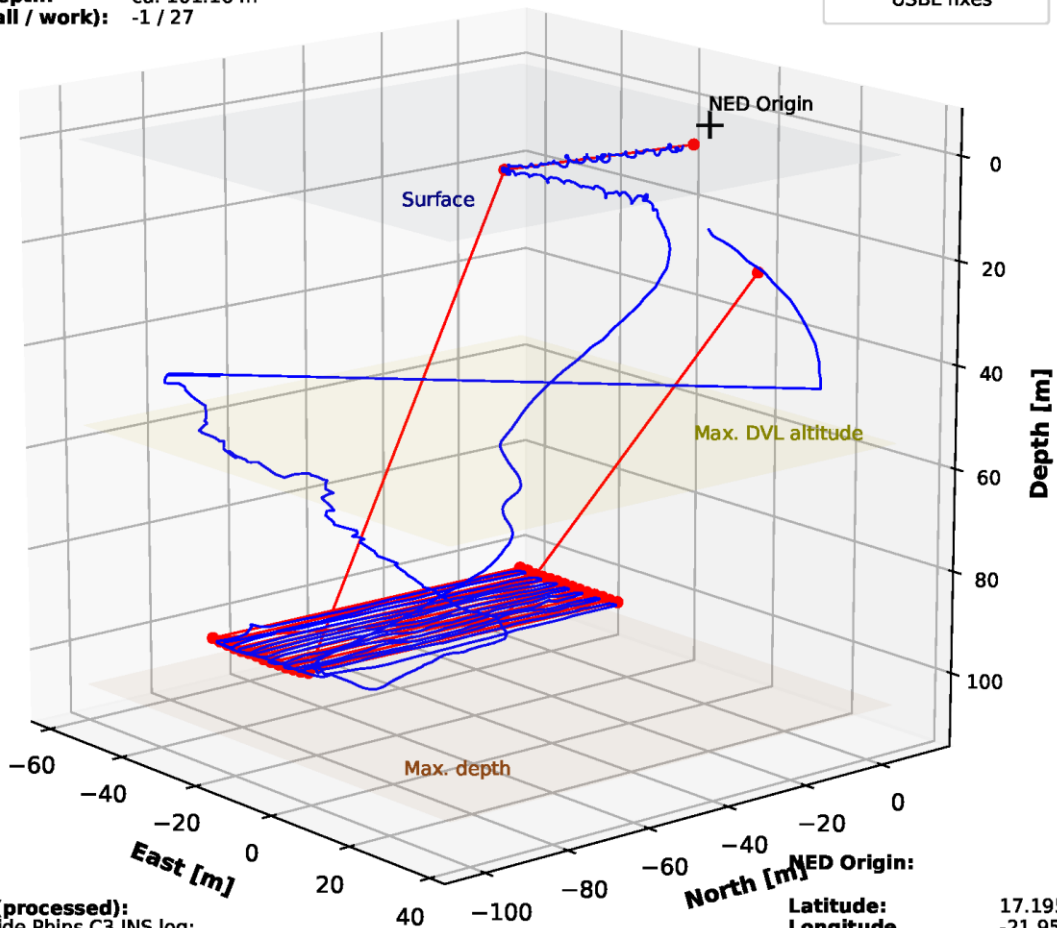
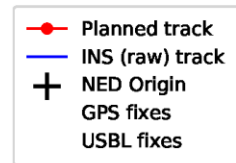
First Girona deployment on M182. Photo survey on top of seamount Senghor.

Mission started: 2022-06-16 13:40
Mission finished: 2022-06-16 14:38

Statistics (planned):

Overall length: 1375.22 m
Overall duration: 00:49 hrs
Working area: 80.0 x 70.0 m = 5596.3 m²
Working depth: ca. 101.16 m
Sections (all / work): -1 / 27

Anton_231



Statistics (processed):
 Please provide Phins C3 INS log:
 1. Enable postprocessing log in iXBlue Phins C3 INS
 2. Open log in iXBlue DELPH software
 3. Run forward/backwards/smoothing processing
 4. Export 'primary navigation' to provided template

Note: All times are UTC

NED Origin:
Latitude: 17.19523°
Longitude: -21.95403°
GPS altitude: 0.00 m
Maximum depth: 106.62 m
Max DVL altitude: 51.29 m

Fig. 5.23 Anton 231 Dive Summary.

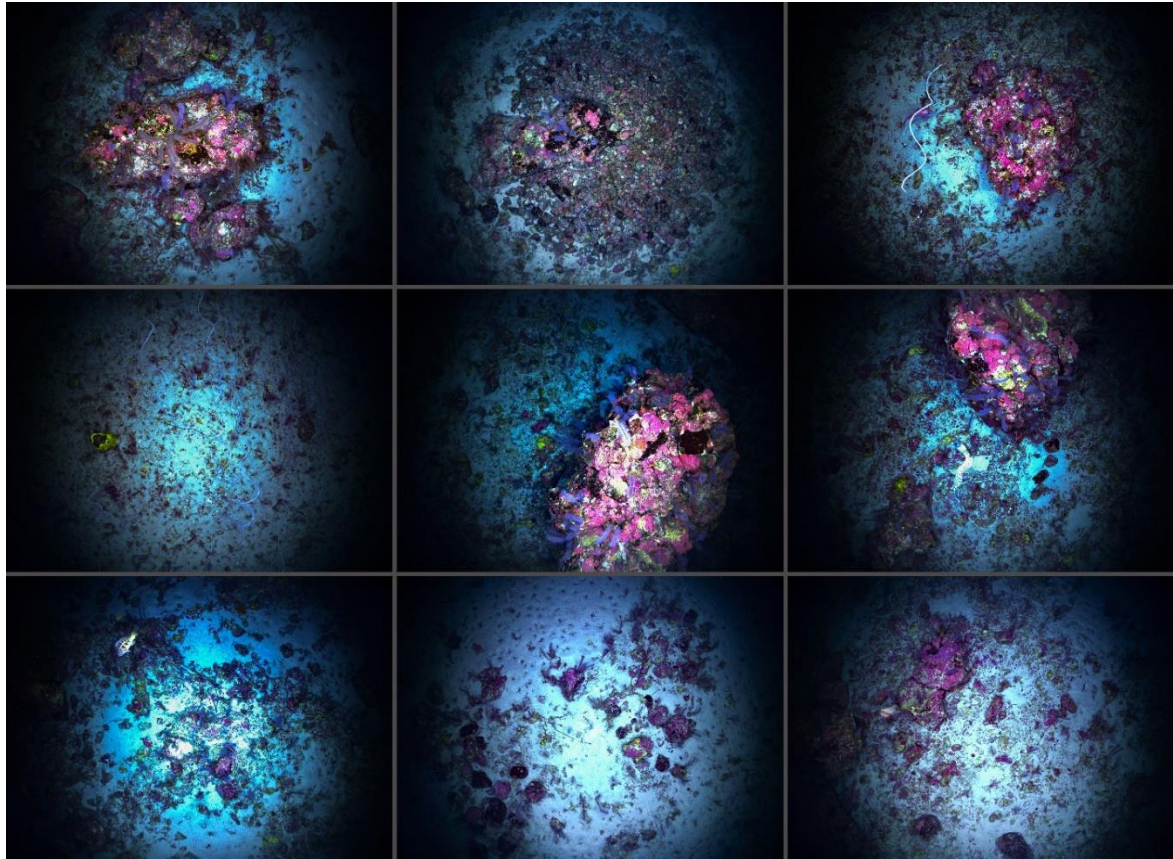


Fig. 5.24 Sample images from ANTON231.

Fig. 5.24 shows a sample set of images made by Anton on dive 231. The images were filtered and processed to a 3D photomosaic of the whole area (Fig. 5.25).

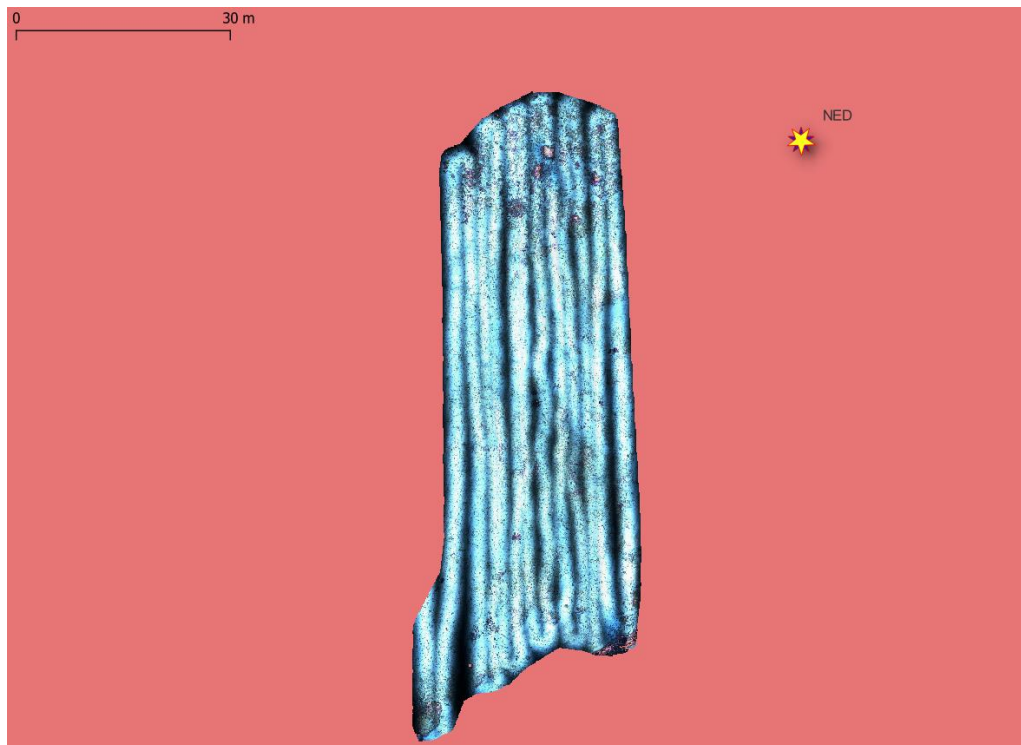


Fig. 5.25 Photomosaic next to NED origin.

Anton 233

The area where the dive will take place is located in the E5 working area off the coast of Mauritania. Before the AUV was deployed in the area, a suitable location for the mission was determined.

The goal was a photo survey of the area. The area is 70 m deep and quite flat (Fig. 5.26).

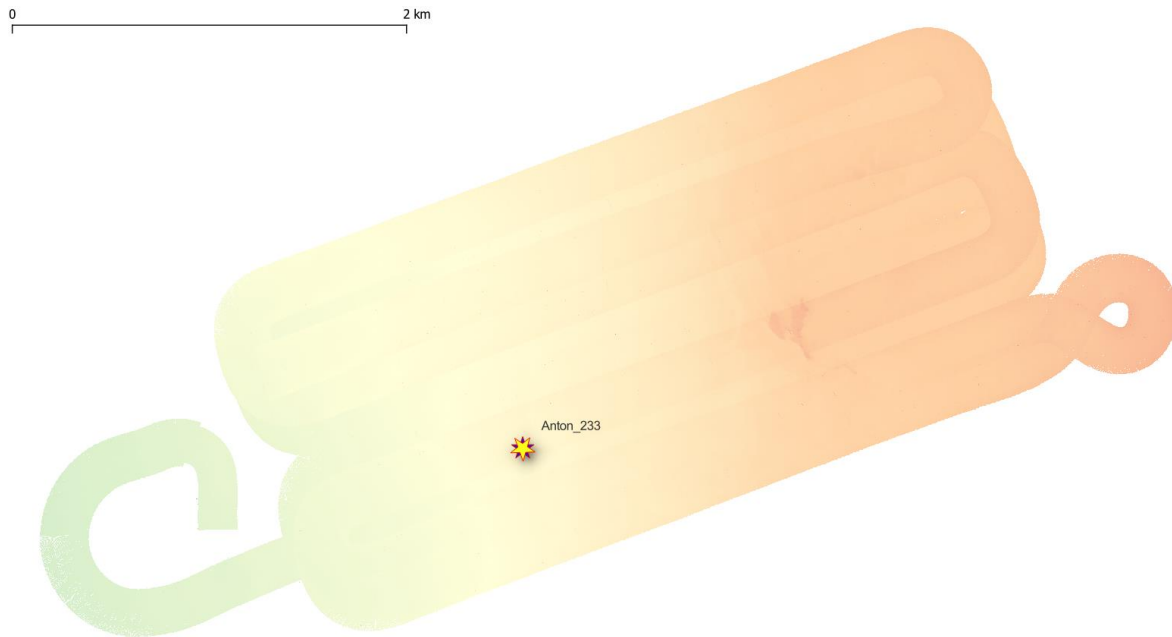


Fig. 5.26 Dive Area for GIRONA500 AUV Anton.

Photo survey in the Mauretania area (E5).

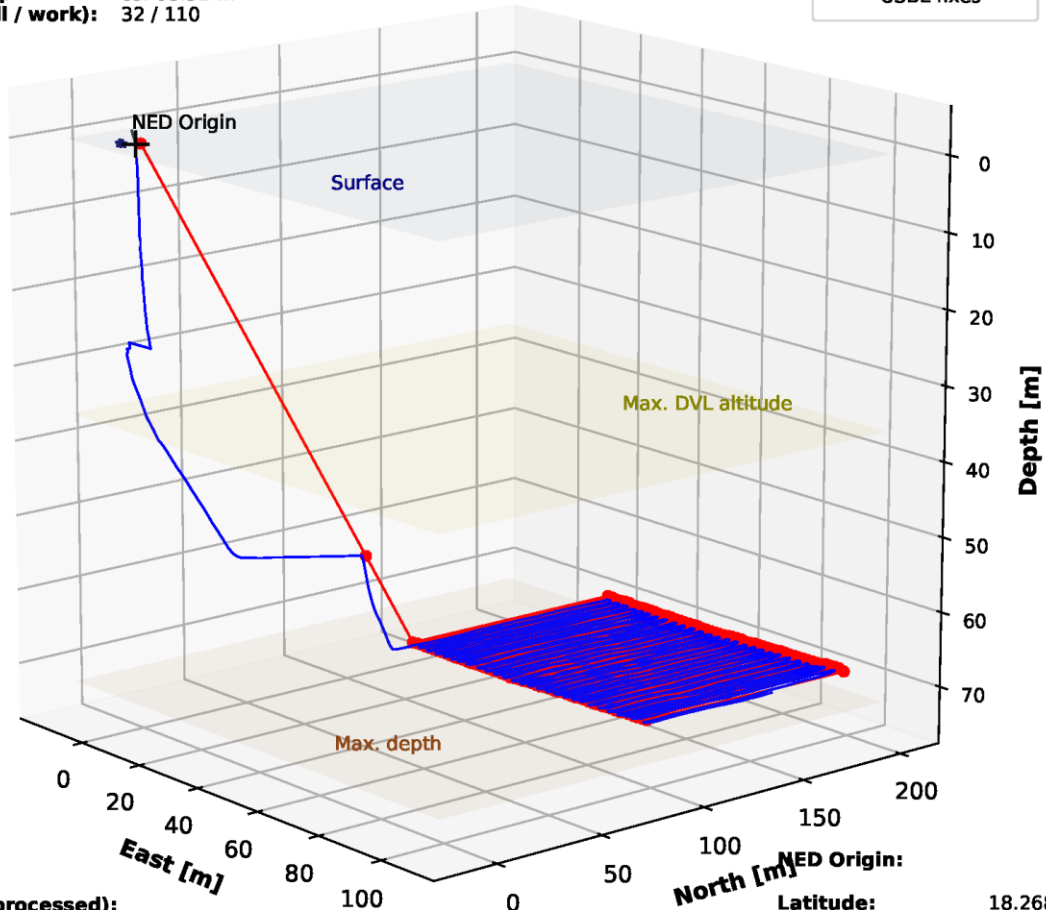
Mission started: 2022-06-30 10:35
Mission finished: 2022-06-30 14:08

Statistics (planned):

Overall length: 5691.22 m
Overall duration: 03:14 hrs
Working area: 194.3 x 102.2 m = 19849.4 m²
Working depth: ca. 68.31 m
Sections (all / work): 32 / 110

Anton_233

—●—	Planned track
—	INS (raw) track
+	NED Origin
*	GPS fixes
	USBL fixes



Statistics (processed):
 Please provide Phins C3 INS log:
 1. Enable postprocessing log in iXBlue Phins C3 INS
 2. Open log in iXBlue DELPH software
 3. Run forward/backwards/smoothing processing
 4. Export 'primary navigation' to provided template

Note: All times are UTC

NED Origin:
Latitude: 18.26834°
Longitude: -16.38154°
GPS altitude: 38.10 m
Maximum depth: 72.26 m
Max DVL altitude: 36.07 m

Fig. 5.27 Anton 231 Dive Summary.

5.7 AUV Tests

(D.Scheppukat, T. B. von See, E. Wenzlaff, T. Kurbjuhn, P.Striewski)

Technical and station description can be found in the appendix (12.6 AUV Test).

Preliminary Results

At station 038-1 the functionality of the software Sinaps and Beluga should be tested. Sinaps is a commercial software from Evologics that is among other things used for the coordinate transformation of the position of an acoustic underwater sender in the coordinate system of the top side USBL modem into the global coordinate system. Beluga is a software that is developed by the AUV team at GEOMAR and shall in the future replace Sinaps and other programs and combine their functionality in one graphical user interface. The test and recalculation afterwards revealed that the lever arms that were used initially are wrong which lead to very high positioning uncertainty. Lever arms describe the three-dimensional distance between the GPS position and the USBL top side unit. They are used in the above-mentioned coordinate transformation. In Fig. 5.28 the ships GPS position during the test is shown as a point cloud together with the transponder positions calculated by Beluga and Sinaps. The Posidonia positions are the positions measured with the ships USBL system which can be seen as the reference for the test. The point cloud calculated with beluga stretches mainly east-westwards while the point cloud calculated with Sinaps stretches homogenously in all directions, as it can be expected. The heading of the ship was approximately 40° so that the distance between the centers of the point clouds is mainly due to the wrong lever arms in x-direction.

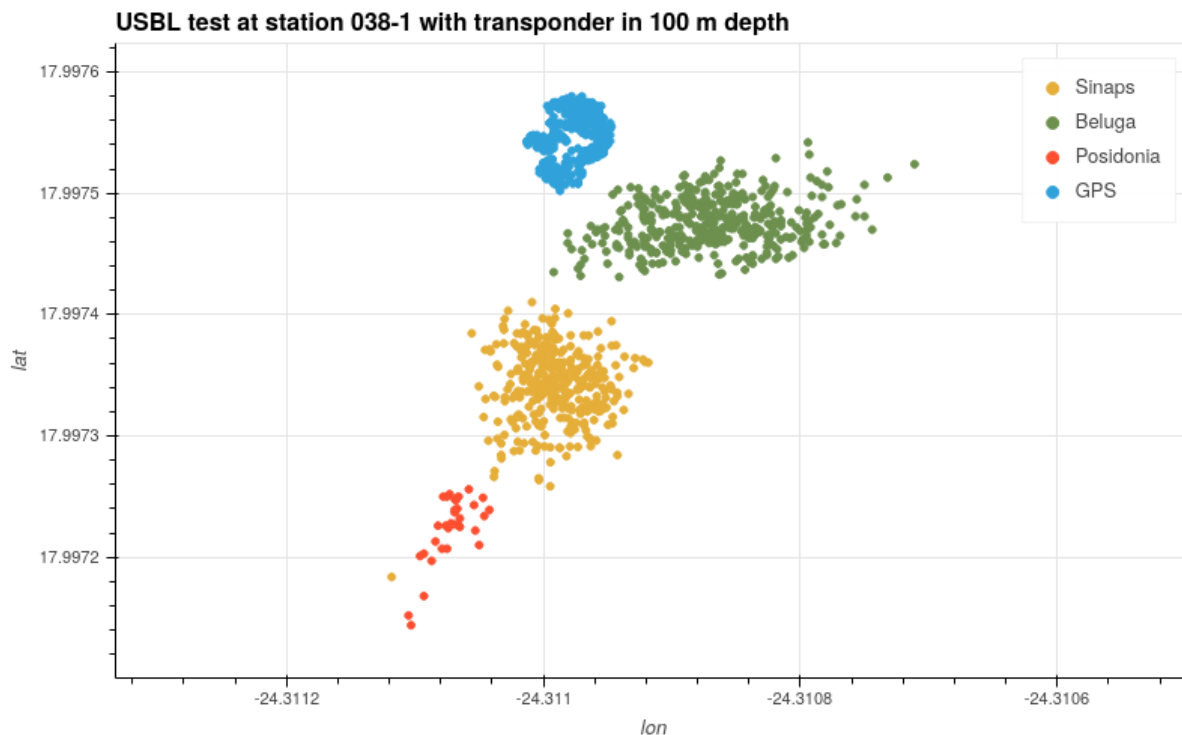


Fig. 5.28 GPS position of the ship and USBL positions of the transponder measured by Sinaps, Beluga and Posidonia at station 038.

For the station 054-1 the lever arms were corrected and the same test was repeated. The result is shown in Fig. 5.29. It can be seen that there is a distinct difference in the positioning of the USBL transponder between Sinaps and Beluga. The centers of the point clouds are roughly at the same position but the positions measured with Beluga are less precise. The diameters for Sinaps, Beluga and Posidonia at the widest extend are roughly 15, 25, and 8 m, respectively. The high uncertainty for Beluga and Sinaps is partly attributed to the mounting of the USBL top side modem on the pipe since its offset to the ships reference point is not measured as accurate as the one of the moon pool and also the construction is not stable but the pipe was swinging with the waves. The offset of approximately 18 m between Posidonia and the other two is due to wrong settings in the Posidonia software.

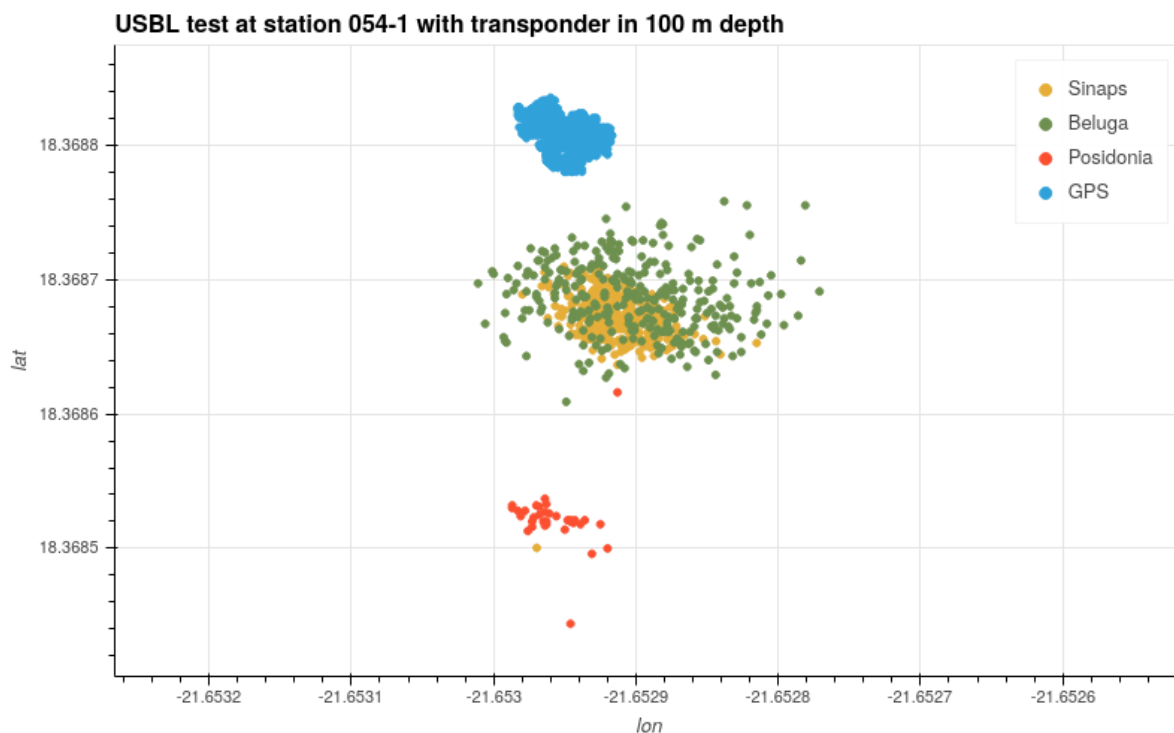


Fig. 5.29 GPS position of the ship and USBL positions of the transponder measured by Sinaps, Beluga and Posidonia at station 054.

At station 133-1 a test for the inertial navigation of the Girona500 AUVs was performed. So far, the AUVs had been mainly used in shallow waters where they have bottom lock with the DVL already at the sea surface. In deep water where no DVL bottom lock is achievable the main driver of the navigation is the integration of the acceleration via the INS. This however is only stable for a short amount of time and tends to drift, therefore it should be stabilized with additional measurements. Here, USBL position updates were used that are send from the top side modem. To prevent the AUV from driving away if the test fails the AUV was mounted on its transportation stand with additional 120 kg of weights. The software architecture was powered on but the thrusters were turned off and the AUV was lowered down into the water with a winch. Since the INS is closed source, the only tuning parameter is the uncertainty of the USBL positions that are send to the INS. The aim of the test was to find good parameters for this uncertainty. Fig. 5.30 shows the path, that the AUV calculated via the INS as well as the ships GPS and the USBL positions calculated by Beluga that were sent to the INS.

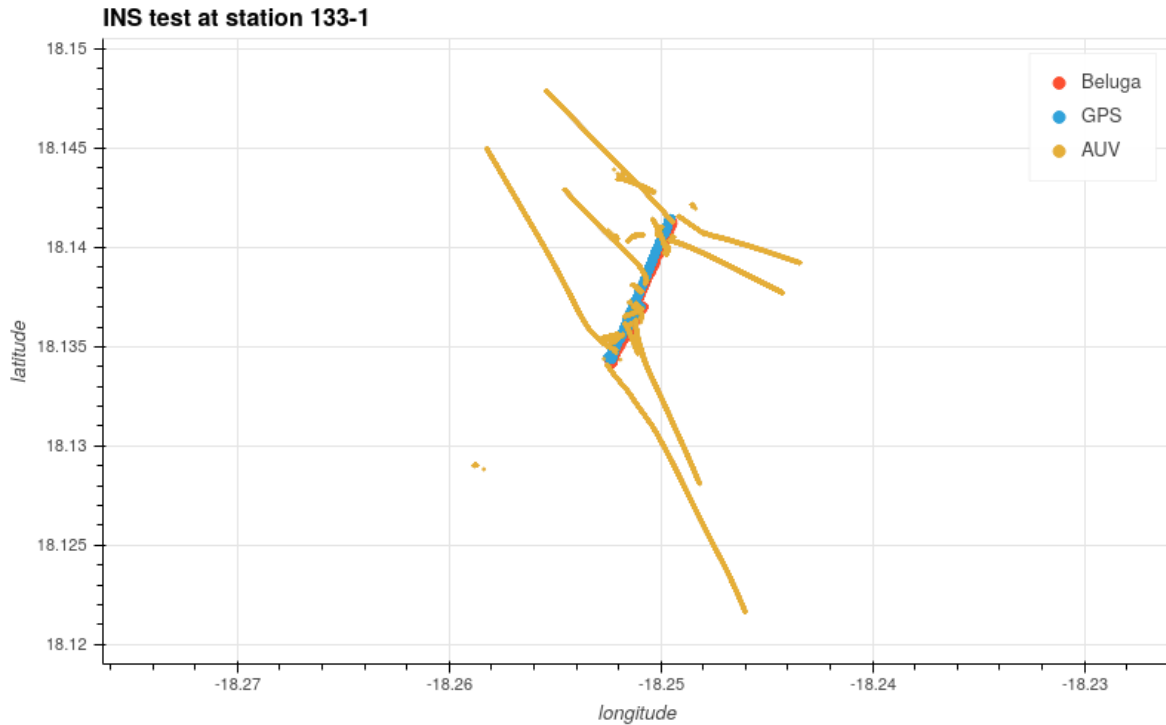


Fig. 5.30 GPS, AUV navigation track and USBL positions for the INS test at station 133.

Fig. 5.31 shows a close-up of the same data. Jumps between lines of the AUV indicate that the INS accepted a USBL position. In the worst case the navigation drifted 1.5 km before a USBL position was accepted by the INS, in the best case it stayed on track for 25 m. None of the parameters seemed to stabilize the INS navigation good enough to ensure safe AUV operation.

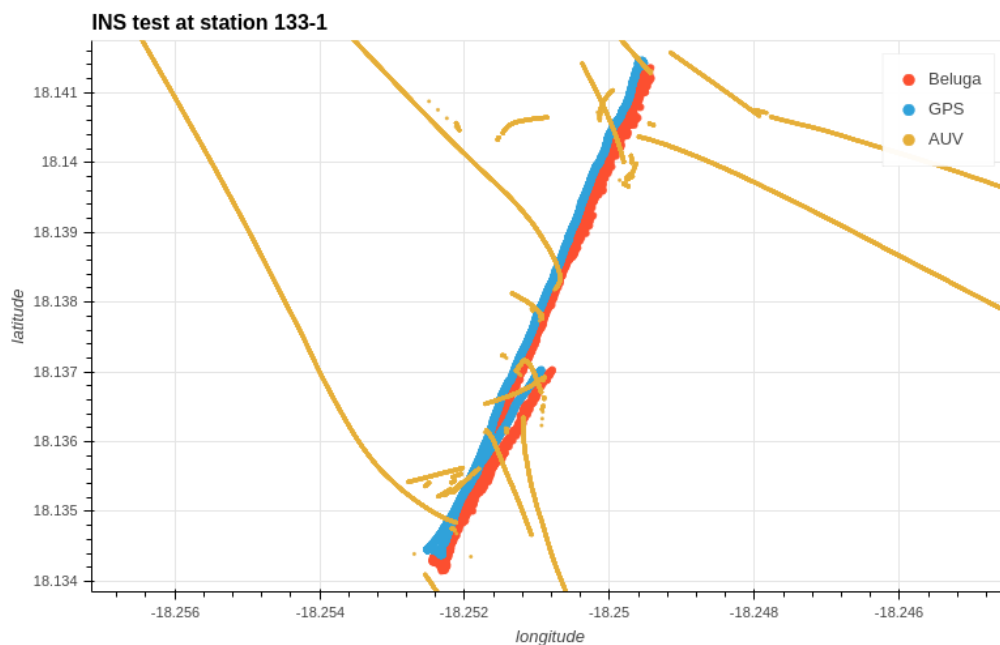


Fig. 5.31 Close-up of GPS, AUV navigation track and USBL positions for the INS test at station 133.

At station 163-1 a lever arm calibration with a USBL transponder from Evologics was performed. This is not necessary on large vessels where the distances between the measurement

devices have been measured professionally but on smaller vessels this is normally not the case. The main aim was to acquire a good dataset to test the calibration routine, that shall be implemented in Beluga. The distances of the professional measurements serve as the reference. To get measurements from many directions and distances the ship drove a circle and an eight around the transponder position.

At station 166-1 an autonomous thermocline detection algorithm was tested with AUV Luise. For this, a mission of three waypoints was created. At the second waypoint, the AUV should switch from the global mission mode to an external mission mode in which the thermocline tracking was implemented and afterwards resume the mission. Four missions were started of which the first three failed to activate the thermocline tracking behavior. The AUV navigation path and the three mission waypoints are shown in Fig. 5.32. The depth of the mission points was increased from 10 (mission 237) to 20 and 30 m in mission 238 and 238, respectively to reach the depth in which DVL bottom lock was achieved. In mission 238 the thermocline tracking was not started due to strong currents that lead to a drift of the AUV as can be seen in Fig. 5.32. For the missions 237 and 239 it is not completely clear why the thermocline tracking was not activated. Before the start of mission 240 the ROS node that was running the thermocline detection was restarted. The AUV navigation path, the mission waypoints and USBL measurements of the AUV position are shown in Fig. 5.33.

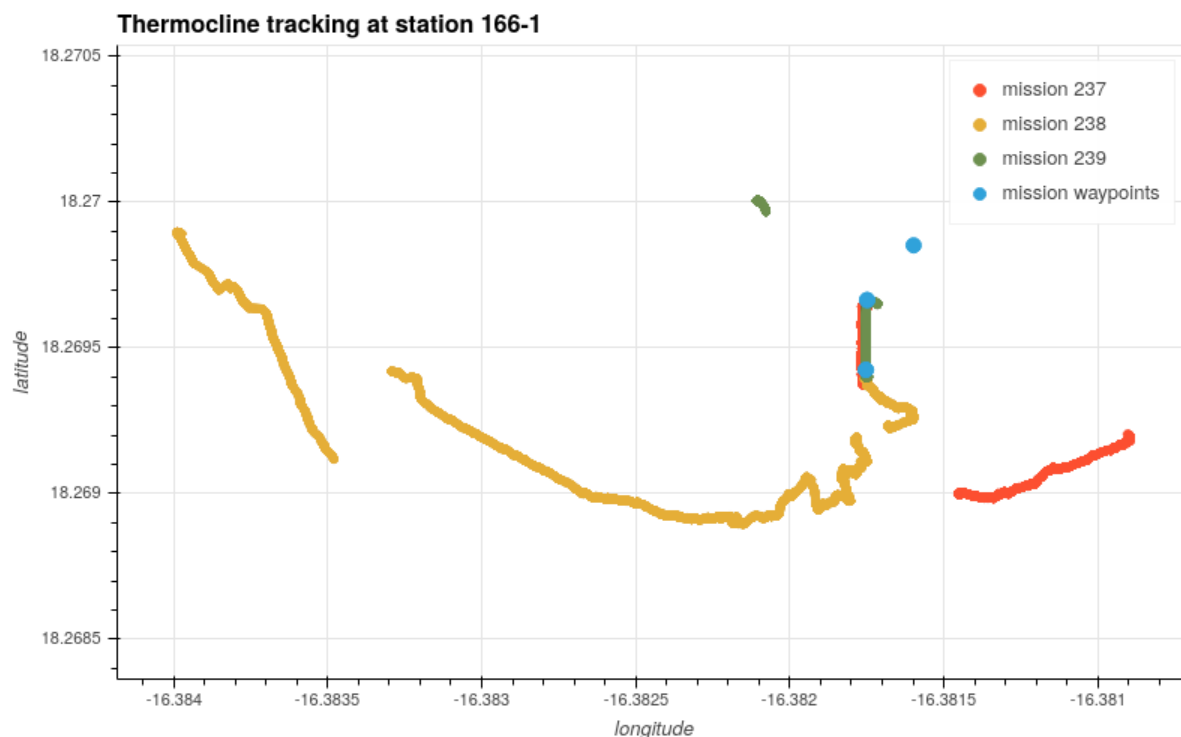


Fig. 5.32 Mission waypoints and AUV navigation tracks for the thermocline tracking missions 237,238 and 239 at station 166.

It can be seen that the AUV reached the second waypoint at which the thermocline tracking behavior was started. The AUV was commanded to drive 100 m to the north, 25 m to the west and 100 m to the south while the thermocline tracking algorithm was used to control the depth of the AUV. Due to a wrong setting in the INS of AUV Luise the DVL bottom lock was

disabled and the AUV navigation drifted. The USBL positions that were triggered manually during the mission show that the AUV did not drift to the west but drove to the south instead. Therefore, the thermocline tracking was disabled. Fig. 5.33 shows the depth and temperature that was measured. It can be seen that the mission started at 20 m depth, then the AUV drove to the second waypoint at 30 m depth at which the thermocline tracking started. The AUV drove to the seafloor to calculate a normalization of the gradient of the temperature with respect to depth. Afterwards it should drive upward until the thermocline layer is reached in which an extremum seeking control (ESC) performs fine tuning of the depth while driving sinusoidal waves. In Fig. 5.34, it can be seen that the ESC was started at the thermocline but also that the AUV did not drive a sinusoidal wave but a triangle.

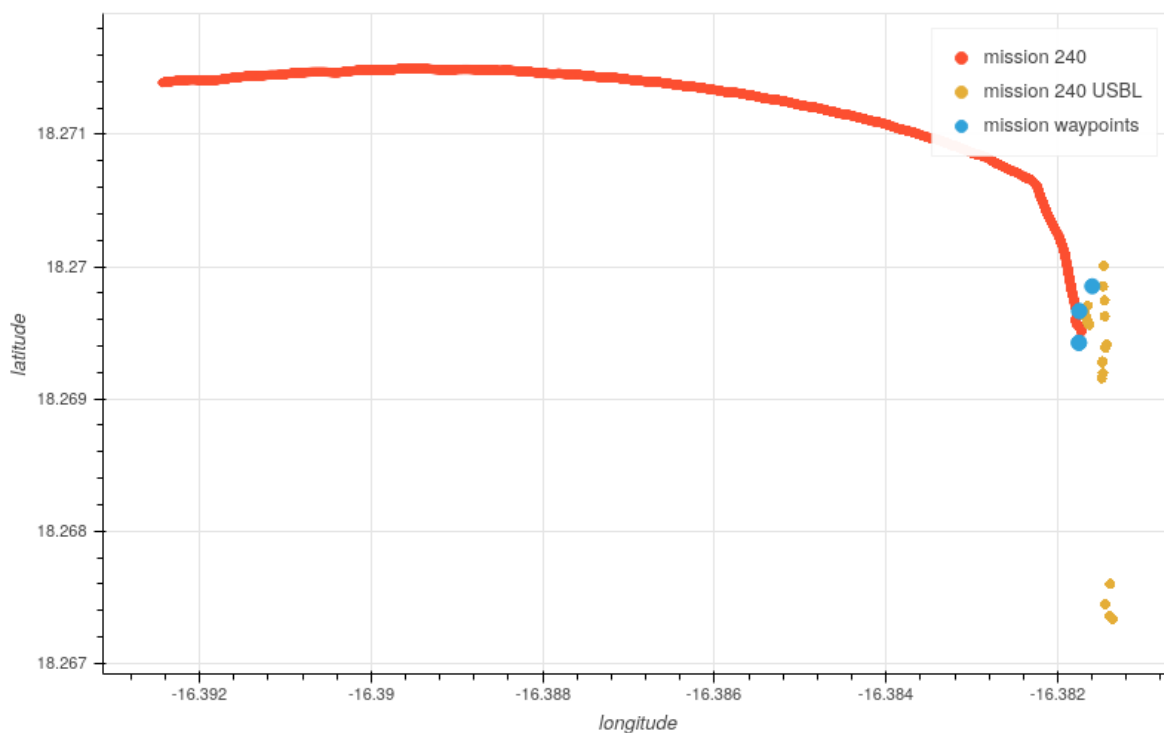


Fig. 5.33 Mission waypoints, AUV navigation track and USBL positions for the thermocline tracking mission 240 at station 166.

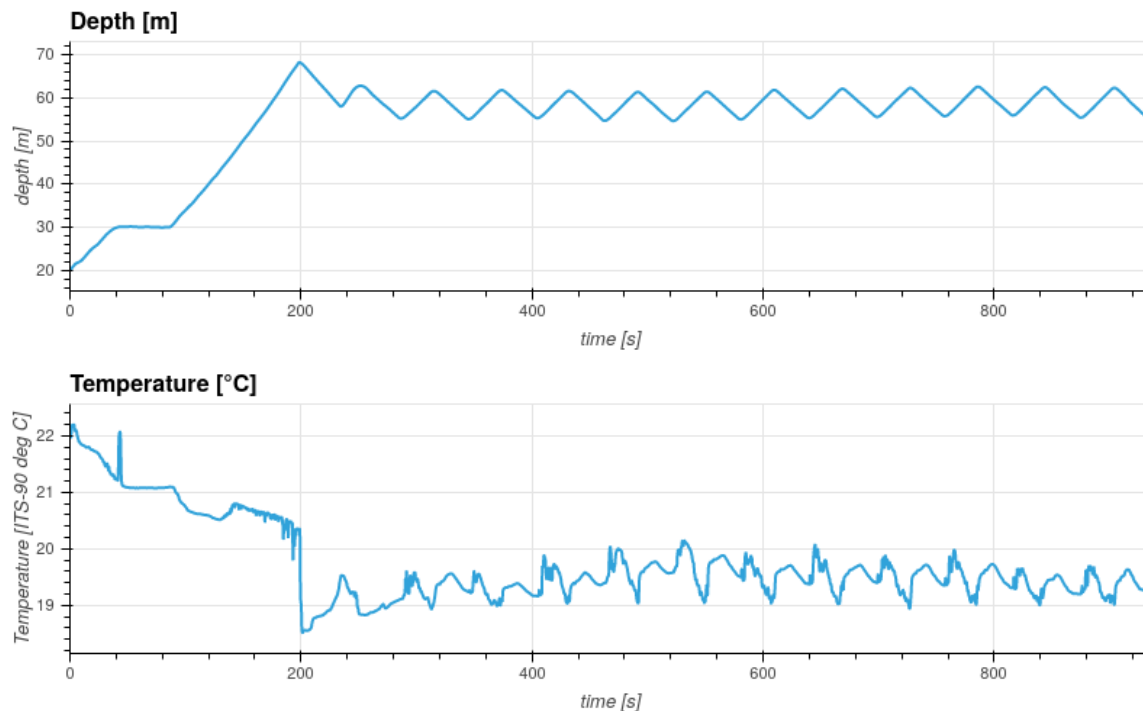


Fig. 5.34 Depth and temperature over time for the thermocline tracking mission 240 at station 166.

The latter is due to wrong settings in the AUV navigation that limited the vertical velocity to ± 0.2 m/s instead of ± 0.4 m/s. This saturation of the control parameter basically disabled the ESC. At the recovery of the AUV it was drawn underneath the ship. Acoustic positioning while the ship was drifting with the currents revealed that the AUV was stuck there so that a command was sent to the AUV to drive to 15m depth close to the ship. After sending the command the acoustic connection to the AUV was lost. The analysis of the log data of the AUV revealed that it stayed in 15 m depth for some time and simultaneously drifted southwards with the currents so that we could not see it when it surfaced. Therefore, AUV Anton that was performing a photo survey 1 km north was recovered and afterwards the ship drove southwards to find AUV Luise. Luckily a ship from the Mauritanian coast guard saw something yellow and told us the direction where we found and recovered the AUV.

Expected Outcome

The expected outcome of the stations 038-1 and 054-1 was to verify that the software Beluga and Sinaps are working properly in order to use them in later AUV tests. The expected outcome of the test at station 133-1 was to find good parameters for the USBL position uncertainty that is attributed to the USBL updates sent to the INS of the AUV. This is essential for a safe operation of the AUV in the water column without DVL bottom lock. The expected outcome of the station 163-1 was to acquire a good dataset to which ground truth values exist. The dataset will be used to test and verify the USBL lever arm calibration that shall be integrated in Beluga. The expected outcome of the thermocline detection tests at station 166-1 was to verify the simulation results and to obtain a dataset of the spatial evolution of the thermocline.

5.8 Dedicated Acoustic Mapping

(M. Kampmeier, J. Mohrmann, A. K. Hinz)

Multibeam EM122, EM710

The EM122 was used for all areas, except of the very shallow one, E5. The 12 kHz system has a resolution of $1 \times 2^\circ$ beam opening angles, which results in 50 - 75 m grid cell size for 3,000 m water depth.

All working areas have been either mapped during M182, or mapping from M156 was extended. The data was logged in *.all format and processed with Qimera. Sound velocity profiles were acquired with an AML sound velocity profiler and added into the Kongsberg acquisition software. The roll offset was corrected and the new value was entered into the system's offset settings inside the acquisition software. Configuration tables are given in the appendix (12.7 Dedicated Acoustic Mapping).

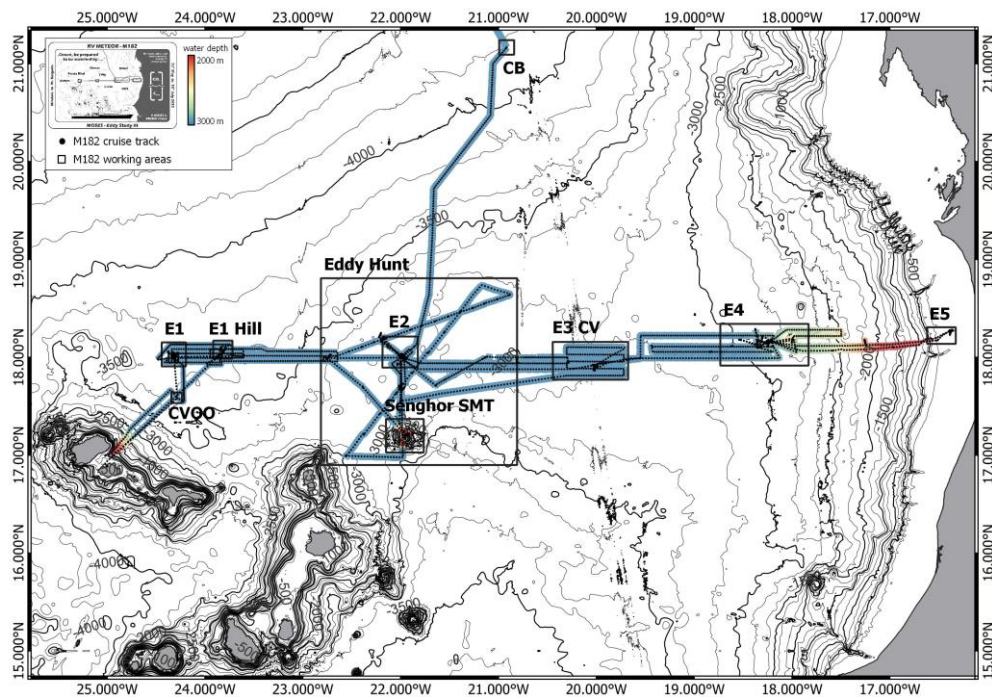


Fig. 5.35 Map with working areas of M182 and total acquired multibeam data. Measured water depths range from 65 to 3800 m.

The plain areas (E1, E2 and E3 CV) show only minor morphology and MBES artefacts become more pronounced. Morphological features and differences in between areas are not visible inside MBES data. Nevertheless, the seafloor north of Cape Verde and west of Mauretania is not completely flat. It is rather characterized by small (E1 Hill) and large seamounts (Senghor Seamount), which extent from the abyssal plain (Fig. 5.35). The ridge of E1 Hill is about 10 km long, 3.5 km wide and 400 m high and has sharp edges and slopes. Compared to that, the diapiric structure in E4 is with approx.40 km 4 times bigger, but less high (300 m) (Fig. 5.36). It seems to have a different development history as it is more gently sloping and parts of it seem to be subsequently eroded by currents.

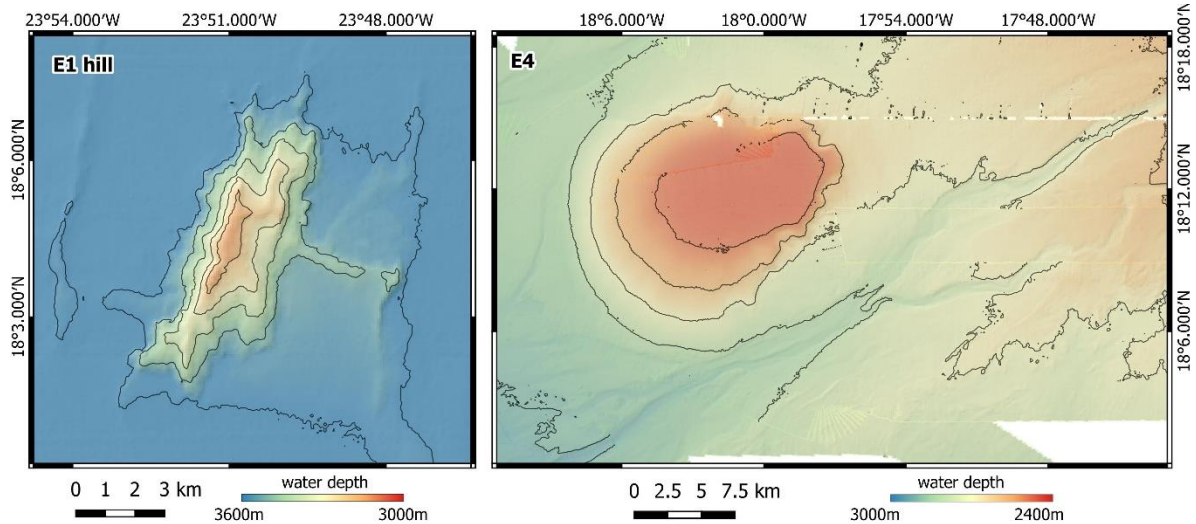


Fig. 5.36 Two seamount structures that were mapped during M182. They can have different shapes and sizes and represent special habitats in the deep sea.

The closer you get to the Mauritanian coast, the more the seabed is criss-crossed by channel systems and canyons. Landslides from the shelf shape the morphology and transport sediment along the channel systems into the deep sea. These channels are prominent in area E4 and reach depths of more than 60 m on a width of around 1 km. The Senghor seamount on the other hand, is around 3,000 m high and has a more or less conic shape with steep slopes to each side. Since water depths are so low, which results in small footprints, only the top and the north-eastern flank could be mapped. The central part forms a plateau with steep and rugged flanks, which decrease to 3,500 m water depth (Fig. 5.37).

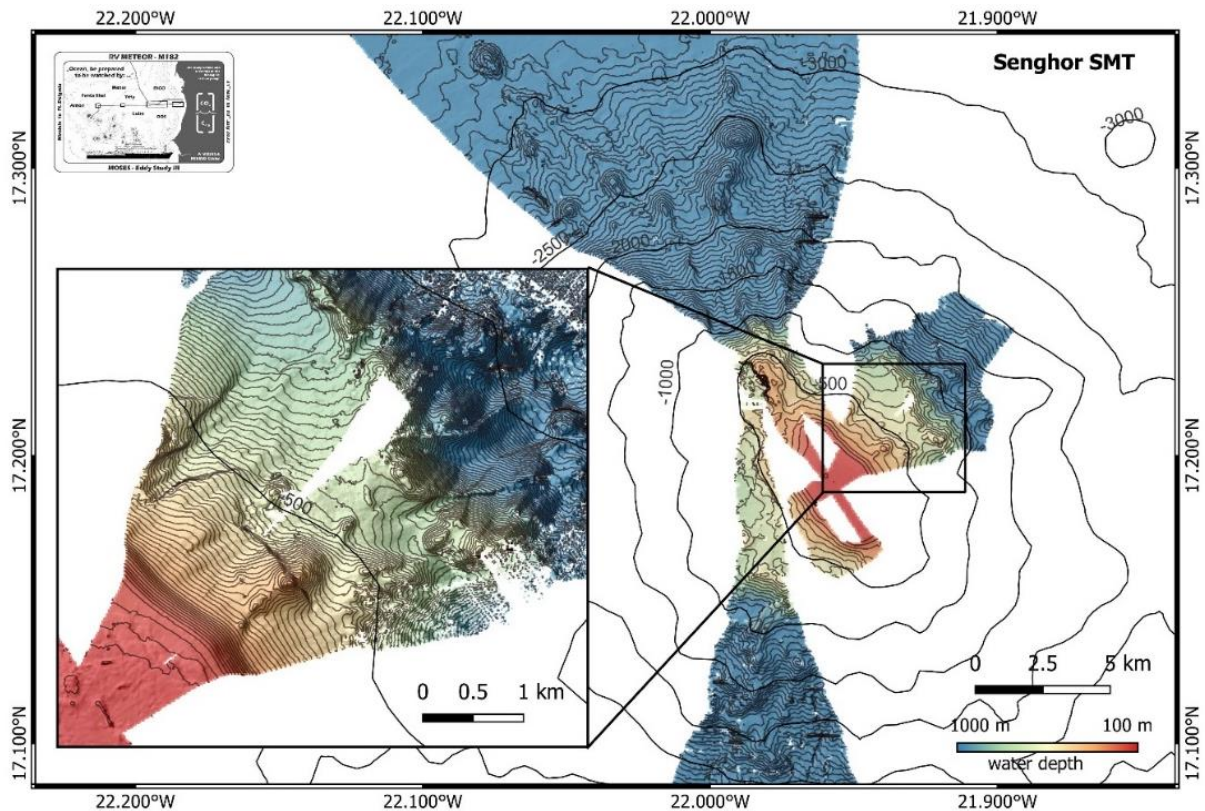


Fig. 5.37 The Senghor Seamount could not be fully mapped, since MBES footprints turned very narrow in low water depths. It extends from 110 m on the plateau, down to 2 km.

The seabed of the very western area E5 is located on the Mauritanian shelf at a water depth of 65 to 75 meters. It is formed by a gently sloping slope to the west and a 3 m high reef structure (Fig. 5.38). Due to the shallow water depth, tide effects reduce data quality. The MBES profiles have been vertically shifted during post-processing, but gradual water level changes could not be fully eliminated.

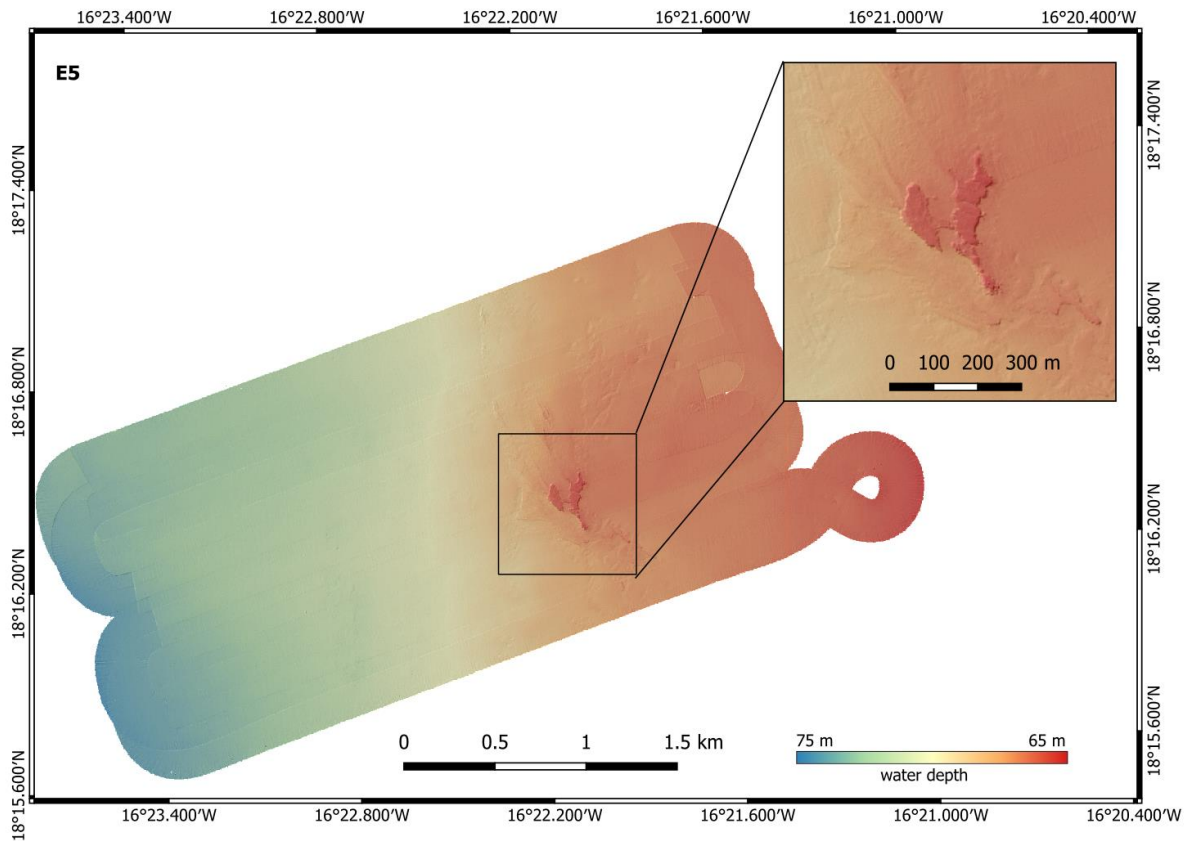


Fig. 5.38 The most shallow research site E5 is located on the Mauritanian shelf and shows a ca 300 m long reef structure.

5.9 Underway Studies

(M.Kampmeier, J. Greinert)

Thermosalinograph

We ran the ship-based thermosalinograph as soon as we left Cape Verdian waters and all data were logged. The SST (sea surface temperature) is an important factor when it comes to the eddy hunt. Satellite images provide sea surface heights, which can be interpreted according to eddy occurrences. SST cross sections can reveal the boundaries of an eddy structure, since temperatures differ outside and inside an eddy. On M182 we followed a cyclonic eddy (anti-clockwise rotating), which creates a depression on the sea surface. At the same time SST becomes lower in the eddy centre compared to the realm (Fig. 5.39).

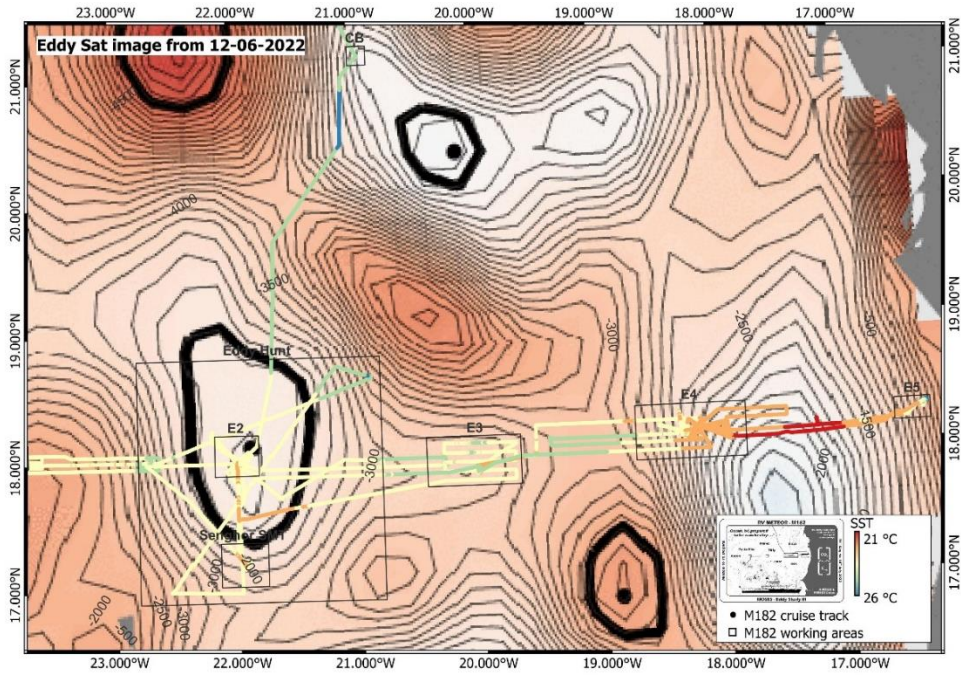


Fig. 5.39 Eddy satellite image with SST, which was recorded during M182 cruise.

38 kHz ADCP

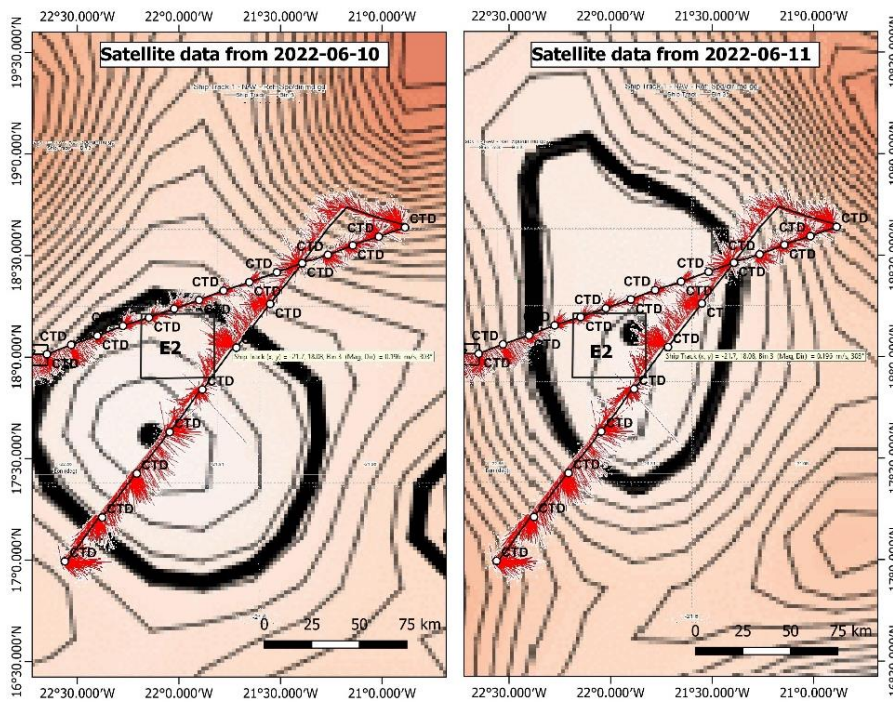


Fig. 5.40 Eddy satellite image with current direction from ADCP 38 kHz (Bin 3; 60 m water depth).

We ran the ship-based 38 kHz ADCP as soon as we left Cape Verdian waters and all data were logged. The data confirmed the presence of the eddy and identified it as a cyclonic (ant-clockwise rotating) eddy (Fig. 5.40). Where current directions swap during the cross profile, the eddy centre is assumed.

5.10 Expected Results

The cruise M182 is the final one of the three cruises in the measuring campaign, addressing the goal to investigate the multi-layered influence of eddies on the lateral transport of biogeochemical properties and the carbon pump in eastern boundary upwelling areas and the effect to the oligotrophic deep-sea periphery. During the cruise, the focus was placed onto the following scientific questions:

- i. Mapping and characterizing an eddy using physical oceanography and satellite data. During M182 a suitable eddy was detected. With diameters of ca 190 (N-S) and 100 m (W-E), it was quite large and kept slowly migrating towards NW while we crossed it from different directions. Subsequently, the position of the eddy center changed its location, but nevertheless, we are confident that we managed to sample the core region.
- ii. Sample the eddy for biogeochemical investigations along a cross-transect. The full CTD section from S1 to E5, encompassing the eddy center, revealed generally low chlorophyll levels, with a slight increase towards the Mauritanian coast; notably, the eddy exhibited significantly lower oxygen concentrations within its core, reaching values well below 60 $\mu\text{mol kg}^{-1}$ between 80 and 100 m depth. Salinity and temperature anomalies were also observed around the eddy center.
- iii. Conduct vertical water column sampling and optical investigations for gelatinous organisms. We introduced a pioneering stereo camera system during horizontal video transects, achieving synchronized 4k resolution videos at 25 fps. Deployed at 10 stations during both day and night, the system provided over 30 hours of unprecedented field-collected footage. This data will be compared in terms of vertical distribution, abundance, and diversity data between stations and between day and night along a west to east productivity gradient.
- iiii. Investigate small-scale heterogeneity of biogeochemical carbon turnover on the seafloor using AUV-based mapping technologies, high-resolution optical seafloor mapping, sediment sampling, and in-situ biogeochemical flux measurements. All working areas have been mapped via ship-based multibeam and high-resolution towed video mapping. Additional benthic sampling via Rover, MUC and BIGO Lander will be linked to the different scales of seafloor heterogeneity.

6 Ship's METEORological Station

6.1 Weather and Route during the Trip M182

(M. Stelzner, M. Knobelsdorf)

The research area of the M182 was located in the area just northeast of the Cape Verde Islands and the coast of Mauritania/West Africa. The aim of the trip was to understand the dynamics of ocean eddies quantitatively, with a focus on CO₂ sources/sink mechanisms and the biological carbon pump. (Abstract from the expedition booklet)

On Tuesday, 31.05.2022 at about 09 o'clock RV METEOR left the port of Mindelo. A subtropical high between Sargasso Sea and the Azores stretched a ridge into the research area at the start of the journey. The steady northeast trade wind with 5 Bft was blowing, the seastate showed 1.5 m with two swells from the northeast and northwest. In addition, from the beginning of the trip, the air was temporarily enriched with Sahara dust of varying thickness. The surface visibility was affected however rarely under 15km. In the next following days, the wind temporarily refreshed to 7 Bft. The north-eastern swell rose to 2m and became the main swell from 03.06. In addition to the windsea, the significant sea level rose to 2.5 m. This weather pattern did not hardly change until 08.06.

The North Atlantic high dominated the weather in the travel area, weakened only on 09.06. Further along, a new high followed from the northwest, which brought a calming in the travel area. During the day, the wind weakened briefly before rising to 4 Bft later. The sea state dropped to 1.5 metres.

On 11.06. the new North Atlantic high migrated somewhat northeast. At the same time, a low over Mauritania shifted somewhat towards the coast. Between these pressure areas, the northeastern trade winds refreshed to 6 Bft and caused the sea state to rise to 2.5 m. The NE 'luy swell persisted, the weather pattern did not change for a whole week.

On the 18.06. the North Atlantic high strengthened und migrated northward. The Mauritanian low weakened, causing the northeastern trade to decline somewhat. For a whole week, the wind showed only 4 Bft with a sea at 1 m. On the 21.06 and 22.06. a second weak swell from the south was observed.

On the 23.06. the extensive north Atlantic high strengthened with the ridge extending southeast. This caused an increase in wind in the research area. On the 25.06. 8 Bft was measured. Until the end of June 5 to 6 Bft was predominant. With the strong wind on 25.06. the significant wave height climbed to 3 to 3,5m, decreasing the next day to 2,5m.

From 29.06. to 01.07. the research area was shifted close to the Mauritanian coast. The impact of the North Atlantic high diminished, leading to a weather improvement. The wind turned northwest and blew at 4 to 5 Bft with the sea dropping under 1.5m.

On the 01.07. RV METEOR turned west, getting under the influence of the high-pressure system. The now again northeasterly wind rose to 6 Bft at times 7 Bft with the sea level reaching the known 2.5m.

Early of the 04.07. the almost one-day transit to the northernmost (21°N) last research area of this journey. Research began on the evening of 05.07. on transit towards Ponta Delgada.

During the transit, the constant northeast trade wind of 5-6 Bft initially blew moderately and gradually declined to 4 Bft. The initial sea level of 2.5m gradually decreased to 1.5m with a swell from the northeast.

On the evening of 09.07. RV METEOR reached the port of Ponta Delgada and ended the journey M182.

7 Station List

Station name	Event Time	Action	USBL-Lat (DD.ddddd)	USBL-Long (DD.ddddd)	Ship-Lat (DD.ddddd)	Ship-Long (DD.ddddd)	Depth (m)	Working Area	remarks
M182_1-1_MN_B9-1	5/31/2022 16:35	max depth/on ground			17.58352	-24.2834	3597	CVOO	
M182_2-1_CTD-1	5/31/2022 18:53	max depth/on ground			17.58353	-24.2833	3597	CVOO	
M182_3-1_TP-1	5/31/2022 23:08	in the water			17.98455	-24.3151	3694	E1	
M182_4-1_TP-1	5/31/2022 23:22	in the water			17.99737	-24.3124	3694	E1	
M182_5-1_CTD-2	6/1/2022 1:15	max depth/on ground			18.0001	-24.3336	3694	E1	
M182_6-1_TP-2	6/1/2022 3:42	information			18.001	-24.3187	3694	E1	
M182_6-1_TP-2	6/1/2022 4:44	information			17.98348	-24.3151	3693	E1	
M182_7-1_EM122-1	6/1/2022 6:30	profile start			18.04992	-24.3743	3710		
M182_7-1_EM122-1	6/1/2022 8:32	profile end			18.04622	-24.3413	3700		
M182_8-1_TVMUC-1	6/1/2022 10:35	max depth/on ground	18.00033131	-24.33355087	18.00007	-24.3336	3701	E1	
M182_9-1_EM122-2	6/1/2022 13:16	profile start			18.04828	-24.3081	3695		
M182_9-1_EM122-2	6/1/2022 15:40	profile end			18.0498	-24.2742	3690		
M182_10-1_BIGO_I-1	6/1/2022 19:14	max depth/on ground	18.00014059	-24.33363496	17.99985	-24.3335	3697	E1	
M182_11-1_XOFOS-1	6/1/2022 23:24	profile start			17.99988	-24.3335	3696	E1	water column
M182_11-1_XOFOS-1	6/2/2022 0:54	profile end			18.00963	-24.3259	3696	E1	water column
M182_12-1_EM122-3	6/2/2022 2:18	profile start			18.03958	-24.2591	3685		
M182_12-1_EM122-3	6/2/2022 14:27	profile end			18.0044	-23.6101	3614		

M182_13-1_MN_B9-2	6/2/2022 15:20	max depth/on ground			18.00027	-23.6093	3614	between E1 hill - E2
M182_14-1_CTD-3	6/2/2022 17:44	max depth/on ground			18.00027	-23.6093	3612	between E1 hill - E2
M182_15-1_BIGO_II-1	6/3/2022 0:31	max depth/on ground	18.05338852	-23.81657415	18.0479	-23.8195	3563	E1 hill
M182_16-1_TVMUC-2	6/3/2022 9:32	max depth/on ground	18.0483414	-23.81978867	18.04808	-23.8197	3562	E1 hill
M182_17-1_EM122-4	6/3/2022 11:44	profile start			18.08448	-23.9251	3645	
M182_17-1_EM122-4	6/3/2022 14:37	profile end			18.08447	-24.3323	3699	
M182_18-1_DSR-1	6/3/2022 20:02	deployed	18.00017334	-24.33291705	17.9998	-24.3329	3693	E1
M182_19-1_XOFOS-2	6/4/2022 0:08	profile start			18.00097	-24.3343	3694	E1
M182_19-1_XOFOS-2	6/4/2022 3:17	profile end			18.0216	-24.3175	3691	E1
M182_20-1_TVMUC-3	6/4/2022 6:53	max depth/on ground	18.03716959	-24.33294987	18.03722	-24.3326	3694	E1
M182_21-1_EM122-5	6/4/2022 8:43	profile start			17.99475	-24.2638	3682	
M182_21-1_EM122-5	6/4/2022 11:07	profile end			17.99405	-23.933	3652	
M182_22-1_CTD-4	6/4/2022 14:19	max depth/on ground			18.04928	-23.8204	3556	E1 hill
M182_23-1_XOFOS-3	6/4/2022 15:30	in the water			18.04998	-23.8213	3553	E1 hill
M182_23-1_XOFOS-3	6/4/2022 18:10	on deck			18.07738	-23.8019	3569	E1 hill
M182_24-1_EM122-6	6/4/2022 19:32	profile start			18.08693	-23.6236	3629	
M182_24-1_EM122-6	6/5/2022 4:27	profile end			17.95942	-22.786	3399	
M182_25-1_MN_B9-3	6/5/2022 5:42	max depth/on ground			18.00203	-22.7864	3414	Senghor SMT
M182_26-1_CTD-5	6/5/2022 7:54	max depth/on ground			18.00202	-22.7863	3414	Eddy Hunt

M182_27-1_TVMUC-4	6/5/2022 10:40	max depth/on ground	18.00223106	-22.78638306	18.002	-22.7864	3414	Eddy Hunt	
M182_28-1_XOFOS-4	6/5/2022 15:53	profile start			17.98075	-22.7568	3397	Eddy Hunt	
M182_28-1_XOFOS-4	6/5/2022 23:47	profile end			18.0253	-22.7232	3401	Eddy Hunt	
M182_29-1_EM122-7	6/6/2022 0:51	profile start			17.96347	-22.7783	3410		
M182_29-1_EM122-7	6/6/2022 8:18	profile end			17.96127	-23.845	3632		
M182_30-1_BIGO_II-2	6/6/2022 11:20	deployed			18.04797	-23.8197	3559	E1 hill	
M182_31-1_TVMUC-5	6/6/2022 14:06	max depth/on ground	18.07433699	-23.85077294	18.07403	-23.8508	3129	E1 hill	
M182_32-1_XOFOS-5	6/6/2022 16:40	profile start			18.07545	-23.8517	3141	E1 hill	
M182_32-1_XOFOS-5	6/6/2022 21:57	on deck			18.104	-23.8391	3445	E1 hill	
M182_33-1_MN_B9-4	6/6/2022 22:50	max depth/on ground			18.10407	-23.8392	3444	E1 hill	
M182_34-1_EM122-8	6/7/2022 0:50	profile start			18.13198	-23.7532	3654		
M182_34-1_EM122-8	6/7/2022 7:27	profile end			17.9889	-24.4829	3699		
M182_35-1_GC-1	6/7/2022 10:08	max depth/on ground			17.99818	-24.3337	3692	E1	
M182_36-1_TP-3	6/7/2022 11:16	information			17.99857	-24.3344	3693	E1	
M182_37-1_TP-3	6/7/2022 12:08	information			17.9855	-24.3158	3690	E1	
M182_38-1_AUV_ANTON-1	6/7/2022 16:08	max depth/on ground			17.99752	-24.311	3691	E1	
M182_39-1_XOFOS-6	6/7/2022 17:51	in the water			17.99825	-24.3104	3691	E1	water column
M182_39-1_XOFOS-6	6/7/2022 19:15	on deck			18.00328	-24.3072	3689	E1	water column

M182_40-1_XOFOS-7	6/7/2022 21:08	profile start	18.00347	-24.3071	3690	E1	water column
M182_40-1_XOFOS-7	6/7/2022 23:55	profile end	18.03998	-24.2834	3689	E1	water column
M182_41-1_EM122-9	6/8/2022 1:19	profile start	17.94862	-24.3926	3683		
M182_41-1_EM122-9	6/8/2022 6:31	profile end	17.92437	-23.9775	3633		
M182_42-1_MN_B9-5	6/9/2022 2:04	max depth/on ground	17.58283	-24.2831	3601	CVOO	
M182_43-1_EM122-10	6/9/2022 3:30	profile start	17.55703	-24.2146	3585		
M182_43-1_EM122-10	6/9/2022 6:54	profile end	17.91153	-24.2212	3664		
M182_44-1_EM122-11	6/9/2022 17:21	profile start	18.0169	-23.5884	3609		
M182_44-1_EM122-11	6/9/2022 23:57	profile end	18.01403	-22.6506	3383		
M182_45-1_CTD-6	6/10/2022 0:44	max depth/on ground	18.01358	-22.6499	3383	Eddy Hunt	
M182_46-1_CTD-7	6/10/2022 2:40	max depth/on ground	18.06002	-22.53	3349	Eddy Hunt	
M182_47-1_CTD-8	6/10/2022 4:37	max depth/on ground	18.10482	-22.4014	3345	Eddy Hunt	
M182_48-1_CTD-9	6/10/2022 6:36	max depth/on ground	18.15347	-22.2755	3335	Eddy Hunt	
M182_49-1_CTD-10	6/10/2022 8:37	max depth/on ground	18.19417	-22.1473	3325	E2	
M182_50-1_CTD-11	6/10/2022 10:43	max depth/on ground	18.23768	-22.0232	3305	Eddy Hunt	
M182_51-1_CTD-12	6/10/2022 12:48	max depth/on ground	18.2808	-21.9003	3275	Eddy Hunt	
M182_52-1_CTD-13	6/10/2022 14:49	max depth/on ground	18.32705	-21.78	3249	Eddy Hunt	

M182_53-1_CTD-14	6/10/2022 16:57	max depth/on ground	18.3688	-21.653	3192	Eddy Hunt
M182_54-1_AUV_ANTON-2	6/10/2022 16:36	in the water	18.36837	-21.6521	3195	Eddy Hunt
M182_55-1_CTD-15	6/10/2022 19:20	max depth/on ground	18.41728	-21.5171	3129	Eddy Hunt
M182_56-1_CTD-16	6/10/2022 21:23	max depth/on ground	18.46142	-21.3917	3103	Eddy Hunt
M182_57-1_CTD-17	6/11/2022 0:43	max depth/on ground	18.50332	-21.2657	3081	Eddy Hunt
M182_58-1_CTD-18	6/11/2022 2:53	max depth/on ground	18.54993	-21.1436	3097	Eddy Hunt
M182_59-1_CTD-19	6/11/2022 4:58	max depth/on ground	18.59297	-21.0156	3131	Eddy Hunt
M182_60-1_CTD-20	6/11/2022 7:06	max depth/on ground	18.63858	-20.8863	3171	Eddy Hunt
M182_61-1_CTD-21	6/11/2022 11:58	max depth/on ground	18.4622	-21.3924	3103	Eddy Hunt
M182_62-1_CTD-22	6/11/2022 14:45	max depth/on ground	18.26163	-21.5502	3161	Eddy Hunt
M182_63-1_CTD-23	6/11/2022 17:27	max depth/on ground	18.04617	-21.7173	3236	Eddy Hunt
M182_64-1_CTD-24	6/11/2022 20:14	max depth/on ground	17.83977	-21.884	3299	Eddy Hunt
M182_65-1_CTD-25	6/11/2022 22:59	max depth/on ground	17.63055	-22.0453	3343	Eddy Hunt
M182_66-1_CTD-26	6/12/2022 1:39	max depth/on ground	17.42587	-22.2073	3356	Eddy Hunt

M182_67-1_CTD-27	6/12/2022 4:24	max depth/on ground			17.20965	-22.3775	3337	Eddy Hunt	
M182_68-1_CTD-28	6/12/2022 7:13	max depth/on ground			16.99325	-22.5616	3088	Eddy Hunt	
M182_69-1_VMADCP_38kHz-1	6/12/2022 7:55	profile start			16.99333	-22.5608	3094	Eddy Hunt	
M182_69-1_VMADCP_38kHz-1	6/12/2022 11:10	profile end			16.9776	-21.9835	3442	Eddy Hunt	
M182_70-1_GC-2	6/12/2022 19:13	max depth/on ground	18.00048048	-22.0007160	18.00003	-22.0007	3295	E2	
M182_71-1_CTD-29	6/12/2022 23:03	max depth/on ground			17.69348	-21.9986	3332	Eddy Hunt	
M182_72-1_XOFOS-8	6/13/2022 0:31	profile start			17.69402	-21.9979	3332	Eddy Hunt	water column
M182_72-1_XOFOS-8	6/13/2022 3:04	profile end			17.73262	-21.9833	3325	Eddy Hunt	water column
M182_73-1_MN_B9-6	6/13/2022 4:44	max depth/on ground			17.69152	-21.9977	3332	Senghor SMT	
M182_74-1_AUV_ABYSS-1	6/13/2022 5:38	in the water			17.6922	-21.9975	3332	Eddy Hunt	
M182_75-1_TP-4	6/13/2022 13:44	in the water			17.99118	-21.9674	3290	E2	
M182_75-1_TP-4	6/13/2022 14:03	in the water			18.00332	-21.967	3290	E2	
M182_76-1_CTD-30	6/13/2022 15:41	max depth/on ground			17.99943	-22.0011	3294	E2	
M182_77-1_BIGO_II-3	6/13/2022 19:05	deployed	18.00015899	-22.0011959	17.99938	-22.0011	3294	E2	
M182_78-1_XOFOS-9	6/13/2022 23:39	profile start			17.99587	-22.0024	3295	E2	
M182_78-1_XOFOS-9	6/14/2022 3:42	profile end			18.0343	-21.9886	3299	E2	
M182_79-1_EM122-12	6/14/2022 6:01	profile start			17.92088	-22.033	3300		

M182_79-1_EM122-12	6/14/2022 8:48	profile end			18.00498	-22.0021	3296		
M182_80-1_TVMUC-6	6/14/2022 10:05	information	17.9999	-22.000956	17.99945	-22.001	3294	E2	
M182_81-1_DSR-2	6/14/2022 15:38	deployed	17.9999504	-22.002658	17.99978	-22.0026	3294	E2	
M182_82-1_AUV_ABYSS-2	6/14/2022 17:30	in the water			17.9847	-21.959	3289	E2	
M182_83-1_CTD-31	6/14/2022 22:05	max depth/on ground			18.10323	-22.1323	0	E2	
M182_84-1_CTD-32	6/14/2022 23:33	max depth/on ground			18.16413	-22.2019	3329	Eddy Hunt	
M182_85-1_XOFOS-10	6/15/2022 0:50	profile start			18.16502	-22.2013	3328	E2 & Eddy Hunt	water column
M182_85-1_XOFOS-10	6/15/2022 3:52	profile end			18.20397	-22.1695	3326	E2 & Eddy Hunt	water column
M182_86-1_MN_B9-7	6/15/2022 5:45	max depth/on ground			18.1616	-22.2009	3328	Senghor SMT	
M182_87-1_EM122-13	6/15/2022 8:05	profile start			17.99847	-22.0032	3295		
M182_87-1_EM122-13	6/15/2022 9:56	profile end			17.82985	-22.0035	3313		
M182_88-1_CTD-33	6/15/2022 12:08	max depth/on ground			17.6945	-21.9974	3332	Eddy Hunt	
M182_89-1_XOFOS-11	6/15/2022 13:30	profile start			17.66787	-22.0167	3336	Eddy Hunt	water column
M182_89-1_XOFOS-11	6/15/2022 16:08	profile end			17.70748	-22.0003	3329	Eddy Hunt	water column
M182_90-1_MN_B9-8	6/15/2022 17:34	max depth/on ground			17.69387	-21.9973	3331	Senghor SMT	

M182_91-1_TVMUC-7	6/15/2022 19:38	max depth/on ground	17.69422835	-21.9972526	17.69393	-21.9973	3332	Eddy Hunt	
M182_92-1_CTD-34	6/15/2022 21:14	max depth/on ground			17.69392	-21.9973	3333	Eddy Hunt	
M182_93-1_CTD-35	6/16/2022 0:47	max depth/on ground			17.32093	-22.0153	2891	Senghor SMT	
M182_94-1_EM122-14	6/16/2022 2:39	profile start			17.20863	-21.97	232		
M182_94-1_EM122-14	6/16/2022 4:30	profile end			17.18798	-21.9589	104		
M182_95-1_XOFOS-12	6/16/2022 5:29	profile start			17.19052	-21.9594	103	Senghor SMT	
M182_95-1_XOFOS-12	6/16/2022 10:02	on deck			17.20625	-21.9277	592	Senghor SMT	
M182_96-1_CTD-36	6/16/2022 10:45	max depth/on ground			17.22125	-21.9146	1154	Senghor SMT	
M182_97- 1_AUV_ANTON-3	6/16/2022 12:30	in the water			17.19467	-21.9568	0	Senghor SMT	
M182_98-1_CTD-37	6/16/2022 20:25	max depth/on ground			17.69513	-22.3873	3342	Eddy Hunt	
M182_99-1_TVMUC-8	6/17/2022 0:57	max depth/on ground	17.99164373	-22.7473905	17.99162	-22.7474	3397	Eddy Hunt	
M182_100- 1_AUV_ABYSS-3	6/17/2022 7:16	in the water			17.9881	-21.9544	0	E2	
M182_101-1_XOFOS-13	6/17/2022 11:51	profile start			18.20788	-22.2208	3337	Eddy Hunt	water column
M182_101-1_XOFOS-13	6/17/2022 14:49	profile end			18.24957	-22.2011	3342	Eddy Hunt	water column

M182_102-1_MN_B9-9	6/17/2022 16:11	max depth/on ground			18.22882	-22.2103	3339	Senghor SMT
M182_103-1_CTD-38	6/17/2022 22:39	max depth/on ground			17.71138	-21.6423	3303	Eddy Hunt
M182_104-1_CTD-39	6/18/2022 5:04	max depth/on ground			17.9995	-21.1349	3123	Eddy Hunt
M182_105-1_CTD-40	6/18/2022 14:03	max depth/on ground			17.99977	-20.3007	3160	E3
M182_106-1_EM122-15	6/18/2022 16:08	profile start			17.93813	-20.2987	3163	
M182_106-1_EM122-15	6/18/2022 20:01	profile end			17.93895	-20.8095	2956	
M182_107-1_TVMUC-9	6/18/2022 21:30	max depth/on ground	17.98451194	-20.8143520	17.98448	-20.8144	2892	Eddy Hunt
M182_108- 1_AUV_ABYSS-4	6/19/2022 9:41	in the water			17.99067	-21.9526	0	E2
M182_109-1_TP-5	6/19/2022 13:15	information			17.99705	-21.9746	0	E2
M182_110-1_TP-5	6/19/2022 13:44	information			17.98643	-21.9701	0	E2
M182_111-1_CTD-41	6/19/2022 22:39	max depth/on ground			17.54928	-22.0002	3353	Eddy Hunt
M182_112-1_EM122-16	6/20/2022 8:33	profile start			17.81378	-20.3025	3180	
M182_112-1_EM122-16	6/21/2022 7:28	information			18.09978	-19.7198	3207	
M182_113-1_TVMUC-10	6/21/2022 10:44	max depth/on ground	17.91587101	-20.0187375	17.9158	-20.0189	3205	E3
M182_114-1_TP-6	6/21/2022 12:19	in the water			17.91087	-19.9991	3208	E3
M182_114-1_TP-6	6/21/2022 12:36	in the water			17.92165	-19.999	3207	E3
M182_115-1_CTD-42	6/21/2022 13:26	max depth/on ground			17.91602	-20.0189	3203	E3
M182_116-1_BIGO_II-4	6/21/2022 19:38	deployed			17.91565	-20.0189	3204	E3

M182_117-1_AUV_ABYSS-5	6/21/2022 21:58	in the water			17.90348	-19.9873	3211	E3 CV	
M182_118-1_CTD-43	6/21/2022 23:56	max depth/on ground			17.9142	-20.0182	3204	E3	
M182_119-1_XOFOS-14	6/22/2022 1:30	profile start			17.91305	-20.0182	3204	E3	water column
M182_119-1_XOFOS-14	6/22/2022 4:20	profile end			17.86737	-20.0182	3209	E3	water column
M182_120-1_XOFOS-15	6/22/2022 6:46	profile start			17.86543	-20.0174	3212	E3	
M182_120-1_XOFOS-15	6/22/2022 10:04	profile end			17.88792	-20.0287	3205	E3	
M182_121-1_GC-3	6/22/2022 13:12	max depth/on ground	17.91242793	-20.0187128	17.91243	-20.0188	3204	E3	
M182_122-1_TP-7	6/22/2022 14:00	information			17.91215	-20.0189	3204	E3	
M182_123-1_TP-7	6/22/2022 14:47	information			17.90697	-20.0015	3208	E3	
M182_124-1_CTD-44	6/22/2022 20:54	max depth/on ground			17.99363	-19.5503	3220	between E3 VC - E4	
M182_125-1_EM122-17	6/22/2022 23:44	profile start			18.21755	-19.5486	3190		
M182_125-1_EM122-17	6/23/2022 9:36	profile end			18.22308	-18.189	2838		
M182_126-1_GC-4	6/23/2022 11:10	max depth/on ground	18.16877807	-18.2208604	18.1688	-18.2209	2864	E4	
M182_127-1_BBL-1	6/23/2022 13:08	in the water			18.16895	-18.2167	0	E4	
M182_128-1_TP-8	6/23/2022 13:58	in the water			18.15827	-18.2521	2877	E4	
M182_128-1_TP-8	6/23/2022 14:17	in the water			18.16993	-18.2517	2878	E4	
M182_129-1_AUV_ABYSS-6	6/23/2022 18:17	in the water			18.14998	-18.2441	2878	E4	
M182_130-1_DSR-3	6/23/2022 22:39	deployed	18.16452541	-18.2210033	18.16447	-18.221	2865	E4	
M182_131-1_XOFOS-16	6/24/2022 1:15	profile start			18.16455	-18.2212	2870	E4	

M182_131-1_XOFOS-16	6/24/2022 4:12	profile end			18.18175	-18.2145	2859	E4	
M182_132-1_TVMUC-11	6/24/2022 6:23	max depth/on ground			18.16882	-18.2209	2866	E4	
M182_133-1_AUV_ANTON-4	6/24/2022 9:15	in the water			18.1377	-18.2506	0	E4	
M182_134-1_XOFOS-17	6/24/2022 12:39	profile start			18.15627	-18.3165	0	E4	water column
M182_134-1_XOFOS-17	6/24/2022 16:57	on deck			18.21723	-18.3027	0	E4	water column
M182_135-1_BIGO_I-2	6/24/2022 19:30	deployed	18.16923346	-18.2257813	18.1688	-18.2257	0	E4	
M182_136-1_EM122-18	6/24/2022 21:24	profile start			18.10952	-18.2038	2886		
M182_136-1_EM122-18	6/25/2022 21:08	profile end			18.05552	-18.1989	2904		
M182_137-1_TVMUC-12	6/25/2022 1:49	max depth/on ground			18.1163	-18.6112	3072	E4	
M182_138-1_CTD-45	6/25/2022 14:57	max depth/on ground			18.05595	-18.8342	3084		between E3 VC - E4
M182_139-1_TVMUC-13	6/25/2022 23:06	max depth/on ground	18.10492464	-18.357915	18.10468	-18.3578	2977	E4	
M182_140-1_XOFOS-18	6/26/2022 0:26	profile start			18.10472	-18.3593	2978	E4	water column
M182_140-1_XOFOS-18	6/26/2022 5:05	on deck			18.16893	-18.3568	2905	E4	water column
M182_141-1_AUV_ABYSS-7	6/26/2022 6:59	in the water			18.15497	-18.2465	2876	E4	
M182_142-1_TVMUC-14	6/26/2022 11:48	max depth/on ground	18.18006513	-18.5409803	18.17978	-18.5409	3052	E4	
M182_143-1_TVMUC-15	6/26/2022 17:06	max depth/on ground	18.28932508	-18.3760131	18.2891	-18.376	2949	E4	
M182_144-1_XOFOS-19	6/26/2022 20:22	profile start			18.0972	-18.3531	2930	E4	

M182_144-1_XOFOS-19	6/26/2022 23:32	profile end			18.12268	-18.3602	2935	E4	
M182_145-1_XOFOS-20	6/27/2022 4:09	profile start			18.17982	-17.9938	2478	E4	
M182_145-1_XOFOS-20	6/27/2022 7:39	profile end			18.15163	-18.0038	2579	E4	
M182_146-1_TVMUC-16	6/27/2022 9:59	max depth/on ground	18.18073195	-17.9937853	18.18042	-17.9938	2478	E4	
M182_147-1_AUV_ABYSS-8	6/27/2022 13:09	in the water			18.1632	-18.2527	2883	E4	
M182_148-1_CTD-46	6/27/2022 17:31	max depth/on ground			18.0563	-17.956	0	E4	
M182_149-1_TVMUC-17	6/27/2022 19:44	max depth/on ground	18.05657579	-17.9561319	18.0563	-17.956	2733	E4	
M182_150-1_EM122-19	6/27/2022 21:46	profile start			18.2185	-17.9873	2471		
M182_150-1_EM122-19	6/28/2022 7:09	profile end			18.16362	-18.2193	2867		
M182_151-1_TP-9	6/28/2022 11:10	information			18.15365	-18.2527	0	E4	
M182_152-1_TP-9	6/28/2022 12:13	information			18.15433	-18.2528	0	E4	
M182_153-1_EM122-20	6/28/2022 15:08	profile start			18.11702	-17.9499	2806		
M182_153-1_EM122-20	6/29/2022 9:00	profile end			18.26365	-16.3964	76		
M182_154-1_CTD-47	6/28/2022 20:30	max depth/on ground			18.12412	-17.2445	2161	between E4 - E5	
M182_155-1_XOFOS-21	6/28/2022 22:56	profile start			18.12402	-17.2453	2159	between E4 - E5	water column
M182_155-1_XOFOS-21	6/29/2022 2:18	profile end			18.17695	-17.259	2185	between E4 - E5	water column
M182_156-1_CTD-48	6/29/2022 7:41	max depth/on ground			18.17385	-16.5142	176	E5	
M182_157-1_CTD-49	6/29/2022 9:15	max depth/on ground			18.26507	-16.3963	77	E5	
M182_158-1_EM710-1	6/29/2022 10:06	profile start			18.26417	-16.3921	75		
M182_158-1_EM710-1	6/29/2022 14:10	profile end			18.27207	-16.3949	74		

M182_159-1_BIGO_I-3	6/29/2022 15:36	deployed	18.27155	-16.3815	71	E5
M182_160-1_TVMUC-18	6/29/2022 16:08	max depth/on ground	18.27153	-16.3818	71	E5
M182_161-1_TVMUC-19	6/29/2022 16:29	max depth/on ground	18.27153	-16.3818	71	E5
M182_162-1_XOFOS-22	6/29/2022 20:12	profile start	18.26863	-16.3666	66	E5
M182_162-1_XOFOS-22	6/29/2022 21:03	profile end	18.27467	-16.3688	432	E5
M182_163-1_TP-10	6/29/2022 22:06	in the water	18.27077	-16.3754	70	E5
M182_164-1_GC-5	6/30/2022 8:26	max depth/on ground	18.27065	-16.3818	72	E5
M182_165-1_AUV_ANTON-5	6/30/2022 10:30	in the water	18.26927	-16.3821	72	E5
M182_166-1_AUV_LUISE-1	6/30/2022 11:14	in the water	18.26928	-16.3821	72	E5
M182_167-1_AUV_ABYSS-9	6/30/2022 19:00	in the water	18.27162	-16.3817	71	E5
M182_168-1_XOFOS-23	6/30/2022 22:11	profile start	18.26967	-16.3813	69	E5
M182_168-1_XOFOS-23	6/30/2022 22:50	profile end	18.27475	-16.3813	72	E5
M182_169-1_XOFOS-24	6/30/2022 23:32	profile start	18.26983	-16.3743	70	E5
M182_169-1_XOFOS-24	7/1/2022 0:01	profile end	18.27388	-16.3743	69	E5
M182_170-1_EM122-21	7/1/2022 9:30	profile start	18.24657	-16.4326	89	
M182_170-1_EM122-21	7/3/2022 7:30	profile end	17.9873	-21.9792	3293	
M182_171-1_TVMUC-20	7/1/2022 11:17	max depth/on ground	18.19535	-16.5836	501	E5
M182_172-1_TVMUC-21	7/1/2022 14:39	max depth/on ground	18.1031	-16.9654	1704	between E4 - E5
M182_173-1_CTD-50	7/1/2022 19:24	max depth/on ground	18.07032	-17.5815	2571	between E4 - E5

M182_174-1_XOFOS-25	7/2/2022 15:36	profile start			17.87085	-20.0304	3208	E3	water column
M182_174-1_XOFOS-25	7/2/2022 17:05	profile end			17.89365	-20.0238	3207	E3	water column
M182_175-1_TP-11	7/3/2022 7:42	in the water			17.99483	-21.9793	3291	E2	
M182_175-1_TP-11	7/3/2022 8:15	in the water			18.01273	-21.9792	3292	E2	
M182_176-1_BBL-2	7/3/2022 12:44	max depth/on ground	18.00347648	-21.9999947	18.00293	-22	3296	E2	
M182_177-1_DSR-4	7/3/2022 18:28	max depth/on ground	18.00533073	-21.9989815	18.00502	-21.999	3296	E2	
M182_178-1_AUV_ABYSS-10	7/3/2022 20:15	in the water			17.9926	-21.9772	3291	E2	
M182_179-1_CTD-51	7/3/2022 22:22	max depth/on ground			18.00727	-21.9795	3290	E2	
M182_180-1_TP-12	7/4/2022 7:56	information			18.00727	-21.9794	3290	E2	
M182_181-1_TP-12	7/4/2022 8:30	information			18.00727	-21.9794	3291	E2	
M182_182-1_EM122-22	7/4/2022 10:25	profile start			18.00838	-21.9751	3291		
M182_182-1_EM122-22	7/5/2022 10:23	profile end			21.16643	-20.9169	4175		
M182_183-1_CTD-52	7/5/2022 11:24	max depth/on ground			21.16662	-20.9166	4176	CB	
M182_184-1_TVMUC-22	7/5/2022 14:11	max depth/on ground			21.16663	-20.9166	4176	CB	
M182_185-1_GC-6	7/5/2022 16:37	max depth/on ground			21.16663	-20.9667	4176	CB	

8 Data and Sample Storage and Availability

The data were collected within the REEBUS project (BMBF) and the MOSES project (HGF). The data management is handled by the GEOMAR data management team. Data sharing and exchange will take place within the Ocean Science Information System (OSIS-Kiel) hosted at GEOMAR. In a first phase data are only available to the project members. After a two-year proprietary time the data management team will publish these data by dissemination to national and international data archives, i.e. the data will be submitted to PANGAEA. Digital object identifiers (DOIs) are automatically assigned to data sets archived in the World Data Centre PANGAEA (Data Publisher for Earth & Environmental Science) making them publically retrievable, citeable and reusable for the future. All metadata are immediately available publically via the following link pointing to OSIS-Kiel in the GEOMAR data management portal (<https://portal.geomar.de/metadata/leg/show/348695>). In addition, the portal provides a single downloadable KML formatted file (<https://portal.geomar.de/metadata/leg/kmlexport/>), which retrieves and combines up-to-date cruise (M182) related information, links to restricted data and to published data for visualization e.g. in GoogleEarth. In adherence to the MOSES Data Policy, basic campaign data, sensor metadata as well as metadata about collected data sets (including links to OSIS and PANGAEA) will be made publically available using the MOSES data portal. This does not affect the two-year proprietary use period for collected data, since only metadata will be published at the MOSES Portal.

9 Acknowledgements

Our thanks goes to master Rainer Hammacher, the officers, and the entire crew of RV METEOR for their exceptional support, creating a highly professional working environment and significantly contributing to the success of this cruise. We are grateful for the friendly atmosphere on board. Special thanks to the Ministère des Pêches et de l'Économie Maritime (République Islamique de Mauritanie) and the Instituto Marítimo Portuário-IMP (Cabo Verde) for their support and permission to conduct research in Mauritanian and Cape Verdian waters. Our gratitude also goes to the German Ministry of Foreign Affairs for their support. Acknowledgments to the Geschäftsstelle des Gutachterpanels Forschungsschiffe (GPF) and the Leitstelle Deutsche Forschungsschiffe (Hamburg) for their valuable assistance. The ship time of RV METEOR and financial support for the cruise logistics were generously provided by the German Research Council, DFG. The project REEBUS is funded by the German Ministry for Education and Research, BMBF.

10 References

- Allredge, A.L., Passow, U., and Logan, B.E. (1993). The abundance and significance of a class of large, transparent organic particles in the ocean. *Deep-Sea Res Pt I Oceanogr Res Pap* 40(6), 1131-1140. doi: 10.1016/0967-0637(93)90129-q.
- Arnosti, C. (2003). Fluorescent derivatization of polysaccharides and carbohydrate-containing biopolymers for measurement of enzyme activities in complex media. *J Chromatogr B Analyt Technol Biomed Life Sci* 793(1), 181-191. doi: 10.1016/s1570-0232(03)00375-1.
- Arnosti, C. (2011). Microbial extracellular enzymes and the marine carbon cycle. *Ann Rev Mar Sci* 3, 401-425. doi: 10.1146/annurev-marine-120709-142731.
- Azam, F. (1998). Microbial control of oceanic carbon flux: The plot thickens. *Science* 280(5364), 694-696. doi: 10.1126/science.280.5364.694.
- Baltar, F., Arístegui, J., Sintés, E., van Aken, H.M., Gasol, J.M., and Herndl, G.J. (2009). Prokaryotic extracellular enzymatic activity in relation to biomass production and respiration in the meso- and bathypelagic waters of the (sub)tropical Atlantic. *Environ Microbiol* 11(8), 1998-2014. doi: 10.1111/j.1462-2920.2009.01922.x.
- Benner, R., and Amon, R.M. (2015). The size-reactivity continuum of major bioelements in the ocean. *Ann Rev Mar Sci* 7, 185-205. doi: 10.1146/annurev-marine-010213-135126.
- Busch, K., Endres, S., Iversen, M.H., Michels, J., Nöthig, E.-M., and Engel, A. (2017). Bacterial Colonization and Vertical Distribution of Marine Gel Particles (TEP and CSP) in the Arctic Fram Strait. *Frontiers in Marine Science* 4. doi: 10.3389/fmars.2017.00166.
- Dale, A. W., Bourbonnais, A., Altabet, M., Wallmann, K., & Sommer, S. (2019). Isotopic fingerprints of benthic nitrogen cycling in the Peruvian oxygen minimum zone. *Geochim. Cosmochim. Acta*, 245, 406– 425.
- Dhakar, S. P. & Burdige, D. J. 1996 A coupled, non-linear, steady-state model for early diagenetic processes in pelagic sediments *Am J Sci* 296:296-330.
- Dittmar, T., Lennartz, S.T., Buck-Wiese, H., Hansell, D.A., Santinelli, C., Vanni, C., et al. (2021). Enigmatic persistence of dissolved organic matter in the ocean. *Nature Reviews Earth & Environment*. doi: 10.1038/s43017-021-00183-7.
- Dundas, K., and Przeslawski, R. (2009). Deep Sea Lebensspuren Biological Features on the Seafloor of the Eastern and Western Australian Margin. *Geoscience Australia Record* 2009/26, 76 pp.
- Engel, A. (2002). Direct relationship between CO₂ uptake and transparent exopolymer particles production in natural phytoplankton. *J Plankton Res* 24(1), 49-53.
- Engel, A. (2009). "Determination of Marine Gel Particles," in *Practical Guidelines for the Analysis of Seawater*, ed. O. Wurl. CRC Press), 408.

- Engel, A., and Galgani, L. (2016). The organic sea-surface microlayer in the upwelling region off the coast of Peru and potential implications for air–sea exchange processes. *Biogeosciences* 13(4), 989-1007. doi: 10.5194/bg-13-989-2016.
- Engel, A., and Händel, N. (2011). A novel protocol for determining the concentration and composition of sugars in particulate and in high molecular weight dissolved organic matter (HMW-DOM) in seawater. *Marine Chemistry* 127(1-4), 180-191. doi: 10.1016/j.marchem.2011.09.004.
- Engel, A., Goldthwait, S., Passow, U., and Alldredge, A. (2002). Temporal decoupling of carbon and nitrogen dynamics in a mesocosm diatom bloom. *Limnology and Oceanography* 47(3), 753-761. doi: 10.4319/lo.2002.47.3.0753.
- Engel, A., Thomas, S., Riebesell, U., Rochelle-Newall, E., and Zondervan, I. (2004). Polysaccharide aggregation as a potential sink of marine dissolved organic carbon. *Nature* 428(6986), 929-932. doi: 10.1038/nature02453.
- Falkowski, P.G., Barber, R.T., and Smetacek, V.V. (1998). Biogeochemical controls and feedbacks on ocean primary production. *Science* 281(5374), 200-207.
- Falkowski, P.G., Fenchel, T., and DeLong, E.F. (2008). The microbial engines that drive Earth's biogeochemical cycles. *Science* 320(5879), 1034-1039. doi: 10.1126/science.1153213.
- Field, C.B., Behrenfeld, M.J., Randerson, J.T., and Falkowski, P. (1998). Primary production of the biosphere: integrating terrestrial and oceanic components. *Science* 281(5374), 237-240.
- Grasshof, K., Kremling, K., and Ehrardt, M. (1999). *Methods of seawater analysis*; 3. compl. rev. and ext.
- Hansell, D.A., and Carlson, C.A. (2015). *Biogeochemistry of marine dissolved organic matter*. New York: Elsevier.
- Hansell, D.A., Carlson, C.A., Repeta, D.J., and Schlitzer, R. (2009). Dissolved organic matter in the ocean. *Oceanography* 22(4), 202-211.
- Hoppe, H.G. (1993). "Use of fluorogenic model substrates for extracellular enzyme activity (EEA) measurement of bacteria," in *Current methods in aquatic microbial ecology*, eds. P. Kemp, B. Sherr, E. Sherr & J. Cole. (Boca Raton: CRC Press), 423-431.
- Kujawinski, E.B. (2011). The impact of microbial metabolism on marine dissolved organic matter. *Ann Rev Mar Sci* 3, 567-599. doi: 10.1146/annurev-marine-120308-081003.
- Lindroth, P., and Mopper, K. (2002). High performance liquid chromatographic determination of subpicomole amounts of amino acids by precolumn fluorescence derivatization with o-phthaldialdehyde. *Analytical Chemistry* 51(11), 1667-1674. doi: 10.1021/ac50047a019.
- Loginova, A.N., Thomsen, S., and Engel, A. (2016). Chromophoric and fluorescent dissolved organic matter in and above the oxygen minimum zone off Peru. *Journal of Geophysical Research: Oceans* 121(11), 7973-7990. doi: 10.1002/2016jc011906.

- Long, R.A., and Azam, F. (1996). Abundant protein-containing particles in the sea. *Aquat Microb Ecol* 10(3), 213-221. doi: DOI 10.3354/ame010213.
- Mari, X., and Kiørboe, T. (1996). Abundance, size distribution and bacterial colonization of transparent exopolymeric particles (TEP) during spring in the Kattegat. *Journal of Plankton Research* 18(6), 969-986. doi: 10.1093/plankt/18.6.969.
- Moran, M.A., Kujawinski, E.B., Stubbins, A., Fatland, R., Aluwihare, L.I., Buchan, A., et al. (2016). Deciphering ocean carbon in a changing world. *Proc Natl Acad Sci U S A* 113(12), 3143-3151. doi: 10.1073/pnas.1514645113.
- Ogawa, H., and Tanoue, E. (2003). <Ogawa-Tanoue2003_Article_DissolvedOrganicMatterInOceani.pdf>. *Journal of Oceanography* 59(2), 129-147. doi: 10.1023/a:1025528919771.
- Omand, M.M., D'Asaro, E.A., Lee, C.M., Perry, M.J., Briggs, N., Cetinic, I., et al. (2015). Eddy-driven subduction exports particulate organic carbon from the spring bloom. *Science* 348(6231), 222-225. doi: 10.1126/science.1260062.
- Parada, A.E., Needham, D.M., and Fuhrman, J.A. (2016). Every base matters: assessing small subunit rRNA primers for marine microbiomes with mock communities, time series and global field samples. *Environ Microbiol* 18(5), 1403-1414. doi: 10.1111/1462-2920.13023.
- Parks, D.H., Chuvochina, M., Waite, D.W., Rinke, C., Skarszewski, A., Chaumeil, P.A., et al. (2018). A standardized bacterial taxonomy based on genome phylogeny substantially revises the tree of life. *Nat Biotechnol*. doi: 10.1038/nbt.4229.
- Pfannkuche, O., Linke, P. (2003) GEOMAR Landers as Long-Term Deep-Sea Observatories, *Sea Technology*, 44, 50-55.
- Pontiller, B., Martínez-García, S., Lundin, D., and Pinhassi, J. (2020). Labile dissolved organic matter compound characteristics select for divergence in marine bacterial activity and transcription. *Front Microbiol* 11, 588778. doi: 10.3389/fmicb.2020.588778.
- Pontiller, B., Pérez-Martínez, C., Bunse, C., Osbeck, C.M.G., González, J.M., Lundin, D., et al. (2021). Taxon-Specific Shifts in Bacterial and Archaeal Transcription of Dissolved Organic Matter Cycling Genes in a Stratified Fjord. *mSystems*. doi: 10.1128/mSystems.00575-21.
- Poretsky, R.S., Gifford, S., Rinta-Kanto, J., Vila-Costa, M., and Moran, M.A. (2009). Analyzing gene expression from marine microbial communities using environmental transcriptomics. *J Vis Exp* 24, 1-6. doi: 10.3791/1086.
- Salazar, G., and Sunagawa, S. (2017). Marine microbial diversity. *Curr Biol* 27(11), R489-R494. doi: 10.1016/j.cub.2017.01.017.
- Salazar, G., Paoli, L., Alberti, A., Huerta-Cepas, J., Ruscheweyh, H.J., Cuenca, M., et al. (2019). Gene expression changes and community turnover differentially shape the global ocean metatranscriptome. *Cell* 179(5), 1068-1083 e1021. doi: 10.1016/j.cell.2019.10.014.

Sanders, R., Henson, S.A., Koski, M., De La Rocha, C.L., Painter, S.C., Poulton, A.J., et al. (2014). The Biological Carbon Pump in the North Atlantic. *Progress in Oceanography* 129, 200-218. doi: 10.1016/j.pocean.2014.05.005.

Satinsky, B.M., Smith, C.B., Sharma, S., Landa, M., Medeiros, P.M., Coles, V.J., et al. (2017). Expression patterns of elemental cycling genes in the Amazon River Plume. *ISME J* 11(8), 1852-1864. doi: 10.1038/ismej.2017.46.

Scholz, F., Löschera, C. R., Fiskal, A., Sommer, S. Hensen. C., Lomnitz, U., Wuttig, K., Göttlicher, J., Kosse, E., Steininger, R., Canfield, D. E. 2016 Nitrate-dependent iron oxidation limits iron transport in anoxic ocean regions *Earth Planet. Sci. Lett.* 454, 272-281.

Sommer, S., Linke, P., Pfannkuche, O., Schleicher, T., Schneider v. Deimling, J., Reitz, A., Haeckel, M., Flögel, S., Hensen, C. (2009) Seabed methane emissions and the habitat of frenulate tubeworms on the Captain Arutyunov mud volcano (Gulf of Cadiz). *Marine Ecology Progress Series*, 382, 69-86.

Sugimura, Y., and Suzuki, Y. (1988). A high-temperature catalytic oxidation method for the determination of non-volatile dissolved organic carbon in seawater by direct injection of a liquid sample. *Marine Chemistry* 24(2), 105-131. doi: [https://doi.org/10.1016/0304-4203\(88\)90043-6](https://doi.org/10.1016/0304-4203(88)90043-6).

Sunagawa, S., Coelho, L.P., Chaffron, S., Kultima, J.R., Labadie, K., Salazar, G., et al. (2015). Structure and function of the global ocean microbiome. *Science* 348(6237), 1261359. doi: 10.1126/science.1261359.

Thornton, D.C.O., and Chen, J. (2017). Exopolymer production as a function of cell permeability and death in a diatom (*Thalassiosira weissflogii*) and a cyanobacterium (*Synechococcus elongatus*). *J Phycol* 53(2), 245-260. doi: 10.1111/jpy.12470.

Verdugo, P., Alldredge, A.L., Azam, F., Kirchman, D.L., Passow, U., and Santschi, P.H. (2004). The oceanic gel phase: a bridge in the DOM-POM continuum. *Mar Chem* 92(1-4), 67-85. doi: 10.1016/j.marchem.2004.06.017.

Weiss, M.S., Abele, U., Weckesser, J., Welte, W., Schiltz, E., and Schulz, G.E. (1991). Molecular architecture and electrostatic properties of a bacterial porin. *Science* 254(5038), 1627-1630. doi: 10.1126/science.1721242.

11 Abbreviations

ADCP Acoustic Doppler velocity profiler

AUV Autonomous Underwater Vehicle

BBL Benthic Boundary Layer

CTD Conductivity Temperature Depth

MBES Multibeam

MUC Multicorer

SST Sea surface temperature

XOFOS eXtended OceanFloor Observation System

12 Appendices

12.1 Water Column Biogeochemistry

CTD Water Sampling

During M182 the GEOMAR GO3 rosette frame equipped with the GEOMAR SBE6, a Seabird Electronics (SBE) 911/917plus underwater unit, was used. The SBE6 was equipped with one Digiquartz pressure sensor (s/n 0615) and double sensor packages for temperature (T), conductivity (C) and oxygen (O₂) (primary set: T1 = s/n 4875, C1 = s/n 2512, O1 = s/n 1312; secondary set: T2 = s/n 4831, C2 = s/n 2537, O2 = s/n 2590). Additionally, a WET Labs fluorescence/turbidity sensor (FLNTURTD, s/n 4775), a PAR light sensor from Biospherical Instruments (s/n 70714), a Valeport altimeter (s/n 42299) to measure the distance to the seafloor with high precision, and an Underwater Vision Profiler 5 (UVP) designed to take photographs and to count and estimate the size of particles bigger than 100 µm (e.g., zooplankton), were mounted on the rosette frame. The FLNTURTD sensor was not installed during the first two CTD casts (M182_002 and M182_005). Thereafter, during the first few CTD deployments, we obtained erroneous scatter signals from the FLNTURTD sensor. Therefore, we decided to turn off the UVP during two consecutive CTD casts (M182_046 and M182_047) to check for potential interference between the UVP and the FLNTURTD sensor. As it turned out, the flashlight from the Underwater Vision Profiler (UVP) caused these erroneous readings through the backscatter of the flashlight on the rosette frame. Moving the sensor position facing outwards of the rosette frame and above the UVP solved the issue, and we did not experience any erroneous readings until the end of the cruise. In total, we deployed the UVP on 48 of the 52 CTD casts (M182_115 and M182_118 – uncharged batteries) and took pictures of a total of about 450.000 objects. The data will undergo post-processing after the cruise by Dr. Rainer Kiko and colleagues and will be published on ecotaxa.obs-vlfr.fr. The CTD data acquisition was done using Seabird SBE Data Processing software (v7.26.7). CTD data from the downcast were used for downstream analysis. For visualization of CTD profiles, raw values were averaged into 1 m bins and plotted using Ocean Data View and R. Water samples were collected with 24 x 10 L Niskin bottles attached to the GEOMAR rosette frame.

Table 12.1 Overview of the conducted CTD profiles and depths of sampled biological and chemical parameters. Abbreviation as follows: Dissolved organic matter (DOM), particulate organic matter (POM), dissolved carbohydrates (DCHO, dissolved amino acids (DAA), chromophoric dissolved organic matter (CDOM), fluorescent dissolved organic matter (FDOM), flow cytometry (FC), dissolved organic carbon (DOC), particulate organic carbon (POC), particulate organic nitrogen (PON), chlorophyll a (Chl a), biogenic silica (BSi), transparent exopolymer particles (TEP), Coomassie stainable particles (CSP), extracellular enzymatic activity (EEA), polysaccharide hydrolysis (PS), and oxygen (O2).

Area Station /	Lat. (°N)	Long. (°W)	Bottom depth (m)	Sampling date	Sampling depth (m) for parameters:					
					DOM (i.e., DOC, DCHO, DAA, DOP, CDOM, FDOM), FC	POM (i.e., POC, PON, Chl a, BSi, TEP, CSP)	EEA	PS	DNA & RNA	O ₂ & nutrients
CVOO	17° 35.000'	24° 17.000'	3596	31.05.2022	10, 80, 200, 450	10, 80, 200, 450	10, 80, 200, 450	-	-	10, 20, 40, 60, 80, 100, 120, 150, 200, 250, 350, 450, 600, 1000, 1500, 2000, 3000, 3500, bottom
S1	17° 59.996'	24° 20.006'	3696	01.06.2022	5, 25, 75, 125, 400, 800	5, 25, 75, 125, 400, 800	5, 25, 75, 125, 400, 800	5, 75, 400, 800	5, 25, 75, 125, 400, 800	5, 25, 75, 125, 400, 800, 1500, 3500

S2	18° 00.016'	23° 36,558'	3612	02.06.2022	5, 25, 60, 100, 350, 800, 1500	5, 25, 60, 100, 350, 800	5, 25, 60, 100, 350, 800, 1500	-	5, 25, 60, 100, 350, 800, 1500	5, 350, 1500, 3500
E1 Hill	18° 02.950'	23° 49,223'	3554	04.06.2022	-	-	-	-	25, 65, 100, 160, 250, 400, 500, 700, 900	-
S3	18° 00.123'	22° 47.179'	3414	05.06.2022	5, 20, 40, 90, 390, 800, 1500	5, 20, 40, 90, 390, 800	5, 20, 40, 90, 390, 800, 1500	-	5, 20, 40, 90, 390, 800, 1500	5, 390, 1500, 3300
ES24	17° 41.645'	21° 59.984'	3332	12.06.2022	5, 45, 80, 200, 420, 800, 1500	5, 45, 80, 200, 420, 800	5, 45, 80, 200, 420, 800, 1500	-	5, 45, 80, 200, 420, 800, 1500	5, 45, 80, 200, 420, 800, 1500
ES25/S4	17° 59.966'	22° 00.063'	3293	13.06.2022	5, 40, 80, 200, 410, 800, 1500, 3100	5, 40, 80, 200, 410, 800	5, 40, 80, 200, 410, 800, 1500	5, 40, 410, 800	5, 40, 80, 200, 410, 800, 1500	5, 40, 80, 200, 410, 800, 1500, 3100
ES27 rim north	18° 09.846'	22° 12.112'	3329	14.06.2022	5, 45, 120, 315, 410, 800, 1500	5, 45, 120, 315,	5, 45, 120, 315,	-	5, 45, 120, 315,	5, 45, 120, 315, 410, 800, 1500

						410, 800	410, 800, 1500		410, 800, 1500	
ES28 core	17° 41.670'	21° 59.845'	3333	15.05.2022	5, 30, 150, 310, 440, 800, 1500	5, 30, 150, 310, 440, 800	5, 30, 150, 310, 440, 800, 1500	-	5, 30, 150, 310, 440, 800, 1500	5, 30, 150, 310, 440, 800, 1500
ES30 south	17° 19.259'	22° 00.918'	2884	16.06.2022	5, 30, 70, 200, 380, 800, 1500	5, 30, 70, 200, 380, 800	5, 30, 70, 200, 380, 800, 1500	5, 30, 380, 800	5, 30, 70, 200, 380, 800, 1500	5, 30, 70, 200, 380, 800, 1500
ES31 seamount	17° 13.273'	21° 54,870'	1154	16.06.2022	5, 40, 58, 200, 350, 800	5, 40, 58, 200, 350, 800	5, 40, 58, 200, 350, 800	-	5, 40, 58, 200, 350, 800	5, 40, 58, 200, 350, 800
ES32 west	17° 41.710'	22° 23.239'	3342	16.06.2022	5, 45, 80, 180, 390, 800, 1500	5, 45, 80, 180, 390, 800	5, 45, 80, 180, 390, 800, 1500	-	5, 45, 80, 180, 390, 800, 1500	5, 45, 80, 180, 390, 800, 1500
ES33 east	17° 42.681'	21° 38.536'	3303	17.06.2022	5, 50, 110, 200, 345, 800, 1500	5, 50, 110, 200, 345, 800	5, 50, 110, 200, 345, 800	-	5, 50, 110, 200, 345, 800, 1500	5, 50, 110, 200, 345, 800, 1500

							800, 1500			
S5	17° 59.965'	21° 08.097'	3123	18.06.2022	5, 38, 50, 200, 380, 800, 1500	5, 38, 50, 200, 380, 800	5, 38, 50, 200, 380, 800, 1500, 3000	-	5, 38, 50, 200, 380, 800, 1500	5, 38, 50, 200, 380, 800, 1500, 3000
S6	17° 59.989'	20° 18.040'	3160	18.06.2022	5, 45, 120, 350, 800, 1500	5, 45, 120, 350, 800	5, 45, 120, 350, 800, 1500	-	5, 45, 120, 350, 800, 1500	5, 45, 120, 350, 800, 1500, 3000
ES34 core new	17° 32.960'	22° 00.017'	3353	19.06.2022	5, 45, 110, 190, 380, 800, 1500	5, 45, 110, 190, 380, 800	5, 45, 110, 190, 380, 800, 1500	5, 110, 380, 800	5, 45, 110, 190, 380, 800, 1500	5, 45, 110, 190, 380, 800, 1500
LAT1	17° 54.917'	20° 01.093'	3203	21.06.2022	5, 35, 80, 200, 330, 800, 1500	5, 35, 80, 200, 330, 800	5, 35, 80, 200, 330, 800, 1500	-	5, 35, 80, 200, 330, 800, 1500	5, 35, 80, 200, 330, 800, 1500, 3100
S7	17° 55.620'	19° 33.024'	3219	22.06.2022	5, 35, 69, 150, 320, 800, 1500	5, 35, 69, 150, 320, 800	5, 35, 69, 150, 320,	-	-	5, 35, 69, 150, 320, 800, 1500, 3100

							800, 1500			
S8	18° 03.330'	18° 49.987'	3085	26.06.2022	7, 23, 140, 220, 370, 800, 1500	7, 23, 140, 220, 370, 800	7, 23, 140, 220, 370, 800, 1500	-	-	7, 23, 140, 220, 370, 800, 1500, 3000
S9	18° 03.374'	17° 57.358'	2732	27.06.2022	5, 19, 60, 180, 360, 800, 1500	5, 19, 60, 180, 360, 800	5, 19, 60, 180, 360, 800, 1500	-	-	5, 19, 60, 180, 360, 800, 1500
S10	18° 07.447'	17° 14.668'	2159	28.06.2022	5, 35, 70, 150, 340, 800, 1500	5, 35, 70, 150, 340, 800	5, 35, 70, 150, 340, 800, 1500	-	-	5, 35, 70, 150, 340, 800, 1500
S11	18° 10.249'	16° 30,852'	176	29.06.2022	5, 19, 70, 100, 150	5, 19, 70, 100, 150	5, 19, 70, 100, 150	-	-	5, 19, 70, 100, 150
S12	18° 04.216'	17° 34.885'	2569	01.07.2022	5, 26, 75, 150, 360, 800	5, 26, 75, 150, 360, 800	5, 26, 75, 150, 360, 800	-	-	5, 26, 75, 150, 360, 800
S13 LTA new	18° 00.435'	21° 58.766'	3290	03.07.2022	5, 52, 82, 180, 380, 800, 1500	5, 52, 82, 180, 380,	5, 52, 82, 180, 380,	-	52*, 82*, 180*, 380*,	5, 52, 82, 180, 380,

							380, 800	800, 1500		800*, 1500*	800, 1500, 3200
S14 Blanc	Cape Blanc	21° 09.985'	20° 55.015'	4175	05.07.2022	6, 42, 85, 220, 380, 800, 1500	6, 42, 85, 220, 380, 800, 1500	6, 42, 85, 220, 380, 800, 1500	-	6, 42, 85, 220, 380, 800, 1500	6, 42, 85, 220, 380, 800, 1500, 3000

* Only DNA was sampled for testing amplicon primers (Dr. Henk-Jan Hoving).

Table 12.2 Overview of conducted CTD profiles for the characterization/hunting of an eddy without water sampling down to 1500 m depth. The distance between stations was 8 nm from ES1 to 15 and 16 nm from ES16 - 23.

Area / Station	Transect direction	Lat. (°N)	Long. (°W)	Bottom depth (m)	Water temperature (°C)	Date
ES1	NE	18° 00.816'	22° 38.995'	3382	23.7	09.06.2022
ES2		18° 03.692'	22° 31.799'	3351	23.6	10.06.2022
ES3		18° 06.284'	22° 24.085'	3344	23.7	
ES4		18° 09.203'	22° 16.538'	3345	23.7	
ES5		18° 11.630'	22° 08.849'	3323	23.8	
ES6		18° 14.259'	22° 01.391'	3305	23.3	
ES7		18° 16.745'	21° 54.019'	3277	23.3	
ES8		19° 19.621'	21° 46.801'	3250	23.4	
ES9		18° 22.104'	21° 39.125'	3193	23.8	
ES10		18° 25.036'	21° 31.025'	3129	23.4	
ES11		18° 27.683'	21° 23.498'	3109	23.6	
ES12		18° 30.201'	21° 15.936'	3080	23.3	11.06.2022

ES13	SW	18° 32.995'	21° 08.615'	3096	23.2		
ES14		18° 35.578'	21° 00.939'	3131	22.9		
ES15		18° 38.312'	20° 53.180'	3171	22.6		
ES16		18° 27.733'	21° 23.544'	3102	23.5		
ES17		18° 15.698'	21° 33.012'	3161	23.9		
ES18		18° 02.768'	21° 43.043'	3236	24.1		
ES19		17° 50.388'	21° 53.039'	3300	24.0		
ES20		17° 37.834'	22° 02.711'	3344	23.9		
ES21		17° 25.552'	22° 12.441'	3354	23.7		
ES22		17° 12.576'	22° 22.647'	3338	23.8		12.06.2022
ES23		16° 59.593'	22° 33.694'	3086	24.0		
ES26	-	18° 06.190'	22° 07.941'	NA	23.8	14.06.2022	

12.2 Water Column Biology

Table 12.3 M182 Station and sample overview of the Deep-Sea Biology Group.

Station	Date	Time	Gear	Devices	Did not work	Depth														Sample Type	Type of Analysis*	Number of Samples	
M182_22	04.06.22	Day	CTD	CTD, bottles, UVP, Fluoresc.		900	700	500	400	250	160	100	65	25							eDNA	Metabarcoding	3/depth + 1 blank
M182_92	15.06.22	Day	CTD	CTD, bottles, UVP, Fluoresc.		900	700	500	400	250	160	100	65	25							eDNA	Metabarcoding	3/depth + 1 blank
M182_115	21.06.22	Day	CTD	CTD, bottles, UVP, Fluoresc.		900	700	500	400	250	160	100	65	25							eDNA	Metabarcoding	3/depth + 1 blank
M182_179	03.07.22	Night	CTD	CTD, bottles, UVP, Fluoresc.		1500	800	380	180	82	52										eDNA	Metabarcoding	3/depth + 1 blank

M182_183	05.07.22	Day	CTD	CTD, bottles, UVP, Fluoresc.		1500	800												eDNA	Metabarcoding	1/depth	
M182_1	31.05.22	Day	Multinet	9 x 335µm nets, CTD, Flowmeter	Flow meter	1000-800	800-600	600-500	500-400	400-300	300-200	200-100	100-50	50-0						Specimen in Formalin	Identification, Measuring	9
M182_13	02.06.22	Day	Multinet	9 x 335µm nets, CTD, Flowmeter	Flow meter	1000-800	800-600	600-500	500-400	400-300	300-200	200-100	100-50	50-0						Specimen in Formalin	Identification, Measuring	9
M182_25	05.06.22	Night	Multinet	9 x 335µm nets, CTD, Flowmeter	Flow meter	1000-800	800-600	600-450	450-300	300-200	200-120	120-80	80-50	50-0						Specimen in Formalin, EtOH	Identification, Measuring	9 & 1
M182_33	06.06.22	Night	Multinet	9 x 335µm nets, CTD, Flowmeter	Flow meter	1000-800	800-600	600-450	450-300	300-200	200-120	120-80	80-50	50-0						Specimen in Formalin	Identification, Measuring	9
M182_42	09.06.22	Night	Multinet	9 x 335µm nets, CTD, Flowmeter	Flow meter	1000-800	800-600	600-500	500-400	400-300	300-200	200-100	100-50	50-0						Specimen in Formalin	Identification, Measuring	9
M182_73	13.06.22	Night	Multinet	9 x 335µm nets, CTD, Flowmeter	Flow meter	1000-800	800-600	600-450	450-300	300-200	200-120	120-80	80-50	50-0						Specimen in Formalin	Identification, Measuring	9
M182_86	15.06.22	Night	Multinet	9 x 335µm nets, CTD, Flowmeter	Flow meter	1000-800	800-600	600-450	450-300	300-200	200-120	120-80	80-50	50-0						Specimen in Formalin	Identification, Measuring	9
M182_90	15.06.22	Day	Multinet	9 x 335µm nets, CTD, Flowmeter	Flow meter	1000-800	800-600	600-450	450-300	300-200	200-120	120-80	80-50	50-0						Specimen in Formalin	Identification, Measuring	9
M182_102	17.06.22	Day	Multinet	9 x 335µm nets, CTD, Flowmeter	Flow meter	1000-800	800-600	600-450	450-300	300-200	200-120	120-80	80-50	50-0						Specimen in Formalin	Identification, Measuring	9
M182_40	07.06.22	Night	XOFOS	Stereo camera, ADCP, CTD		900	700	500	375	250	160	100	65	25						2x 4k by 4k 25fps footage	Annotation, Measuring	13 min transects
M182_72	13.06.22	Night	XOFOS	Stereo camera, ADCP, CTD		25	65	100	160	250	375	500	700	900						2x 4k by 4k 25fps footage	Annotation, Measuring	13 min transects
M182_85	15.06.22	Night	XOFOS	Stereo camera, ADCP, CTD	CTD, ADCP	25	65	100	160	250	325	375	500	700	900					2x 4k by 4k 25fps footage	Annotation, Measuring	13 min transects
M182_89	15.06.22	Day	XOFOS	Stereo camera,	CTD	25	65	100	160	250	375	500	700	900						2x 4k by 4k 25fps footage	Annotation, Measuring	13 min transects

				ADCP, CTD																		
M182_101	17.06.22	Day	XOFOS	Stereo camera, ADCP, CTD		25	65	100	160	250	375	500	700	900	450					2x 4k by 4k 25fps footage	Annotation, Measuring	13 min transects
M182_119	22.06.22	Night	XOFOS	Stereo camera, ADCP, CTD		25	65	100	160	250	375	450	500	700	900					2x 4k by 4k 25fps footage	Annotation, Measuring	13 min transects
M182_134	24.06.22	Day	XOFOS	Stereo camera, ADCP, CTD		25	65	100	160	250	375	450	500	700	900	1100	1300	1000		2x 4k by 4k 25fps footage	Annotation, Measuring	13 min transects
M182_140	26.06.22	Night	XOFOS	Stereo camera, ADCP, CTD		25	65	100	160	250	375	450	500	700	900	1000	1100	1300	1500	2x 4k by 4k 25fps footage	Annotation, Measuring	13 min transects
M182_155	28.06.22	Night	XOFOS	Stereo camera, ADCP, CTD	ADC P	25	65	36/45	100	160	250	375	450	500	700	900	1100			2x 4k by 4k 25fps footage	Annotation, Measuring	13 min transects
M182_174	02.07.22	Day	XOFOS	Stereo camera, ADCP, CTD	ADC P	250	450	500	700	900										2x 4k by 4k 25fps footage	Annotation, Measuring	13 min transects

12.3 Benthic Biogeochemistry

Methods

An overview of the sampling stations where porewater geochemistry was analyzed is given in Table 12.4. Sediment cores were retrieved using a multiple-corer (MUC) and a gravity corer (GC). The MUC was equipped with 7 Perspex liners 60 cm long and with an internal diameter of 10 cm. The MUC was lowered into the sediment with a speed of 0.3 m s^{-1} in all deployments. Once on the seafloor, the liners were pushed into the sediment under gravity by a set of lead weights. Penetration did not exceed ca. 35 cm. Long sediment cores up to 460 cm were retrieved with a gravity corer (GC), consisting of a 5 m steel barrel attached to a weight of 1600 kg that pushes the core into the sediment. The GC was lowered into the sediment with a speed of 0.8 to 1.0 m s^{-1} . On retrieval, the inner plastic liner (11 cm inner diameter) was cut into 1-m long segments. Separate BIGO cores were taken by pushing the short liners (diameter 10 cm, length ca. 20 cm) into the sediment within the incubation chambers once the BIGO was back on deck. After retrieval, all MUC and BIGO cores were transferred to a cooling lab at 5°C (the bottom water temperature at the sampling stations was mainly ca. 2°C , increasing to 15°C on the Mauritanian shelf). The GC was sampled immediately in METEOR's geo-laboratory after each 1-m segment was cut lengthwise into a sampling half and an archive half. The two halves were then transferred into protective cases (D-tubes) for long-term storage (4°C) at GEOMAR's refrigerated core repository.

The MUC and BIGO cores were sliced at a resolution of 1 cm close to the surface increasing to 4 cm at sediment depths > 20 cm. GCs were sampled at 15 cm intervals. For all measurements and sub-sampling for redox-sensitive parameters (e.g. dissolved Fe, nutrients) from the MUC cores, the sediments were sectioned inside an argon filled glove bag. Supernatant bottom water samples of the MUC cores were also taken. Sediment samples were spun in a refrigerated centrifuge at 4000 G for 20 min at 3°C to separate the porewater from the particulates. Subsequently, the porewater samples were filtered ($0.2 \mu\text{m}$ cellulose-acetate syringe filters) under argon. All BIGO cores were processed in the same way but under ambient atmosphere. Porewater extraction yielded 5-30 ml of porewater at each depth interval. Sediment samples were also taken for the calculation of sediment density and water content as well as solid phase constituents in the onshore laboratory. Porewater from the GCs was extracted using rhizon filters ($0.2 \mu\text{m}$) attached to Perspex syringes. The loss of sediment from the top of the GC resulting from the penetration of the core barrel through the sediment was determined by aligning the concentrations of porewater constituents from the MUC and GC. This way, sediment loss of $\sim 0 - 15$ cm was determined, depending on the site.

A total of 479 porewater samples were recovered and analyzed (Table 12.1). Porewater analyses of the following parameters were carried out onboard: ferrous iron (Fe^{2+}), nitrate (NO_3^-), nitrite (NO_2^-), ammonia (NH_4^+), phosphate (PO_4^{3-}), silicate (H_4SiO_4), total alkalinity (TA), sulfate (SO_4^{2-}) and dissolved hydrogen sulfide (H_2S). NO_3^- , NO_2^- , NH_4^+ , PO_4^{3-} , and H_4SiO_4 were determined using standard methods (Grasshoff et al., 1997). NO_3^- and NO_2^- were always measured on a Quattro Autoanalyzer (Seal Analytic). NH_4^+ , PO_4^{3-} and H_4SiO_4 were measured either on the autoanalyzer or using a Hitachi U-2001 spectrophotometer, depending on the expected concentrations. The two instruments showed an agreement to within $< 5\%$ on

most samples. For the analysis of dissolved Fe^{2+} concentrations, sub-samples of 1 ml were taken within the glove bag, immediately stabilized with ascorbic acid and analysed within 30 cm after complexation with 20 μl of Ferrozin. Samples for TA were analyzed by titration of 0.5-1 ml pore water according to Ivanenkov and Lyakhin (1978). Titration was ended when a stable pink colour appeared. During titration, the sample was degassed by continuously bubbling nitrogen to remove any generated CO_2 and H_2S . The acid was standardized using an IAPSO seawater solution. Untreated filtered samples were analyzed for SO_4^{2-} , Cl^- and Br^- using ion-chromatography. H_2S was only determined at the shallow E5 station. An aliquot of pore water was diluted with appropriate amounts of oxygen-free artificial seawater and the sulphide was fixed by immediate addition of zinc acetate gelatine solution. Analytical precision and detection limits of each method are given in Table 12.5.

Acidified sub-samples (30 μl suprapure HNO_3^- + 3 ml sample) were prepared for analyses of major ions (K, Li, B, Mg, Ca, Sr, Mn, Br, and I) and trace elements by inductively coupled plasma optical emission spectroscopy (ICP-OES) at the home laboratory. Further subsamples are listed in Table 12.4.

Table 12.4 Stations, sampling areas and planned analyse for sediment samples measured in multiple cores (MUC), gravity cores (GC) and benthic lander cores (BIGO). Data are organized by station number.

Core ID ^a	Area	Depth (m)	Geochemistry ^b	Phys. Prop.	Organics ^d	¹⁵ N ^e	Nd	Microbiology	eDNA	No. samples ^f
008MUC1	E1	3701	X	X	X	X				13
016MUC2	E1 hill	3560	X	X	X			X		13
020MUC3	E1	3553	X	X	X			X		13
027MUC4	S3	3414					X		X	
028XOFOS4	S3	3400					X			
031MUC5	E1 hill	3134	X	X	X			X	X	12
035GC1	E1	3692	X	X		X				23
070GC2	E2	3295	X	X		X				34
080MUC6	E2	3294	X	X	X	X			X	15
091MUC7	Eddy core	3339	X	X	X				X	15
099MUC8	S3	3399	X	X	X				X	14
107MUC9	E2/ E3	2894	X	X	X			X	X	15

113MUC10	E3 CV	3203	X	X	X			X	X	14
121GC3	E3 CV	3204	X	X		X				32
126GC4	E4	2864	X	X		X				31
132MUC11	E4	2862	X	X	X	X				17
135BIGO1-2 K1	E4	2858	X	X						10
137MUC12	E4	3070	X	X	X					15
137MUC12B	E4	3070		X						
139MUC13	E4	2972	X	X	X					16
142MUC14	E4	3052	X	X	X					18
143MUC15	E4	2947	X	X	X					16
146MUC16	E4	2478	X	X	X					16
149MUC17	E4 (S6)	2739	X	X	X					16
157CTD49	E5	77					X			
159BIGO1-3 K2	E4	71	X	X						9
160MUC18	E5	70	X	X	X	X				14
161MUC19	E5	70					X			
164GC5	E5	72	X	X						11
171MUC20	E5	501	X	X	X					14
171MUC20B	E5	501		X						
172MUC21	E4/ E5	1704	X	X	X		X			16
184MUC22	CB	4184	X	X	X	X				15
185GC6	CB	4190	X	X		X				32

^a K1, K2 denotes if sediments from chamber 1 or chamber 2 (respectively) were sampled using a push-core.

^b Details of geochemistry of BIGO chamber samples are given in the benthic lander section.

^c Sediment physical properties including particulate organic carbon and nitrogen, porosity, and grain size.

^d Surface samples for phaeopigments and amino acids.

^e For the ¹⁵N of dissolved inorganic N species in sediment porewaters

^f Number of porewater samples measured on board.

Table 12.5 Analytical methods of onboard geochemical analyses.

Parameter	Method	Detection limit	Analytical precision
NH ₄ ⁺	Photometer	1 µmol/l	5 %
PO ₄ ³⁻	Photometer	1 µmol/l	5 %
Fe ²⁺	Photometer	1 µmol/l	5 %
H ₄ SiO ₄	Photometer	5 µmol/l	2 %
Alkalinity	Titration	0.05 meq/l	3 %
NO ₃ ⁻	Autoanalyzer	1 µmol/l	1 %
NO ₂ ⁻	Autoanalyzer	0.1 µmol/l	2 %
NH ₄ ⁺	Autoanalyzer	0.2 µmol/l	2 %
PO ₄ ³⁻	Autoanalyzer	0.05 µmol/l	2 %
H ₄ SiO ₄	Autoanalyzer	1.7 µmol/l	2 %
H ₂ S	Photometer	1 µmol/l	3 %
SO ₄ ²⁻	Ion chromatography	200 µmol/l	1 %

12.4 Benthic Insitu-Fluxes

A total of 7 Lander deployments (BIGO, Biogeochemical Observatory) were conducted at the main stations E1 to E5-SFB754 including the E1 Hill site and the additional site E3_CV, Table 12.6. E3_CV was foreseen for the long-term deployment of the DOS Lander and the DSR Panta Rhei, but due to the rough small scale topography of the sediments this area was considered as inappropriate for the Rover deployment.

Table 12.6 Station data of the in-situ flux measurements using the BIGO-I, BIGO-II and the DSR Panta Rhei. Height measurements of the benthic chambers (ch.) are needed to calculate the volume of the enclosed water body inside the benthic chambers.

Station	Gear	Date/ time	Lat. N	Long. W	Depth (m)	Habitat/ height measures of ch.
M182_10-1	BIGO-I-1	01.06.22 19:14	17°59.991'	24°20.010'	3697	E1 , K1: 27.8, 25.8, 26.1, 27.0 K2: none
M182_15-1	BIGO-II-1	03.06.22 00:31	18°02.874'	23°49.170'	3563	E1 hill failed
M182_18-1	DSR-1	03.06.22 20:02	17°59.988'	24°19.976'	3693	E1 successful, 5 series
M182_30-1	BIGO-II-2	06.06.22 11:20	18°02.878'	23°49.179'	3559	E1 Hill , no heights
M182_77-1	BIGO-II-3	13.06.22 19:05	17°59.963'	22°00.064'	3294	E2 , K1: 29.9, 29.3, 27.7, 28.2 K2: only Schleppezeiger

M182_81-1	DSR-2	14.06.2022 15:38	17°59.987'	22°00.157'	3294	E2 successful, 6 series
M182_116-1	BIGO-II-4*	21.06.2022 19:38	17°54.939'	20°01.131'	3204	(E3_CV) K1: none K2: 25.2
M182_130-1	DSR-3	23.06.2022 22:39	18°09.868'	18°13.261'	2865	E4 , Rover did not move, 1 series
M182_135-1	BIGO-I-2*	24.06.2022 19:30	18°10.128'	18°13.539'	2867	E4 plain K1: 19.3, 19.5, 21.0, 19.5 K2: Schleppezeiger
M182_159-1	BIGO-I-3*	29.06.2022 15:36	18°16.293'	16°22.887'	71	E5 SFB754 K1: 23, 22.5, 25 K2: 25, 23.6, 22.6, 22.5
M182_177-1	DSR-04	03.07.2022 18:28	18°00.301'	21°59.939'	3296	E2 long-term

* biogeochemical measurements in addition to the total oxygen uptake

For the measurement of solute fluxes across the sediment water interface and sediment retrieval two structurally similar BIGOs (BIGO I and BIGO II) were deployed as described in detail by Sommer et al. (2009) and Pfannkuche & Linke (2003). In brief, each BIGO contained two circular flux chambers (internal diameter 28.8 cm area 651.4 cm²). A TV-guided launching system allowed controlled placement of the observatories at selected sites on the sea floor. After a delay of few hours after the observatories were placed on the sea floor the chambers were slowly driven into the sediment (~ 30 cm h⁻¹). During this initial time period where the bottom of the chambers was not closed by the sediment, the water inside the flux chamber was periodically replaced with ambient bottom water. The water body inside the chamber was replaced once more with ambient bottom water after the chamber has been driven into the sediment to flush out solutes that might have been released from the sediment during chamber insertion. To trace fluxes of nutrients 8 sequential water samples were removed from either flux chamber with a glass syringe (volume of each syringe ~ 47 ml) by means of glass syringe water samplers. The syringes were connected to the chamber using 1 m long Vygon tubes with a dead volume of 5.2 ml. Prior to deployment these tubes were filled with distilled water. Eight undiluted water samples were taken from the water body enclosed by the benthic chambers using an eight-channel peristaltic pump, which slowly filled glass tubes (quartz glass). These samples will be used for the analyses of TA and DIC. To monitor the ambient bottom water geochemistry an additional syringe water sampler and another series of eight glass tubes were used. The positions of the sampling ports were about 30 – 40 cm above the sediment water interface. O₂ was measured inside the chambers and in the ambient seawater using optodes (Aanderaa) that were two point calibrated before each lander deployment.

In addition to the fluxes measured using the BIGO's, the novel DeepSea Rover (DSR) Panta Rhei was used to measure repeatedly oxygen uptake of the sediment. The DSR represents a six-wheeled vehicle (weight in air 1200 kg, 80 kg in water, dimensions 3 x 2 x 1.7 (L, W, H)), which is specifically designed to carry out repeated benthic oxygen flux measurements inside two benthic incubation chambers at the front of the vehicle for prolonged time periods of up to one year, Fig. 12.1. Oxygen is measured using fibre-optic oxygen sensors (Pyroscience, Bremen), three were placed inside each chamber, two sensors record the oxygen variability in the ambient bottom water. The volume of the two benthic chambers is determined automatically by injecting pure water into the benthic chambers after the measurement and

simultaneously recording the change of the conductivity (Aanderaa conductivity sensors). Additionally, the Rover carries two camera systems, one of which is forward looking, the other one takes photographs of the seafloor behind the vehicle. The Rover further comprises a current profiling instrument (ADCP), a Seabird SBE 19plus CTD for the recording of physical parameters (conductivity, temperature, depth) in the bottom water, and a Wetlab turbidity sensor. A flashlight and a radio beacon allows for easy location of the Rover when floating on the sea surface after its mission. Two releaser (KUM) are used for the recovery of the Rover. The ascend velocity from the seafloor to the sea surface is about 0.4 to 0.5 m s⁻¹. A flashlight and a radio beacon allows for easy location of the Rover when floating on the sea surface after its mission.

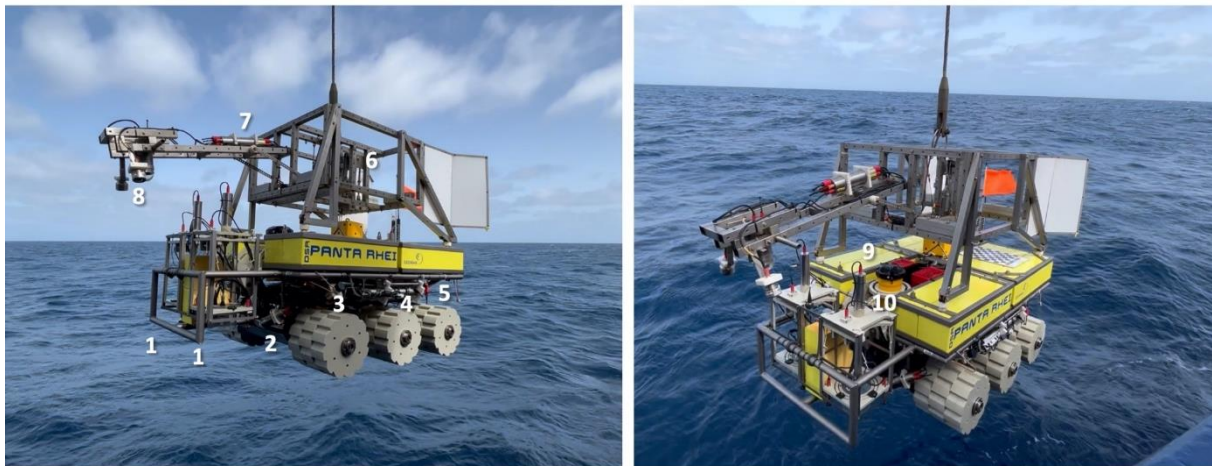


Fig. 12.1 Deployment of the DSR Pantar Rhei at the E2 working area for the long-term measurement of TOU until January 2023. (1) two chambers for benthic flux measurements, (2) one of three cameras, (3) Wetlab turbidity sensor, (4) Seabird CTD SBE 19plus (5) rear camera, (6) launching unit from which the Rover is uncoupled using an electric releaser when the seafloor is reached (7) telemetry for signal and energy transfer (8) camera and lights of the launching unit, (9) profiling current meter (ADCP), (10) pump for volume determination. Photos Gabriel Nolte.

During deployment, the following sequence of activities is performed by the Rover: i. after its placement at the seafloor it moves a distance of 10 m away from its landing site into an undisturbed area, ii. subsequently the benthic chambers are flushed, iii. it takes photos of the area that will be sampled by the two benthic chambers iv. then the benthic chambers are inserted into the sediment and flushed prior to the start of flux measurement, v. directly thereafter photos are taken from of either chamber whilst inserted into the sediment, vi. measurement phase, duration was set to 16 hours, the sampling interval of the optodes was set to 5 min. For the long-term deployment (see below) the measurement phase was set to 40 hours, vii. when the measurement phase is terminated, pure water is injected to determine the volume of both chambers, the change of conductivity is monitored for 20 min at an increased sampling rate, viii subsequently the chambers were retrieved out of the sediment and photos of the sampled area are made, ix the Rover moves a distance of 0.7m to the next measurement area and repeat this sequence. Flux measurements will be conducted until the Rover is recovered.

Four Rover deployments were performed during cruise M182, Table 12.6. The last Rover deployment (DSR 04) will last until mid-January 2023 and recovered during the cruise MSM114 with RV Maria S. Merian. The Rover was deployed in order to measure variability

of sediment oxygen consumption in response to enhanced carbon deposition during the passage of a productive eddy at sea surface.

12.5 Benthic Observations

XOFOS

The X-tended Ocean Floor Observation System is planned, constructed and made by GEOMAR Helmholtz Center for Ocean Research Kiel. It is designed to deliver high resolution video footage of the seafloor in combination with most reliable underwater positioning. For its purpose it is equipped with one 4k forward looking video camera, one HD downward looking video camera, one downward looking still camera, LED lights (designed by GEOMAR as well) and flashes (Fig. 12.2). For the positioning there is an USBL Beacon attached. A downward facing 300 kHz ADCP with bottom log functions as DVL and records the speed and direction over ground, which enhances the navigation significantly.

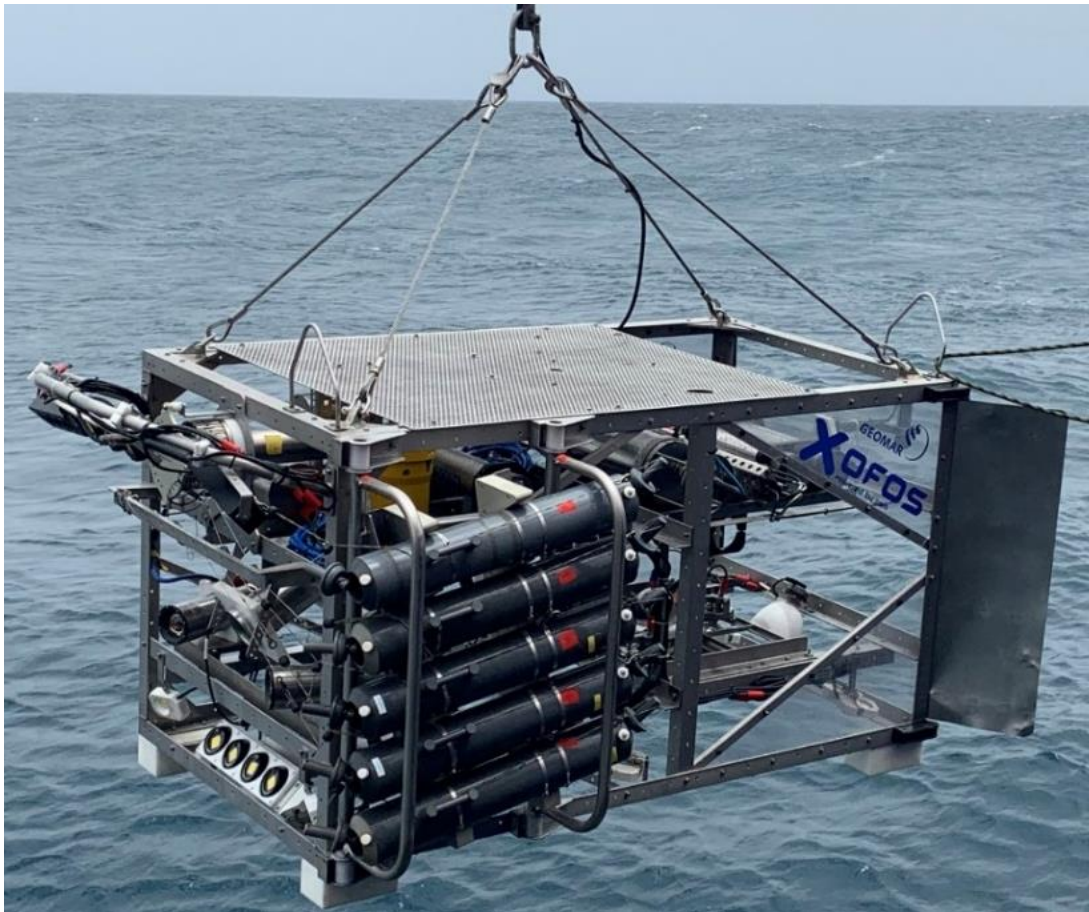


Fig. 12.2 Deployment of the XOFOS. Five Niskin bottles for water sampling are attached to the portside of the frame.

In addition, the XOFOS holds a CTD with an altimeter and 3 Laser points indicate the height over ground. The distance in between the laser points on the seafloor is 45 cm. It can be optionally equipped with 10 (5 bottles at each side) remotely closable Niskin bottles for water sampling.

CTD and ADCP is recorded by the software OFOP and written into a text file with timestamp and ship and USBL navigation. Online annotations were made in real-time during the dive and also logged via OFOP.

The still Ocean Imaging Camera System (OIS) is set to 1 picture per 5, 10 or 15 seconds, which are stored on an SD card inside the camera housing. The videos are recorded via video recorder from Aja KI Pro Ultra and Aja KI Pro Ultra Plus in HD quality on the XOFOS PC. Because times on the cameras and PCs have been synchronized, they can be linked to the navigation recorded in OFOP.

In total 13 dives had been conducted for benthic observations. For best vessel stability, the XOFOS profiles had to be planned with 0.5 knots straight against the waves. The videos were recorded in HD split into frames (1 Hz). After colour-correction via the software Darktable the frames are merged to photo mosaics and DEMs in the software Metashape.

Even though, the online annotations are biased due to several reasons (individual annotator, visibility, height over ground, etc.), differences in the benthic properties do become obvious. Nevertheless, those observations have to be treated carefully and cannot be taken for quantitative analyses. However, the georeferenced photo mosaics provide a more precise method to spatially map and quantify structures on the seafloor.

AUV Mapping

The system comprises the AUV itself, a control and workshop container and a mobile Launch and Recovery System (LARS) (Fig. 12.3) with a deployment frame that was installed at the afterdeck of RV METEOR. The self-contained LARS was developed by Woods Hole Oceanographic Institution to support ship-based operations so that no Zodiac or crane is required for launch and recovery. The LARS is mounted on steel plates, which are screwed to the deck of the ship.

The LARS is configured in a way that the AUV can be deployed over the stern or port/starboard side of the German medium and ocean-going research vessels. The AUV Abyss can be launched and recovered at weather conditions with a swell up to 2.5 m and wind speeds of up to 6 Beaufort. For the recovery the nose float pops off when triggered through an acoustic command. The float and the ca. 17 m recovery line drift away from the vehicle so that a grapnel hook can snag the line. The line is then connected to the LARS winch, and the vehicle is pulled up. Finally, the AUV is brought up on deck and secured in the LARS. The AUV missions were planned based on ships bathymetry.

Depending on scientific needs different sensors can be used, following are part of the standard configuration: Reson T-50 multibeam echosounder, Edgetech 2205 sidescan sonar, designed to provide 120/410 kHz Side Scan. Seabird SBE 49 FastCat and Wet Labs ECO FLNTU fluorometer and turbidity sensor. Optional configurations instead of the MBES (Multibeam Echosounder) are the Edgetech 2205, 4-24 kHz Sub Bottom Profiler or the Deep Survey Cam with different LED settings (4m and 7m Altitude) can be installed. The REDOX potential sensor by Ko-ichi Nakamura on request.

The navigation of Abyss is mainly based on the Kearfott Inertial Navigation System (INS). The INS is capable to determine acceleration and angular velocity in 3-dimensional space and it usually requires an initial position by GPS to dead reckon its own position. Since the dead reckoning based navigation is associated with an increasing error, the Long Base Line Positioning (LBL) has been used successfully to aid. The LBL concept make use of acoustic transponders moored to the seabed. The transponder positions are known from a preceding calibration from the surface vessel. The AUV position is computed from range measurements to the transponders. The downward looking doppler velocity log (DVL) stabilizes continuously the INS navigation by exact ground velocity values. The AUV depth is determined by a separate pressure sensor (Paroscientific 8B7000). The above mentioned DVL (Teledyne RDI Workhorse Navigator) provide the altitude (height above seabed), too. Once the AUV is surfaced and is within the WIFI range, it can be controlled from the ship. The vehicle can detect obstacles in its pre-field and escape upwards.



Fig. 12.3 Recovery of AUV Abyss with the LARS (launch and recovery system).

AUV Abyss

The AUV system and its corresponded containers were placed on the stern of the vessel. This means the LARS and the Ops-Van. The OPS Van is placed right behind the LARS with its main doors directed to the stern. The container for the LARS and the spare container are not needed for AUV operations, but for the sake of maintenance and storage place there are placed

nearby. The AUV needs two subsystems for proper operation, that are apart from the Ops-Van. The acoustic positioning and communication system is placed in the moonpool of the vessel. An antenna system which maintains wifi and iridium connection is placed on the monkey deck, to get a line of sight to the vehicle when it is in the water. On METEOR a third system was in use, since the AUV requires a different wifi system after the core overhaul. This wifi system was placed near to the Ops-Van to keep cabling short.



Fig. 12.4 Top left: Launch and recovery system (LARS) on aft deck of RV METEOR. Top right: Mounting of the LARS on deck via steel plates. Bottom left: Container for AUV operation. Bottom right: Steel plates are temporary welded to the aft deck via Z-profiles.

The metal plates which adapt the LARS on the ship are welded to the deck by the use of Z-shaped connector pieces (Fig. 12.4). The used metal plates are intentionally made for RV Sonne. Next to the LARS the HPU (Hydraulic Power Unit) is placed.



Fig 12.5 Top left: Hydraulic unit for operating the LARS. Center and bottom left: Detailed photos of Z-profiles. Top right: Stacked AUV containers on board RV METEOR.

AUV Abyss mission and preparation summary

During the cruise M182, 10 AUV mission were flown by AUV Abyss. Out of these ten missions, eight were flown successfully with minor issues, two were aborted due to major issues with the vehicle. M182 was the first deep water test of the overhauled AUV system. It brought up a lot of difficult conditions with the vehicle itself and with the supporting equipment.

Table 12.7 Overview of AUV Abyss dives during M182.

Station Number	Dive Number	Area	Sensors (MBES, SSS120, SSS410, camera)	Date	Mission Time	Distance In meter
074-1	Abyss-1 0356	Eddy	Camera water column (OK)	13.06.2022	4:15h	20490
082-1	Abyss-2 0357	E2	Camera, 7m SSS 120, 30m	14.06.2022	2:04h	7486
100-1	Abyss-3 0358	E2	Camera, 7m SSS120, 30m (OK)	17.06.2022	11:18h	51828
108-1	Abyss-4 0359	E2	Camera, 7m SSS410, 7m (OK) SSS120, 18m (OK) SSS410, 18m (OK)	19.06.2022	7:25h	32346
117-1	Abyss-5 0360	E3- CV	Camera, 7m (OK) SSS410, 18m (OK)	21.06.2022	17:58h	93629
129-1	Abyss-6 0361	E4	MBES, 75m	23.06.2022	15:58h	79381
141-1	Abyss-7 0362	E4	MBES, 60m SSS410, 18m	26.06.2022	4:18h	15372
147-1	Abyss-8 0363	E4	MBES, 60m (OK) SSS410, 12m (OK)	27.06.2022	19:06h	100727
167-1	Abyss-9 0364	E5	Camera 7m and 4m (OK), no LBL because of shallow water (70m)	30.06.2022	1:50h	9885
178-1	Abyss-10 0365	E2	SSS410, 7m (OK) Camera, 7m (OK)	3.07.2022	13:25h	69174

The first dive happened very late on the cruise because there was an O-Ring missing for the INS pressure housing. The reason was because the navigation unit needed to be dismantled and taken on the air plane to arrive in Mindelo. This happened due to customs and export regulations. Checking the factory spare part list of the AUV with supply that had been send in the container suggested that the needed O-ring is already on board. Unfortunately, it was not because the factory spare part list was faulty. A replacement O-ring could not be found on the ship (US-extra size) so that a hand delivery of the O-ring, plus another spare part box, which was still in customs in Mindelo, had to be arranged. This was successful and the INS was working as expected.

During the preparation phase of the in AUV an error with the iridium system showed up. The iridium system is mandatory for diving with the AUV because it maintains communication after a successful dive. When the AUV is submerged and floats free, the ship gets constantly the position of the AUV and knows were to collect it after station work. Without a running iridium system it is very likely to lose the AUV. After some days of troubleshooting it turned

out, that the Iridium provider deleted a telephone number the AUV is using for data communication.

Transponder Deployments

The whole cruise only one set of Transponders was used (Fig. 12.6). The deployment went smooth from the stern of the vessel with help of the crane for the benthos spheres. The transponder was deployed by hand. When the ship was on position the ground weight was slipped and dropped.



Fig. 12.6 LBL Transponders with floating spheres.


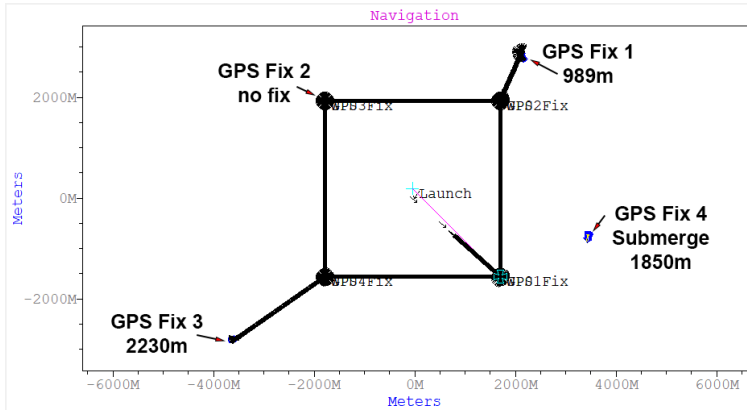
Table 12.8 Overview of LBL transponder deployments.

Transponder #	Type	Position	Transducer depth (m)	Deployment	Released	Recovered
1A	DT4A-LF	17° 59.059' N 24° 18.916' W	3666	31.05.2022 23:08	07.06.2022 11:00	07.06.2022 12:15
2B	DT4B-LF	17° 59.826' N 24° 18.762' W	3666	31.05.2022 23:21	07.06.2022 12:07	07.06.2022 13:07
Transponder	Type	Position	Transducer depth (m)	Deployment	Released	Recovered
3A	DT4A-LF	18° 00.171' N 21° 58.018' W	3264	13:06.2022 14:04	19.06.2022 13:43	19.06.2022 14:55
4B	DT4B-LF	17° 59.441' N 21° 58.048' W	3264	13:06.2022 13:45	19.06.2022 13:13	19.06.2022 14:23
Transponder	Type	Position	Transducer depth (m)	Deployment	Released	Recovered
6A	DT4A-LF	17° 55.252' N 19° 59.908' W	3187	21.06.2022 12:35	22.06.2022 14:47	22.06.2022 15:50
5B	DT4B-LF	17° 54.587' N 19° 59.965' W	3188	21.06.2022 12:19	22.06.2022 14:00	22.06.2022 15:03

Transponder	Type	Position	Transducer depth (m)	Deployment	Released	Recovered
7A	DT4A-LF	18° 10.097' N 18° 15.079' W	2856	23.06.2022 14:17	28.06.2022 12:00	28.06.2022 13:02
8B	DT4B-LF	18° 09.389' N 18° 15.102' W	2856	23.06.2022 13:58	28.06.2022 11:10	28.06.2022 12:10
Transponder	Type	Position	Transducer depth (m)	Deployment	Released	Recovered
9A	DT4A-LF	17° 59.665' N 21° 58.757' W	3271	03.07.2022 08:15	04.07.2022 08:30	04.07.2022 09:40
10B	DT4B-LF	18° 00.677' N 21° 58.767' W	3273	03.07.2022 07:42	04.07.2022 07:52	04.07.2022 09:04


AUV Abyss dives

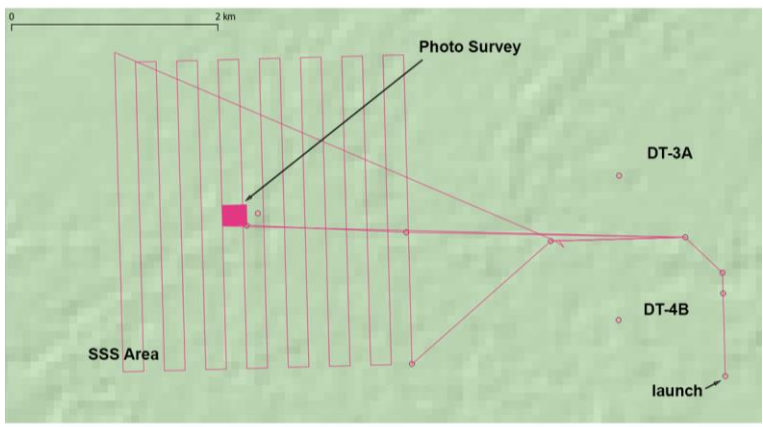
Abyss0356

Station	M182/074-1		Day (UTC)	13.06.2022
Dive	Abyss0356		Mission goal:	Zigzag dive through the top 300m of the water column; main sensor CTD and fluorometer. Cam attached for watercolumn pictures
			Times (UTC)	
			Launch	5:40
			Mission start	5:40
			Survey start	5:40
			Survey finished	9:53
			Mission finished	9:53
			Recovery	11:40
			Distance travelled	20490m

		Mission comments	Depth Triange Objective used for water column survey, AUV had wrong navigation at the end. Got only two GPS fixes inbetween	
Depth / Altitude	- Zig Zag from 20m to 300m			
Sensor	DSC Deep Survey Cam			
Total raw files		First file		
		Last file:		
Survey area covered:		Average coverage:		
Sensor	Eh / REDOX Sensor (Koichi Nakamura)			
Total raw files	1 file (.txt) / 1.53 MB	File name	Abyss356_REDOX.txt	
Comments	- Sensor data positions are not shifted to the corrected vehicle track			
Sensor	SeaBird SBE49 FastCAT CTD (S/N: 4955482-0198)			
Total raw files	1 file (.txt) / 8.1 MB	File name	Abyss356_CTD.txt	
Comments	- Sensor data positions are not shifted to the corrected vehicle track			
Sensor	Wetlabs ECO FLNTU (Chlorophyll / Turbidity) (S/N: FLNTURTD-939)			
Total raw files	1 file (.txt) / 1 MB	File name	Abyss356_ECO.txt	
Comments	- Sensor data positions are not shifted to the corrected vehicle track			
Comments	The AUV performed the mission ok. From 3 planned inbetween GPS fixes only 2 were done, because on GPS fix 2 (see image) the vehicle was to deep to submerge in the given time. This led to a big offset on GPS fix 3			

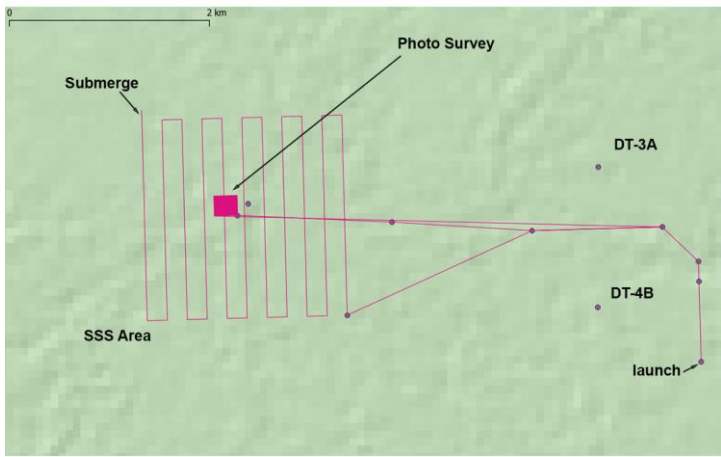
Abyss0357

Station	M182/82-1		Day (UTC)	14.06.2022
Dive	Abyss0357			
			Mission goal:	Camera mission over BIGO Lander and Pantha Rhei Rover, SSS mapping 120kHz
			Times (UTC)	
			Launch	17:31
			Mission start	17:33

	Survey start	-
	Survey finished	-
	Mission finished	-
	Recovery	19:34
	Distance travelled	7486
	Mission comments	Mission aboard because of Altitude sensor misconfiguration. No data from seafloor
Depth / Altitude	- Altitude Mode 7m - Depth 3200m	
Sensor	DSC Deep Survey Cam	
Total raw files	-	First file: - Last file: -
Survey area covered:	Average coverage:	
Sensor	Eh / REDOX Sensor (Koichi Nakamura)	
Total raw files	1 file (.txt) / 496 kB	File name: Abyss357_REDOX.txt
Comments	- Sensor data positions are not shifted to the corrected vehicle track	
Sensor	SeaBird SBE49 FastCAT CTD (S/N: 4955482-0198)	
Total raw files	1 file (.txt) / 1.1 MB	File name: Abyss357_CTD.txt
Comments	- Sensor data positions are not shifted to the corrected vehicle track	
Sensor	Wetlabs ECO FLNTU (Chlorophyll / Turbidity) (S/N: FLNTURTD-939)	
Total raw files	1 file (.txt) / 773kB	File name: Abyss357_ECO.txt
Comments	- Sensor data positions are not shifted to the corrected vehicle track	
Comments	Mission was not successful due to misconfiguration of the AUV Altimeter. The AUV didn't get a bottom lock. In order to that no navigation could be established on the seafloor. The AUV got redirected thru a manual modem command (Abort and redirect) to submerge at a specific position.	


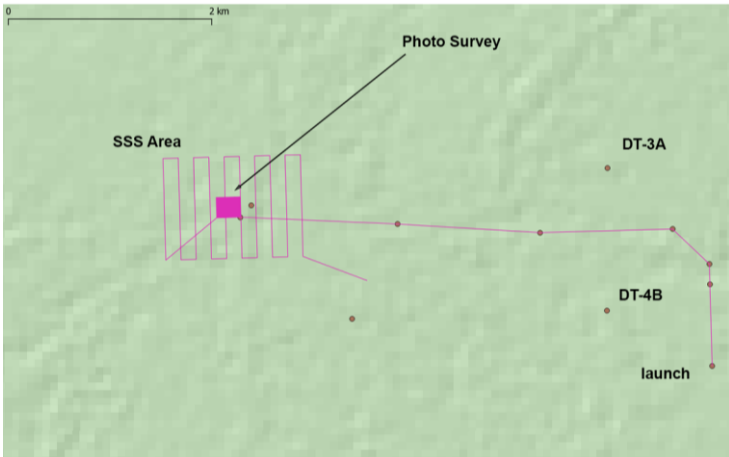
Abyss0358

Station	M182/100-1		Day (UTC)	17.06.2022
Dive	Abyss0358			

	Mission goal:	Camera mission over BIGO and Rover, SSS mapping 120kHz	
	Times (UTC)		
	Launch	07:18	
	Mission start	07:20	
	Survey start	09:27 SSS(12:50)	
	Survey finished	11:23 SSS(17:18)	
	Mission finished	17:18	
	Recovery		
	Distance travelled	51828	
	Mission comments	Retry of dive 0357. Camera did not work because of camera sensor error, SSS data acquired. On submerge ascent weight gone	
Depth / Altitude	- 7m Alt Camera / 30m SSS - Depth 3200m		
Sensor	SSS 120kHz		
Total raw files	31 files (.jsf) 3.24GB	First file	20220617.121508.000000
		Last file:	20220617.121508.000030
Survey area covered:	Average coverage:	1.4km ²	
Sensor	Eh / REDOX Sensor (Koichi Nakamura)		
Total raw files	1 file (.txt) / 2.37 MB	File name	Abyss358_REDOX.txt
Comments	- Sensor data positions are not shifted to the corrected vehicle track		
Sensor	SeaBird SBE49 FastCAT CTD (S/N: 4955482-0198)		
Total raw files	1 file (.txt) / 19 MB	File name	Abyss358_CTD.txt
Comments	- Sensor data positions are not shifted to the corrected vehicle track		
Sensor	Wetlabs ECO FLNTU (Chlorophyll / Turbidity) (S/N: FLNTURTD-939)		


Total raw files	1 file (.txt) / 3.65 MB	File name	Abyss358_ECO.txt
Comments	- Sensor data positions are not shifted to the corrected vehicle track		
Comments	The Camera did not take pictures due to a hardware error in the sensor cleaning mechanism. That prohibited the software to get access to the camera and take pictures. Camera was changed and sensor cleaning mechanism was deactivated on new camera. At the end of the dive, the vehicle recognized a missing pickupfloat, therefore the ascent weight was released and the mission aborted.		

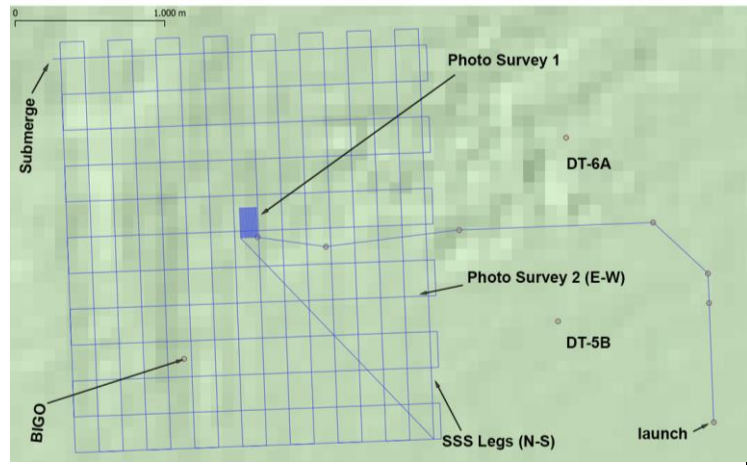
Abyss 0359

Station	M182/108-1		Day (UTC)	19.06.2022
Dive	Abyss0359		Mission goal:	Camera mission with parallel 410kHz SSS; subsequent, combined 120 and 410 kHz SSS survey
			Times (UTC)	
			Launch	09:41
			Mission start	09:42
			Survey start	11:48 13:58
			Survey finished	13:44 15:58
			Mission finished	15:58
			Recovery	
			Distance travelled	32346
			Mission comments	Camera did not work due to software issues. All side scan surveys accomplished. Pick up float released. Abort weight gone.
			Depth / Altitude	- 7m DSC & 410kHz / 18m SSS combined - Depth 3200m
Sensor	SSS 410kHz			
Total raw files	14 files (.jsf) 1.65GB	First file	20220619.113203.0000000	

		Last file:	20220619.113203.0000013
Survey area covered:		Average coverage:	50000m ²
Sensor	SSS 120/410kHz		
Total raw files	14 files (.jsf) 2.93GB		First file
		Last file:	20220619.113203.0000026
Survey area covered:		Average coverage:	1.4km ²
Sensor	Eh / REDOX Sensor (Koichi Nakamura)		
Total raw files	1 file (.txt) / 1.54 MB	File name	Abyss359_REDOX.txt
Comments	- Sensor data positions are not shifted to the corrected vehicle track		
Sensor	SeaBird SBE49 FastCAT CTD (S/N: 4955482-0198)		
Total raw files	1 file (.txt) / 12.4 MB	File name	Abyss359_CTD.txt
Comments	- Sensor data positions are not shifted to the corrected vehicle track		
Sensor	Seabird ECO FLNTU (Chlorophyll / Turbidity) (S/N: 6590)		
Total raw files	1 file (.txt) / 2.26 MB	File name	Abyss359_ECO.txt
Comments	- Sensor data positions are not shifted to the corrected vehicle track		
Comments	Retry of dive Abyss358. Camera did not work due to software issues. These were fixed in a new release of the camera software.		

Abyss0360

	M182/117-1		Day (UTC)	21.06.2022
Dive	Abyss0360			
			Mission goal:	Camera and 410kHz SSS over BIGO 1 st cam, 2 nd SSS, 3 rd cam
			Times (UTC)	
			Launch	21:58
			Mission start	22:00
			Survey start	23:44 / 0:41 / 9:34

	Survey finished	0:41 / 9:34 / 15:30	
	Mission finished	15:30	
	Recovery		
	Distance travelled	93629	
	Mission comments	Camera and SSS successful, images blurred	
Depth / Altitude	- DSC 7m / SSS 410kHz 18m / DSC 7m - Depth 3200m		
Sensor	DSC Deep Survey Cam		
Total raw files		First file	
		Last file:	
Survey area covered:		Average coverage:	26000m ²
Sensor	SSS 410kHz		
Total raw files	54 files (.jsf) 5.94GB	First file	20220622.004124.0000000
		Last file:	20220622.004124.0000053
Survey area covered:		Average coverage:	7.28km ²
Sensor	DSC Deep Survey Cam		
Total raw files		First file	
		Last file:	
Survey area covered:		Average coverage:	Swath width on 32km
Sensor	Eh / REDOX Sensor (Koichi Nakamura)		
Total raw files	1 file (.txt) / 4.21 MB	File name	Abyss360_REDOX.txt
Comments	- Sensor data positions are not shifted to the corrected vehicle track		
Sensor	SeaBird SBE49 FastCAT CTD (S/N: 4955482-0198)		
Total raw files	1 file (.txt) / 34.2 MB	File name	Abyss360_CTD.txt
Comments	- Sensor data positions are not shifted to the corrected vehicle track		
Sensor	Seabird ECO FLNTU (Chlorophyll / Turbidity) (S/N: 6590)		
Total raw files	1 file (.txt) / 6.24 MB	File name	Abyss360_ECO.txt
Comments	- Sensor data positions are not shifted to the corrected vehicle track		
Comments	Final camera dive which worked out. Images were taken, but are blurred. Prefocus in air was not successful. Second camera leg was activated by power		

	on of the sensor. Software mixed up image folders and put new images in old folders. Got fixed in new software release.
--	---

Sample Data:

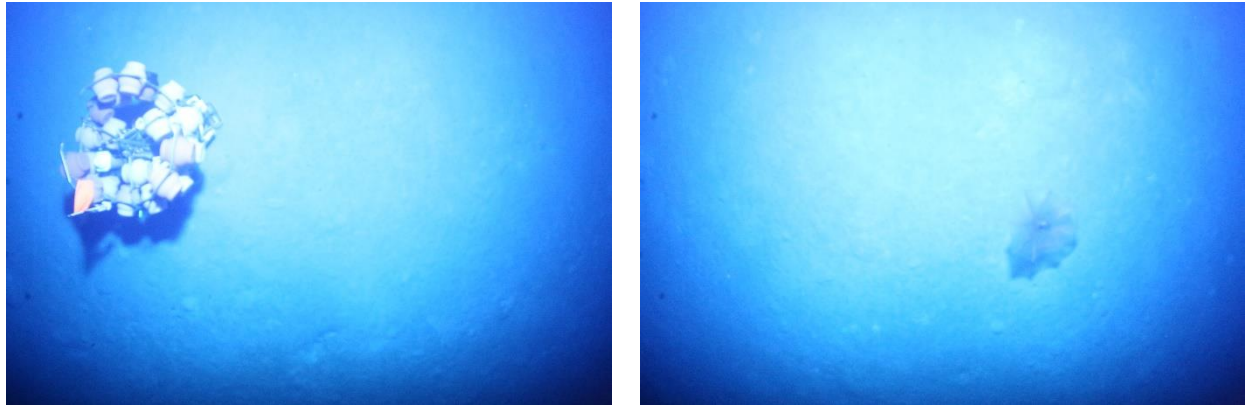

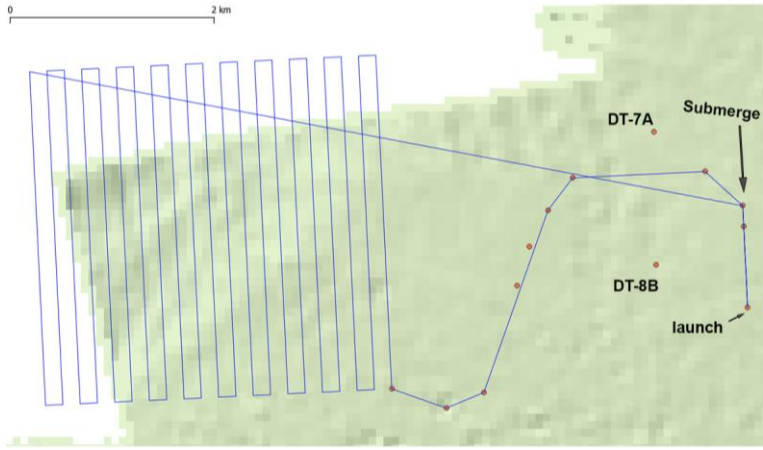


Fig. 12.7 The images show the defocussing of the camera during the dive.

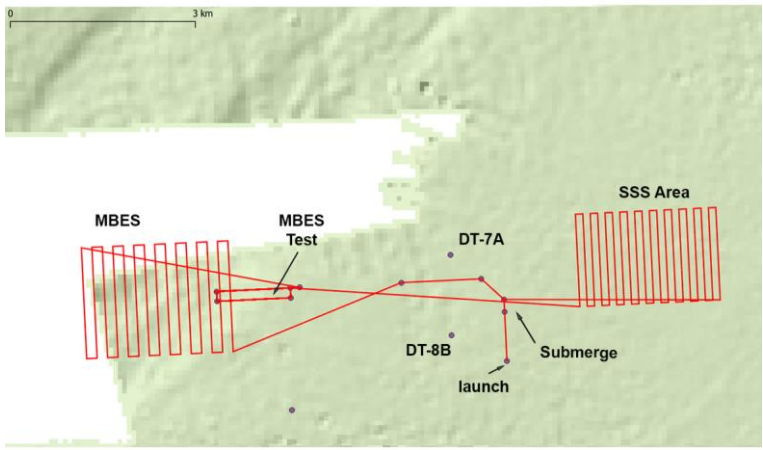
Abyss0361

Station	M182/129-1		Day (UTC)	23.06.2022
Dive	Abyss0361		Mission goal:	Multibeam Dive with test of adapter software
			Times (UTC)	
			Launch	18:17
			Mission start	18:20
			Survey start	20:10
			Survey finished	09:09 (aborted)
			Mission finished	
			Recovery	
			Distance travelled	79381


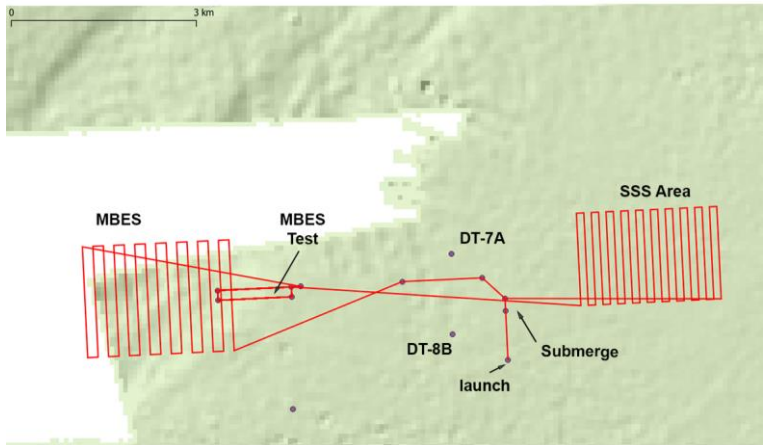
		Mission comments	
		MBES data of very low quality Mission aborted, ascent weight gone	
Depth / Altitude	- 75m Altitude -2900m Depth		
Sensor	Multibeam Reson T-50		
Total raw files	93 files (.s7k) 17.1GB	First file	20220623_193500
		Last file:	20220624_090736
Survey area covered:		Average coverage:	12.25km ²
Sensor	Eh / REDOX Sensor (Koichi Nakamura)		
Total raw files	1 file (.txt) / 3.47 MB	File name	Abyss361_REDOX.txt
Comments	- Sensor data positions are not shifted to the corrected vehicle track		
Sensor	SeaBird SBE49 FastCAT CTD (S/N: 4955482-0198)		
Total raw files	1 file (.txt) / 28.1 MB	File name	Abyss361_CTD.txt
Comments	- Sensor data positions are not shifted to the corrected vehicle track		
Sensor	Seabird ECO FLNTU (Chlorophyll / Turbidity) (S/N: 6590)		
Total raw files	1 file (.txt) / 5.06 MB	File name	Abyss361_ECO.txt
Comments	- Sensor data positions are not shifted to the corrected vehicle track		
Comments	The mission tests several feature of the multibeam. Adaptive gates, Tracker and other. The data is not usable due to a lack of roll information from vehicle to multibeam. On top there was a time offset and the multibeam got a wrong bottom detection in the beginning which was persistent. The Ascent weight was released to an error with the proximity sensor threshold.		

Abyss0362

Station	M182/141-1		Day (UTC)	26.06.2022
Dive	Abyss0362		Mission goal:	MBES Test dive and SSS

 <p>The map displays a survey track in red lines over a green bathymetric background. Key features include: 'MBES' and 'MBES Test' at the start of the track; 'DT-7A' and 'DT-8B' marked with dots; 'Submerge' and 'launch' points on the track; and a 'SSS Area' (Shallow Scattering Surface) indicated by a red hatched area on the right. A scale bar at the top left shows 0 to 2 km.</p>	Times (UTC)	
	Launch	06:59
	Mission start	07:01
	Survey start	08:39
	Survey finished	10:11 aborted
	Mission finished	
	Recovery	
	Distance travelled	15372
	Mission comments	Aborted mission because of ascent weight error.
	Depth / Altitude	- 75m Altitude - Depth 2900m
Sensor	Multibeam Reson T-50	
Total raw files	17 files (*.s7k) 2.56GB	First file 20220626_083739
		Last file: 20220626_100517
Survey area covered:	Average coverage:	
Sensor	Eh / REDOX Sensor (Koichi Nakamura)	
Total raw files	1 file (.txt) / 761kB	File name Abyss361_REDOX.txt
Comments	- Sensor data positions are not shifted to the corrected vehicle track	
Sensor	SeaBird SBE49 FastCAT CTD (S/N: 4955482-0198)	
Total raw files	1 file (.txt) / 6.02 MB	File name Abyss361_CTD.txt
Comments	- Sensor data positions are not shifted to the corrected vehicle track	
Sensor	Seabird ECO FLNTU (Chlorophyll / Turbidity) (S/N: 6590)	
Total raw files	1 file (.txt) / 1.1 MB	File name Abyss361_ECO.txt
Comments	- Sensor data positions are not shifted to the corrected vehicle track	
Comments	The ascent weight error was persistent from dive 361 to this one. The proximity sensor was changed and the position rearranged. The threshold was raised from 8 to 10.	

Abyss0363

Station	M182/147-1		Day (UTC)	27.06.2022
Dive	Abyss0363		Mission goal:	MBES and SSS retry of Abyss 0362. MBES Survey, MBES tests and SSS
			Times (UTC)	
			Launch	13:09
			Mission start	13:34
			Survey start	MB 15:06 / SSS 1:30
			Survey finished	MB 20:27 / SSS 7:23
			Mission finished	08:40
			Recovery	09:18
			Distance travelled	100727
			Mission comments	GFI in MBES test survey
			Depth / Altitude	- 60m Altitude - 2900m depth
Sensor	Multibeam Reson T-50			
Total raw files	290 files (*.s7k) 64.2 GB	First file	20220627_150420	
		Last file:	20220628_003653	
Survey area covered:		Average coverage:	4.86km ²	
Sensor	SSS 410kHz			
Total raw files	46 files (*.jsf)	First file	20220627.101555.0000000	
		Last file:	20220628.003646.0000040	
Survey area covered:		Average coverage:	5.1km ²	
Sensor	Eh / REDOX Sensor (Koichi Nakamura)			
Total raw files	1 file (.txt) / 4.49MB	File name	Abyss363_EH_SENSOR.txt	
Comments	- Sensor data positions are not shifted to the corrected vehicle track			
Sensor	SeaBird SBE49 FastCAT CTD (S/N: 4955482-0198)			

Total raw files	1 file (.txt) / 36.3 MB	File name	Abyss363_CTD.txt
Comments	- Sensor data positions are not shifted to the corrected vehicle track		
Sensor	Seabird ECO FLNTU (Chlorophyll / Turbidity) (S/N: 6590)		
Total raw files	1 file (.txt) / 6.6 MB	File name	Abyss363_ECO.txt
Comments	- Sensor data positions are not shifted to the corrected vehicle track		
Comments	Dive was successful. In MBES test pattern the vehicle had GFI. After this dive the multibeam showed several issues. Due to bad navigation and issues with the dvl, we exchanged Kearfott data and power interface.		

MBES Problems: There are multiple artifacts present in the survey data. No straight forward solution exists to create a map out of the dataset. Previous missions had similar (though not necessary the same) problems. These findings are based on the M182_147-1_Abyss-8_0363 Multibeam dataset.

Issue 1 – Incorrect Depth Calculation for Pings

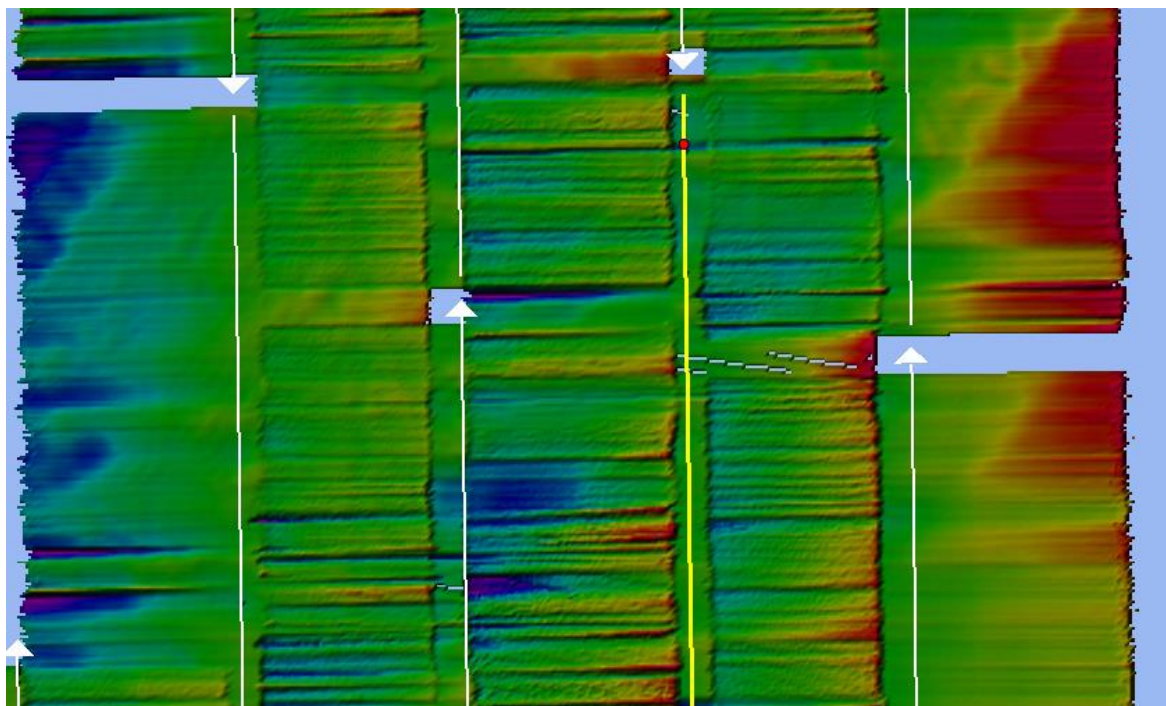


Fig. 12.8 Surface from directly after importing .s7k raw data into Qimera: colormap range from -83.472 to -71.272.

When importing the raw .s7k data into Qimera, the swath depth seems to be calculated incorrectly. In Fig. 12.8 the color scale is set about -80m, while in reality the seafloor is at around -2900m. The depth is however correctly displayed when plotted directly for a file (see Fig. 12.9). As a result, only the relative distance AUV-seafloor seems to be displayed. The reason for this is unknown, however Exporting and Re-Importing the depth seems to solve the problem. This issue seems to be exclusive to Qimera however, as with MB-System (after using mbpreprocess) this issue did not occur.

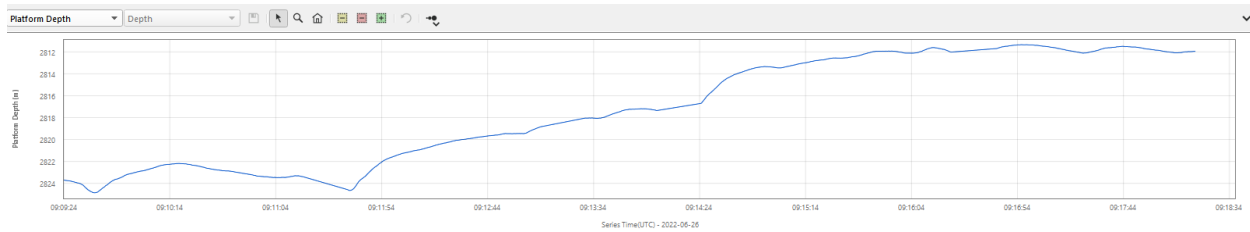


Fig. 12.9 Platform depth for an individual s7k file.

Issue 2 – Missing Navigation Data in File Records

As seen in Fig. 12.8 data at the end of a file is missing. The issue here is, that the navigation record of an .s7k file ends before the data recording itself. MB-System confirms that the data record relative to the navigation record is misaligned for individual files. (Using mblist and mbnavlist and comparing timestamps yields this result)

In Qimera this issue is solved by allowing to get navigation data from neighboring files (see Fig. 12.13). The issue was not resolved for MB-System. The files had to be processed on an individual basis. Using datalists for the preprocessing yielded errors, while using a script to run the commands on individual files did work (there were still errors and data bits were skipped). The MB-System version used was preinstalled on the METEOR Poseidon machine (MB-System Version 5.5.2315). The Current Version as of time of writing this is 5.7.8. There is a chance that this issue is resolved with a newer version. As of now the only attempt to resolve it (Exporting Navigation using Qimera and Importing to MB-System) failed – while the navigation was integrated, the individual files still maintained the shift in the navigation to data records.

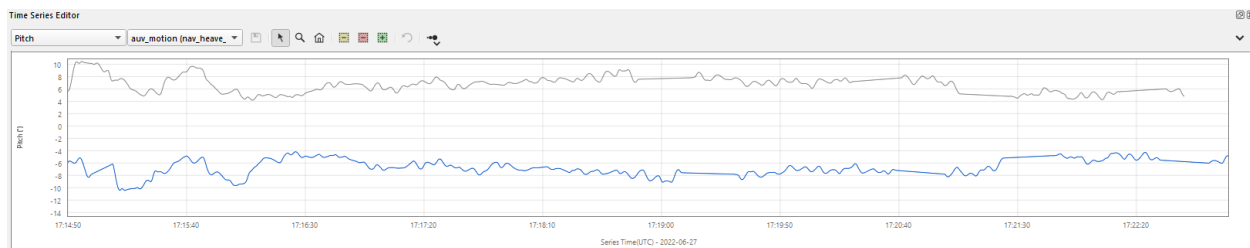


Fig. 12.10 Pitch over time for a single file. The grey line represents the original data, the blue line is from a corrected version. In both cases periods are present where no data is recorded (flat line). Those lines persist not only for the pitch, but other motion data.

A different issue is that apparently there are time windows where no new navigation is recorded. This is visible in the navigation records using Qimera (compare Fig. 12.10).

Issue 3 – Offset between neighboring lines

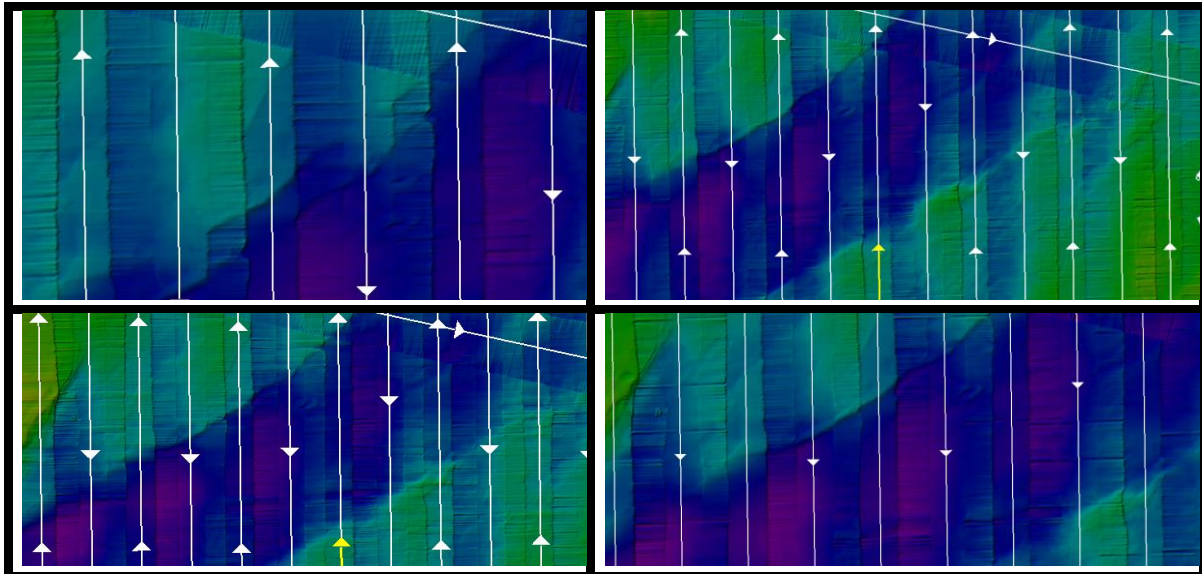


Fig. 12.11 Parts of the same survey treated with different offsets. Top-left: Original data. Top-right: Survey with 30m offset along track - this aligns the cliffs in north and south. Bottom-Left: Survey with 25° pitch offset. Bottom-right: Survey with 17 seconds time offset. The cliff feature matches for alternating lines.

In Fig. 12.11 cliffs are shown. Upon further inspection, it becomes clear that the lines from south-west to north-east actually form one continuous cliff. The difference between these features is however quite large (around 75m) and visible between lines with alternating headings. Such an offset over multiple lines can generally be explained by three static offsets (Pitch – Translation along the vehicle and Time). All of them have been considered:

Translation Offset: An offset of 30 m along track is in fact able to align the cliffs and other similar features as seen in Fig. 12.11. However, other artefacts remain. In addition, an offset of 30 m is physically impossible given the length of the AUV. While this does confirm the presence of a 30 m offset in the data, a translation between AUV navigation unit and Multibeam cannot (exclusively) be the reason.

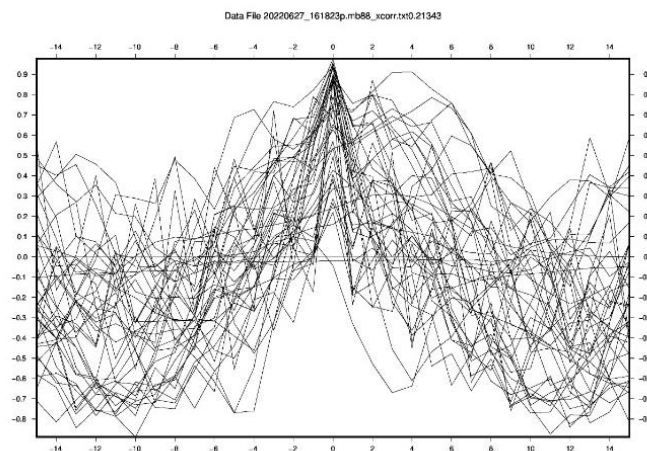


Fig. 12.12 Output Graph of the MB roll-time lag tool from MB-System. It shows the cross correlation over time between measured roll and apparent bottom slope of the seafloor. It clearly shows peaks at 0 degree - Which means there is no time lag present in the data.

Pitch Offset: A similar result can be achieved using a 25-degree pitch. The value was found using the Qimera patch test tool. The features are aligned, but other artifacts persist and such a large offset would be easily identified when attaching the multibeam.

Time Offset: MB-System provides a very useful tool to determine a lag between multibeam data and the roll in particular. The Cross correlation of the roll and the apparent bottom slope is calculated for different time lags. A clear maximum should exist for the correct time lag (compare). In this case there exists a clear indication of a time lag of 0 – so no time lag at all. Interestingly enough this is not reflected in Qimera. Applying a time offset of 17 seconds the cliffs are aligned between alternating survey directions (compare Fig. 12.8).

During the AUV mission, the platforms propeller occasionally stops. As a result, the vehicles roll spikes (see Fig. 12.14). If a time offset exists between roll and MB-data, the result can be seen twice. Once when the roll occurs in the data, but not in the navigation and once when the navigation sees a roll, but there is not actual movement from the Multibeam. The propeller stop can happen every other minute and results in periodic spikes, visible in the bathymetry (see Fig. 12.15). We can exploit this feature to increase the accuracy of our time lags. Using Qimeras Wobbly Tool, we can align the two roll spikes with sub second precision (see Fig. 12.16). This method is more precise than aligning based on features, but is less useful for determining large offsets. The time lags are not constant across the mission, but are increasing with time (during the whole mission the time lag changes by a whole second). In theory we could try to determine the best lag for each individual file and apply it there, in practice we used a reasonable value that in the middle of the two extremes in the beginning and end (18.15 seconds). The correct time lag eliminates the roll spike artifacts as well.

Why MB-System and Qimera seem to treat the data differently is not known, but it is clear that a non-constant time lag is causing at least some of the issues with the multibeam. The time lag probably is the cause for the misalignment of navigation and bathymetry (compare Issue 2 – Missing Navigation Data in File Records) records, too.

Roll-Offset: Even with the correct time offset, there are artifacts present that are not accounted for. These artifacts look like a roll offset and could be solved if the lines would go in the same direction. Since they are opposing lines however, this is not the correct solution. One observation however that can be made, is that the measured roll differs between lines. While south-north lines have an average roll of close to 0° , the north-south lines do have an average roll of close to -1° .

Since the underlying cause is unknown, the opposing lines were treated using a different roll offset (see Fig. 12.17). This somewhat corrects the data, but is not recommended, since it is not solving the underlying issue is complicated to implement and is not precise.

Results

The final result (see Fig. 12.18) is not optimal. The misalignment of navigation and MB-data is easily solved. The drifting time delay is the bigger challenge and while it can be solved on a per file basis, this method is tedious and relies on the roll spikes, which in return are something

to be avoided in the first place. Both issues should be addressed on the recording site and not on the postprocessing site.

The last issue of the apparent roll could not be solved and no underlying issue is determined. Further inspection is necessary.

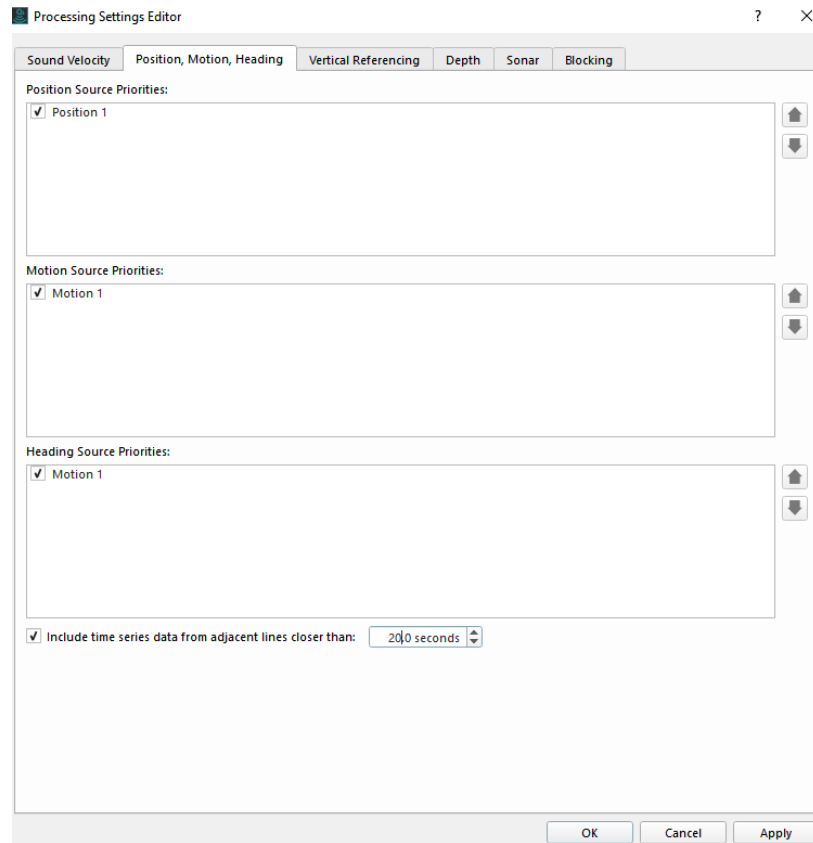


Fig. 12.13 Increasing the value for "Include time series data from adjacent lines closer than:" closes the navigational gaps in the data records

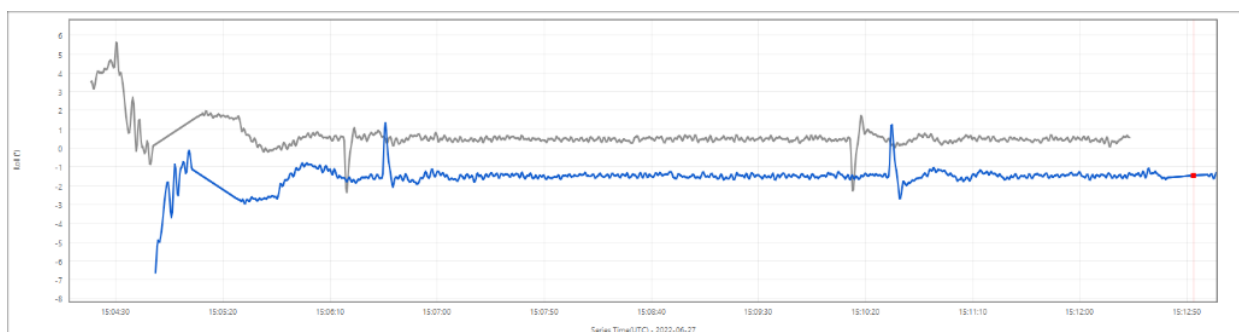


Fig. 12.14 Roll over time for a single .s7k file. The grey line corresponds to the original navigation, the blue line to the time shifted navigation. Additionally, the roll was changed from roll positive port down to postivie port up.

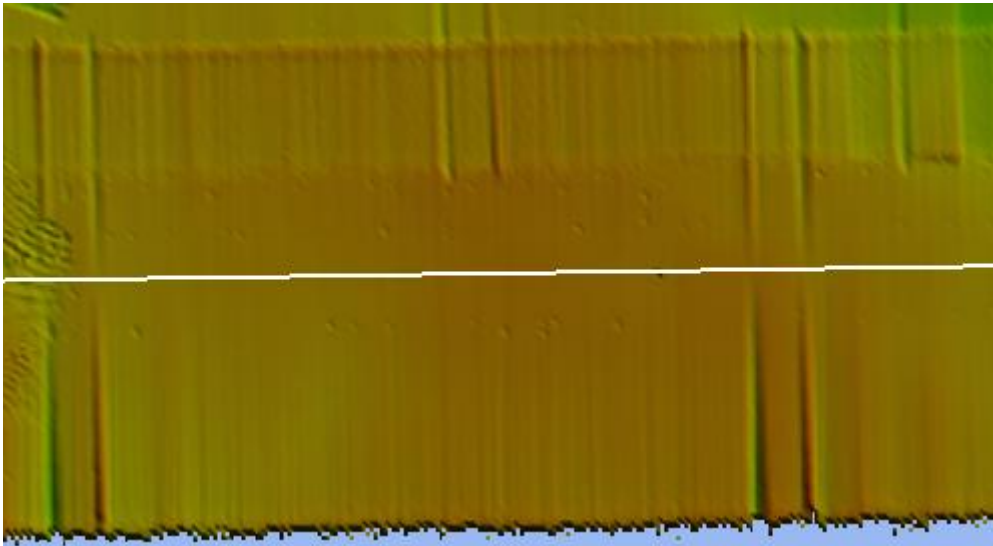


Fig. 12.15 Survey lines with roll artifacts clearly visible. The propeller stopped twice resulting in four roll artifacts.

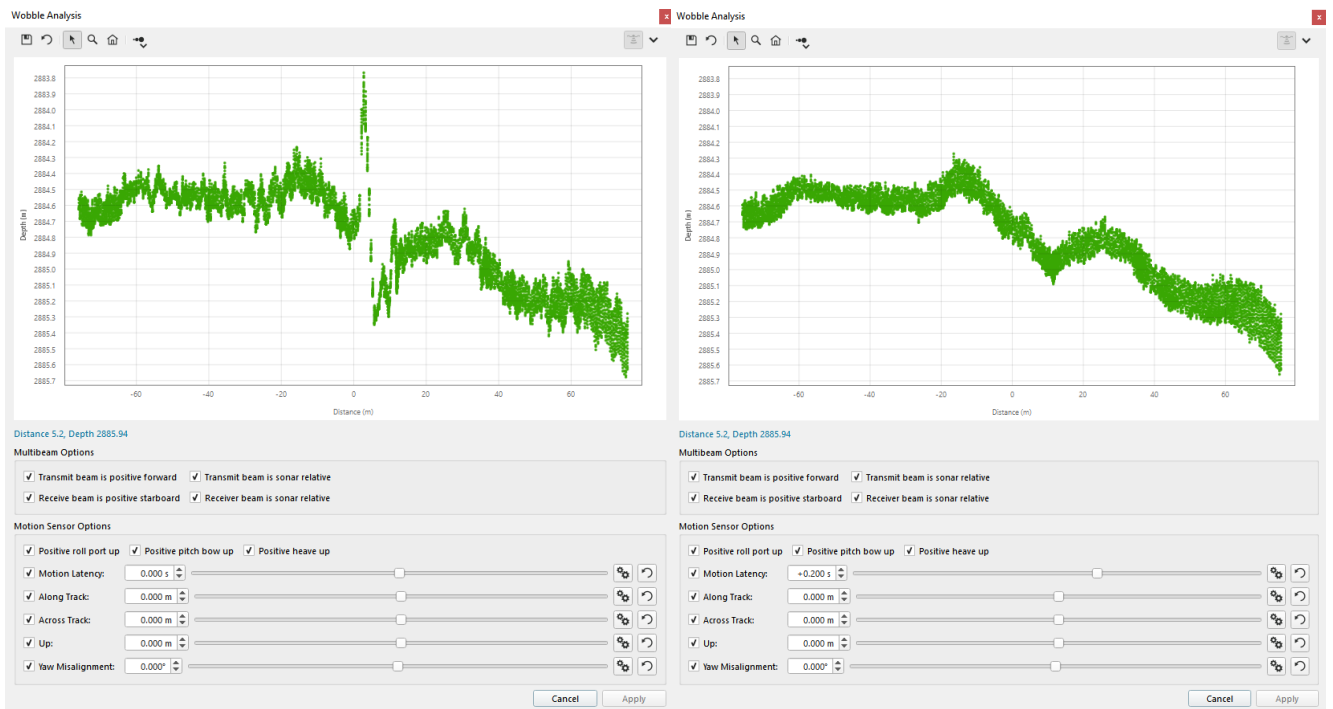


Fig. 12.16 Qimeras Wobbly Tool is useful to determine small time offsets. Especially if sudden changes in the roll are present. While the relative time offset between the left and right example are only 0.2 seconds, it is important to note, that the whole survey was already corrected by 18.15 seconds beforehand.

MRU Offsets:

	Latency (s)	Heave Delay (s)	Pitch (°)	Roll (°)	Heading (°)
2022-06-27 15:04:30	-18.150	0.000	0.000	-1.000	0.000
2022-06-27 15:24:47	-18.150	0.000	0.000	1.000	0.000
2022-06-27 15:48:19	-18.150	0.000	0.000	-1.000	0.000
2022-06-27 16:09:59	-18.150	0.000	0.000	1.000	0.000
2022-06-27 16:31:38	-18.150	0.000	0.000	-1.000	0.000
2022-06-27 16:53:14	-18.150	0.000	0.000	1.000	0.000
2022-06-27 17:14:50	-18.150	0.000	0.000	-1.000	0.000
2022-06-27 17:34:29	-18.150	0.000	0.000	1.000	0.000
2022-06-27 17:58:04	-18.150	0.000	0.000	-1.000	0.000
2022-06-27 18:19:39	-18.150	0.000	0.000	1.000	0.000
2022-06-27 18:41:12	-18.150	0.000	0.000	-1.000	0.000
2022-06-27 19:02:48	-18.150	0.000	0.000	1.000	0.000
2022-06-27 19:24:22	-18.150	0.000	0.000	-1.000	0.000
2022-06-27 19:45:56	-18.150	0.000	0.000	1.000	0.000
2022-06-27 20:07:32	-18.150	0.000	0.000	0.000	0.000

Fig. 12.17 The roll offset seems to be dependent on the direction of survey lines. In order to account for this problem, multiple vessel configuration files need to be created in Qimera.

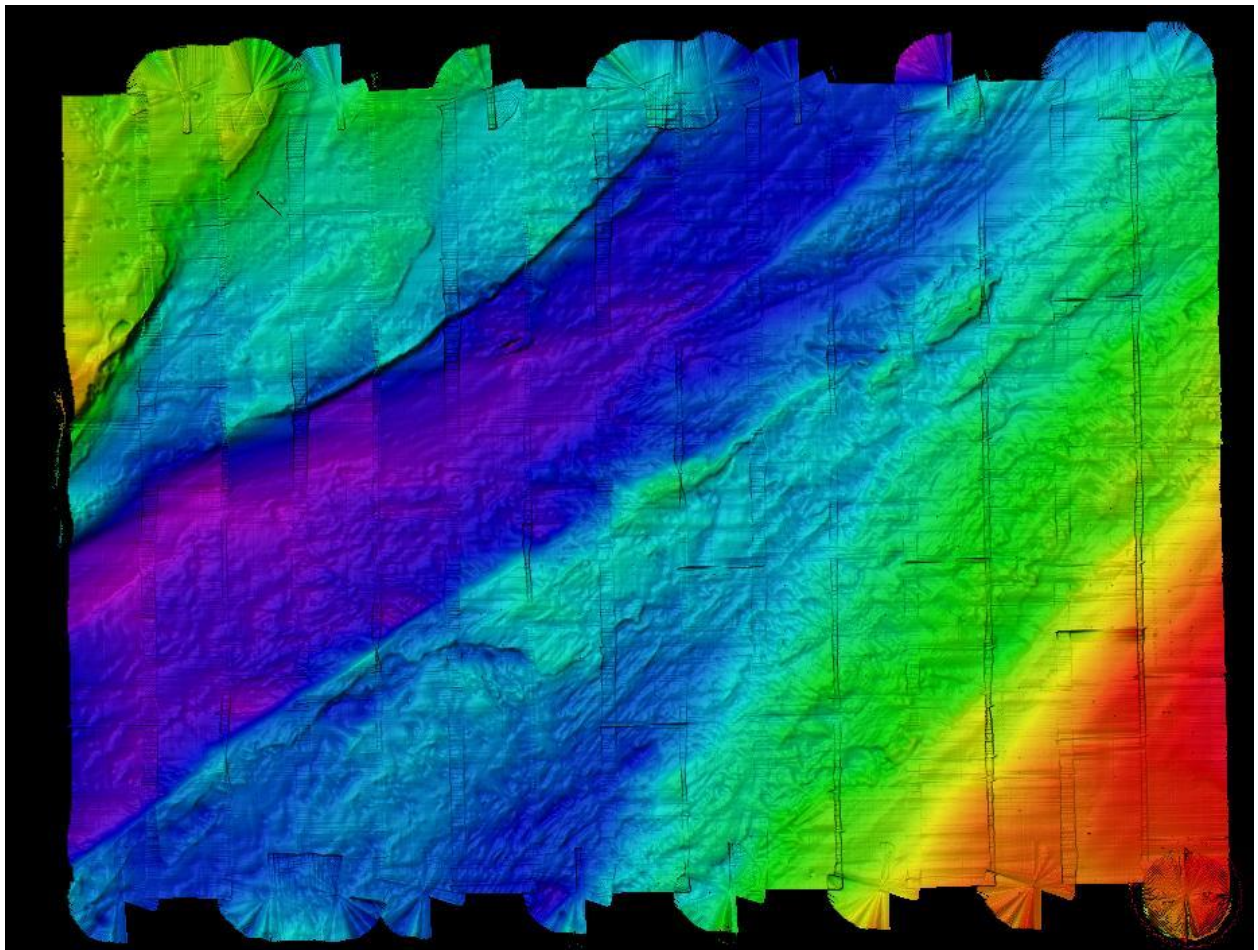

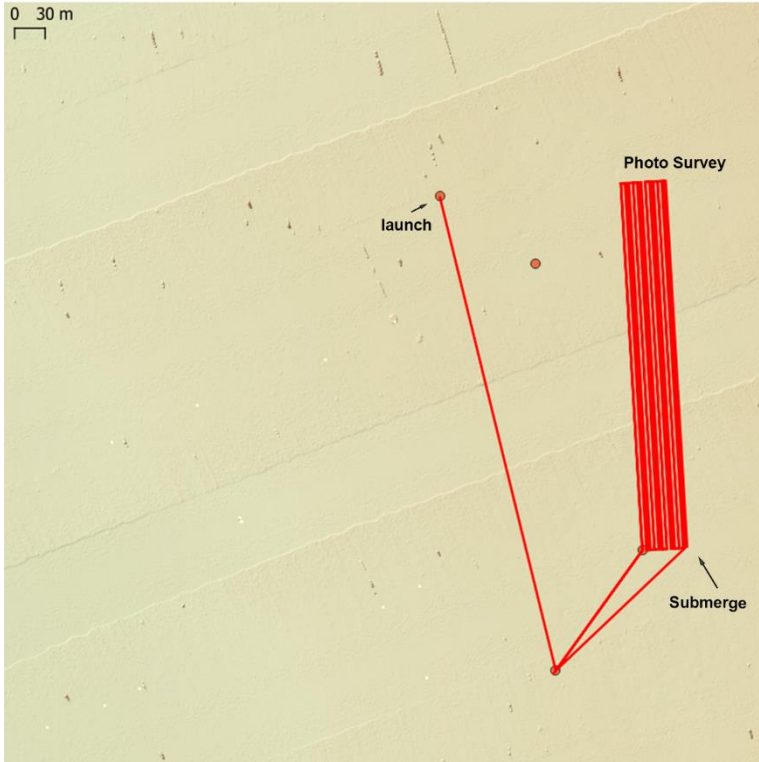


Fig. 12.18 Final surface for the dive M182_147-1_Abyss-8_0363 with 3m resolution.

Abyss0364

Station	M182/167-1		Day (UTC)	30.06.2022
Dive	Abyss0364		Mission goal:	Camera test at 4 and 7m water depth, GPS fix in between
			Times (UTC)	
			Launch	19:01
			Mission start	19:03
			Survey start	19:11
			Survey finished	20:51
			Mission finished	20:53
			Recovery	21:18
			Distance travelled	9885
			Mission comments	Camera worked good, images slightly out of focus or just blurred from marine snow in water column
			Depth / Altitude	- 7m and 4m Altitude - 70m depth
Sensor	DSC Deep Survey Cam			
Total raw files	4499 files (.jpg) 28.3GB	First file		
		Last file:		
Survey area covered:		Average coverage:		
Sensor	Eh / REDOX Sensor (Koichi Nakamura)			
Total raw files	1 file (.txt) / 444kB	File name	Abyss364_REDOX.txt	
Comments	- Sensor data positions are not shifted to the corrected vehicle track			
Sensor	SeaBird SBE49 FastCAT CTD (S/N: 4955482-0198)			
Total raw files	1 file (.txt) / 3.48 MB	File name	Abyss364_CTD.txt	

Comments	- Sensor data positions are not shifted to the corrected vehicle track		
Sensor	Seabird ECO FLNTU (Chlorophyll / Turbidity) (S/N: 6590)		
Total raw files	1 file (.txt) / 646 kB	File name	Abyss364_ECO.txt
Comments	- Sensor data positions are not shifted to the corrected vehicle track		
Comments	Successful test dive. The pictures are not clear because of marine snow and jellies in the water column. The AUV performed navigation without transponders very good		

Sample Data:

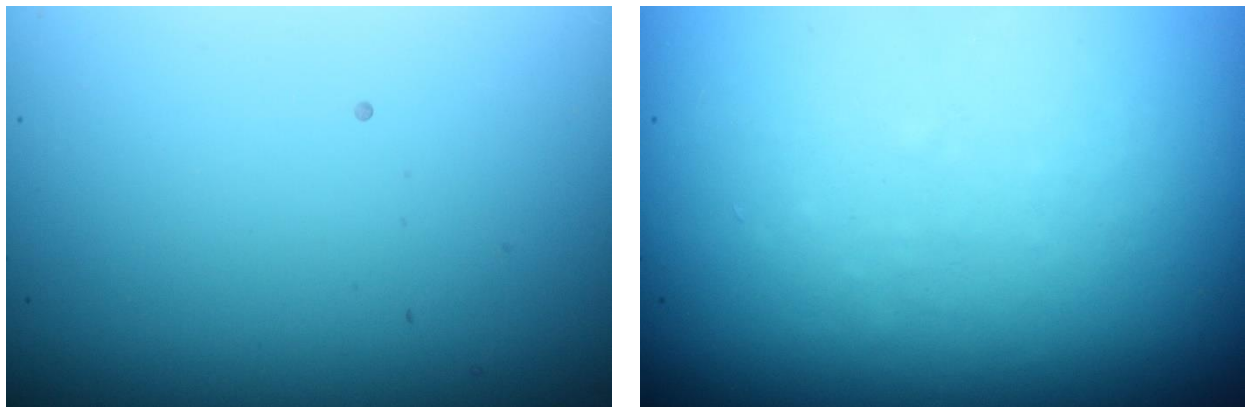

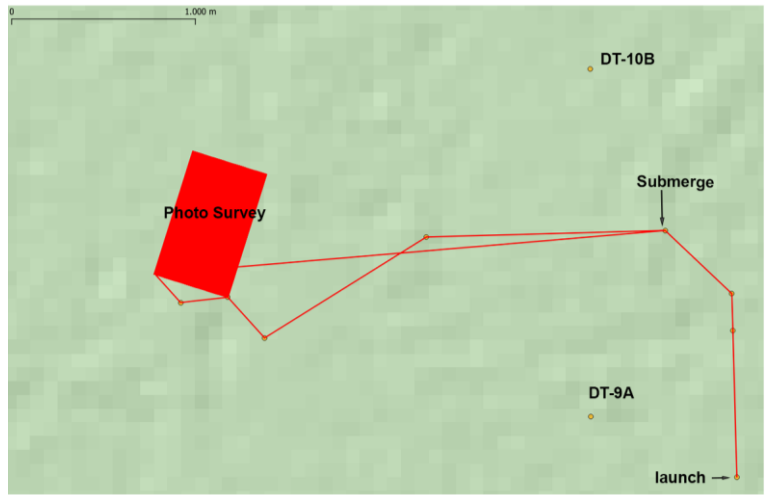


Fig. 12.19 These images show blurriness which is introduced by marine snow and a lot of fauna in the water column.

Abyss0365

Station	M182/178-1		Day (UTC)	03.07.2022
Dive	Abyss0365		Mission goal:	SSS and Camera over BBL and Rover
			Times (UTC)	
			Launch	20:15
			Mission start	20:16
			Survey start	21:38 / 07:29
			Survey finished	07:26 / 08:35

	Mission finished	09:41	
	Recovery	10:05	
	Distance travelled	69174	
	Mission comments	Area of longterm deployment, SSS and Camera worked, but LBL navigation was off so that the wrong area was mapped	
Depth / Altitude	- 7m Alt DSC & SSS		
Sensor	DSC Deep Survey Cam		
Total raw files	35000 files (*.jpg) 219 GB	First file	
		Last file:	
Survey area covered:	Average coverage:	294.550m ²	
Sensor	SSS 410kHz		
Total raw files	8 files (*.jsf) 949MB	First file	20220703.111139.0000000
		Last file:	20220704.072901.0000006
Survey area covered:	Average coverage:	294.550m ²	
Sensor	Eh / REDOX Sensor (Koichi Nakamura)		
Total raw files	1 file (.txt) / 3.15 MB	File name	Abyss365_REDOX.txt
Comments	- Sensor data positions are not shifted to the corrected vehicle track		
Sensor	SeaBird SBE49 FastCAT CTD (S/N: 4955482-0198)		
Total raw files	1 file (.txt) / 25.4 MB	File name	Abyss365_CTD.txt
Comments	- Sensor data positions are not shifted to the corrected vehicle track		
Sensor	Seabird ECO FLNTU (Chlorophyll / Turbidity) (S/N: 6590)		
Total raw files	1 file (.txt) / 4.65 MB	File name	Abyss365_ECO.txt
Comments	- Sensor data positions are not shifted to the corrected vehicle track		
Comments	The final dive was another retry. The plan was a photomission over BBL Lander and Pantha Rhei Rover. Due to unknown problems the AUV did not manage to get LBL positioning. In order to that error the flight was blind an the map has an offset of 420m.		

Sample Data:

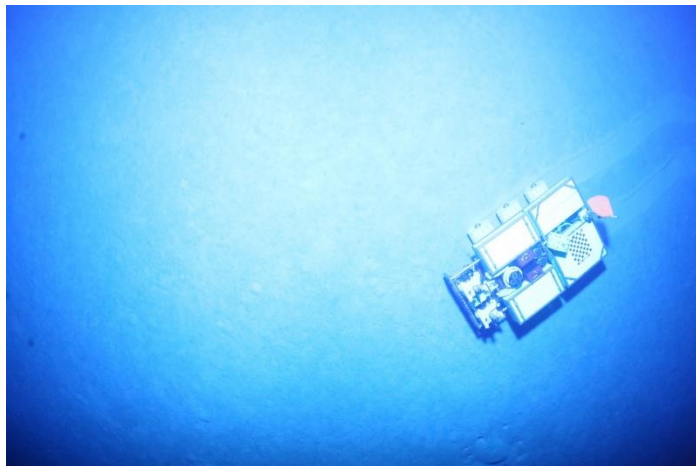


Fig. 12.20 Photo of the DSR Pantha Rhei, taken by the AUV Abyss.

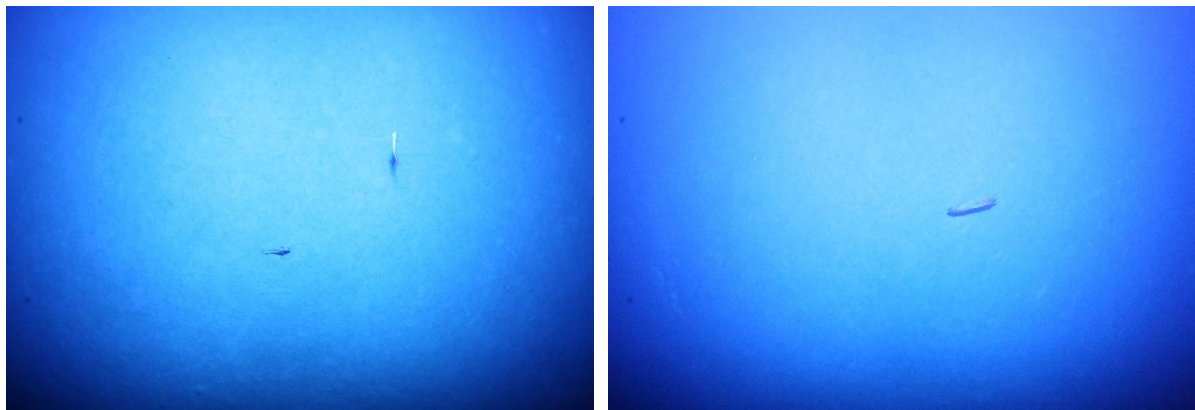


Fig. 12.21 Images taken by the AUV Abyss of the deep seafloor.

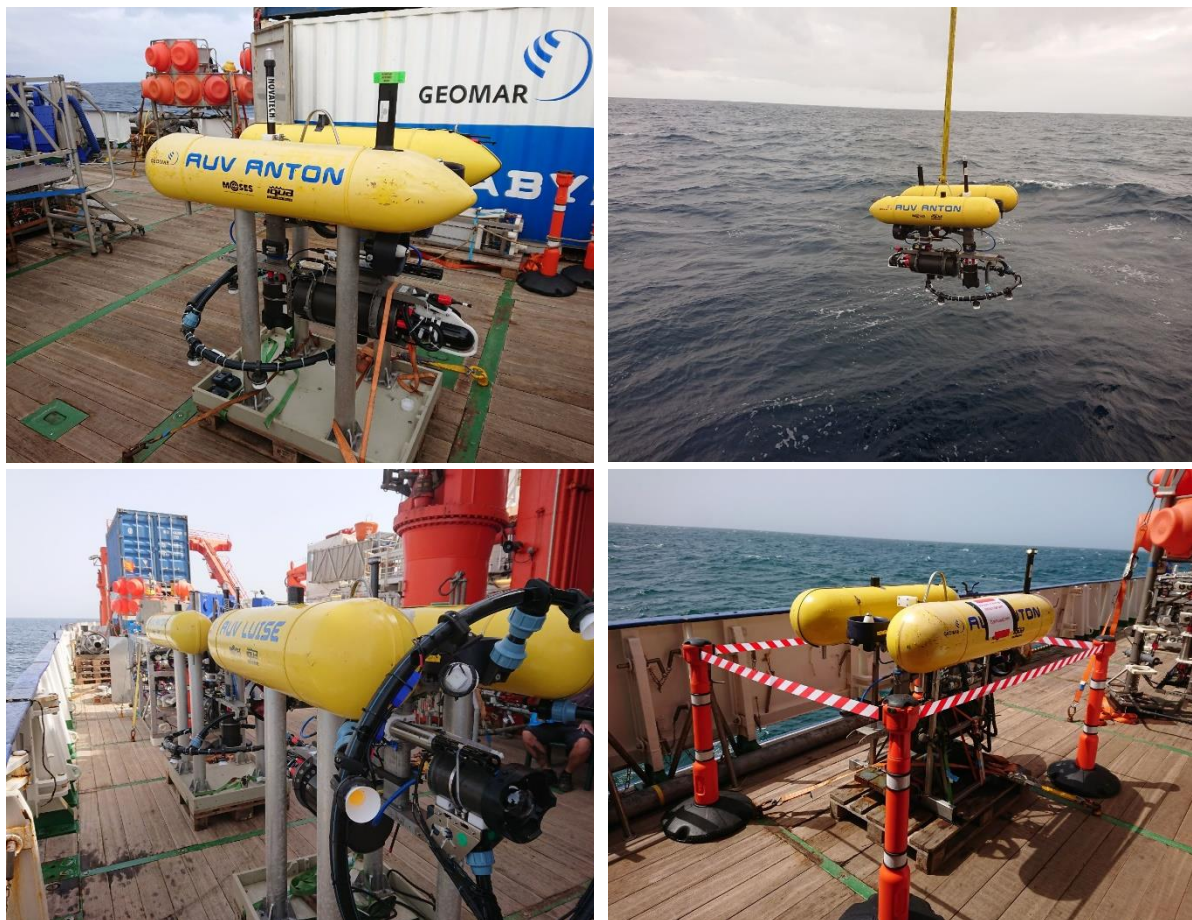
AUV GIRONA 500

Fig. 12.22 Images of the GIRONA500 AUVs Anton and Luise on deck of RV METEOR and during deployment (top right).

The overall dimensions of the vehicle are 1 m in height, 1 m in width, 1.5 m in length and a weight of less than 200 kg. The two upper hulls, which contain the flotation foam and the electronics housing, are positively buoyant, while the lower one contains the heavier elements such as the batteries and the payload. This particular arrangement of the components makes the separation between the centre of gravity and the centre of buoyancy about 11 cm, which is significantly more than any typical torpedo shape design. This provides the vehicle with passive stability in pitch and roll, making it suitable for imaging surveys. One characteristic of the Girona 500 is its capacity to reconFig. for different tasks.

Standard sensors

- INS: iXblue Phins Combat C3

The internal navigation unit that processes sensor data and provides position information. The error of this INS is in range of $0,15^\circ$ for heading and $0,05^\circ$ for roll and pitch. This leads to a 0,3% DT position accuracy.

- DVL: Teledyne RDI Explorer 600kHz

This device measures the velocity relative to the sea floor and its altitude.

- CTD: Sea-Bird SBE 49 FastCAT

This measurement device acquires the conductivity, temperature and the pressure of the water and calculates the sound velocity.

- Pressure sensor: Valeport ultraP

This sensor measures the pressure and converts it to water depth.

- USBL: Evologics S2CR 18/34

The Evologics S2CR 18/34 modem combines underwater acoustics and positioning.

- GPS: Quectel l86 GNSS module

The GPS is used to determine the absolute position at the surface.

Additional Sensors

- Imagenex 837B DeltaT 4000

The optionally mounted multibeam sonar is used for mapping purposes.

- CoraMo mk II Camera

Down or forward looking camera system for photographic surveys with an image rate of up to 2 images per second with a resolution of 12.34MP. CoraMo brings connection for 8 high power LEDs

12.6 AUV Test

To test the functionality of the software Sinaps and beluga the USBL transponder from Evologics was used which is rated for 6000 m water depth. For the stations 038-1 and 054-1 it was mounted on the Panta Rhei launcher and the CTD, respectively and for station 163-1 it was used in the classical way with a weight and buoyancy foam.

For the first two stations the top side USBL modem 'S2C R 18/34 USBL' from Evologics was mounted on an 8 m long tube that was fixed on the starboard rail. For the last three stations it was mounted in the moon pool of RV METEOR at the port-front position with an adapter. The lever arms are shown in Table 12.10.

Table 12.9 Station overview of AUV dives.

Station number	Dive number	Area	Task	Sensors	Comment
038-1	n.a.	E1	USBL test	USBL Transponder	The USBL Transponder was mounted on the Panta Rhei launcher to test Sinaps, Beluga and the ship offsets
054-1	n.a.	Eddy Hunt	USBL test	USBL Transponder	The USBL Transponder was mounted on the CTD to test Sinaps, Beluga and the ship offsets

133-1	Anton 232	E4	INS test	INS, CTD	AUV Anton was fixed on the transport stand together with 120 kg weights and lowered into the water with the ship winch
163-1	n.a.	E5	lever arm calibration	USBL Transponder	Strong wind and currents and therefore none ideal calibration patterns
166-1	Luise 237, 238, 239, 240	E5	Thermocline detection	CTD, Camera, Oxygen Optode, Fluorescence	large navigation drift due to wrong INS settings

Table 12.10 Lever arms of RV METEOR for Sinaps and Beluga.

Sinaps			Beluga		
	GPS [m]	USBL [m]		GPS [m]	USBL [m]
x	-6	-19,17	x	3	-10,17
y	-0,36	-0,65	y	1,54	1,25
z	-32,81	7,09	z	-32,81	7,09

12.7 Dedicated Acoustic Mapping

Table 12.11 Calibration offsets for the EM122 MBES.

Parameter	EM122 -old		EM122 -new	
	Tx	Rx	Tx	Rx
Pitch [°]	0.270	0.350	0.270	0.350
Roll [°]	-0.060	-0.090	-0.340	-0.370
HDG [°]	359.940	359.870	359.940	359.870
Stbd [m]	-1.960	-1.911	-1.960	-1.911
Fwd [m]	5.662	10.533	5.662	10.533
Up [m]	-7.043	-7.015	-7.043	-7.015

Table 12.12 Calibration offsets for the EM710 MBES.

Parameter	EM710 -old		EM710 -new	
	Tx	Rx	Tx	Rx
Pitch [°]	0.370	-0.360	0.370	-0.360
Roll [°]	0.100	-0.080	0.410	0.230
HDG [°]	0.060	179.980	0.060	179.980
Stbd [m]	-0.908	-0.807	-0.908	-0.807
Fwd [m]	12.341	11.622	12.341	11.622
Up [m]	-7.005	-7.010	-7.005	-7.010

Table 12.13 Main settings for EM122 acquisition.

Max. angle [°] port	50
Max. angle [°] starboard	50
Angular coverage mode	AUTO
Beam spacing	HD EQDST
Dual swath mode	Dynamic
Pitch stabilization	yes
Yaw stabilization	off
Heading filter	Weak

12.8 Maps of the Research Areas

Working area CVOO

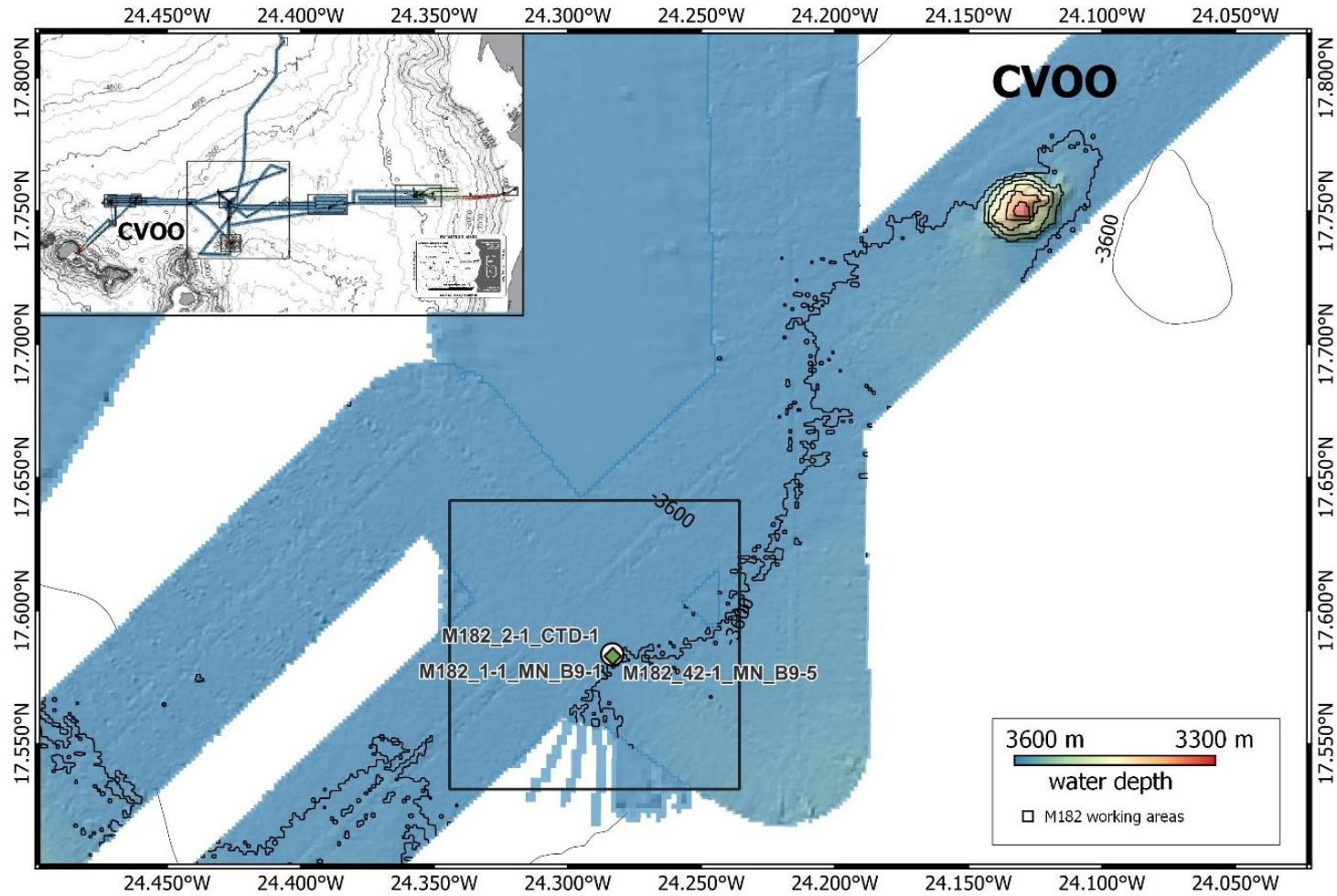


Fig. 12.23 Bathymetry data of M182 cruise of research area CVOO with sampling stations.

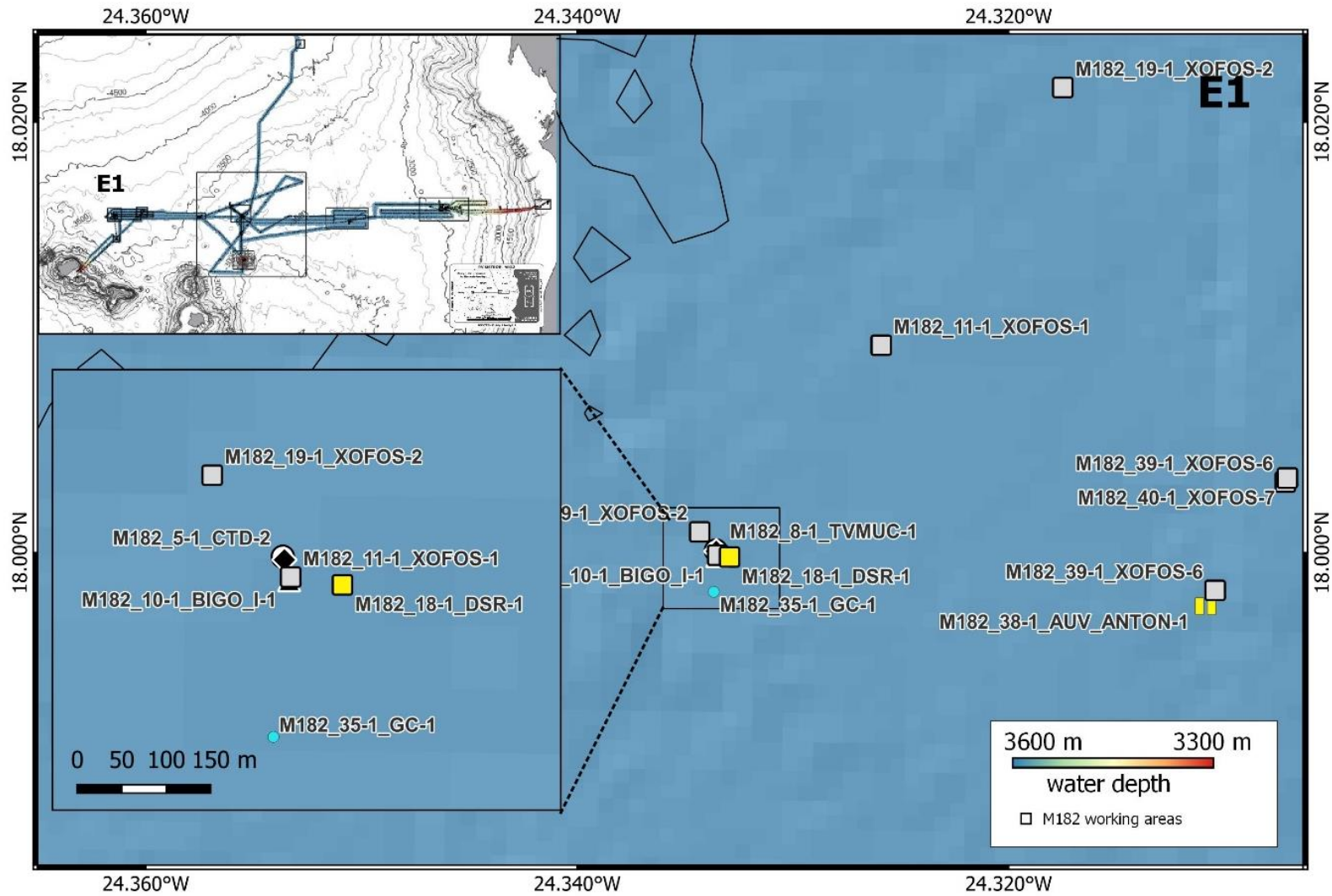
Working area E1

Fig. 12.24 Bathymetry data of M182 cruise of research area E1 with sampling stations.

Working area E1 Hill

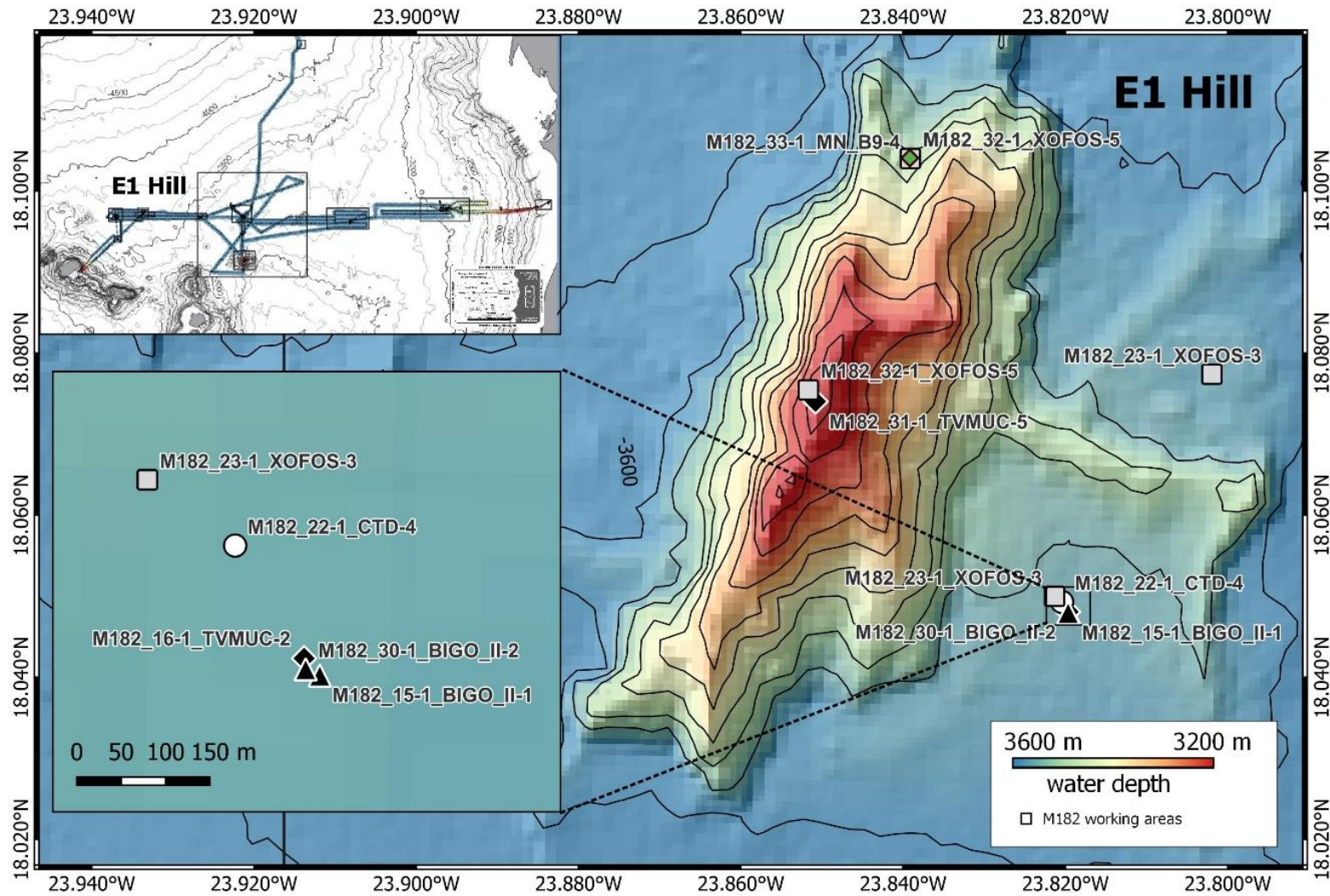


Fig. 12.25 Bathymetry data of E1 Hill cruise of research area CVOO with sampling stations.

Working area E2

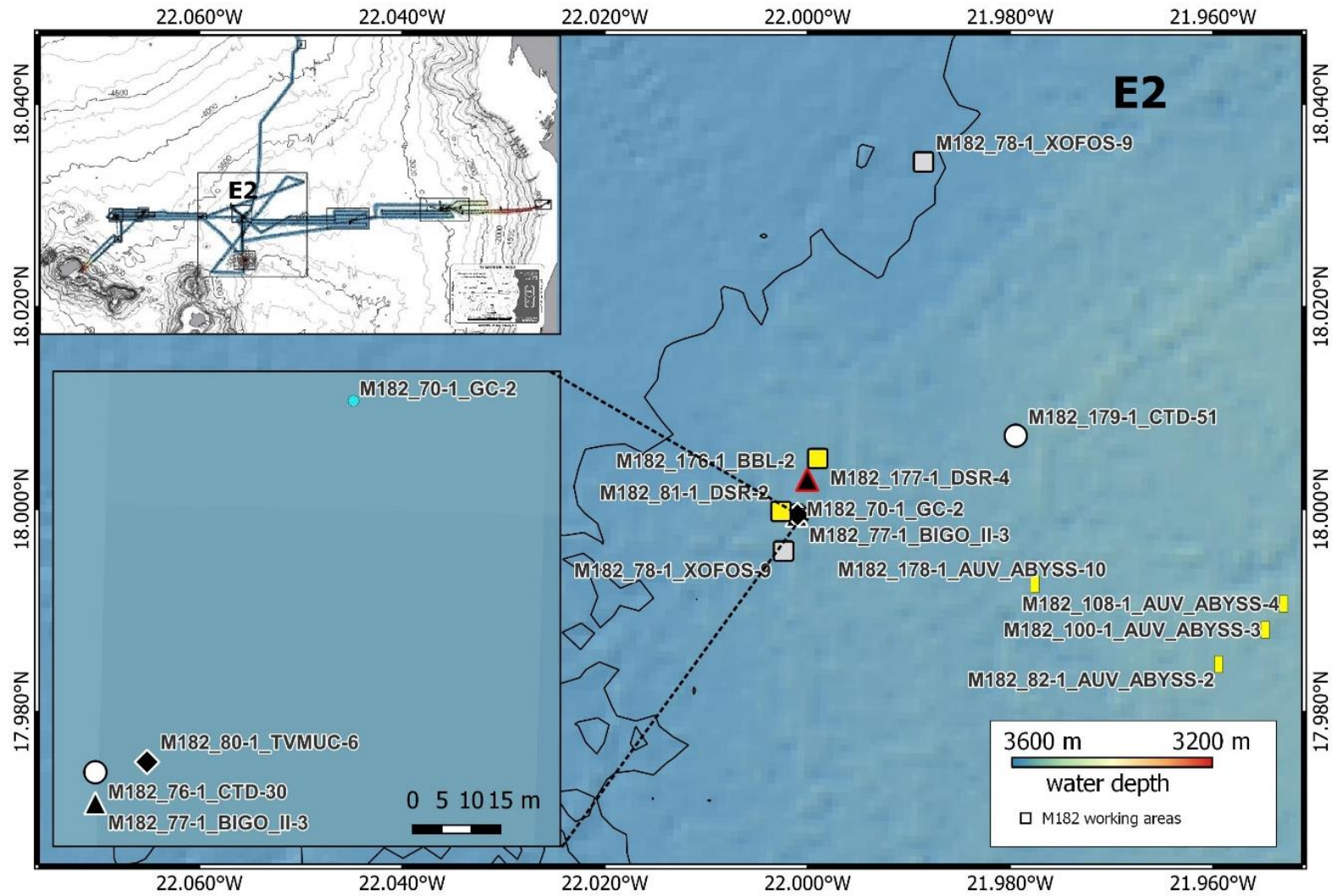


Fig. 12.26 Bathymetry data of M182 cruise of research area E2 with sampling stations.

Working area E3

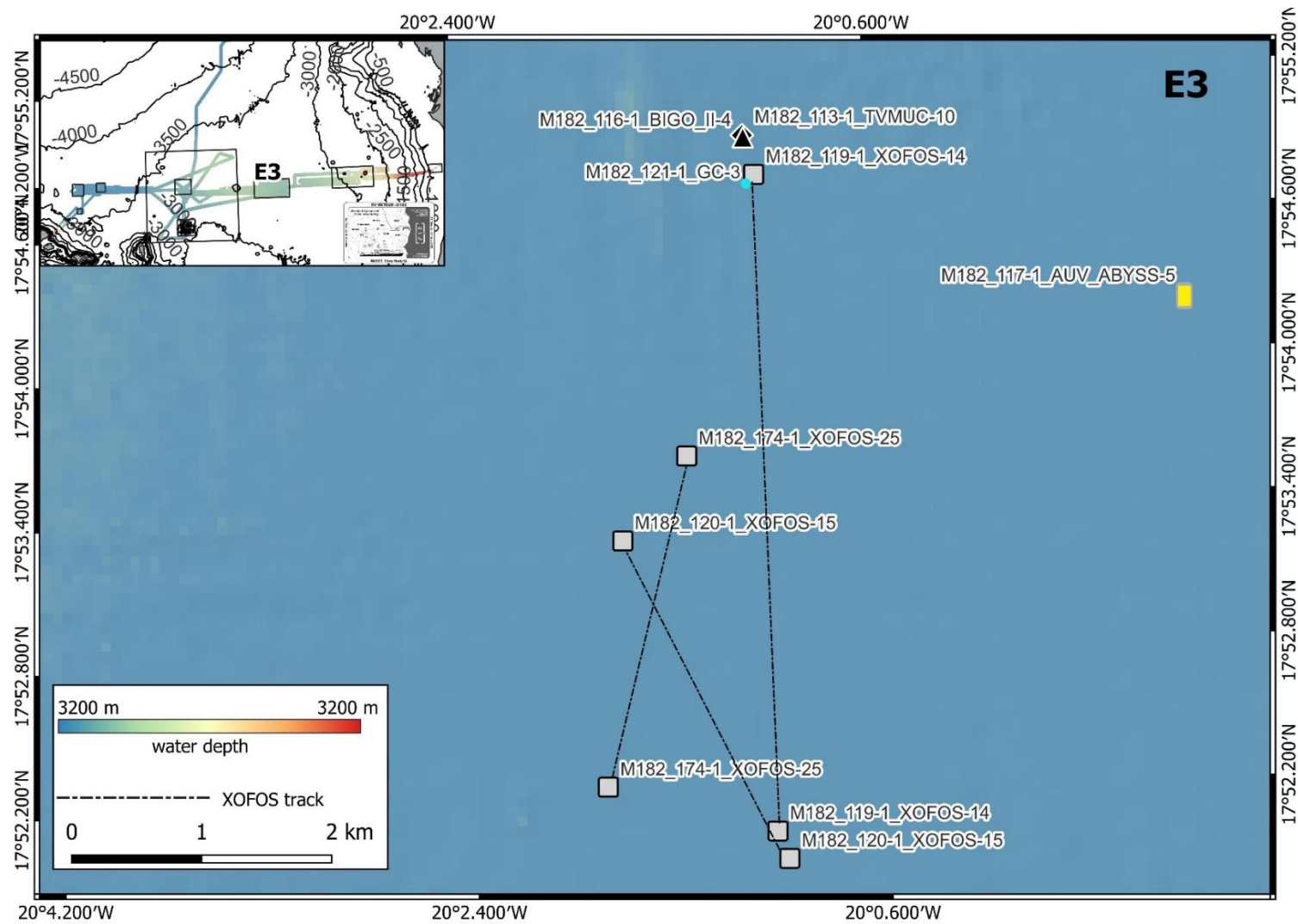


Fig. 12.27 Bathymetry data of M182 cruise of research area E3 with sampling stations.

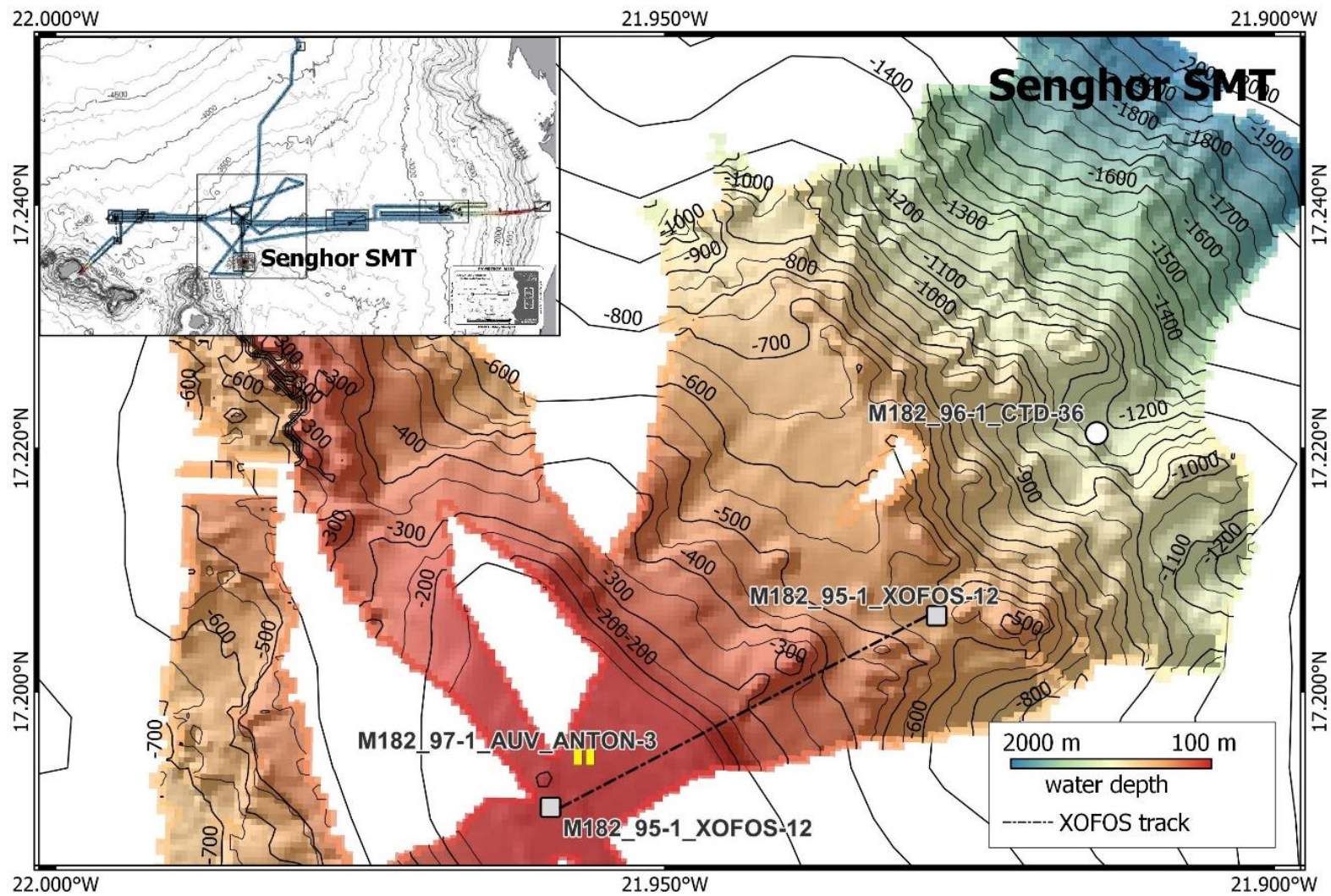
Working area Senghor Seamount

Fig. 12.28 Bathymetry data of M182 cruise of research area Senghor SMT with sampling stations.

Working area E4 (a)

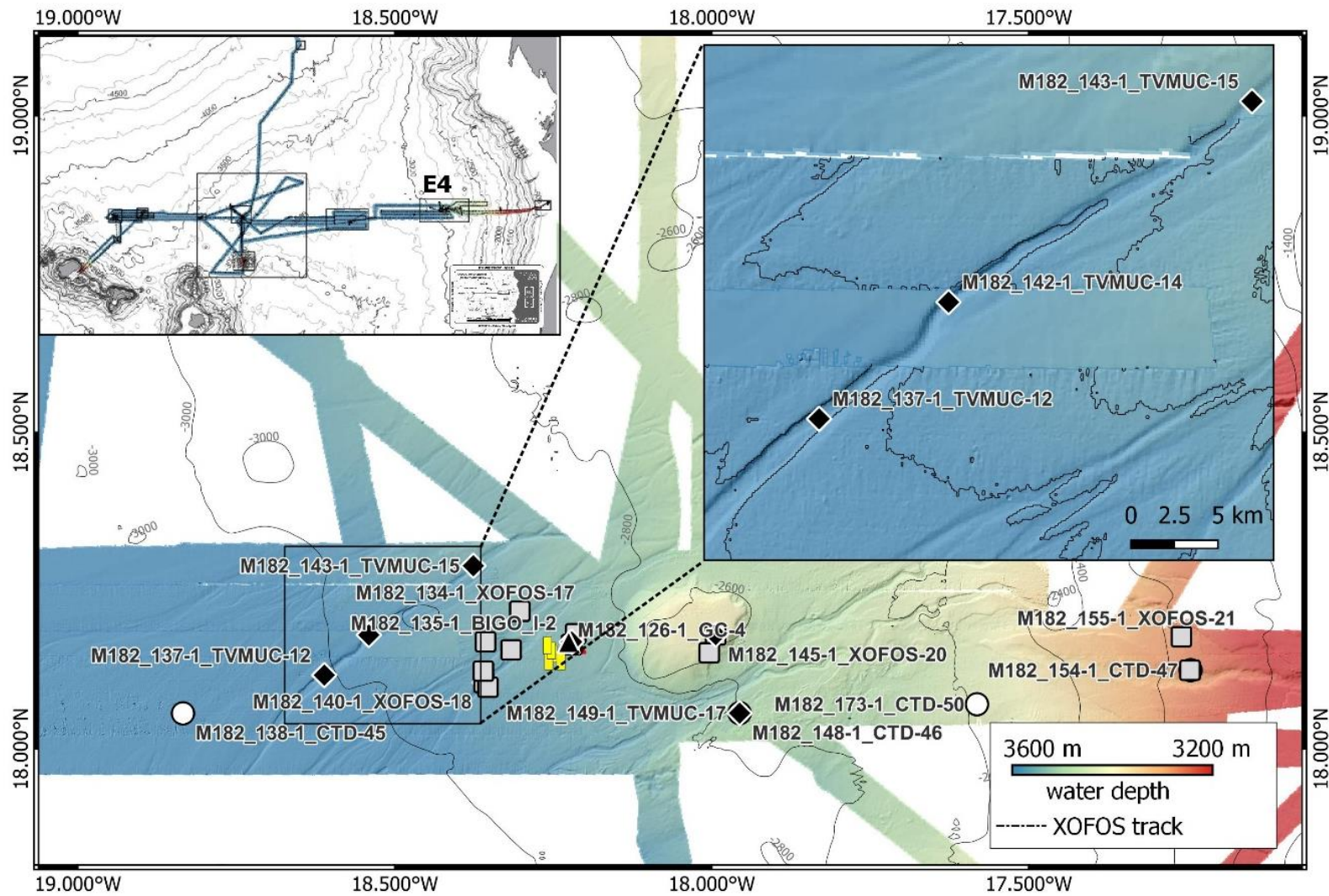


Fig. 12.29 Bathymetry data of M182 cruise of research area E4 (a) with sampling stations.

Working area E4 (b)

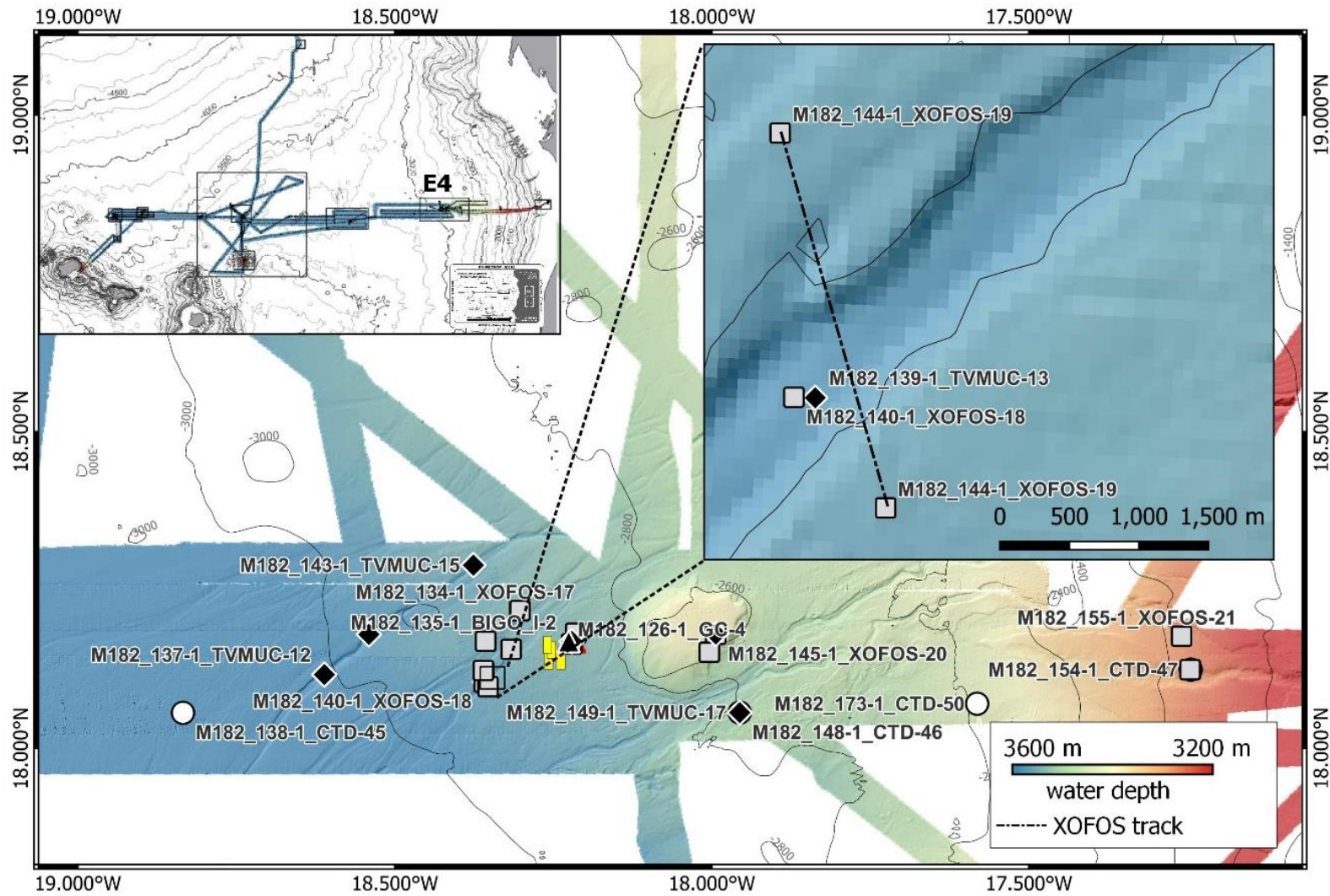


Fig. 12.30 Bathymetry data of M182 cruise of research area E4 (b) with sampling stations.

Working area E4 (c)

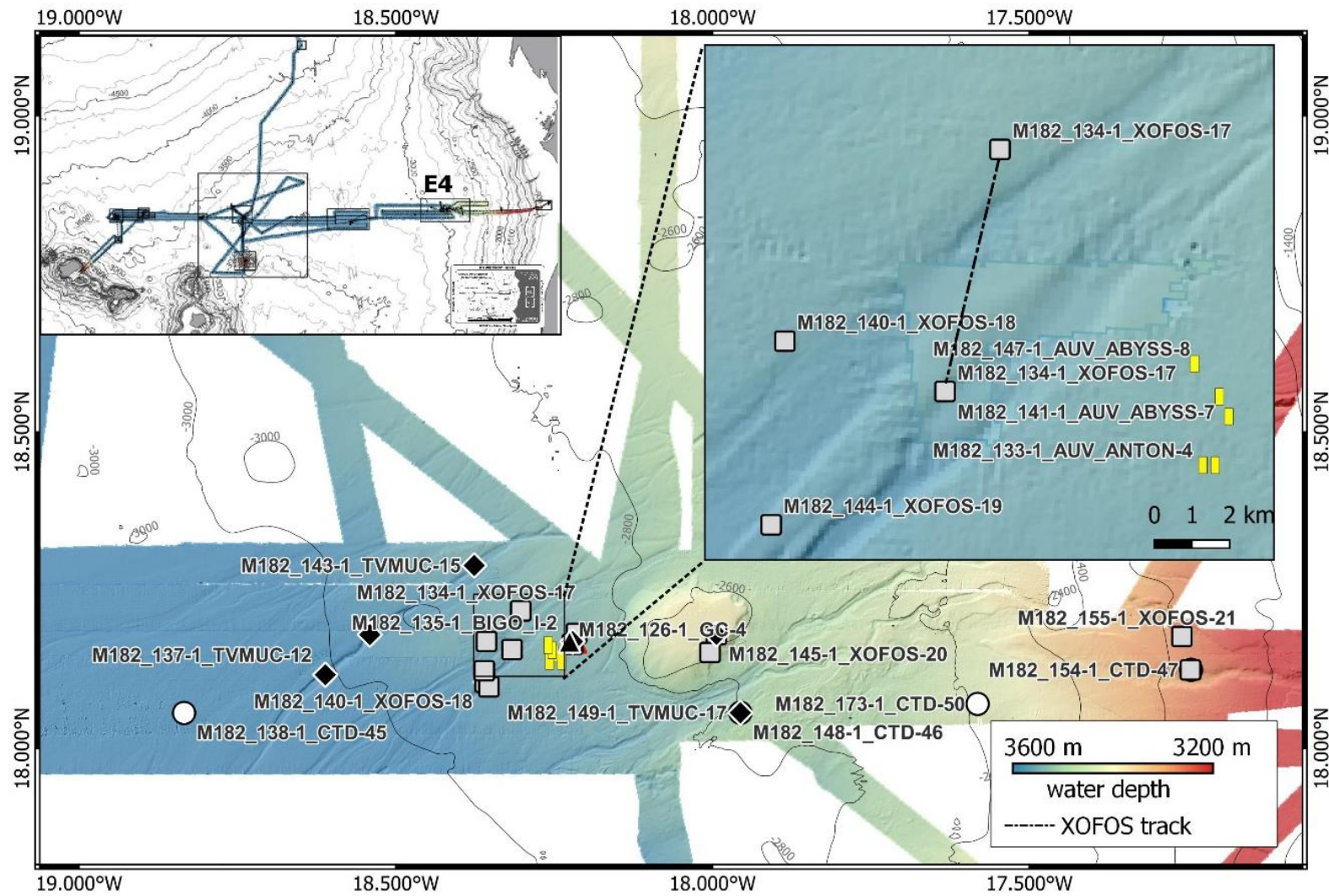


Fig. 12.31 Bathymetry data of M182 cruise of research area E4 (c) with sampling stations.

Working area E4 (d)

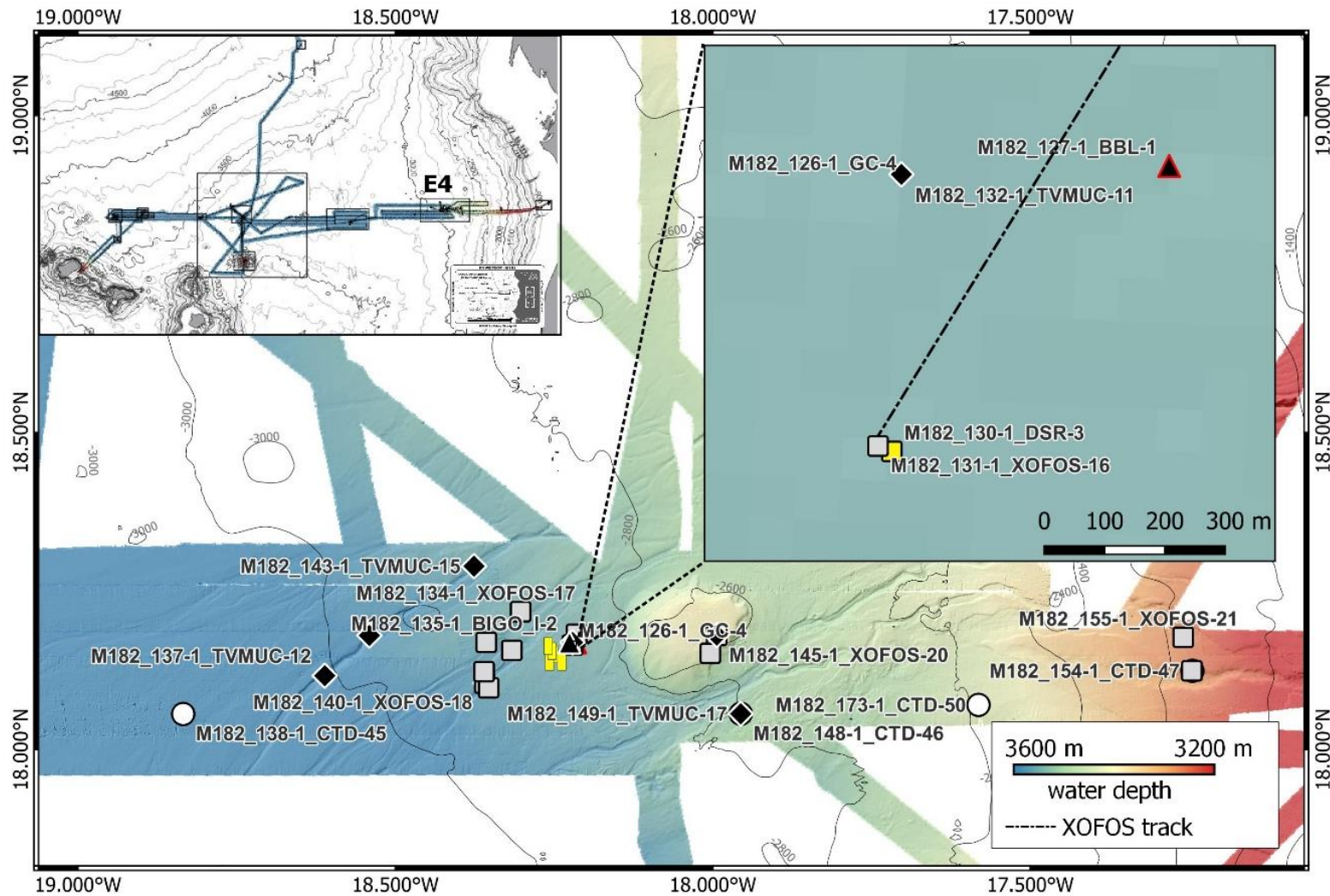


Fig. 12.32 Bathymetry data of M182 cruise of research area E4 (d) with sampling stations.

Working area E4 (e)

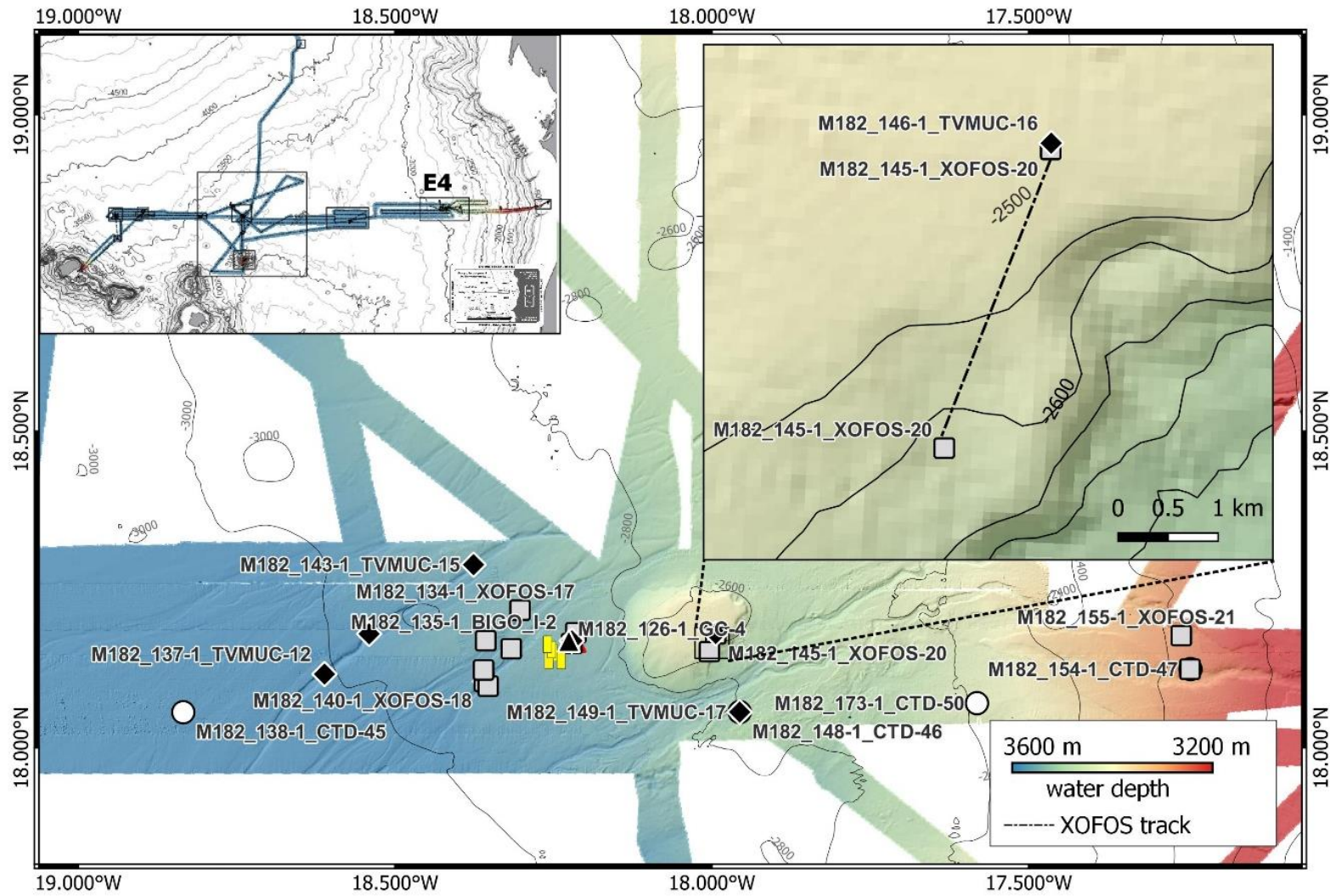


Fig. 12.33 Bathymetry data of M182 cruise of research area E4 (e) with sampling stations.

Working area E4 (f)

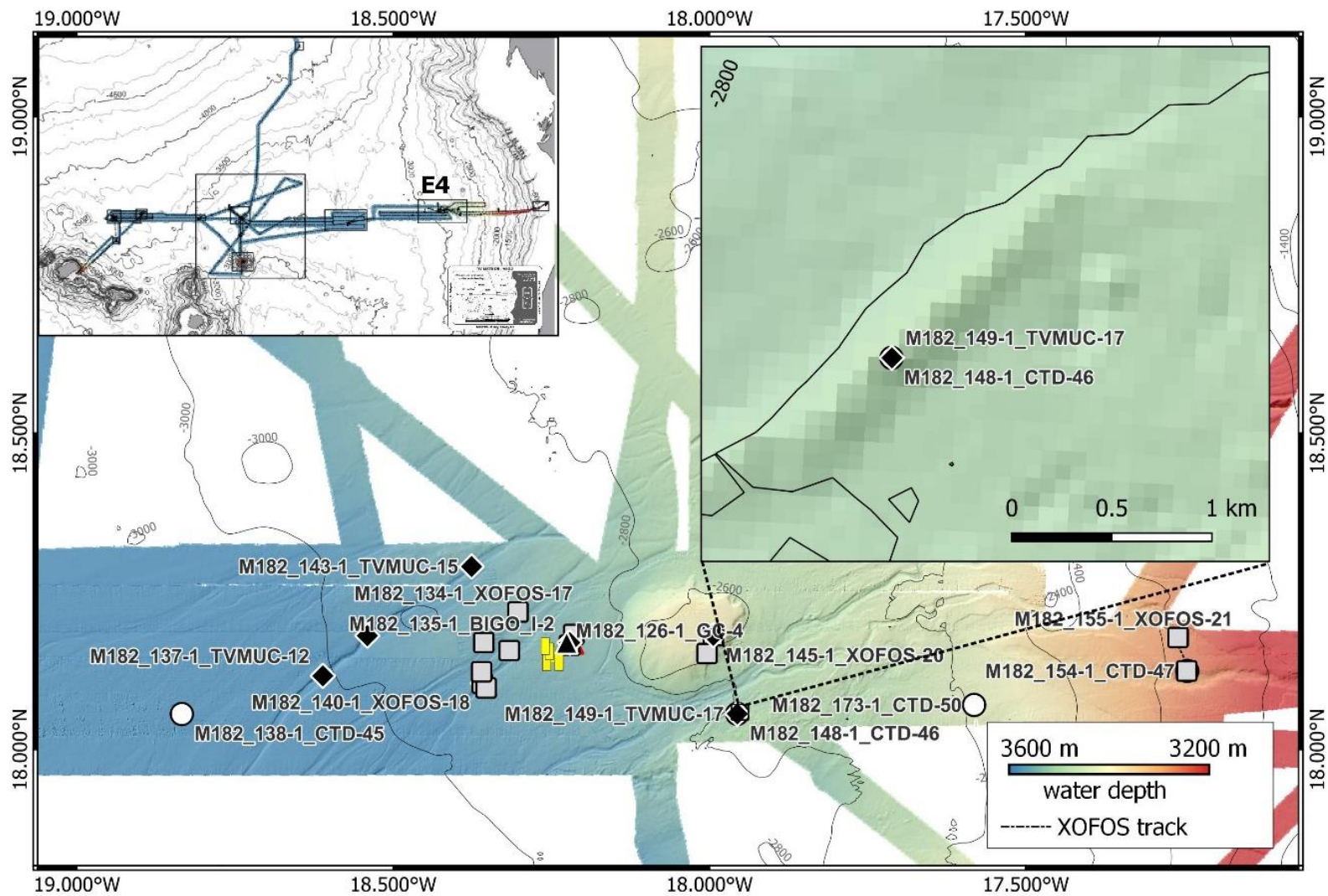


Fig. 12.34 Bathymetry data of M182 cruise of research area E4 (f) with sampling stations.

Working area E4 – E5

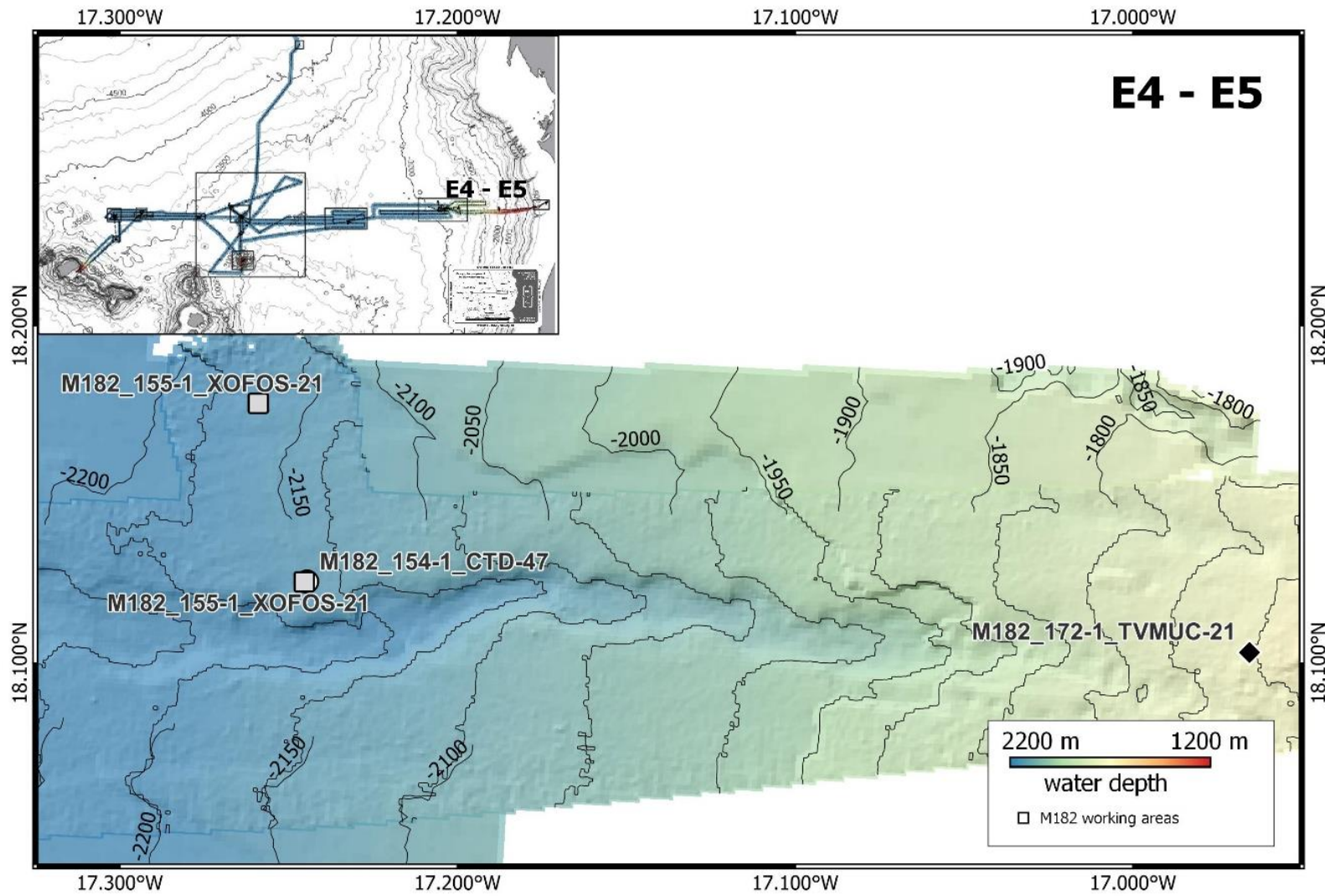


Fig. 12.35 Bathymetry data of M182 cruise of research area E4 - E5 with sampling stations.

Working area E5 (a)

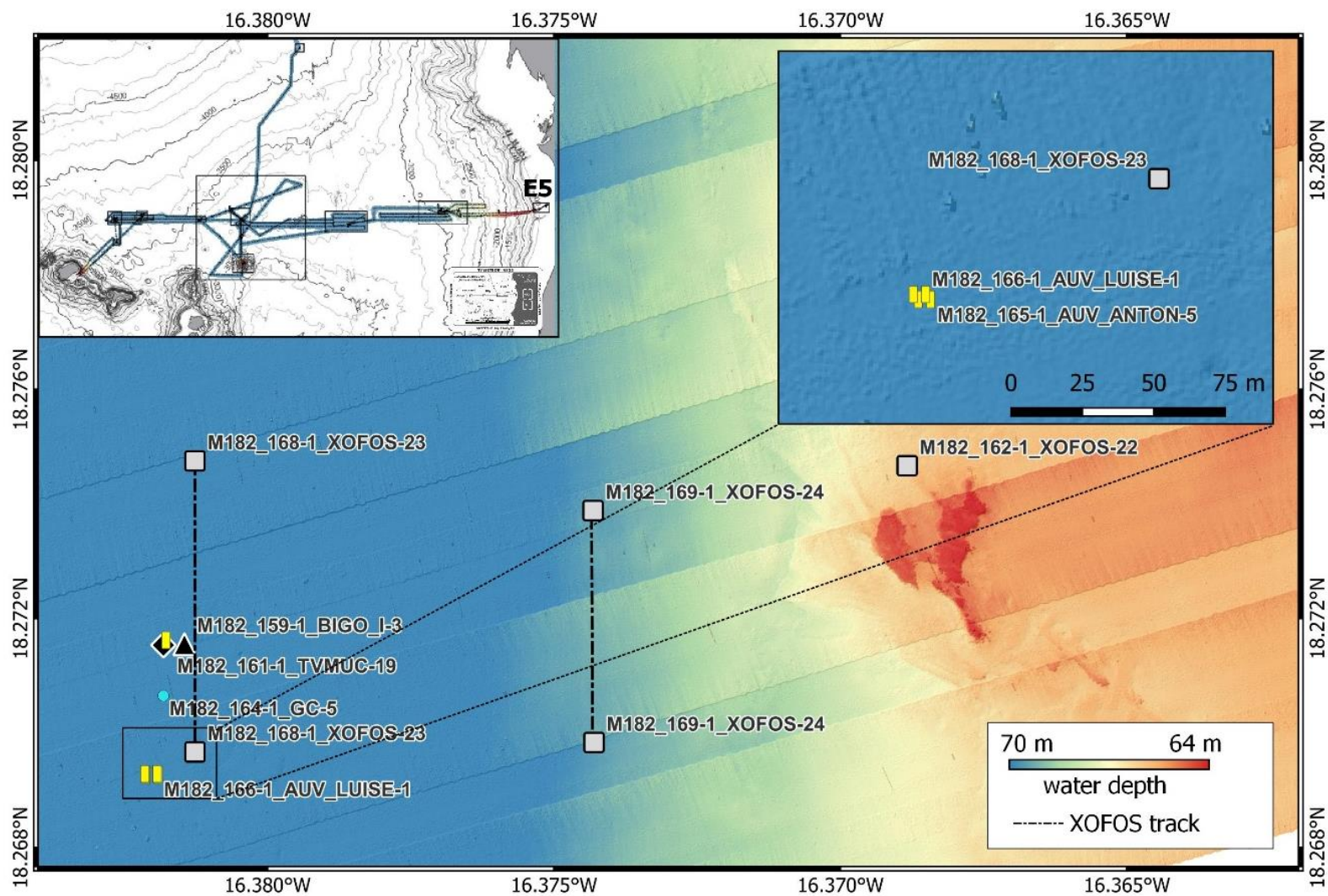


Fig. 12.36 Bathymetry data of M182 cruise of research area E5 (a) with sampling stations.

Working area E5 (b)

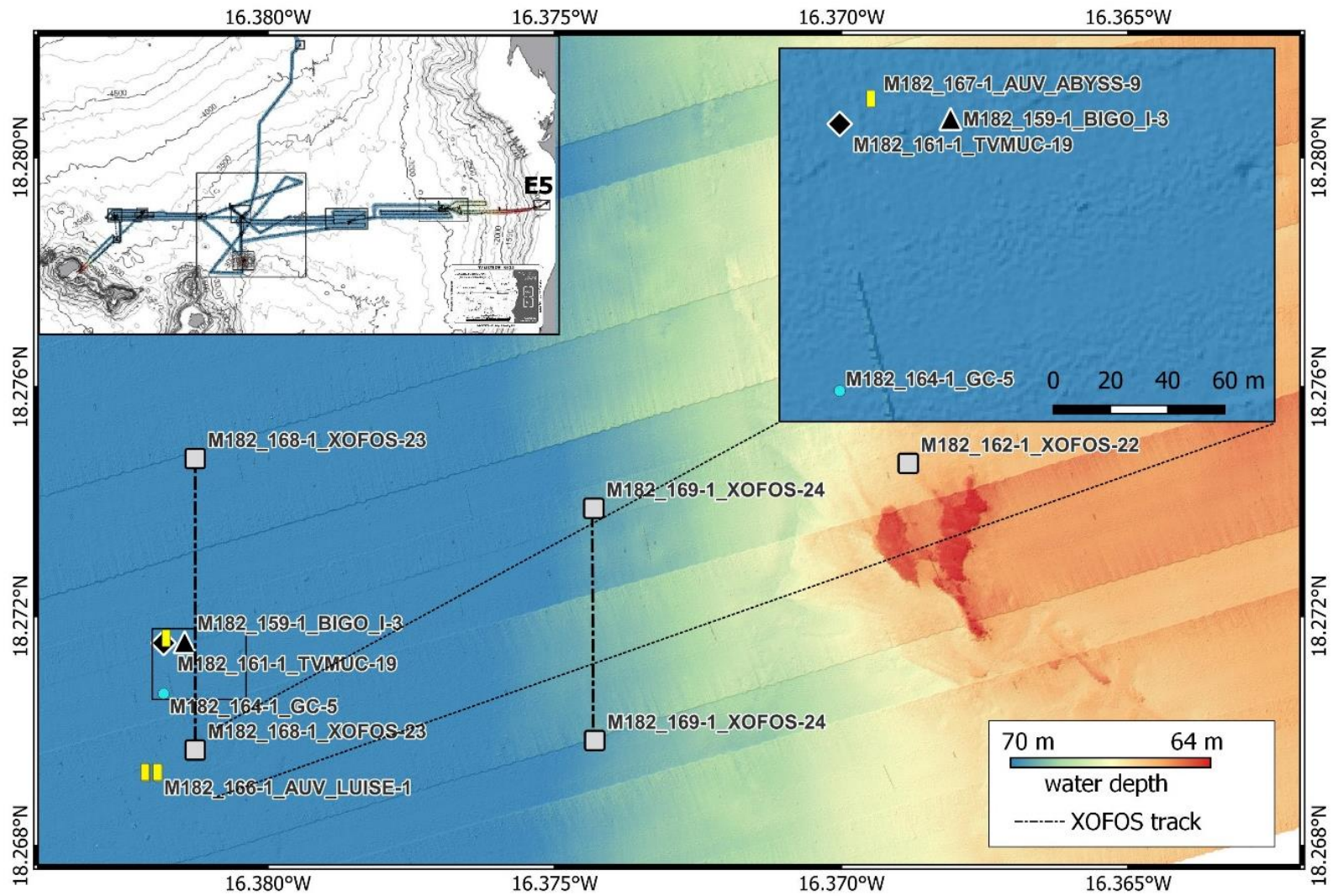


Fig. 12.37 Bathymetry data of M182 cruise of research area E5 (b) with sampling stations.

Working area Eddy Hunt Core

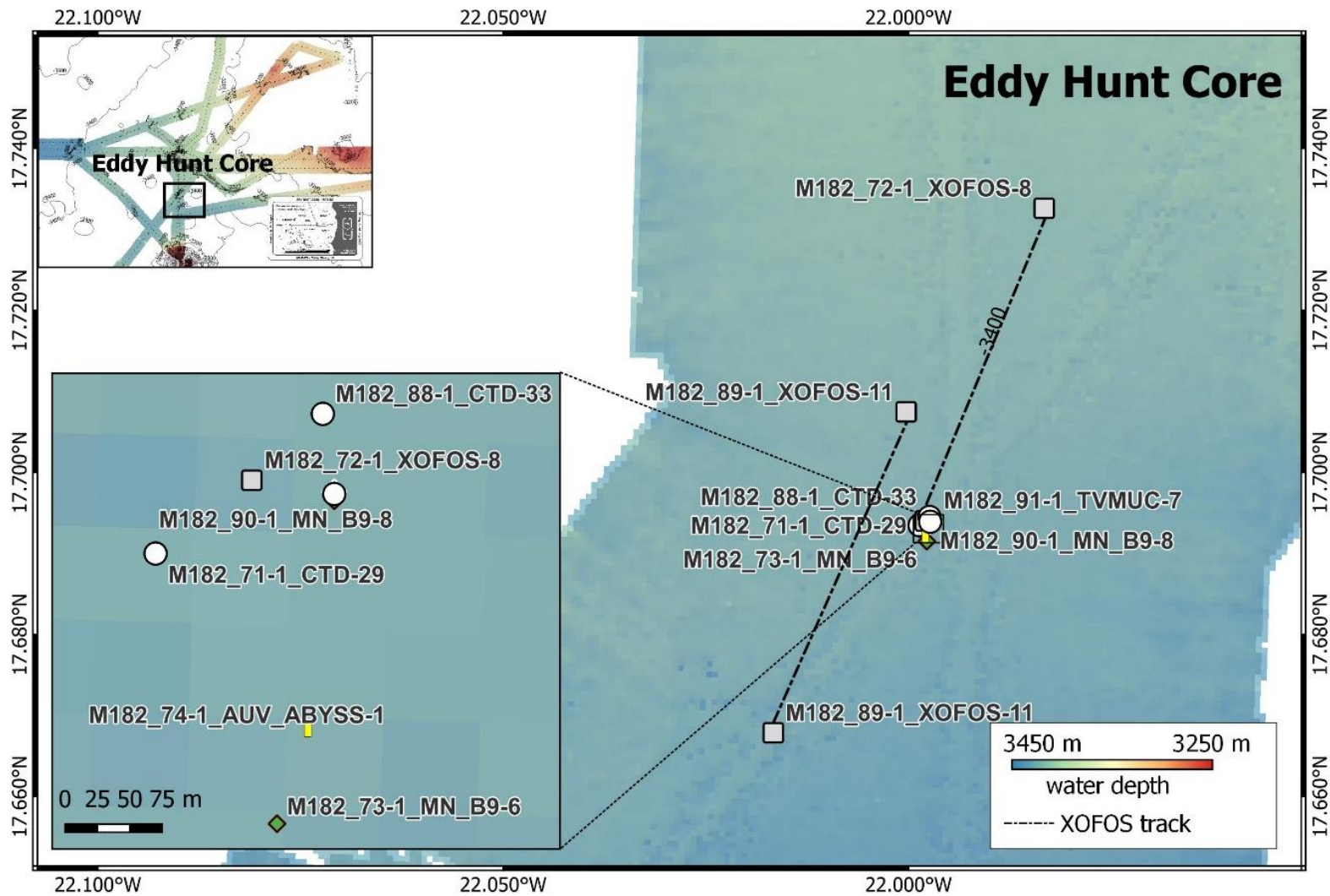


Fig. 12.38 Bathymetry data of M182 cruise of research area Eddy Hunt Core with sampling stations.

Working area Eddy Hunt Periphery N

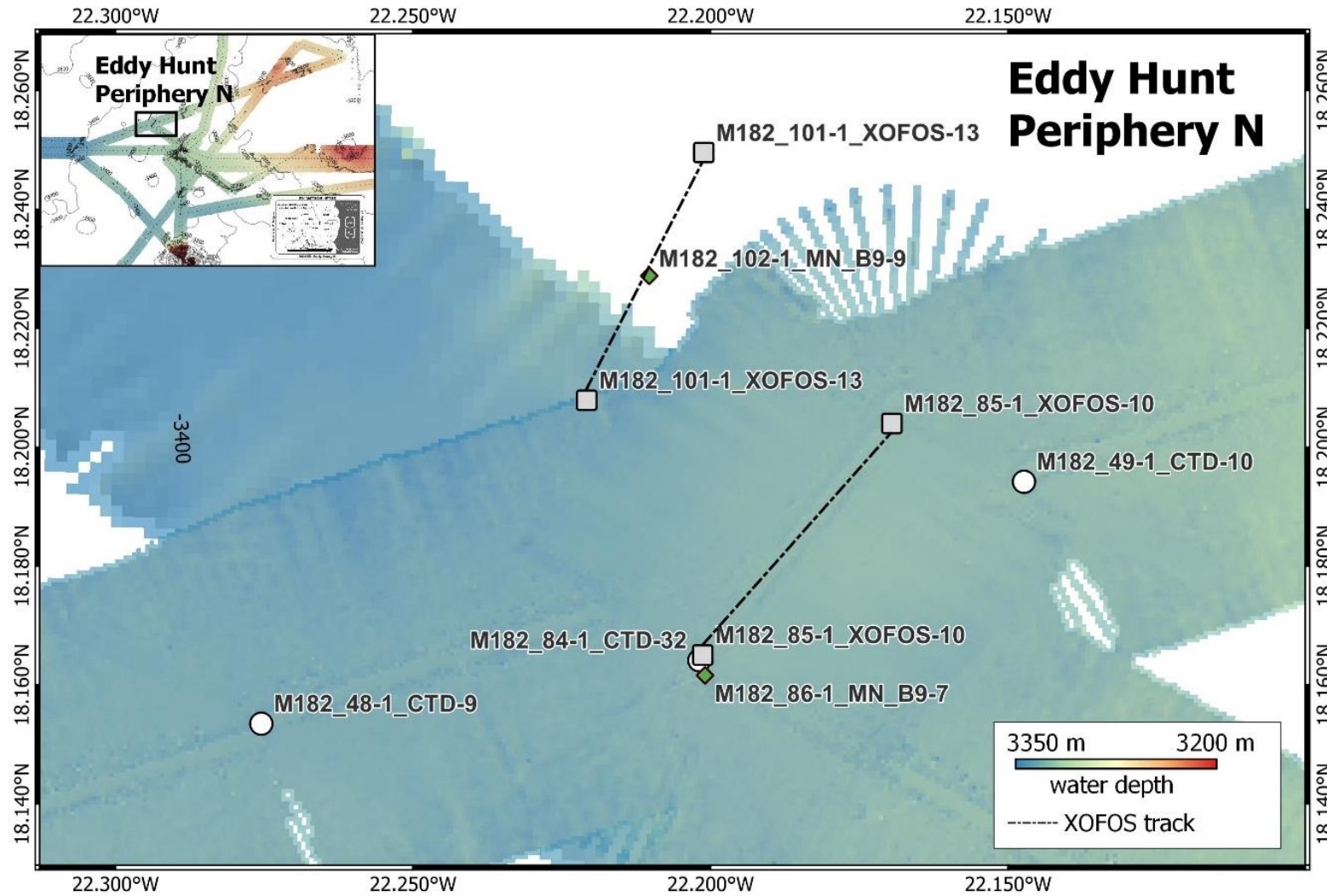


Fig. 12.39 Bathymetry data of M182 cruise of research area Eddy Hunt Periphery N with sampling stations.

Working area Eddy Hunt Periphery NW

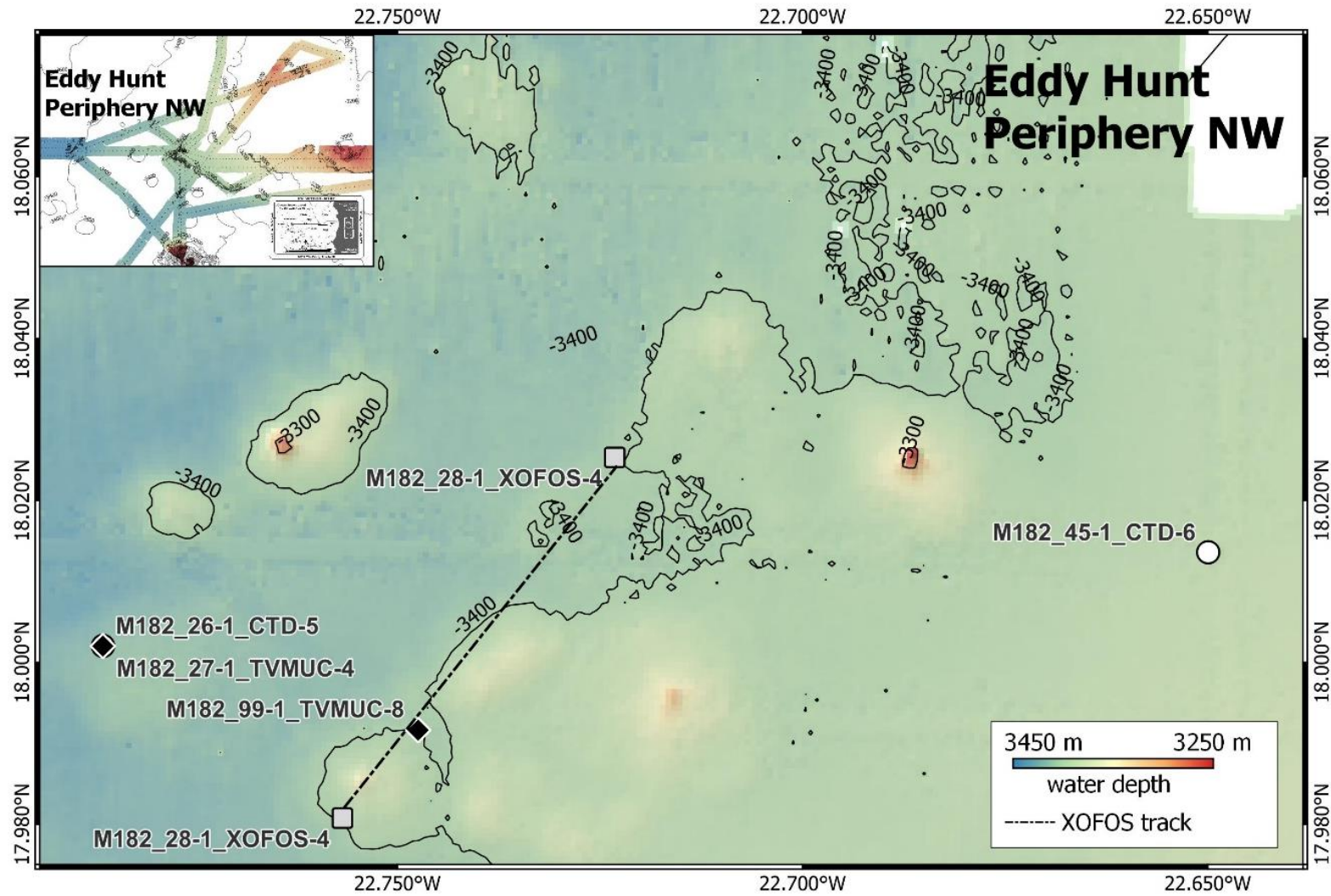


Fig. 12.40 Bathymetry data of M182 cruise of research area Eddy Hunt Periphery NW with sampling stations.

Working area Eddy Hunt

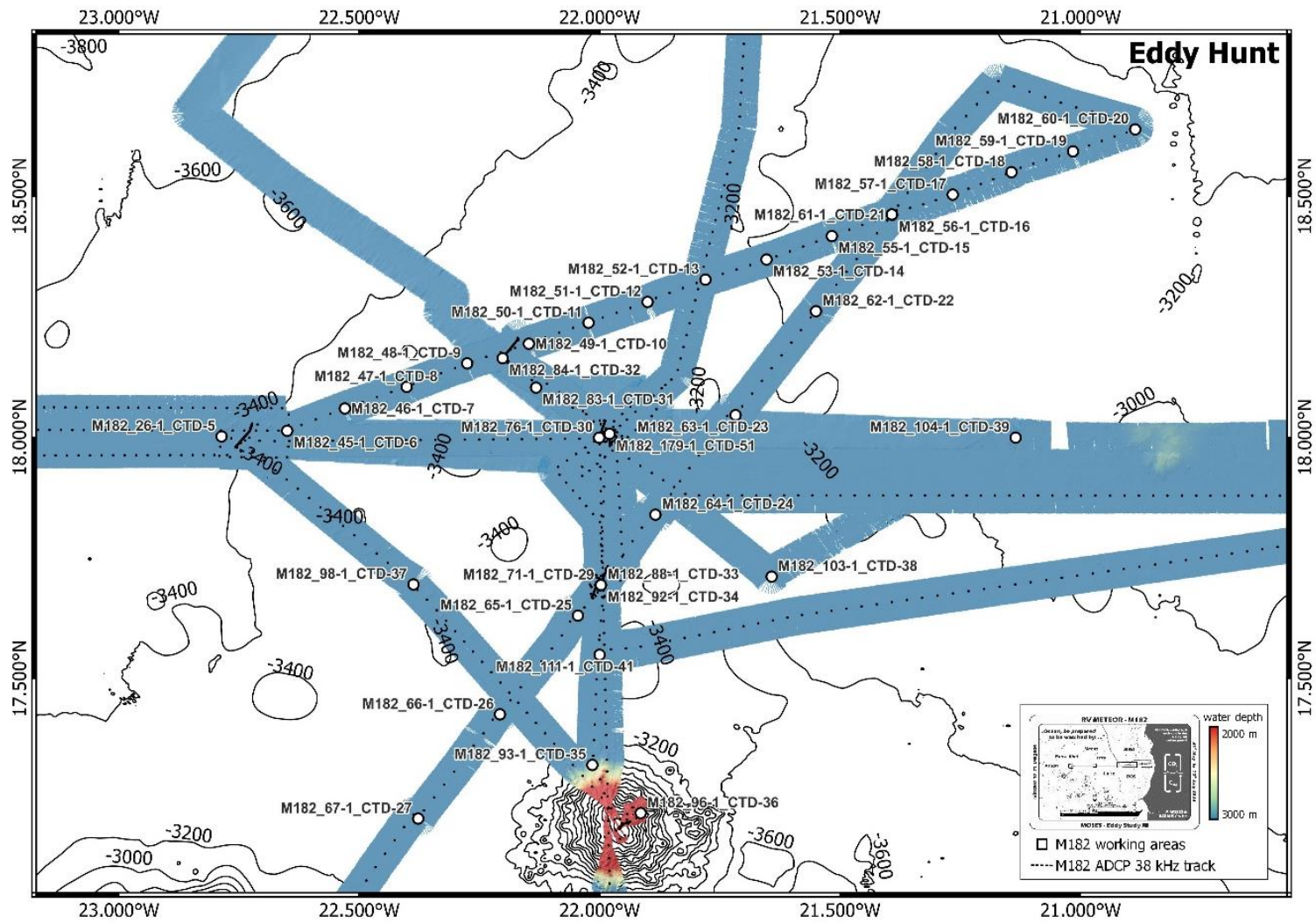


Fig. 12.41 Bathymetry data of M182 cruise of research area Eddy Hunt with sampling stations.

Overall CTD Stations

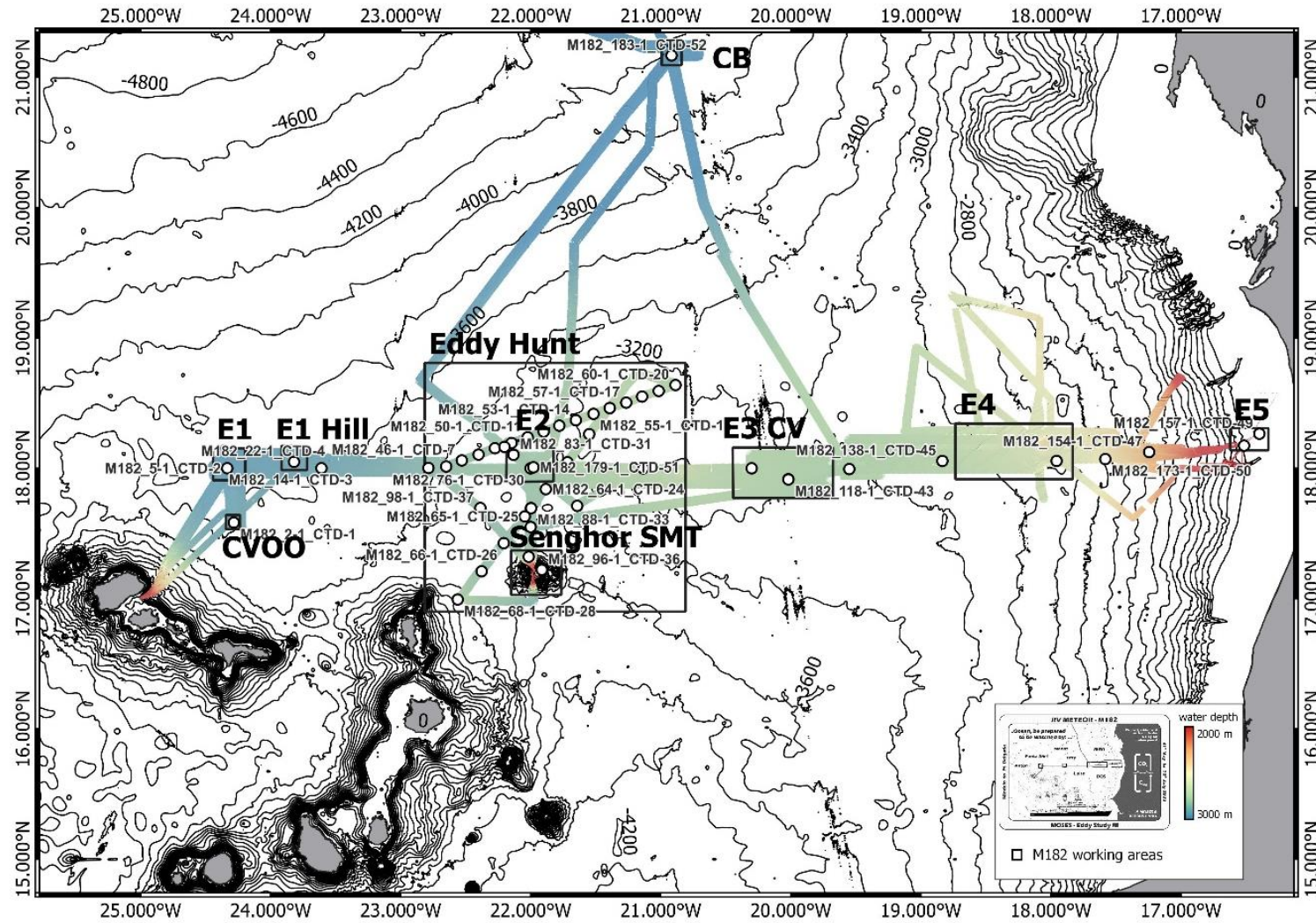


Fig. 12.42 Bathymetry data of M182 cruise of research areas with CTD stations.

Overall MUC Stations

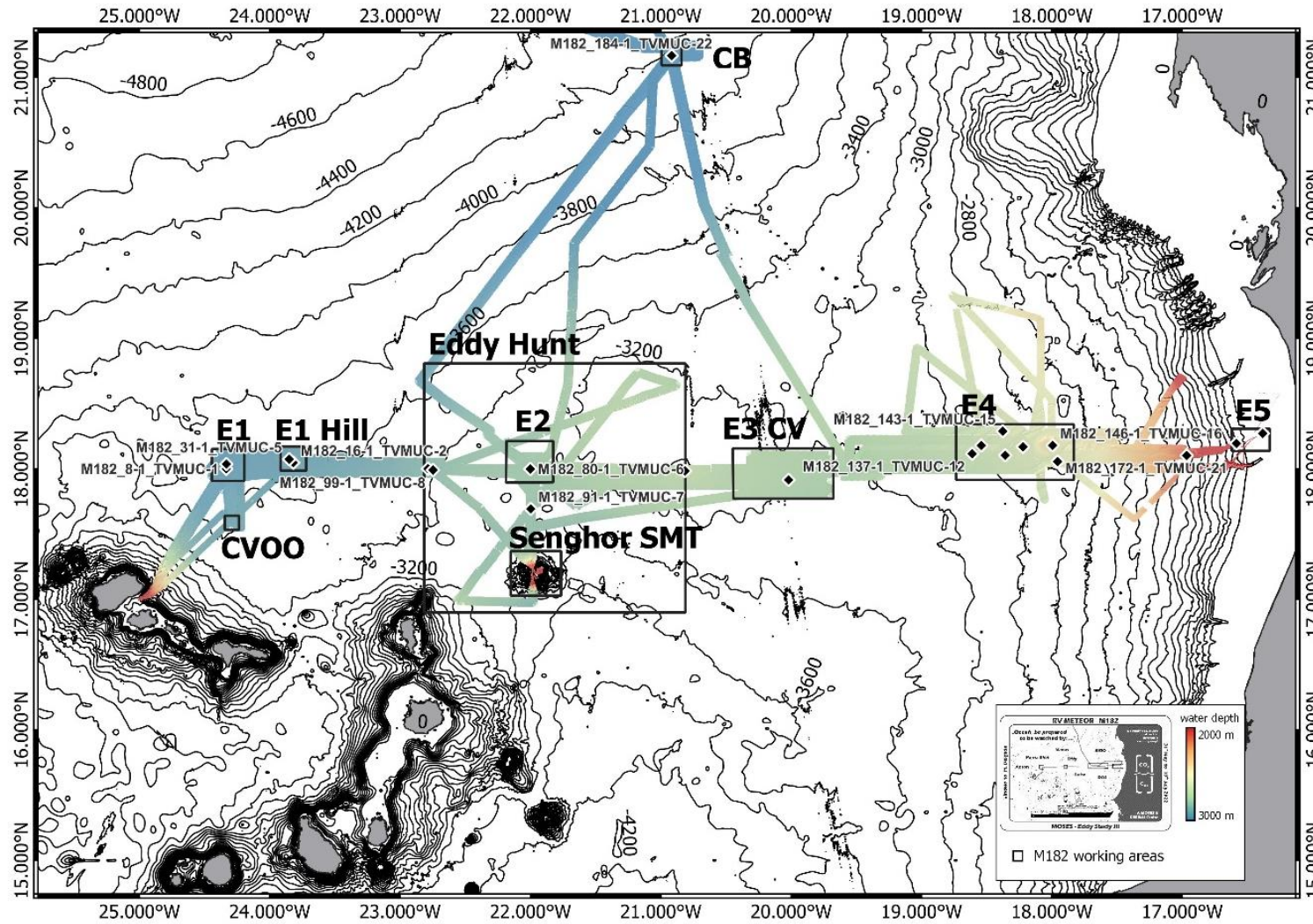


Fig. 12.43 Bathymetry data of M182 cruise of research areas with MUC stations.